Kari Moen

Quantitative measurements of mineral microstructures

Development, implementation and
use of methods in applied mineralogy

Thesis for the degree doktor ingeniør

Trondheim, November 2006

Norwegian University of Science and Technology
Faculty of Engineering Science and Technology
Department of Geology and Mineral Resources Engineering

NTNU
Innovation and Creativity

"....the mountains must indeed be examined with the microscope."

H.C. Sorby, 1856

Preface

The work presented in this doctoral thesis was conducted at the Department of Geology and Mineral Resources Engineering at the University of Science and Technology (NTNU) in Trondheim during the period 2001-2006. The supervisors for the project were Professor Terje Malvik at the Department of Geology and Mineral Resources Engineering and Professor Jarle Hjelen at the Department of Materials Science and Engineering.

The project was initiated by Professor Terje Malvik, as a part of the strategic university program (SUP) "The value chain from mineral deposit to beneficiated product with emphasis on Quartz" funded by the Norwegian Research Council. This particular part of the SUP was partly funded by the Norwegian mining companies Titania A/S, Hustadmarmor A/S and Norwegian Crystallites AS. These companies also provided samples and cases for the studies.

Co-adviser during this work, Professor Jarle Hjelen provided equipment, software and expertise on the experimental and instrumental part.

In addition to collaboration with the mineral industry, projects were carried out together with Researcher Lisbeth Alnæs at Sintef Rock and Soil Mechanics and Professor Mai Britt Mørk at the Department of Geology and Mineral Resources Engineering.

The papers presented in this doctoral thesis are the main contributions during the project period. In addition, papers and posters have been presented at several international conferences and meetings.

Abstract

The project has been in applied mineralogy. Advanced characterisation techniques have been developed and used as a tool for quantitatively describing geological raw materials, middlings and end products for optimal exploitation of mineralogical materials. The overall purpose has been to develop skills and techniques on detection and quantification of mineralogy and microstructures by means of various scanning electron microscopy (SEM) techniques. A premise for success was then to develop a close cooperation with the staff at the electron microscopy laboratory at Department of Materials Science and Engineering at the initiation of the project. A specific objective has been to develop and implement automatic SEM-based quantitative measurements on major and trace minerals in rocks, ores and milled products in order to measure modal mineralogy, microstructures and particle texture including mineral liberation and mineral association. Through collaboration with engineers and researchers in different aspects of mineral production, the work has included development of software, implementation and testing of software, and case studies for the industry and other collaborators. Five papers are included in the thesis. Papers 1 and 2 present methods for quantitative measurements of minerals covering the principles of PTA and EBSD analysis and some case studies. Papers 3-5 present microstructure studies of marble and deeply buried sandstone. In addition, Chapter 5 treats the development of the PTA more thoroughly.

The main conclusions from the study are:

A method for detailed, quantitative measurements of main and trace minerals and particle texture has been developed in close relation with the industry. The data acquisition is based on commercial hard- and software and the results are post-processed in the developed PTA software. In the future, the PTA will be further developed and it is a goal to launch the system on the commercial market.

Several cases of raw material, middlings and end products from the mineral industry were investigated by means of PTA analysis throughout the doctoral study. Modal mineralogy, mineral liberation, mineral associations and mineral intergrowths and the contribution from various minerals to certain elements, have been studied. The cases have demonstrated the strength and the possibilities of the programme.

Electron backscatter diffraction was tested and evaluated as a relatively new approach in applied mineralogy, characterising the crystallography. EBSD is not found suitable for ordinary particle analysis, but the technique is superior when studying polymorphs, and in quantitative measurements of lattice orientation and fabric parameters obtained from the measurements of crystal orientations.

The microstructure of marble used for exterior cladding panels were investigated with respect to deterioration. Several aspects of the microstructure were measured and analysed, and a prediction model for bowing of marble slabs was calculated. For direction dependent bowing, the grain shape orientation (foliations, lineation) was regarded as most important together with lattice preferred orientation because of extremely anisotropic thermal behaviour of calcite. The variables that influenced the intensity of bowing in the prediction model were grain shape or roughness of the grain boundaries and the shape of the grain-size distribution curve.

Optical and electron microscopy techniques were used to investigate relations of diagenesis and microstructure in quartz grains and quartz cement in reservoir sandstones from offshore Norway to search for possible evidences of compaction induced deformation. The quartz overgrowths were indistinguishable from the host grain in EBSD maps supporting syntaxial growth. From low-angle boundary studies it was concluded that cement growth was not accompanied by recrystallisation. Dauphiné twins were common both in cemented and non-cemented samples and it was suggested that some of the twins at quartz grain edges and quartz cement-grain contacts may be related to burial compaction. This implies a mechanism of grain-boundary deformation in burial diagenesis, which is invisible using conventional petrographic tools.

During the development and implementation of systems and techniques, competence has been developed in the intersection between geology and materials technology. The research groups have become integrated with a common instrument laboratory and knowledge to further develop the laboratory as a resource in applied mineralogical research.

Acknowledgements

Table of contents

Part Two:

Paper 1: Particle Texture Analysis in process mineralogy

Paper 2: EBSD – a potential supplementary technique in quantitative characterisation of minerals

Paper 3: EBSD microstructure measurements of marble

Paper 4: Quantitative measurements of marble microstructure – a model for predicting deterioration of marble

Paper 5: Reconnaissance study of compaction microstructures in quartz grains and quartz cement in deeply buried sandstones using combined petrography - EBSD analysis

Appendix

Contributions to the papers

The papers are based on projects that have involved collaboration with other people. The contributions to the papers are therefore given below:

1. PARTICLE TEXTURE ANALYSIS IN PROCESS MINERALOGY

Kari Moen, Terje Malvik, Torkjell Breivik, Jarle Hjelen

Moen has been a central partner in the development of PTA, she planned and performed the experimental and analytical work and wrote the paper. Malvik assisted with ideas for the PTA and has evaluated the work throughout the process. Breivik has performed all the programming and has been of vital importance in the development. Hjelen has supported with important guidance related to electron microscopy and contact with Oxford Instruments.

2. EBSD - A POTENTIAL SUPPLEMENTARY TECHNIQUE IN QUANTITATIVE CHARACTERISATION OF MINERALS.

Kari Moen, Jarle Hjelen, Terje Malvik, John Rasmus Leinum

Moen performed the experimental work and wrote the paper. Hjelen and Malvik provided guidance with the approach to the problem, EBSD theory and writing. Leinum assisted in the experimental work.

3. EBSD MICROSTRUCTURE MEASUREMENTS OF MARBLE.

Kari Moen, Terje Malvik, Jarle Hjelen, John Rasmus Leinum, Lisbeth Alnæs

Moen planned and performed the experimental and analytical work and wrote the paper. Malvik and Hjelen provided guidance and assistance. Leinum helped in the experimental work and in the analytical discussions. Alnæs provided background information and the overall picture and assisted in writing.

4. QUANTIFICATION OF MARBLE MICROSTRUCTURE

Kari Moen, Terje Malvik, Lisbeth Alnæs, Jarle Hjelen

Moen planned and performed the experimental and analytical work and wrote the paper. Malvik and Hjelen provided guidance and assistance. Alnæs provided background information and the overall picture and assisted in writing.

5. RECONNAISSANCE STUDY OF COMPACTION MICRO-STRUCTURES IN QUARTZ GRAINS AND QUARTZ CEMENT IN DEEPLY BURIED SANDSTONES USING COMBINED PETROGRAPHY - EBSD ANALYSIS

Mai Britt Mørk and Kari Moen

Mørk had the idea, planned the experimental work and wrote the paper. Moen performed the experiments, post-processed the data and joined in the interpretation discussion.

Abbreviations

ADC	Analogue to Digital Converter
BSE	Backscatter Electron
CCD	Charged Couple Device (Digital camera technology (light sensitive)
CL	Cathodoluminescence
CMOS	Complementary Metal Oxide Semiconductor (Digital Camera technology)
DD	Detector Distance (EBSD)
EBSD	Electron Backscatter Diffraction
EBSP	Electron Backscatter Pattern
EDS	Energy Dispersive System (X-rays detector)
EPMA	Electron Probe Micro-Analyser
HIS	Hue Saturation Intensity
IA	Image Analysis
MRD	Multiples of Random Distribution (EBSD pole-figure intensity)
OM	Optical microscopy
PC	Pattern Centre (EBSD)
PC	Point counting
PLS	Partial Leas Squares (regression)
PTA	Particle Texture Analysis
RGB	Red Green Blue
SE	Secondary Electron
SEM	Scanning Electron Microscope
TEAM	Testing and Assessment of Marble and Limestone, EC-project
WDS	Wavelength Dispersive System (X-rays detector)

Introduction

1.1   GENERAL

1.1.1   The Norwegian mining industry

During recent decades the Norwegian mining industry has undergone a marked shift from being an industry largely based on exploitation of metallic ores to one almost entirely producing non-metallic ores. During the 1980s and 1990s several old sulphide ore mines were closed down, while there was a strong growth in the production and export of industrial minerals, aggregates and dimension stone (Kleiv, 2001). The production and export value of industrial minerals have continued to increase considerably. The industrial mineral production is characterised both by the variety of minerals and mineral products and by the fact that Norway is the world's major producer of certain minerals such as olivine, nepheline and beneficiated carbonates (GCC) used in paper. In addition, Norway produces quartz/quartzite, graphite, talc, anorthosite, feldspar, mica, dolomite and ilmenite. The production value of mineral resources in Norway, except for oil/gas, was about 8,25 thousand million NOK in 2004. Out of this, 2,84 thousand million NOK came from the industrial minerals, 2,66 thousand million from crushed rocks/aggregates, 1,1 thousand million from natural stone

and only 0,62 thousand million NOK from metallic ores. The remainder 1,0 thousand million NOK results from an increased coal production at Svalbard (NGU, 2005). The growth in industrial mineral production exceeds the decline in metallic ores, and it is recognised that there is a considerable future growth potential in industrial mineral production in Norway. The value of industrial minerals is primarily created during the beneficiation and the production of special products, needing both competence and sophisticated technology. For instance, crushed carbonate may be priced at 35 – 40 NOK/t, while beneficiated carbonate filler used in paper may reach prices above 1000 NOK/t. There is a gradual transition from mineral beneficiation to material technology. The research activity in industrial minerals has been fairly low in Norway. Most of the research is carried out by the industry itself, and the results are generally kept in company files. However, to produce valuable and special products reaching high prices in the market, there is a considerable need for skill and competence (Malvik, 2005).

1.1.2   Applied and theoretical mineralogy

1.1.2.1   *Applied mineralogy*

As reviewed a number of times by Professor Richard D. Hagni (Hagni, 1982; 1988, 1991, 1995b) applied mineralogy differs from theoretical mineralogy in various aspects. Whereas applied mineralogy focuses on industrial problems, theoretical mineralogy focuses on mineralogical issues that may have no direct application to current problems in the mineral industry (Hagni, 1991). Applied mineralogy papers commonly present case studies describing solutions to industrial problems by applying various mineralogical techniques, development of new mineralogical techniques or application of mineralogical technology (Hagni, 1991). The questions asked in theoretical geology, differ fundamentally from the ones in applied mineralogy. After characterising the mineral material the theoretical mineralogist is principally interested in questions of petrogenesis. "How did the minerals form?", "What do they tell us about the origin of the rock?" etc. The applied mineralogist, on the other hand, asks questions such as: "How can these minerals be separated?", "In which minerals are the elements of value or damage?", "Is there a mineralogical reason for low recovery?" (Vaughan et al., 2004), "What is the reason for high porosity of the reservoir

rock?", "Why does certain dimensional stones deteriorate?". Focus in applied mineralogy is put on solving practical problems rather than discovering fundamental facts (Hagni, 1991).

The scope of applied mineralogy is nicely illustrated in the books of William Petruk (2000), Meurig Jones (1987) and the proceedings of meetings of the International Congress of Applied Mineralogy and the Commission on Applied Mineralogy of the International Mineralogical Association (see for example Hagni, 1995a) (Vaughan et al., 2004).

1.1.2.2 *Process mineralogy*

Hagni (1991) states that "Often used interchangeably, the phrases "process mineralogy" and "applied mineralogy" encompass somewhat different spheres of applications. Process mineralogy deals with mineralogy as applied to the products of industrial processes, including beneficiation, hydrometallurgy, pyrometallurgy, coking, Portland cement-making, refractory manufacture, electronic materials production and others. Applied mineralogy, on the other hand, includes all of process mineralogy as well as mineralogical techniques for minerals exploration, environmental concerns, the medical profession and other areas".

For applied mineralogists it is necessary to extend their knowledge beyond that classically associated with mineralogists and geologists. Applied mineralogists should acquire knowledge of nomenclature, processes and challenges found within the industry (Hagni, 1991).

Up to 1979 only sporadic papers within the applied mineralogy discipline were published although some of the larger mining companies of the world employed applied mineralogists. The results of their research were typically stored in company files. The most important impetus of the development of applied mineralogy was the initiation of the "Process Mineralogy Committee" which is a committee of the Society of Mining, Metallurgy and Exploration Engineers (SME) and the Minerals Metallurgical and Materials Society (TMS). The committee sponsored the first process mineralogy session in 1979. During the 1980s, the developments in applied or process mineralogy were spectacular (Hagni, 1991).

1.2 PROJECT BACKGROUND AND FUNDING

1.2.1 Strategic university programme

The strategic university programme (SUP) "The value chain from mineral deposit to beneficiated product with emphasis on quartz" was initiated by the Department of Geology and Mineral Resources Engineering in 2000 and gradually started during 2001. In accordance with recommendations given by the "National Working Group" (Elverøy et al., 1999) a close co-operation with staff at the Department of Materials Technology was strongly emphasised in this project. The research activity in industrial minerals has been fairly low in Norway. Most of the research has been carried out by the industry itself, and the results are generally kept secret. However, to produce valuable and special products reaching high prices in the market, there is a considerable need for skill and competence. Being the only university in Norway responsible for research and teaching in mineral production, the research programme has been of major importance.

The programme comprised three areas of research:

- Genesis of industrially applicable high purity quartz in igneous and metamorphic environments
- Beneficiation of quartz
- Advanced characterisation of industrial minerals and beneficiated products.

Collaboration with other universities as well as with industrial partners which also gave financial support to the project has been vital. The following departments and institutions have collaborated in the programme: Department of Geology and Mineral Resources Engineering, (IGB), NTNU, Department of Materials Technology, NTNU, SINTEF Rock and Soil Mechanics, The Geological Survey of Norway (NGU) and The Department of Geology, University of Oslo (UiO). Industry partners have been TITANIA A/S, Hustadmarmor A/S, Norwegian Crystallites AS, North Cape Minerals and Elkem A/S.

The time plane of the project was 5 years, from 1st of January 2001 to 31th of December 2005. Financial support was given by the Norwegian Research Council (NFR), Hustadmarmor, Norwegian Crystallites and Titania and from NGU as field contribution from researchers. Within the programme, 5 doctoral

candidates, one post doc and researchers at NTNU and NGU performed research.

1.2.2 Cooperation with the industry

The importance of being able to quantify the mineralogical parameters is fully recognized by the industry. Three industry partners (Titania, Hustadmarmor, and Norwegian Crystallites) have supported the project in order to benefit from the developments being made. An online measurement system where the industry partner can take an active part in the measurements has been developed. Combined with flexible solutions and measurement settings these have led to techniques being able to describe most mineralogical and textural phenomena occurring in rocks/ores and in mineral products. By use of new and advanced laboratory equipment, mineralogical and textural properties of industrial minerals and beneficiated products can be determined. The results may be used to define areas for new applications of minerals or establish correlations between material properties and geological processes leading to different mineral raw materials.

1.2.3 The TEAM project

Parallel to the SUP project, cooperation with researcher Lisbeth Alnæs at the research organization SINTEF, has been fertile. Through a European Union project, Testing and Assessment of Marble and Limestone (TEAM), two papers on microstructure measurements of marble used as dimensional stone have been accomplished. The cooperation followed by funding has been valuable.

1.3 PURPOSE AND SCOPE OF WORK

This thesis is the main contribution to the research area "Advanced characterisation of industrial minerals and beneficiated products" within the strategic university programme further described in chapter 1.2.1, where the development of quantitative methods to describe raw materials and mineral products has been the superior purpose of the project. The specific objective throughout the work has been to develop automatic SEM based quantitative techniques in order to:

- Quantify the mineral content, both major and trace minerals in rocks/ores and in milled products;
- Quantify the occurrence of minerals in different types of particles in milled materials and mineral products;
- Quantify the mineral texture.

After initialising the work on these techniques, it was evidently experienced that quantification of microstructures is a widespread need and an important contribution both in process mineralogy and in applied mineralogy on a wider scale. The main effort has therefore been put into development of a system able to quantify modal mineralogy and appearance of minerals in particles, while the overall scope of work has been focused on detection and quantification of microstructures by means of several scanning electron microscope techniques.

1.4 THESIS ORGANISATION

1.4.1 General organisation

This thesis consists of two main parts. While the scientific work of the study is presented as research papers in the second part, the first part contains a general introduction to the project, aims and scope of work, background information presenting a review of the research field and method chapters describing the analytical techniques used and an overview of the experimental equipment and samples used in the papers. In Chapter 6 the development of the Particle Texture Analysis system is more thoroughly described than in Paper 1. A brief summary of the papers and a general discussion are given along with overall conclusions from the study. Suggestions for further research are also presented. In the appendix some additional application notes on EBSD analysis in applied mineralogy are presented. These are not extensive enough for papers but demonstrate typical tasks that can be solved by means of quantitative measurements. Consequently, Part One provides a complete overall picture of the project while Part Two contains 5 research papers.

1.4.2 The research papers

The papers presented in the second part of this doctoral thesis compose the main contributions during the project period comprising of both papers from a quite

early phase and recent papers still in press. In addition, papers and posters not included have been presented at international conferences and meetings. Each of the research papers is an independent unit which can be read separately. In order to give adequate background information in Part One, a limited number of sections are repeated and are therefore found both in the first part as well as in the papers. It is the author's opinion that this will enhance the ease of reading the thesis.

1.5   STRATEGIES

The objective of the project is already described in the chapters above. The strategy to obtain this, however, has been to develop a new particle system along with competence within the field by means of close cooperation with the industry and early publication of papers at international conferences to get feedback through the whole process. Some of the arguments for making a new particle system were the fact that our laboratory is a multi-purpose laboratory, and the available commercial systems were expensive and dedicated systems dependent on predetermined microscope contractors. Another important argument was that fact that this would also develop valuable competence along with the development of the system.

To gain publicity about the project and to get feedback from researchers in the fields covered by the theses, early publications were aimed at international conferences.

1.6   REFERENCES

Elverøy, A., Haldorsen, S., Bergh, S., Roaldset, E., Kristoffersen, Y., Haugan, P. M., Killingtveit, Å., and Eliassen, A., 1999, Geofagplanen - Plan for norsk geofaglig forskning og undervisning i U&H-sektoren, *in* NFR, ed.: Oslo, Norges forskningsråd, p. 43.

Hagni, R. D., 1982, Process Mineralogy: Past, Present, and Future: Symposium on Process Mineralogy, AIME Annual Meeting, Dallas, Texas, 1982, Process Mineralogy, p. 29-36.

Hagni, R. D., 1988, The Status of Process Mineralogy in 1988: JOM Journal of Metals, v. 40, p. 25.

Hagni, R. D., 1991, A Decade of Developments in Applied Mineralogy: JOM Journal of Metals, v. 43, p. 25-26.

Hagni, R. D., 1995a, Process Mineralogy XIII: Rolla, Missouri, The Minerals, Metals & Materials Society, 377 p.

Hagni, R. D., 1995b, Recent Developments in the Application of Process Mineralogy: JOM Journal of Metals, v. 47, p. 46.

Jones, M. P., 1987, Applied mineralogy: a quantitative approach: London, Graham & Trotman, 259 p.

Kleiv, R. A., 2001, Heavy metal adsorption on silicate tailings. A study of nepheline syenite and olivine process dust.: Unpub. Article collection thesis, Norwegian University of Science and Technology, 142 p.

Malvik, T., 2005, Project description; Background for the programme, Strategic University Programme(SUP) "The value chain from mineral deposit to beneficiated product with emphasis on quartz": Trondheim, NTNU.

NGU, 2005, Mineralressurser i Norge, Bergindustrien 2004, *in* Neeb, P.-R., ed., NGU rapport 2005.041: Trondheim, Geological Survey of Norway, NGU, p. 1-25.

Petruk, W., 2000, Applied Mineralogy in the Mining Industry: Ottawa, Ontario, Canada, Elsevier, 268 p.

Vaughan, J., Davidson, L., Nemchin, A., and Quinton, S., 2004, Teaching process mineralogy in Australia: Journal of Geoscience.

Background

2.1 GENERAL REMARKS

This chapter provides basic and supplementary information, which is meant to assist in the reading of the papers and put the project into a framework where the motivation of the research performed is more thoroughly discussed.

2.2 MINERAL ANALYSIS IN THE INDUSTRY

All mineral processes treat particles and not chemical elements. The particles contain one or more minerals. To achieve high quality products meeting the different requirements from the customers, and with a minimum waste, a thorough and detailed knowledge concerning the occurrence of the minerals in raw materials, products and waste is needed.

For a long time in investigations of particularly the base metal sulphides and precious minerals, automatic scanning electron microscope-based (SEM) image analysers have been used to quantify the occurrence of the minerals. Special emphasis has been laid on determining the liberation properties of the economic minerals to avoid under or over grinding of the minerals for further separation. It

is recognized that the behaviour of particles in separation processes is a function of different properties of which the most important are:

- Mineralogical parameters (minerals in particle, mineral chemistry);
- Textural properties (size, shape, grain boundaries, type of intergrowths (particle texture));
- Physical properties of the minerals (specific gravity, surface tension, magnetic property etc.).

During recent decades the Norwegian mining industry has shifted from the exploitation of metallic ores to a strong and positive development within industrial minerals. In production of industrial minerals, bulk analysis and manual microscopy have been used to describe raw material and concentrates, but the research activity has been fairly low. Most of the research has been carried out by the industry itself, and the results are generally kept in company files. However, to produce valuable and special products reaching high prices in the market, there is a considerable need for skill and competence. This project aims at developing automatic methods which can be used on industrial minerals as well as any other crystalline material (Malvik, 2005).

2.3 DEVELOPMENT OF METHODS IN QUANTITATIVE GEOLOGY

2.3.1 Introduction

In mineral processing, minerals are separated by means of relative differences in physical properties. It is therefore important to determine mineralogical characteristics that affect the behaviour of minerals during processing (Lastra et. al. 1998).

Mineralogical characteristics that are valuable from a process mineralogist's point of view could be:

- Mineralogy in feed, products and waste;
- Mineral chemistry of every mineral;
- Modal mineralogy / mineral distribution ;
- Mineral liberation of important minerals;
- Minerals associated in composite particles;
- Type of lockings/intergrowths in the composite particles.

Most of these aspects need a quantitative approach requiring the analysis of a representative amount of mineral particles to give a valid answer. Petruk (2000) describes the acquisition of quantitative data for mineral processing. Of particular interest are bulk analyses as x-ray diffraction analysis of powders and calculations from chemical assays in addition to microscope techniques using thin or polished sections. He describes the strength and weakness of the different analyses and concludes that bulk analyses are semi-quantitative when it comes to mineralogy and give no information about how the minerals occur. Microscope analysis, therefore, provides vital information in combination with bulk analysis techniques. The quantities of economic minerals have traditionally been determined by point counting (Glagolev 1934) with an optical microscope. As observed in Lastra et al (1998): "Point counting is a slow and tedious process and, because of the paucity of grains counted and the subjectivity of the technique, commonly the data are statistically poor. With the arrival of the computer, automation became possible not only in scanning devices for data acquisition, but also in data recording and data treatment". A new challenge is to present the enormous amount of data that can be collected in appropriate ways.

The following chapters aim to review the development and possibilities regarding quantitative description of mineralogy and particle texture by microscope techniques with a special emphasis on the following items: methods for measuring relative areas in thin sections, image analysis and automated scanning electron microscope based mineral liberation systems. This analysis of methods will include both historical perspectives and *state-of-the-art* techniques dealing with quantitative description of mineralogical characteristics applied to process mineralogy. The analysis ends with discussion of future potential developments.

2.3.2 Methods of measuring relative areas in thin sections

2.3.2.1 *Early developments*

Hetzner (1998) describes today's automated image analysis systems as being the culmination of microscope developments spanning more than 100 years. After the first microscopes were created and systems and know-how for identification of minerals were established, the next logical question was how much of some

constituent was present. As Hetzner (1998) observes: "From these questions quantitative microscopy had its roots".

In his classical book " Petrographic Modal Analysis" Chayes (1956) reviews the development of techniques and instrumentation for modal analysis. The French petrograph A. Delesse is the first name mentioned in the literature followed by his disciple Rosiwal (1898). Delesse developed a statement of the relation between relative areas and volumes and a technique by which he actually estimated areas. He actually placed a piece of waxed paper over a polished surface and traced the outlines of the underlying minerals areas. The pattern was transferred to a tin foil and the various areas cut apart. Foils representing sections of the same mineral were then assembled and weighed, the whole process without the use of a microscope (Delesse, 1848). As Chayes (1956) stated, this technique "seems tedious and crude" and the "possibilities of error seem fabulous". All modal analyses depend on the relation of area and volume from Delesse, but direct area measurements became less important for many years to come. Like Delesse, Rosiwal developed a technique rather than an instrument. His name is generally applied to procedures which are purposely designed to yield estimates of relative areas by means of lines traversing the minerals and by use of an eyepiece micrometer. The use of parallel equidistant traverses were yet later introduced (Chayes, 1956). The modern development of the subject begins with Shand. He did not concern himself about the geometrical basis but designed an instrument which for the first time brought modal analysis into practical scientific activity – the recording micrometer (Shand, 1916). The measuring was done by the traversing mechanism of the stage. Calibrated wheels were fitted on two opposed treads and the thin section drawn across the table of microscope by rotation of either tread. At the end of each traverse the dial readings were recorded and at the end of the analysis the differences between successive readings were summed for each dial. Now a full analysis for one constituent at the time could be completed within an hour (Chayes, 1956).
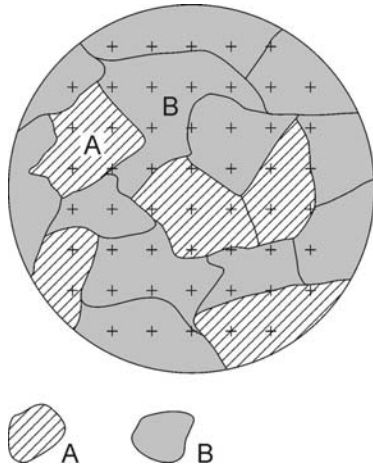
Figure 2-1. Principles of point counting on a two-dimensional surface. The relative amount of points for each constituent reflects the volume fraction of the respective constituent (Figure: Terje Malvik).

2.3.2.2 *Continuous line integrators and point counting*

The later continuous line integrators were all direct descendents of the Shand micrometer stage, however permitting simultaneous analysis of several constituents, motor-driven stage, mechanism for selection of traverses and linkage between tallying and traversing mechanism (Chayes, 1956).

Later the substitution of points for lines in the estimation of areas became common. Point counting is now the classical way to manually estimate the volume fraction of a specific constituent in thin and polished sections (Chayes, 1956; Hetzner, 1998). The principle of point counting is based on the fact that if a point grid is introduced onto a two-dimensional surface, the relative amount of points for each constituent reflects the volume fraction of each constituent, see Figure 2-1. The relationship between volume and fraction of points in a test grid was established both by Thompson and Glagolev in 1930 and 1931, as well as by other subsequent workers in other disciplines. (Chayes, 1956; Hetzner, 1998). The present known stereological relationships have evolved from these works.

Glagolev (1934) introduced the point counter device. The principal of his device is as follows: a prepared specimen is placed on a specially constructed mechanical stage in the microscope and the operator focuses on the phase under the cross-hairs. When the operator presses the key selected for the component that appears at the point, one count is registered on the recording meter. With the pressing of the key the section is automatically shifted a definite distance (Glagolev, 1934). Glagolev also introduces the concept of probable error as a function of amount of constituents and number of points counted.

Even though our optical microscopes have developed since the 1930s, Glagolev's method and a similar kind of counting device are still frequently used

for quantitative measurements of phases and microstructures all around the world. The advantages of this simple device are its low cost and the ease of use. There are naturally limitations when it comes to accuracy, objectiveness and statistical errors. One also has to assume that the material is isotropic, but that applies equally to all kinds of two-dimensional analyses. The most evident progress on recent point counting device is computer-controlled point counting and electronic driving of stage.

As Hetzner (1998) mentions: "Regarding image analysis, point counting will be shown to be equally important. In reality an image analysis system is only a simple point counter. However, when working in conjunction with an electronic computer, highly sophisticated analysis algorithms can be performed rapidly."

Fundamental statistic relations regarding modal analysis by means of point counting involves important properties as the total amount of points as a function of relative error and quantity of minerals. Chayes (1956) has shown that the standard deviation σ, of an estimate p of the probability that a point will lie in the mineral of interest based on n points, is in percentage of the whole:

Standard deviation:

$$\sigma_n = 100 \sqrt{\frac{p(1-p)}{n}} \quad \text{(\%)} \qquad\qquad \textbf{I}$$

If the volume percentage V_i of mineral i is regarded as an estimate for p, the relation can be rewritten:

Standard deviation:

$$\sigma_n = \sqrt{\frac{V_i(100-V_i)}{n}} \quad \text{(\%)} \qquad\qquad \textbf{II}$$

The relative error can be written:

$$E_n = \frac{\sigma_n}{p} * 100 \Rightarrow E_n = \frac{\sigma_n}{V_i} * 100 \quad \text{(\%)} \qquad \textbf{III}$$

When replacing σ_n:

$$n = \frac{10000 * (100 - V_i)}{V_i E_n^2} \qquad\qquad \textbf{IV}$$

Figure 2-2 shows the relationship between the total amounts of points, n as plotted against relative error E_n for several volumes, V_i of phase i. The figure shows that for a certain amount of phase i, the relative error converges against a certain level where increasing the number of points analysed does not further decrease the relative error significantly.
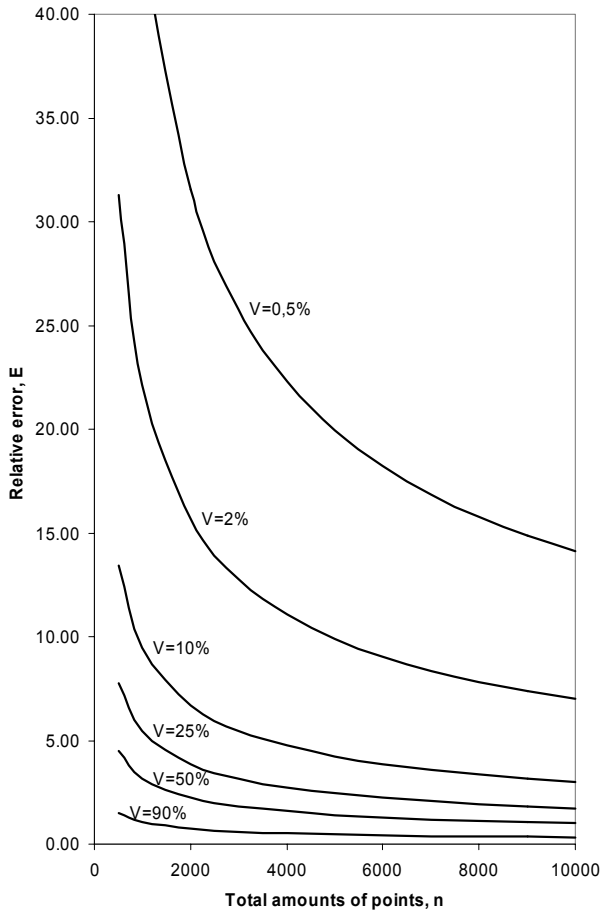
Figure 2-2. Relationship between total amounts of points (n), relative error (E_n) and the volume percentage of phase i (V_i).

2.3.2.3 *Mineral liberation analysis in optical microscope*

To be able to predict how a raw material will behave in a beneficiation process or evaluate the performance of a process by means of the resulting mineral concentrate, a quantification of how the minerals occur in free and composite particles is needed. It is also important to quantify which minerals occur together in composite particles and the nature of intergrowths of the minerals.

When performing such analyses on a ground mineral product, the material has to be split and sieved in narrow fractions. These fractions can then be investigated under the microscope as powder or preferably embedded in epoxy resin in thin or polished sections. Manual mineral liberation analysis is performed by means of the same principle as modal analysis by point counting. Instead of measuring pure phase or microstructure information, a classification of particle type is carried out for every particle analysed by means of a geometric reference system (Malvik, 1976).

The results are generally presented as a function of particle size in the grinding product. As described by Barbery (1991), the procedure was first presented by Gaudin (1939), and is still the basis of most grain counting procedures for liberation assessment. Henley (1983) presents a description of present-day technique: Points falling on each particle during traverses across a plane are counted. The points are decided by means of a mechanical stage or a graticule. The information counted is dependent of the classification categories used, usually based on Amstutz (1961). Amstutz classification system for unliberated grains is found in Figure 2-3. Malvik (1976) used a classification system based on Amstutz where he used the area proportion classifications as follows inTable 2-1:

Table 2-1. Area proportion classification system according to Malvik (1976)

Class	Explanation
Free grain	100% of the mineral, the mineral is apparently liberated
Locked grain 50	Composite particle with an average content of 50% of the mineral of interest, ranging from 20-80% relative amounts
Locked grain 5-20	Composite particles with a major and a minor mineral, the minor mineral occurs in amounts of 5-20% of the particle
Locked grain <5	Composite particle with a major and a minor mineral, the minor mineral occurs in amounts less than about 5% of the particle

Type 1a Simple intergrowth or locking type; rectilinear or gently curved boundaries. Most common type, many examples.

Type 1b Mottled, spotty, or amoeba-type locking or intergrowth. Simple, common pattern; many examples.

Type 1c Graphic, myrmekitic, or "eutectic" type. Common; examples: chalcopyrite and stannite; quartz and feldspars; etc.

Type 1d Disseminated, emulsion-like, drop-like, buckshot or peppered type. Common; examples: chalcopyrite in sphalerite or stannite; sericite, etc. in feldspars; tetrahedrite in galena; etc.

Type 2a Coated, mantled, enveloped, corona-, rim-, ring-, shell-, or atoll-like. Common; examples: chalcocite or covellite around pyrite, sphalerite, galena; etc.; kalyphite rim, and other rims.

Type 2b Concentric-spherulitic, or multiple shell-type. Fairly common; ex.: uranite with galena, chalcopyrite, bornite; cerussite-limonite; Mn- and Fe-oxides; etc.

Type 3a Vein-like, stringer-like, or sandwich-type. Common; ex.: molybdenite-pyrite; silicates; carbonates; phosphates; etc.

Type 3b Lamellae-layered, or polysynthetic type. Less common; examples: pyrrhotite-pentlandite; chlorite-clays; etc.

Type 3c Network, boxwork, or Widmanstatter-type. Less common; ex.: hematite-ilmenite-magnetite; bornite or cubanite in chalcopyrite; millerite-linneite; metals; etc.

Figure 2-3. Amstutz' (1961) classification system for composite particles.

GRID

CROSS HAIRS

BINOCULAR MICROSCOPE
Powder

POL. MICROSCOPE
Section
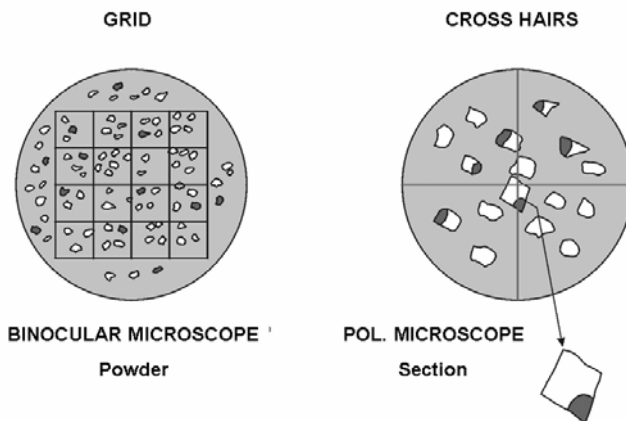
Figure 2-4. Reference systems for mineral liberation analysis (Figure: Terje Malvik).

17

To be able to perform a statistically valid analysis, a reference system such as points or grids as shown in Figure 2-4 is needed.

This kind of analysis has today been more or less replaced by an automatic image analysis system based on optical or scanning electron microscopes, but it can nonetheless be carried out as an indicative and cost-effective method. The greatest advantage of manual liberation analysis is the knowledge and feeling the researcher gains about the material. Even though manual systems possess several limitations, some knowledge and visual judgements are lost with the automation process. Manual inspection in an optical microscope to get to know the material should never be excluded, though. Historical and elementary methods are still important as part of a mineralogical study, along with the automatic and advanced techniques. A skilled mineralogist is therefore still needed for doing the setups, evaluating the performance of the analysis and the results.

2.3.3 Automatic Image analysis

2.3.3.1 *General*

Once the principle of analysing plane sections of mineral particles had become accepted for liberation analysis, the application of automatic techniques instead of human methods was the certain second step (Barbery, 1991). Automatic analysis of digital images within all ranges of disciplines is known as image analysis (IA).

As observed by Lastra, et al. (1998): "Image analysis has greatly increased the accuracy and reliability of quantitative mineralogical data." The materials analysed are generally heterogeneous and contain many phases. To get statistically valid quantitative data, many thousands of particles have to be analysed. Hence, automatic and unattended image analysis is desirable for performing mineralogical analysis.

The age of automation started back in 1963 as the first analysis system to use a television camera as the input device was developed. This system was made by Metals Research Ltd., Cambridge, England, which was the predecessor of Leica (Hetzner 2003). A more detailed description of the development of these systems is provided by Hetzner (1998) as well as Henley (1983).

2.3.3.2 *Image analysis system*

An image analysis system for automatic mineralogical analysis consists principally of the following components (Lastra et al., 1998):

- An imaging unit (optical microscope with a camera, scanning electron microscope (SEM) or microprobe (EPMA));
- A motorised stage that can be moved precisely with software in the x and y direction;
- An image analyser that includes calibrated image acquisition.

2.3.3.3 *Procedure for image analysis*

An image analysis is generally performed by carrying out the following operations (Barbery, 1991; Lastra et al., 1998; Russ, 2002):

- Image acquisition: Image acquisition can be obtained by an analogue or digital video camera or a digital camera on the microscope or a SEM/EPMA. Image analysers allow acquisition of images in several digital formats, for example 256x256, 512x512 or 1024x1024. The image analyser has to be calibrated so that each format has a geometric scale;
- Image enhancement: The images can be improved by applying different filters for enhancing the contrast and brightness, to get rid of biased illumination, and to smooth the grey-levels, reduce noise and sharpen the edges;
- Segmentation: Discrimination   of   mineral   grains   is   done   by segmentation of grey-levels into binary images. This can be done interactively by setting the lower and upper value for each maximum of the grey-level histogram, see Figure 2-5. If there is more than one grey-level or colour of interest; more windows have to be set.
- Feature identification: In optical systems, the operator has to know which minerals correspond to a grey-level or a colour. In the electron optic systems, several signals are generated by the primary electron beam and more signals might therefore be applied. X-ray information can then be combined with the image information to identify the minerals or phases.
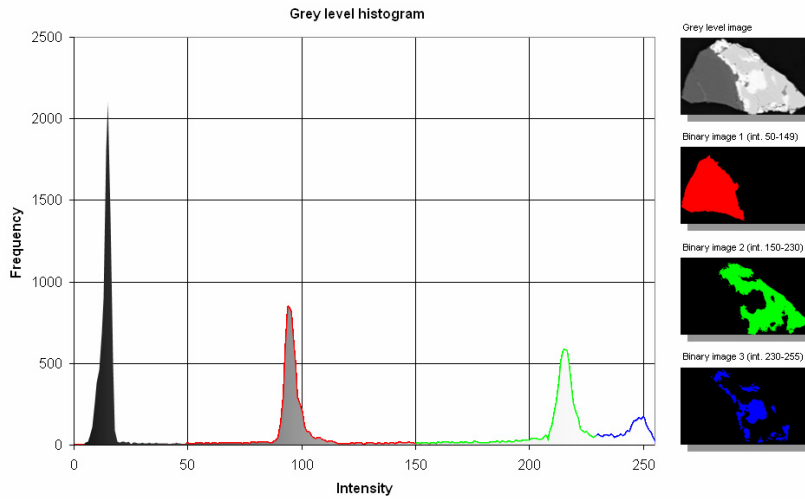
Figure 2-5. Principle of segmentation of grey-levels in a grey-level image.

- Binary operations: Usually, binary operations have to be performed on binary images of mineral particles before measurements can take place. These are mathematical morphological analyses including image erosion, dilatation, skeletonization and other concepts, in addition to the use of Boolean binary logic (Hetzner, 1998). Erosion removes pixels from a feature, dilatation adds pixels while skeletonization removes all pixels but the skeleton of features. Boolean logics are used to combine images. Typical reasons for applying binary operations to particles embedded in epoxy resin are small artefacts that do not represent minerals, touching particles that can be misidentified as one particle, particles which are bigger or smaller than the fraction that has been selected, particles that cross the frame of the image etc.

- Measurements: Several parameters can be measured and used to characterise particles by image analysis. There are two types of measurements that are common to all IA systems. These are field-specific and object-specific measurements where field-specific measurements only allow the measurement of one given parameter for the overall field. Examples are total area or total perimeter for all structural elements. Object-specific measurements consist of measurements for each identified structural element (Hetzner, 1998;

20

Malvik, 1991) and includes parameters as area, perimeter, equivalent circle diameter etc.

- Data analysis: In the end, the data obtained have to be analysed according to the scope of the work carried out. Typically these analyses include: tables and plots for mineral quantities, size distributions, shape factors, mineral liberation tables and mineral association tables and diagrams.

Image processing and analysis is more thoroughly described and discussed in Chapter 5.

2.3.4 Automated Scanning Electron Microscope based Mineral Liberation systems

2.3.4.1 *General*

Quantitative descriptions of mineralogy and textures are important subjects in applied mineralogy. Manual methods and image analysis in the optical microscope are cheap and appropriate for many purposes, but in general a more advanced method is needed especially when studying complex or trace mineralogy, fine particles or e.g. silicates and carbonates that can not be uniquely defined by image analysis in the optical microscope. It is then favourable to turn to an automatic scanning electron microscope (SEM) based image analysis system (Barbery, 1991; Moen et al., 2003).

As described by Barbery (1991) Jones developed the concept that minerals could be identified automatically in the SEM or Microprobe in the 1970s (Barbery, 1991; Jones, 1987; Jones and Gravilovic, 1970).

The two types of signals most appropriate for this application are:

- *Back Scattered Electrons (BSE):* The amount of electrons elastically backscattered is dependent on the average atomic number of the phases scanned by the primary electron beam.
- *Characteristic X-ray*s: Inelastic scattering of the beam electrons can ionize the atoms in the sample, which can lead to the emission of characteristic x-rays which again provide information about chemical composition (Goldstein et al., 1992).

Several systems have been developed for mineral liberation (Butcher, 2004; Gottlieb et al., 2000; Gu, 2003; Jones, 1987; King, 1993; Lastra et al., 1998; Petruk, 2000; Pignolet-Brendom and Reid, 1988). Recent advances, particularly

in computer technology, have made fast and user-friendly mineral liberation systems possible (Gu, 2003).

Stable backscattered electron (BSE) signals from a modern SEM can be used to generate images from the sample from which the most important minerals can be quantified using modern image analysis methods. Each grain outlined from BSE images can be identified with x-ray analysis, either positioned at the centre of the grain or collected from scanning the whole grain. Minerals of similar BSE intensities can be discriminated using x-ray mapping (Gu, 2003, 2004).

2.3.4.2 *Systems*

Barbery (1991) tries to summarise the *state-of-the-art* and mentions most systems and suppliers, however some changes have naturally occurred during the last 15 years.

- The system developed by Jones at Imperial College, London, UK, represents the introduction of the concepts of linear image analysis, in which line scans are made by moving the polished section under the beam of an Electron Microprobe (Jones, 1987; Jones and Gravilovic, 1970; Jones and Horton, 1979). Four wavelength dispersive x-ray analysers are used for primary data collection, and mineral identification and discrimination are based on combination of signals from the four spectrometers (Barbery, 1991).

- The system developed by Petruk (1989; Petruk, 2000) is called MP-SEM-IPS, an acronym for Microprobe - Scanning Electron Microscope - Image Processing System. The system was put together at CANMET, Ottawa, Canada, which is a part of Natural Resources Canada, Mining and Mineral Sciences Laboratories and consists of a microprobe, fitted with an energy dispersive x-ray analyser and an image analysis system from Kontron (Hetzner, 1998). An analysis is performed by setting up the BSE grey-level ranges of all the different minerals. For minerals with overlapping grey-levels, EDS is used to establish detectable differences by x-ray count rates and x-ray mapping. Image analysis and arithmetics are then performed on the BSE images and the x-ray dot maps to discriminate the different minerals and perform mineral liberation analysis (Lastra et. al. 1998).

- The MLA system developed by Gu and his crew at the Julius Kruttschnitt Mineral Research Centre, JKMRC, at the University of Queensland, Australia (Gu, 2003, , 2004) is also based on BSE image analysis and mineral discrimination by x-ray analysis. The problem of touching particles is initially overcome by an automated de-agglomeration function that removes the background and uses particle shape to evaluate if a particle is agglomerated. The de-agglomeration process has different break-up strategies. The MLA image segmentation function then outlines grains of more or less homogeneous grey-level in every particle image. Overlapping and similar grey-levels for the minerals are solved with x-ray analysis. The MLA system typically performs one x-ray analysis for each grey-level region in a particle. If two minerals have similar grey-levels but different chemical composition, x-ray mapping is used. However x-ray mapping is more time consuming, and avoided when grey-levels are unique (Gu, 2003).
- The Particle Texture Analysis (PTA) system developed at Norwegian University of Science and Technology (NTNU) (Moen et al., 2006) is based upon the same principals as the former, but uses commercial software for data acquisition. The BSE image is segmented using grey-levels and overlapping and similar grey-levels for the minerals are solved with x-ray analysis. This part of the system is based on the Oxford Instruments Inca Feature software. The database and the images are then post-processed off line by the PTA software that performs mineral liberation and mineral association analysis using image analysis and x-ray information from the database.
- The QEMSEM system developed over more than 20 years by the division of Mineral and Process Engineering of CSIRO in Australia is based on a different concept. It has been the object of a number of papers since the initial paper of Grant and his crew. presented the concept in 1976 (Barbery, 1991). The system has now been transferred to an independent company, Intellection, continuing the technology through the QEMSCAN and some related products. The system consists of a SEM equipped with four x-ray detectors. The principle of the QEMSCAN technology is to image the particles by means of the BSE signal, perform image analysis to outline each particle to make

individual images of them. QEMSCAN then identifies the mineral present at each point inside these images by rapidly collecting an energy dispersive x-ray spectrum that is analysed to give the chemical composition in every point (Butcher, 2004; Gottlieb et al., 2000).

The work of the research group at Imperial College seems to have ceased while the group at CANMET Mining and Mineral Sciences Laboratories in Canada is still active both in research and assisting clients in the mining industry. Currently both MLA and QEMSCAN provide commercial research, consulting and image analysis systems. Additionally, there exist several software programs for particle analysis, but none of them can currently provide the same kind of data that the established research groups can.

The two Australian systems have different advantages depending on the application area. This is confirmed by the fact that big research centres like that of Anglo Platinum in South Africa have invested in both instruments. These are providing analysis for different purposes. While the MLA is used for rare mineral searches, the QEMSCAN is used for detailed quantification of the process material. Nevertheless, QEMSCAN has an advantage in detailed particle mapping while MLA leads in speed and fitting the efforts to the category of investigation. QEMSCAN also has an advantage when it comes to quantification of whole rocks where no background can be removed. The biggest disadvantage of both of these systems is the investment cost, the commitment to one SEM and EDS contractor system and the dedication of use. Many laboratories have to deal with a range of research activities and are already equipped with a certain scanning device and EDS system. The Feature/PTA system has an advantage when it comes to flexibility and cost, but is at the moment a simpler version. For most cases it provides valid information and the system is still being improved. The speed is slower since it depends on a standard semi-quantitative EDS system, but for many laboratories, the chance to perform a mineral distribution or liberation analysis at a reasonable cost is probably more important than the speed. Both Australian systems have recently started to disengage from specific instrument contractors, and it may be possible to buy software rather than a big and expensive system.

2.3.5 Analytical procedures

The data quality obtained from microscopy analysis is always at the mercy of the sampling strategy. To obtain statistical valid results for the population investigated, some analytical procedures have to be followed. Common analytical procedures for image analysis and statistical considerations including stereology are presented in Chapter 5.

2.3.6 Summary and future potential

As stated in the introduction 2.3.1, this section aims to review the options regarding automatic quantification of mineral texture by microscope techniques including both historical perspectives and focus on the *state-of-the-art* techniques. The review can be summarised as follows:

- Manual and elementary methods are still important as a part of a mineralogical study along with automatic and advanced methods. Manual microscopy in the optical microscope is cost-effective and gives valuable qualitative knowledge about the material studied.
- To get a statistically valid quantitative dataset for a material containing several minerals, automatic image analysis should be used. Image analysis has an advantage compared to indirect bulk analysis mentioned in the introduction, because of its ability to visualise the microstructures and to quantify how the minerals occur in free and composite particles.
- To be able to identify fine particles and to a greater extent be able to discriminate between minerals, the use of an automatic SEM based image analysis system is recommended. Several concepts have been developed and some of them are commercially available. The main principle is the use of the BSE signal and the characteristic x-ray signal together with image analysis and automation procedures. The latest improvements in electronic and computer technology have made fast and user-friendly mineral liberation systems possible.
- If the analytical procedures are not followed and the samples analysed are neither representative nor isotropic the data quality will be poor.

- Future trends in the quantification of applied mineralogical properties will probably be based on flexible systems that can by adapted to any kind of instruments.

- The most important improvements in the future will most probably be systems that combine BSE signals, characteristic x-ray signals and electron backscatter diffraction (EBSD) signals. This allows for three approaches in assessing the mineralogy: average atomic number, chemical composition and crystallographic properties. Such an approach will definitely be an improvement over the existing techniques.

- Three dimensional systems may be the solution in the future, but still there is a lack in techniques resolving the microfabrics as well as in measure procedures. Dual beam microscopy consisting of a SEM and a focused ion beam (FIB) can be used for eroding the sample while analysing, but the erosion is slow and is best fitted for small areas. X-ray tomography can be used for tree-dimensional mapping of pore space and coarse structures, but will not resolve fine structures. Nuclear magnetic resonance (MR) techniques are used as a standard well logging tool in the petroleum industry. MR imaging is also used for investigating porosity distributions. These techniques have potential for some applications, but are too coarse for mineralogical and microstructure investigations.

2.4 **REFERENCES**

Amstutz, G. C., 1961, Microscopy applied to mineral dressing, Colorado School of Mines Quat., 443-482 p.

Barbery, G., 1991, Mineral liberation: measurement, simulation and practical use in mineral processing: Quebec, Canada, Les Editions GB, 351 p.

Butcher, A., 2004, Automation, Integration and Interpretation - the Future for Process Mineralogy and Practising Mineralogists: 8th International Congress on Applied Mineralogy, ICAM 2004, Sao Paulo, Brazil, 2004.

Chayes, F., 1956, Petrographic Modal Analysis: New York, John Wiley & Sons, Inc., 113 p.

Delesse, A., 1848, Procédé méchanique pour déterminer la composition des roches: Ann, mines, v. 13, p. 379-388.

Gaudin, A. M., 1939, Principles of mineral dressing: New York, McGraw Hill.

Glagolev, A. A., 1934, Quantitative analysis with the microscope by the point method: Eng. Mining J, v. 135, p. 399-400.

Goldstein, J. I., Newbury, D., Echlin, P., Joy, D., Romig, A. D., Lyman, C., Fiori, C., and Lifshin, E., 1992, Scanning Electron Microscopy and X-ray Microanalysis: New York, Plenum Press, xviii, 820 p.

Gottlieb, P., Wilkie, G., Sutherland, D., Ho-Tun, E., Suthers, S., Perera, K., Jenkins, B., Spencer, S., Butcher, A., and Rayner, J., 2000, Using Quantitative Electron Microscopy for Process Mineral Applications: JOM Journal of Metals, v. 52, p. 24-25.

Gu, Y., 2003, Automated Scanning Electron Microscope Based Mineral Liberation Analysis: Journal of Minerals & Materials Characterization & Engineering, v. 2, p. 33-41.

Gu, Y., 2004, Rapid Mineral Liberation Analysis with X-ray and BSE Image Processing: 8th International Congress on Applied Mineralogy, ICAM 2004, Sao Paulo, Brazil, 2004, p. 119-122.

Henley, K. J., 1983, Ore dressing mineralogy - a review of techniques, applications and recent developments: 1st ICAM, Hohannesburg, South Africa, 1983, p. 175-200.

Hetzner, D. W., 1998, Quantitative Image Analysis, Part 1 Principles: Buehler's "Tech-Notes", v. 2, p. 5.

Jones, M. P., 1987, Applied mineralogy: a quantitative approach: London, Graham & Trotman, 259 p.

Jones, M. P., and Gravilovic, J., 1970, Automatic quantitative mineralogy in mineral technology: Rudy, v. 5, p. 189-197.

Jones, M. P., and Horton, R., 1979, Recent developments in the stereological assessment of composite (middling) particles by linear measurements: XIth CommonwealthMining and Metallurgical Congress, London, 1979, p. 113-122.

King, R. P., 1993, Basic image analysis for mineralogy, ICAM'93 Demonstration Workshop Manual, p. 119-139.

Lastra, R., Petruk, W., and Wilson, J., 1998, Image-analysis techniques and application to mineral processing, *in* Cabri, l. J., and Vaughan, D. J., eds., Modern Approaches to Ore and Environmental Mineralogy, 27. Short Course Series: Ottawa, Ontario, Mineralogical Association of Canada, p. 327-366.

Malvik, T., 1976, En undersøkelse av malmmineralers frimalingsegenskaper, NTH, 276 p.

Malvik, T., 1991, Partikkelkarakterisering ved bruk av bildeanalyse: Konferens i Mineralteknik, Luleå, 1991.

Malvik, T., 2005, Project description; Background for the programme, Strategic University Programme(SUP) "The value chain from mineral deposit to beneficiated product with emphasis on quartz": Trondheim, NTNU.

Moen, K., Malvik, T., Breivik, T., and Hjelen, J., 2006, Particle Texture Analysis in Process Mineralogy: XXIII IMPC 2006, Istanbul, Turkey, 2006.

Moen, K., Malvik, T., Hjelen, J., and Leinum, J. R., 2003, EBSD-A Potential Supplementary Technique in Quantitative Characterisation of Minerals: XXII IMPC, Cape Town, South Africa, 2003.

Petruk, W., 1989, The Capabilities of the Microprobe Kontron Image Analysis System: Scanning Microscopy, v. 2, p. 1247-1256.

Petruk, W., 2000, Applied Mineralogy in the Mining Industry: Ottawa, Ontario, Canada, Elsevier, 268 p.

Pignolet-Brendom, S., and Reid, K. J., 1988, Mineralogical characterization by QUEM*SEM, *in* Carson, D. J. T., and A.H., V., eds., Process Mineralogy VIII: Warrendale, PA, TMS, p. 337-346.

Rosiwal, A., 1898, Ueber geometriches Gesteinanalysen usw.: Verh. der k. k. Geolog. Reichsanstalt Wien, p. 143-175.

Russ, J. C., 2002, The Image Processing Handbook: Raleigh, CRC Press, 732 p.

Shand, S. J., 1916, A recording micrometer for rock analysis: Journal of Geology, v. 24, p. 394-403.

<div align="right">

3.   CHAPTER

Experimental overview

</div>

3.1   INTRODUCTION

The doctoral project has been highly experimental and has included development and implementation of software and techniques in addition to case studies of several geological materials. In the following sections, overviews of the samples studied and the experimental equipment used in the various papers are displayed.

3.2   SAMPLES

In Table 3-1 the main samples analysed in Papers 1-5 and the main methods used to study them, are listed. All samples are either thin-sections, polished sections or polished thin-sections. The samples studied by the EBSD technique were chemical-mechanically polished in addition to standard preparation techniques (see Chapter 4.3.6.3) to remove surface damage. These samples were not carbon-coated but rather investigated in a low-vacuum microscope.

Table 3-1. Samples analysed in Papers 1-5 accompanied with main methods used.

Paper	Sample	Material	Methods
1	Normal feed	Normal feed, ilmenite ore 63-212 μm	PTA-analysis
1	Normal conc.	Normal lab. conc. of ilmenite 63-212 μm	PTA-analysis
1	Feed 1	Anomalous feed, ilmenite ore 63-212 μm	PTA-analysis
1	Conc. 1	Anomalous lab. conc. ilmenite 63-212 μm	PTA-analysis
1	GCC tailings	Fractions of a tailings stream of GCC	PTA-analysis
1	Quartz feed	Fractions of high purity quartz feed	PTA-analysis
2	Ilmenite oree	Ilmenite Norite from Tellnes, Norway	EBSD
2	Olivine	Dunite form Åheim, Norway	EBSD
2	Iron ore	Hematite/magnetite ore from Rana, Norway	EBSD
2	Marble	Carrara marble	EBSD
3	Itq1	Carrara marble	EBSD
3	Itq2	Carrara marble	EBSD
4	Marbles	25 marbles form around Europe	OM, IA, CL, BSE
5	3185 (A)	Reservoir sandstone with quartz cement	OM, PC, IA, CL, BSE
5	4205(A)	Reservoir sandstone with quartz cement	OM, PC, IA, CL, BSE
5	5040(B)	Reservoir sandstone with quartz cement	OM, PC, IA, CL, BSE
5	5243(C)	Reservoir sandstone with clay lamina	OM, PC, IA, CL, BSE

PTA=Particle Texture Analysis, EBSD=Electron Backscatter Diffraction, OM=Optical microscopy, PC=Point counting, IA=Image analysis, CL=Cathodoluminescence, BSE=Backscatter electrons

3.3 **SCANNING ELECTRON MICROSCOPES**

The different microscopes used in Papers 1-5 are listed in Table 3-2.

Table 3-2. Microscopes used in Papers 1-5.

Paper	Technique	Microscope type	Microscope	Comments
4, 5	Optical	Polarisation microscope	Nikon Eclipse E600	Equipped with 2 mega-pixel digital camera
1	PTA	Field Emission SEM	Hitachi S-4300SE	Stable, high resolution
2, 3	EBSD	Low vacuum SEM	Hitachi S-3500N	Non-conductive samples
2	EBSD	Conventional SEM	JEOL 840	

3.4 **PARTICLE TEXTURE ANALYSIS (PTA)**

The PTA system is programmed in a graphic language (LabVIEW) from National Instruments (NI), using structured query language (SQL) towards databases (Access), and NI Vision library for image processing and analysis. The data acquisition is based on Oxford Inca Feature which is compatible with PTA. The equipment used for PTA is listed in Table 3-3, typical SEM settings during data acquisition are found in Table 3-4 and typical image- and x-ray-settings are found during data acquisition are displayed in Table 3-5.

Table 3-3. Equipment applied for PTA analysis.

Equipment	Type
Field Emission SEM	Hitachi S-4300SE
EDS detector	Oxford SiLi light element detector
Acquisition software	Inca Feature (© Oxford Instruments Analytical Limited)
Post-processing	PTA (© NTNU) Programmed in LabVIEW using SQL towards Access databases

Table 3-4. Typical SEM settings during PTA analysis.

Parameter	Setting
Working distance	15 mm
Accelerating voltage	20 kV
Gun brightness (extr. voltage)	1.9 kV
Aperture	2 (50 μm) and 3 (30 μm)
Beam current	0.25-0.75 nA
Magnification	40-600x

Table 3-5. Typical BSE image and x-ray acquisition settings.

Parameter	Setting
Resolution	1024*896 pixels
Image dwell time	20 microseconds/pixel
Smallest features	20 pixels
Grey image processing	Median filter, 3x3 matrix, rank 4
Binary processing	Separation
X-ray live time	0.5-2 sec
X-ray process time	4-5 (medium-high)

3.5 **ELECTRON BACKSCATTER DIFFRACTION (EBSD)**

For EBSD analysis, the TSL OIM software has been used (© Edax) with the exception for dunite in Paper 2, which was analysed by a JEOL 840 equipped with HKL Channel 5. Table 3-6 summarises the equipment used for EBSD analysis and Table 3-7 summarises the main running and processing conditions during analysis.

Table 3-6 Equipment applied for EBSD mapping

Equipment	Type
Low-vacuum SEM	Hitachi S-3500N
EBSD camera	Nordif CD200 EBSD dig. camera
EBSD software	TSL, OIM

Table 3-7 Running and processing conditions for EBSD mapping

Parameter	Setting
WD	20 mm
V_{acc}	20 kV
Pressure	<50 Pa
Tilt	70°
Binning	2x2
Step size	1-50 μm
Pole figure processing	Gaussian convolution Half with 15° Expansion L=22 Harmonic calculus

Scanning Electron Microscopy

4.1   GENERAL INTRODUCTION

This doctoral project has been developed under the working title "Advanced Characterisation of Minerals" and the project initial phase and funding resulted in the purchase of two modern scanning electron microscopes (SEM) at the lab of Department of Materials Science and Engineering in cooperation with Department of Geology and Mineral Resources Engineering. Developing the expertise and possibilities regarding characterisation and quantification of minerals using signals generated by an electron beam has therefore been the main focus of this thesis. When characterising a material, bulk chemical analyses are fundamental for obtaining information about the material. To obtain information about how the minerals occur however, one has to turn to microscopy. Optical microscopy is always important as a first approach; this thesis, however, is mainly focused on the possibilities available when using signals in the scanning electron microscope. In the SEM several signals can be

combined to obtain the appropriate information. This chapter will therefore cover the main principals of the SEM techniques.

4.2   **SCANNING ELECTRON MICROSCOPY**

4.2.1   Principle

The scanning electron microscope is a valuable instrument when heterogeneous materials are to be characterised on a micro-scale. The area investigated is scanned by a thin focused electron beam. The beam can be stationary or scanning a raster over the sample surface. When the focused beam hits the sample surface, it gives rise to several signals that can be detected. The signals are illustrated in Figure 4-1, and can give information regarding chemical composition, topography, crystallography, average atomic number and others. The most common signals detected in SEM are x-rays, backscattered and secondary electrons (Hjelen, 1989).

Goldstein et al. (2003) divide the SEM into two major components consisting of an electron column and a control console. The schematic sketch in Figure 4-2 is according to Hjelen (1989). He describes the principle as follows: The electrons from filament F are accelerated through a potential field that can vary between 1-40 kV. The electrons go through a column consisting of magnetic lenses. L_1 and L_2 are condenser lenses, while L_3 is the objective lens (some instruments only contain L_1 and L_3). Focusing the narrow electron beam on the specimen surface (S) is the main purpose of the lenses. The column and the specimen chamber are set under extreme vacuum in the range of 10^{-3} Pa (equals 10^{-5} Torr) for conventional filaments, down to 10^{-8} for field emission guns and in a variable pressure microscope non-conductive specimens can be studied up to 250 Pa (and even up to 2700 Pa in E-SEM). The scanning coils (SC) are often placed between lens 2 and 3 and provide the electron beam to scan a raster of the specimen surface analogue to an electron beam scanning a TV screen. The current through the scan coils also goes through the corresponding deflection coils in a cathode ray tube (CRT) such that a corresponding, but bigger raster on the fluorescent screen (CRT) is obtained. Today most CRTs are replaced by LCD screens. When the electron beam hits the specimen, secondary electrons will be liberated from the sample surface. Some of these go to a collector (C). The electron current is amplified and the signal is used to modulate the light

intensity on the screen. It is now a one-to-one-correspondence between the number of secondary electrons from a unique point on the specimen and the light intensity on the corresponding point on the screen. Large magnifications are now easy to obtain while small magnifications are more difficult because of the deflection angle of the beam (Hjelen, 1989).

The most important variables that affect the resolution and the performance are accelerating voltage of the electrons, beam current, aperture size and the working distance between the specimen and the objective lens.
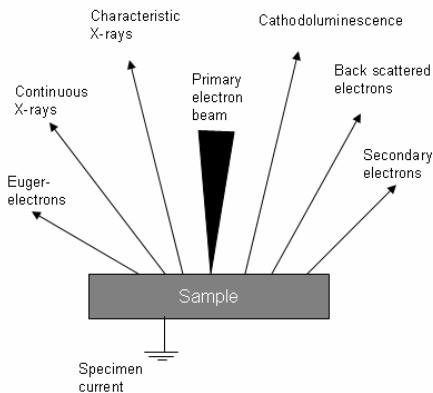
Figure 4-1. Signals that can be detected in a scanning electron microscope (based on Hjelen, 1989)
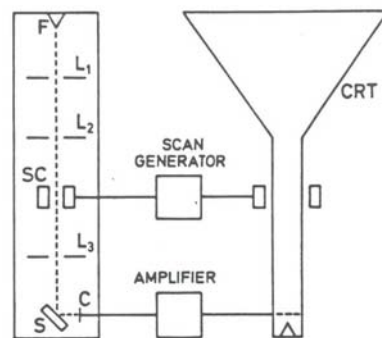
Figure 4-2. Schematic sketch of a SEM (based on Hjelen, 1989)

4.2.2 Microscopes

There exist some different types of scanning electron microscope devices. The main types are:

- Conventional SEM with W-hairpin or LaB_6 filament
- Low vacuum / variable pressure / environmental SEM where the microscope can be run with gas or vapour in the specimen chamber at a pressure from 10-2500 Pa. This arrangement results in an instrument where biological tissue, oil saturated reservoir rocks or insulating specimens can be studied.
- Field emission microscopes where the gun is a sharpened W single crystal which is optimised for high resolution microscopy.

The performance and properties of the different device is further discussed by Goldstein et al. (2003).

4.2.3 Preparation of geological samples in SEM analysis

Sample preparation is vital when doing SEM analysis. If the sample is not well prepared the result will never be successful. Skills within this area are therefore vital for any research laboratory. Important references concerning preparation of geological samples are Lloid (1985), Prior et al. (1999) or Goldstein et al. (2003).

4.2.4 Signals

4.2.4.1 *Backscattered electrons*

Backscattered electrons (BSE) provide an extremely useful signal for imaging in scanning electron microscopy (Goldstein et al., 2003) and is a basis for the PTA system described in Chapter 6. A significant fraction of the incident electron beam is elastically scattered by single or multiple scattering events in which the electron trajectory is changed by more than 90°. The electrons are then able to propagate back to the detector usually placed under the objective lens (Goldstein et al., 1992). To be able to interpret the image generated by BSE, it is necessary to understand the properties of BSE as a function of signal parameters and the specimen characteristics.

The most important property of BSE is the fact that the backscatter coefficient is atomic number dependent. The backscatter coefficient is defined as

$$\eta = \frac{n_{BSE}}{n_B} = \frac{i_{BSE}}{i_B} \qquad\qquad \mathbf{I}$$

where n_B is the number of beam electrons incidentally hitting the specimen and n_{BSE} is the number of backscattered electrons. The coefficient can also be expressed in terms of currents. The fraction BSE increases along a polynomial function as the average atomic number increases (Figure 4-3). This correlation makes the BSE signal good for compositional imaging displaying Z-contrast.

Other important variables influencing the BSE signal are accelerating voltage, especially influencing the interaction volume from where BSEs are generated (see Figure 4-9), and the tilt angle of the specimen which will influence

marginally the magnitude of the backscatter coefficient but considerably the EBSD pattern. (Goldstein et al., 2003; Hjelen, 1989).

4.2.4.2 *Secondary electrons*

Secondary electrons (SE) are defined as emitted electrons with less energy than 50 eV. As explained by Goldstein et al. (2003) they are generated as a result of interaction between high energy holding primary electrons and loosely bound outer shell electrons from the specimen atoms. These receive sufficient kinetic energy during inelastic scattering of the beam electrons to be ejected from the atom and set in motion. These will propagate through the solid and some will escape through the surface (Goldstein et al., 2003). SEs are generated both from primary electrons (type I) and backscattered electrons (type II). In contrast to the backscatter coefficient, the similar coefficient for SE, δ, is not systematically dependent on the average atomic number (Figure 4-3). An important property of SEs, on the other hand, is that they are generated from a very small emission volume (Figure 4-9). This is because of the low kinetic energy and leads to a very good resolution for SE imaging (Goldstein et al., 2003; Hjelen, 1989). The good resolution of the SE signal and the high speed of the SE detector make this signal practical to use for sample navigation, focusing and beam optimisation even when other signals are to be used during analysis. SE imaging is also useful for studying topography since the number of SEs generated is strongly influenced by the angle of the sample surface.
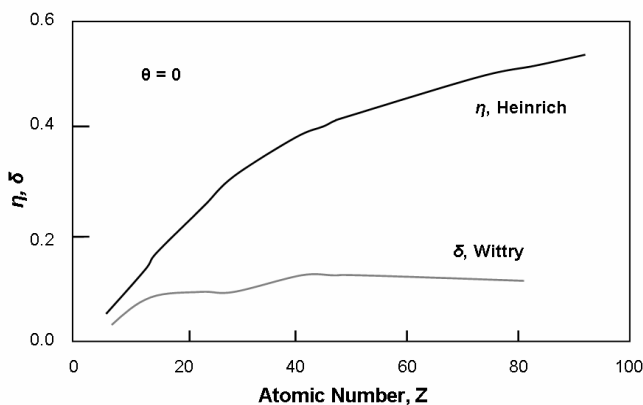
Figure 4-3. Comparison of backscattered (η) and secondary (δ) electron coefficients as a function of atomic number, E_0=30 keV [After data of Wittry (1966) and Heinrich (1966)] (based on Goldstein et al., 2003).
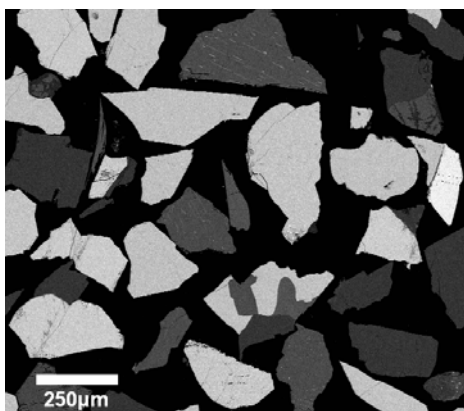
Figure 4-4. BSE image of a polished section of mineral particles from an ilmenite ore (Photo: Kari Moen).
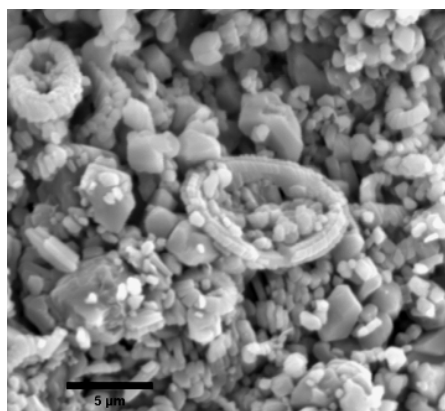
Figure 4-5. SE image of the upper cretaceous chalk deposit, Flamborough Head, Yorkshire (Photo: Kari Moen).

4.2.4.3 *Cathodoluminescence*

As described by Reed (2005), in non-metallic material incident electrons cause excitation by rising electrons in the valence band to the normally empty conduction band, from which they return to their original state in one or more steps. The surplus energy can be dissipated in various ways, one of which is the emission of photons. Only energies of a few electron volts are involved and the wavelengths fall within the visible region, occasionally extending into ultra-violet and infer-red. This radiation is referred to as cathodoluminescence (CL). Examples of minerals that exhibit CL include diamond, quartz, corundum, rutile, fluorite, spinel, calcite, dolomite, apatite, sphalerite, zircon, feldspar, diopside, wollastonite, forsterite and fayalite (Reed, 2005). What play an important role in CL emission are localised energy levels in the gap between valence and conduction bands arising from lattice defects, interstitial ions or substitutional impurity atoms (Reed, 2005). Certain elements behave as 'activators' others have the effect of 'quenching' CL emission. Some forms of CL are also influenced by density of defects which in turn is dependent of temperature of formation, cooling rate, deformation and irradiation. The colour of CL emission depends on the difference in energy between states concerned. The colour is commonly not narrowly defined but takes place over a band (Reed, 2005). Because of the complexity of the factors involved, absolute information is problematic using CL emission; but nevertheless, information not easily

obtained by other means in a range of geological applications is especially interesting when studying generations of a mineral, provenance studies or deformation. As explained by Reed (2005) CL can also be observed with an optical microscope fitted with a relatively simple device where the specimen is bombarded by a broad electron beam. The advantage is the possibility to image the emission by a colour camera while the drawbacks are both the high current that can damage the specimen and lower resolution and magnification (Reed, 2005). When it comes to resolution and interaction volume, the CL signal has poor resolution compared to the previously described SEM signals, exceeding also the x-ray signal.

CL imaging is used in Paper 5 to discriminate the detrital quartz grains from the diagnetic quarts overgrowths as shown in Figure 4-6. The technique is also extensively applied by the other doctoral candidates within the SUP project (e.g. Jacamon and Larsen, 2005; Sørensen et al., 2005) to study generations and deformation of quartz, see for example Figure 4-7.
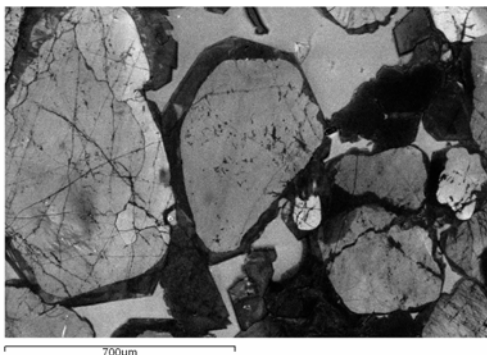
Figure 4-6. CL emission image of quartz sandstone where the detrital quartz grains illuminate while the later cement shows no CL emission (Photo: Kari Moen).
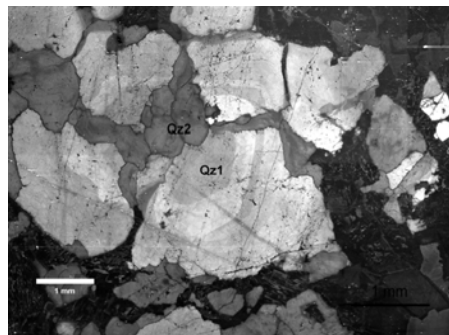
Figure 4-7. CL emission of igneous quartz from the Oslo rift. Qz1 is bright primary quartz with oscillatory growth zoning while Q2 is new quartz precipitated from fluids (with permission from Jacamon and Larsen, 2005).

4.2.4.4 *Generation of X-Rays*

Chemical analysis by means of characteristic x-rays in SEM or microprobe is a central technique in applied mineralogy and in the PTA technique. It is therefore

important to have a certain insight to the generation and the variables influencing the generation and detection of x-rays.

Goldstein (2003) describes the situation when primary electrons undergo deceleration in the electrostatic field of the specimen atoms, x-rays radiation forming a continuous electromagnetic spectrum is generated. This radiation is referred to as "Bremsstrahlung". The loss of electron energy ΔE that occurs is emitted as a photon. The energy of this photon is $\Delta E = h\nu$, where h is Planck's constant and ν is the frequency of the electromagnetic radiation (Goldstein et al., 2003). Photons of all energies up to the original energy of the incident beam E_0, will be emitted. This continuous x-ray radiation is an unwanted background radiation which limits the characterisation of the chemical composition of the specimen.

Characteristic x-rays are the result of the interaction between the beam electron and the tightly bound inner shell electrons of a specimen atom, ejecting an electron from a shell. The electrons of the specimen atom is found on discrete energy levels (K-, L-, M-shell) given from the quant numbers for the atom. When the primary electrons have enough energy to knock out electrons and ionise the atom, the atom is left in an excited state with a missing inner shell electron. The atom relaxes to its ground state within approximately 1 ps through a limited set of allowed transitions of outer shell electron(s) filling the inner-shell vacancy. The energy differences between electron shells is a characteristic value for each element and the excess energy can be released from the atom during relaxation in one of two ways, either through the Auger process or the x-ray process. In the Auger process the difference in the shell energies can be transmitted to another outer shell electron, ejecting it from the atom as an electron with a specific kinetic energy. In the characteristic x-ray process, the difference in energy is expressed as a photon of electromagnetic radiation which has a sharply defined energy (Goldstein et al., 2003). For low atomic numbers the Auger process is favoured, while for the high atomic numbers the x-ray process is favoured. Detection of characteristic x-ray photons are therefore evidence for the presence of the corresponding elements in the specimen (Hjelen, 1989). Several transition events are possible when an electron from the K-shell is knocked out. Examples of these are electrons from respectively the L- and M-shell falling down to the vacant positions in the K-shell generating respectively a K_α- or K_β-photon. Vacancies in the L shell give rise to L radiation

etc. The voltage necessary to generate characteristic x-ray radiation is called critical excitation voltage and increases as the atomic number increases. For example for Molybdenum, the critical excitation voltage is 20.01kV meaning that the accelerating voltage has to be greater than 20 kV to obtain characteristic x-rays. To be able to generate a certain amount of these, an over-voltage of at least 50% is however recommended during analyses.

When doing elemental analysis in SEM, emission depth is important. When analysing small particles, the emission depth has to be smaller than the particle. The emission depth is a function of the density of the material, accelerating voltage and the relation between accelerating voltage and critical excitation voltage. It decreases with increasing atomic number (Figure 4-8 and Figure 4-9)(Hjelen, 1989).

Characteristic x-rays can be detected by wavelength dispersive spectrometer (WDS) consisting of a crystal diffracting the photons whenever Bragg's law is fulfilled or an energy dispersive spectrometer (EDS) consisting of a solid state SiLi spectrometer where the photons passed through a thin beryllium or polymer window into a cooled Li doped Si-crystal. By means of semi-conductor theory, the x-ray photon is converted to a voltage pulse (see for example Goldstein et al., 2003). The WDS has its advantage in high spectral resolution, high signal to background ratio while EDS has its advantage in the ability to analyse all elements at the same time and also a lower investment cost. Most SEMs are therefore equipped with an EDS system.

Both EDS and WDS are qualitative techniques, but the relatively poor energy resolution of EDS can lead to spectral inference and inability to separate members of the x-ray families. Using flat-polished samples and a proper experimental setup, quantitative analyses of chemical composition with an accuracy and precision approaching 1% can be conducted (Goldstein et al., 2003). The analyses can be performed quantitatively with element standards or standard-less semi-quantitatively.
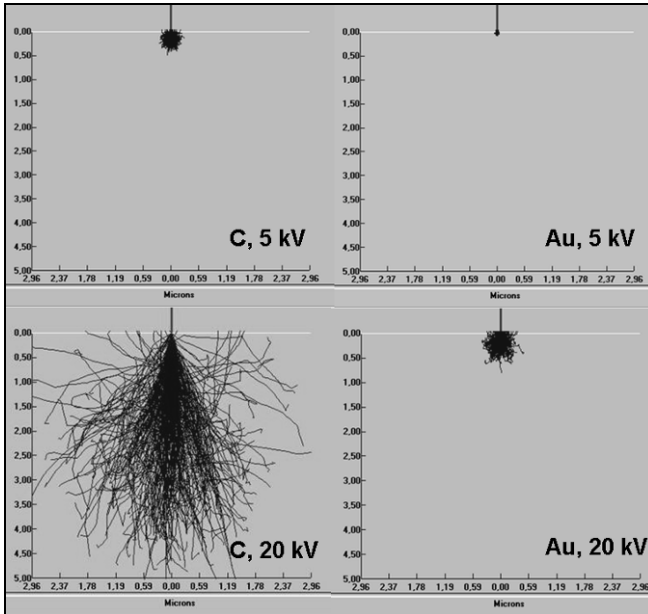
Figure 4-8. Interaction volumes for low and high accelerating voltages and atomic numbers in SEM. The volume expands with decreasing atomic numbers of the phase and increasing accelerating voltages. The volume expansion from low to high accelerating voltage is smaller for high atomic number materials than for low ones (Monte Carlo simulations: Morten Raanes).
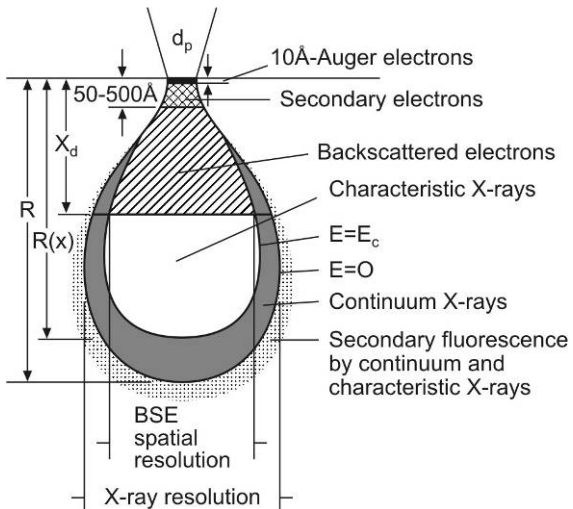
Figure 4-9. Resolution of the different signals in SEM. The CL emission volume exceeds that of all other signals (based on Goldstein, 1974).

4.3 ELECTRON BACKSCATTER DIFFRACTION – EBSD

4.3.1 General

Diffraction patterns generated by BSEs can be used to provide crystallographic information about a crystalline sample. The technique is used in Papers 2, 3 and 5 and will be described in the following chapters.

The EBSD technique is based on the weak diffraction pattern that forms when a focused, stationary, primary electron beam is located at a specific point on a highly tilted sample. Initial elastic scattering of the incident beam causes the electrons to diverge from a point just below the sample surface and to impinge upon crystal planes in all directions, generating Bragg diffraction. The diffraction patterns can be imaged using a transparent phosphor screen that converts the electrons to light and that is viewed by a sensitive camera. The camera is usually positioned horizontally, so that the phosphor screen is close to the sample in order to capture a wide angle of the diffraction patterns (Hjelen 1990) see Figure 4-11. Where the traces of electrons intersect with the phosphor screen, they appear as thin bright bands (see Figure 4-10 and Figure 4-14). These are called backscatter "Kikuchi" bands (Kikuchi, 1928). The resulting pattern is made up of many Kikuchi bands. Every band in the diffraction pattern represents a set of lattice planes in the crystal that is analysed, and the points of intersection between the bands represent crystallographic directions of the crystal. The diffraction pattern is therefore characteristic for the crystal structure and space orientation of the crystal. Rapid developments in both hardware and software in the past 10 years have made EBSD easy to use and ideal for the rapid analysis of microstructures of crystalline materials. Where the patterns were formerly manually indexed, the technique is now based on automated indexing of the diffraction patterns. The resulting pattern provides information on the crystal lattice within the diffracting volume of the electron beam, and the software rapidly reads the pattern and calculates the crystallographic orientation with respect to a given reference system (Wright, 2005). The whole process from start to finish can take from 0.025-1 second (1-40 patterns/sec) dependent on the phases analysed, the pattern quality, the binning of pixels etc. A method for further increasing the speed by storing the images directly on disk will improve the pattern acquisition speed (not indexed) to > 200 patterns/sec (Jarle Hjelen personal communication 2006). The spatial resolution of this technique is

superior to x-rays, since elastic backscattered and diffracted electrons have a much smaller interaction volume than x-rays (Figure 4-9). The interaction volume is dependent on acceleration voltage and atomic number of the analysed minerals, but is usually in the sub-micron range (Humphreys, 2001; Pettersen et al., 1998).
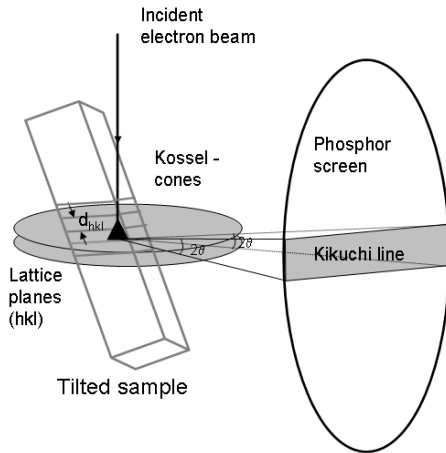
Figure 4-10. Origin of Kikuchi lines from EBSD (based on O. Engler in Schwartz et al., 2000)
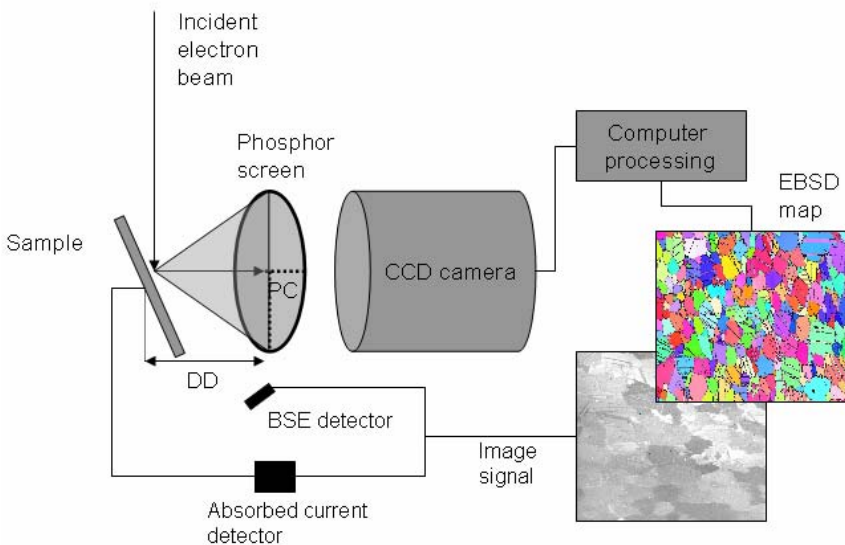
Figure 4-11. Typical EBSD hardware setup inside the SEM. (PC is pattern centre, DD is detector distance).

4.3.2 EBSD maps

EBSD patterns can be captured and indexed by the computer over a large array of measurement point. The recorded data can then be used to generate maps based on the orientation data for each point, see Figure 4-12. These maps enable the researcher to visualise the spatial distribution of crystallographic orientations in the sample. The fact that there is orientation data for each point analysed, "misorientation" between points can be calculated. This capability allows grain boundaries to be visualised. The ability to generate statistical measures of orientation, misorientation, grain boundaries, grain-size and others to provide critical insight into the evolution of microstructure is important to the material scientist (Wright, 2005). Some examples are found in Figure 4-16 and also in the appendix in addition to Papers 2, 3 and 5.
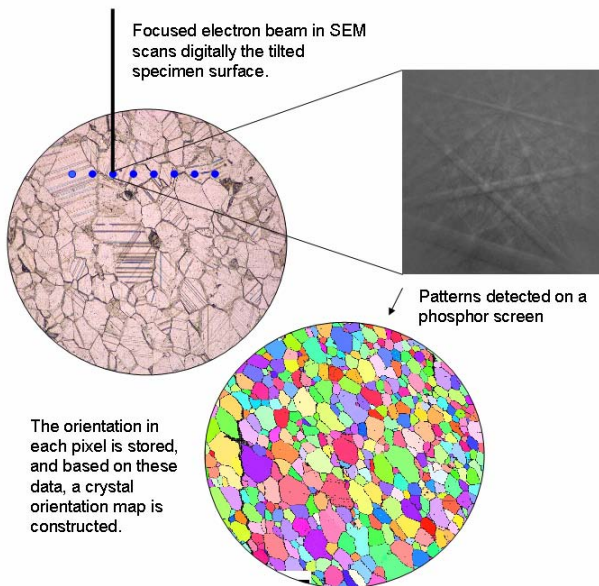
Figure 4-12. Generation of EBSD maps.

4.3.3 Bragg diffraction in the EBSD specimen

Prior et al. (1999) have reviewed the application of EBSD to textural problems in rocks. As described in the review, electrons that pass close to a nucleus will be scattered through larger angles than those that pass more distantly. The

diameter of the electron beam probe (>1 nm) is larger than the atomic spacing (~0.1-0.3 nm). Electrons will impact to all possible distances from nuclei of the specimen, so that interaction of the incident beam and the specimen will give rise to a population of scattered electrons with all possible trajectories. The scattered electron intensities will be a function of scatter angle. This population of scattered electrons acts as the source for EBSD in the SEM.

Trajectories that satisfy the Bragg condition for diffraction give rise to high intensities in the pattern. When θ is the diffraction angle, n is the order of diffraction, λ is the wavelength of the electron beam energy (corresponds with accelerating voltage) and d_{hkl} is the lattice plane spacing, the Bragg equation is given:

$$n\lambda = 2d_{hkl}\sin\theta \qquad\qquad \textbf{II}$$

Wherever the Bragg condition for diffraction is satisfied by atomic lattice planes in the crystal, two cones of diffracted electrons are produced (Figure 4-10). These cones are produced for each family of lattice planes (Schwartz et al., 2000). A network of bands will then be imaged on the phosphor screen. The edges of the bands are conic sections of the two diffraction cones. One edge will be brighter than the other, reflecting the distribution of scattered electron intensities in relation to scatter angle. The Bragg angle for electron diffraction is small, typically 0.5^{o}, leading to opening angles close to 180° for the diffraction cones. Thus the diffraction cones approximate planes and the bands appear straight (Prior et al., 1999). The bisector of each band is the direct projection of a family of lattice plane and the band which is equal to 2θ. The intersection between two bands corresponds to a zone axis or a crystallographic axis.

The highly tilted angle of the sample increases the backscatter yield as shown for example by Goldstein et al. (2003). This is an advantage because the increased signal improves the ability to collect EBSD patterns. The BSE from the tilted sample have close to initial electron beam energy producing the crystallographic information in the EBSD pattern. The lower energy electrons contribute to the overall background intensity or noise of the pattern. See Prior et al. (1999 with references) for a more rigorous treatment.

4.3.4 Resolution

A model using only single event elastic scattering for beam-specimen interactions is oversimplified. In general the primary electrons will penetrate into the specimen causing a series of scattering events. It means that the source of scattered electrons is not a point but a volume. This will cause some blurring of the diffraction bands and it is the geometry of this volume that controls spatial resolution of the EBSD technique (Prior et al., 1999). In addition multiple order diffraction will give rise to multiple bands and lower energy electrons will give rise to a diffuse background signal decreasing the resolution of the technique.

Monte Carlo simulations have shown that the resolution is directly related to the electron probe size. Hence it is apparent that field emission (FE) electron guns increase the spatial resolution due to smaller beam size. The spatial resolution is also a function of the accelerating voltage and the atomic number of the sample (Farstad et al., 1998; Hjelen and Nes, 1990; Humphreys, 2001; Pettersen et al., 1998). In aluminium (similar atomic number to the average atomic number of many silicates) Monte Carlo simulations show that the maximum source depth is 2-2.5 μm for typical EBSD working conditions (70° tilt and V_{acc}=20 kV), the majority of the signal coming from <1 μm. The resolution is better in the direction parallel to the tilt axis than perpendicular because of the tilting. Resolution studies reviewed by Humphrey et al. (2001) using a FE SEM show that Al-patterns can be distinguished by about 100 nm in the perpendicular direction and by 30 nm parallel to the tilt axis. This observed resolution is better than that calculated by simulations and is probably caused by patterns formed entirely from electrons that have experienced only one elastic interaction (D. Dingley, personal communication (in Prior et al., 1999)).

The resolution obtained in metals is not currently obtainable in non-conducting samples mainly due to charging problems. Resolution in the area of 1 μm is common using a tungsten filament and on the order of 0.25 μm using a FE gun (Prior et al., 1999). Resolution studies for non-conductive samples analysed in low vacuum mode is not yet published, but it is indicated that optimised conditions in low-vacuum mode can increase the resolution.

4.3.5 Indexing

Indexing is the process by which the pattern of a known phase is used to calculate the crystallographic orientation at the source point. Indexing the patterns requires calculation of the solid angles between planes that project as bands on the phosphor screen. The positions and orientations of bands are measured relative to the pattern center (PC) using a Hough transformation of the digital images (Hough, 1962; Krieger-Lassen, 1998). The Hough transformation expressed in formula III makes it possible to describe the bands by their distance ρ from the origin and the rotation θ of its normal vector as illustrated in Figure 4-13.

$$\rho = x \cdot \cos\theta + y \cdot \sin\theta \qquad\qquad \textbf{III}$$

Thus, a line in image space transforms to a point (peak) in Hough Space (Figure 4-14). The position of the pixel transformed from the pattern is given by the x and y values. These curves in the Hough space intersect at a point at a ρ, θ coordinate corresponding to the angle of the line (θ) and its position relative to the origin (ρ). The position of the peaks can be determined by standard peak finding techniques. The positions of the peaks correspond to the diffracting planes in the sample and the crystal orientation can be found by an algorithm that calculates possible orientations of the crystal. These give a match to the actual phase within given tolerances when a sufficient number of planes are determined (Dingley, 1998) see Figure 4-14. As explained by Prior et al. (1999) the configuration of the phosphor and the specimen are usually predetermined by the hardware or the user. The position of the source point relative to the phosphor is usually expressed as the position of the pattern center (PC) and the detector distance (DD) (see Figure 4-11). Several calibration methods have been tested (Day, 1993; Hjelen et al., 1993; Randle, 2003), it is common however, to calculate the PC and DD by collecting a high quality pattern. Once initial calibration is made, it is possible to refine the calibration parameters for the actual material and pattern (Krieger-Lassen, 1996).

In order to apply indexing algorithms, the following information is needed according to Prior et al. (Prior et al., 1999): (1) unit-cell lattice parameters, (2) crystal symmetry, and (3) a reflector file containing a list of the lattice planes that give rise to visible bands in the patterns. Items I and 2 are available for most minerals, the third requirement is less trivial. There are an unlimited number of

reflectors in a crystal structure and using all will slow down the process and make more incorrect orientation solutions. Kinematic models (Schmidt and Olesen, 1989) based on atomic scattering factors together with site occupancy data, provide good simulations for most minerals. (Prior et al., 1999).
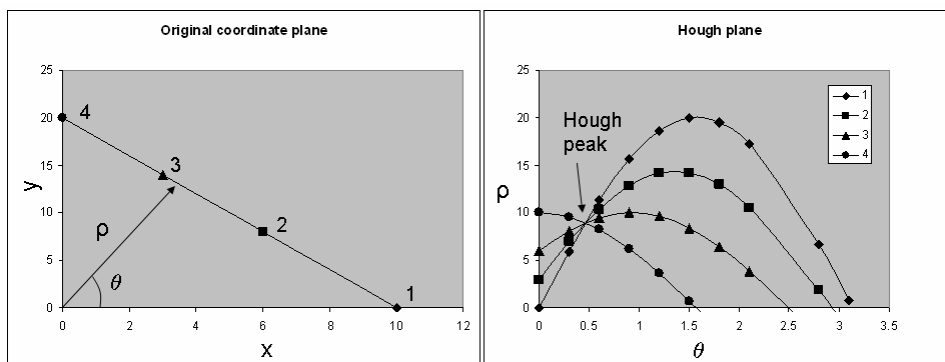
Figure 4-13. The principle of the Hough transformation where a line in image space is transformed to a point in Hough space.
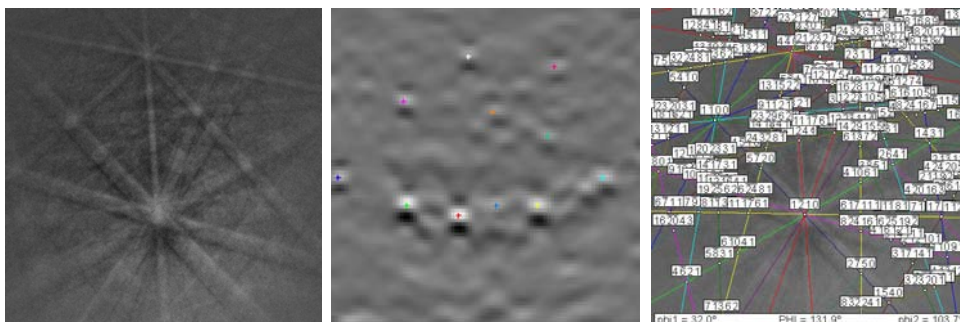
Figure 4-14. Left: an EBSD pattern from one orientation of calcite, middle: the Hough transformed image where the peaks are detected, right: the indexed pattern.

4.3.6 EBSD as a tool in mineralogy

4.3.6.1 *General*

In their review on application of EBSD to textural problems in rocks, Prior et al. (1999) state that "EBSD is a relatively new technique to the petrologist".

The main application area of EBSD in geology is to study microfabrics of a rock including spatial and geometrical configuration of all those components that make up a rock. Microsfabric includes the terms texture, microstructure and

crystallographic preferred orientation as defined by Passchier and Trouw (2005). Phenomena interesting to study by means of EBSD can for example be any kind of deformation mechanisms including lattice preferred orientations, absolute (mis)orientations between grains/crystals, recrystallisation, twinning, recovery and response to in-situ treatment by temperature or pressure, grain-size distributions, grain-shape distribution, grain-shape orientation, phase identifications of known polymorphs (Al_2SiO_5, SiO_2) or phase-identification, discrimination and distribution in multi-component systems. Typical capabilities of EBSD on geological samples are listed in Table 4-1.

Table 4-1. Capabilities of EBSD in mineralogy.

Property	Capability
Spatial resolution	<1µm (minerals)
Angular resolution	1-3 deg
Indexing speed	1-30 patt./sec.
Typical SEM conditions	20 kV, 2 nA, WD 20mm, 1-50Pa

4.3.6.2 *Samples*

Samples that are to be analysed by EBSD have to be crystalline. All minerals can in principal be analysed, several minerals are however challenging because of complex crystallography.

Whole rock or particles embedded in epoxy can be investigated. If absolute orientation of crystals or structures is to be studied, the sample should be oriented in space according to important directions such as lineation, foliation plane, in- situ rock stress etc.

4.3.6.3 *Sample preparation*

For EBSD analyses the specimens have to be prepared by cutting, grinding and polishing, to give a polished rock section. The diffraction patterns form in the uppermost atom layers and after mechanical polishing these atom layers are disturbed. To be able to get a pattern that can be indexed, the crystal lattice at the sample surface has to be undeformed. To obtain this, a post-mechanical preparation is required (Lloyd, 1985). After mechanical polishing, the surface damage in the uppermost layers has to be removed by electro polishing, etching, ion-beam milling or chemical-mechanical polishing (colloid silica polishing).

As explained by Prior et al. (1999), for geological, non-conductive samples, chemical-mechanical polishing provides a damage-free surface for most minerals although some dissolve rapidly in the colloid silica and some soft minerals present preparation problems.

Etching provides damage-free surface, but introduces topography that can be a problem during EBSD analysis.

Ion-beam milling is an unexplored alternative, but is limited to only small surfaces (Prior et al., 1999).

Figure 4-15 shows examples of patterns from quartz before and after chemical-mechanical polishing displaying only indications of a pattern before the chemical-mechanical treatment. A poster illustrating chemical-mechanical polishing of quartz was published by the author at a conference in 2003 (Moen et al., 2003) and is printed in the appendix. All EBSD samples used in this thesis are treated by chemical-mechanical polishing.
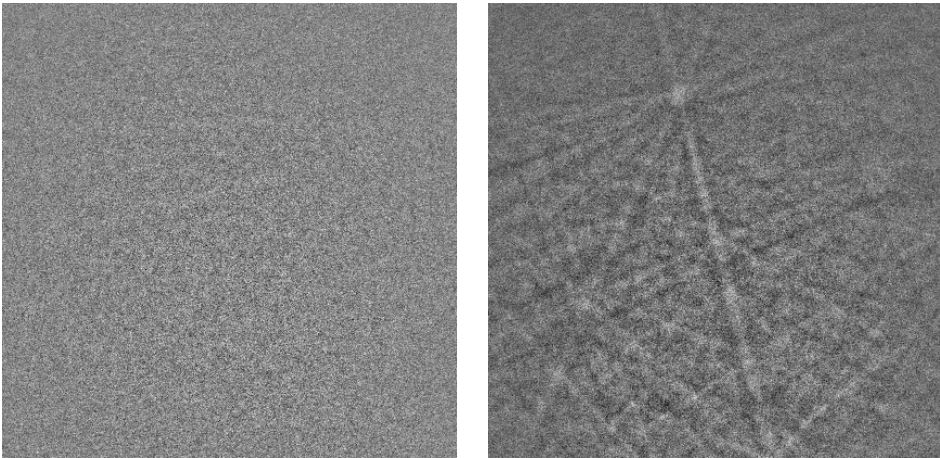
Figure 4-15. Electron backscatter pattern of quartz after mechanical polishing to the left and after 240 sec of chemical-mechanical polishing to the right (Moen et al., 2003).

Insulating samples will experience charging under the electron beam and can prevent meaningful EBSD work. Coating the sample with conductive material such as carbon or gold removes the charging problem, but reduces the quality of the EBSD patterns. Patterns from samples with 4-6 nm of carbon coat require significant higher (one-two orders of magnitude) beam current than that of

uncoated samples (Prior et al., 1999). Thus, coating requires an increased current that in place will reduce spatial resolution. EBSD work on insulating samples should therefore preferably be conducted in a low vacuum SEM without any conductive coating.

4.3.6.4 *Examples*

Some examples of results from EBSD in mineralogy are presented in Figure 4-16. Some application notes on EBSD are found in the appendix in addition to the Papers 2, 3 and 5.
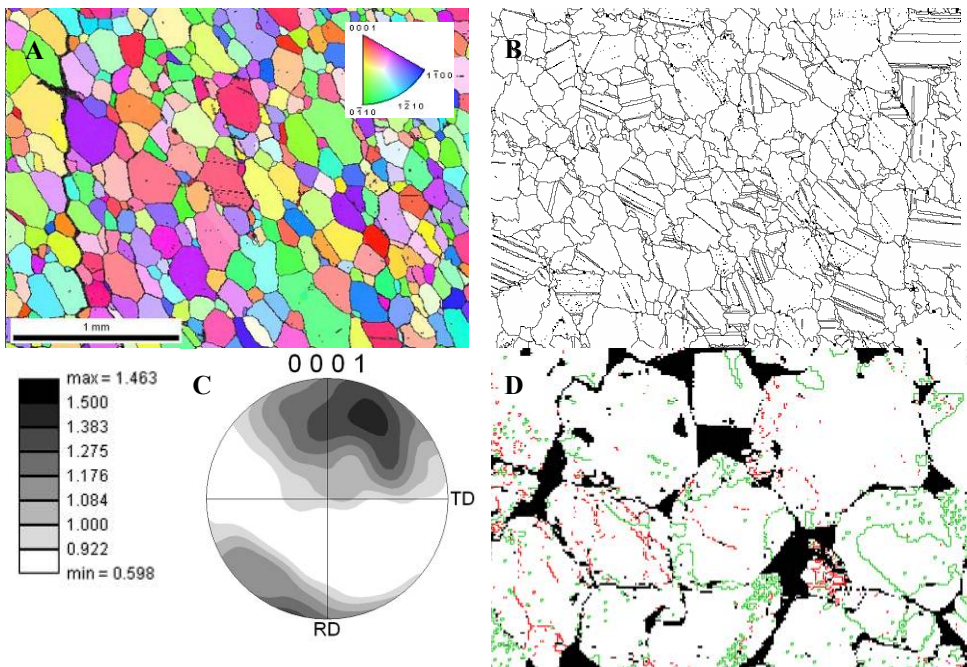
Figure 4-16. Examples of results from EBSD: A) Inverse polefigure map of a calcitic marble. B) Grain boundaries and twin boundaries in a calcitic marble. C) Polefigure of c-axis orientation of a lattice texture, grey scale is multiples of random distribution. D) Dauphinè twin boundaries (green) and low angle boundaries (red) in deeply buried reservoir quartz sandstone.

4.4 **REFERENCES**

Day, A., 1993, Developments in the EBSP technique and their application to grain imaging, University of Bristol.

Dingley, D. J., 1998, Developments in on-line crystal orientation determination, Institute of Physics Conference Series, 98, p. 473-476.

Farstad, T., Johannessen, K., and Hjelen, J., 1998, Spatial resolution of EBSP using fully automated pattern indexing: 14th Int. Congress on ELectron Microscopy ICEM 14, Cancun, Mexico, 1998, p. 753-754.

Goldstein, I. J., 1974, Metallography - a practical tool for correlating the structures and properties of materials, ASTM Special Technical Publication 557, ASTM, p. 86.

Goldstein, J. I., Newbury, D., Echlin, P., Joy, D., Romig, A. D., Lyman, C., Fiori, C., and Lifshin, E., 1992, Scanning Electron Microscopy and X-ray Microanalysis: New York, Plenum Press, xviii, 820 p.

Goldstein, J. I., Newbury, D., Joy, D., Lyman, C., Echlin, P., Lifshin, E., Sawyer, L., and Michael., J., 2003, Scanning Electron Microscopy and X-ray Microanalysis: New York, Kluwer Academic/Plenum Publishers, 689, 1 CD-ROM p.

Heinrich, K. F. J., 1966, In Proceedings of the 4th International Conference on X-ray optics and Microanalysis, Paris, 1966, p. 159.

Hjelen, J., 1989, Scanning elektron-mikroskopi: Trondheim, Metallurgisk institutt, NTH, 106 p.

Hjelen, J., and Nes, E., 1990, Spatial Resolution Measurements of Electron Backscatter Diffraction Patterns (EBSPs) in the Scanning Electron Microscope: XIIth International Congress for Electron Microscopy, Seattle, USA, 1990.

Hjelen, J., Ørsund, R., Hoel, E., Runde, P., Furu, T., and Nes, E., 1993, EBSP, Progress in Technique and Applications: Textures and Microstructures, v. 20, p. 29-40.

Hough, P. V. C., 1962, Methods and means for recognizing complex patterns, 3,069,654: USA.

Humphreys, F. J., 2001, Grain and subgrain characterisation by electron backscatter diffraction: Journal of Materials Science, v. 36, p. 3833-3854.

Jacamon, F. P., and Larsen, R. B., 2005, Relationship between SEM-cathodoluminescence and trace element chemistry of quartz in granitic igneous rocks from the Oslo continental rift: Eos, v. 86(52).

Kikuchi, S., 1928, Diffraction of cathode rays by mica: Jap. J. Phys, v. 5:83.

Krieger-Lassen, N. C., 1996, The relative precision of crystal orientations measured from electron backscattering patterns: Journal of Microscopy, v. 181, p. 72-81.

Krieger-Lassen, N. C., 1998, Automatic high-precision measurements of the location and with of Kikuchi bands in electron backscatter diffraction patterns: Journal of Microscopy, v. 190, p. 375-391.

Lloyd, G. E., 1985, Review of Instumentation, Techniques and Applications of SEM in mineralogy, *in* White, J. C., ed., Short Course in Applications of Electron Microscopy in the Earth Sciences, 11: Fredericton, Mineralogical Association of Canada, p. 151-188.

Moen, K., Hjelen, J., and Malvik, T., 2003, Preparation of Quartz Samples for EBSD Analysis: Applied Mineralogy '03, Helsinki, Finland, 2003.

Passchier, C. W., and Trouw, R. A. J., 2005, Microtectonics Berlin Springer, 366 p.

Pettersen, T., Heiberg, G., and Hjelen, J., 1998, Measurements of spatial resolution of EBSP in the SEM as a function of atomic number and high voltage The 14th International Congress on Electron Microscopy, Cancun, Mexico, 1998.

Prior, D. J., Boyle, A., P., Brenker, F., Cheadle, M., C., Day, A., Lopez, G., Peruzzi, L., Potts, G., Reddy, S., Spiess, R., Timms, N., E., Trimby, P., Wheeler, J., and Zetterstrom, L., 1999, The application of electron backscatter diffraction and orientation contrast imaging in the SEM to textural problems in rocks: American Mineralogist, v. 84, p. 1741-1759.

Randle, V., 2003, Microtexture Determination and Its Applications, , , 146 p.

Reed, S. J. B., 2005, Electron Microprobe Analysis and Scanning Electron Microscopy in Geology: Cambridge, Cambridge University Press, 192 p.

Schmidt, N.-H., and Olesen, N. O., 1989, Computer-aided determination of crystal-lattice orientation from electron channeling patterns in the SEM: The Canadian Mineralogist., v. 27, p. 15-22.

Schwartz, A. J., Kumar, M., and Adams, B. L., 2000, Electron backscatter diffraction in materials science: New York, Kluwer Academic/Plenum Publishers, XVI, 339 s. ill. p.

Sørensen, B. E., Austrheim, H., and Larsen, R. B., 2005, Fluid-related recovery and deformation textures in quartz in partly retrogressed high-grade quartzites from the Bamble sector, v. 86(52).

Wittry, D. B., 1966, In Proceedings of the 4th International Conference on X-ray optics and Microanalysis, Paris, 1966, p. 168.

Wright, S., 2005, A Collection of OIM Applications, *in* Wright, S., ed., Edax TSL, p. 106.

5.   CHAPTER

Image processing and analysis

5.1   INTRODUCTION

Whereas image processing is the science of rearrangement of images, image analysis is the science of extracting information from the image. Within these terms, several operations are necessary, including techniques for acquisition and preparation of images and measurement of the features and structures present. Features and structures are quantifiable and can be used to characterise, classify and compare images by means of numerical values. As expressed by Russ (2002) "the measurement of images generally requires that features be well defined, either by edges or unique brightness, colour, texture, or some combination of these factors". Image analysis is generally dependent on the following operations:

- Image acquisition;
- Image enhancement;
- Segmentation and thresholding;
- Processing of binary images;

- Measurements;
- Analysis.

See for example (Barbery, 1991; Lastra et al., 1998; Russ, 2002). Image processing and analysis is important for all papers in this thesis. Especially in the PTA software further described in Chapter 6 and Paper 1, image analysis is vital.

5.2 **IMAGE ACQUISITION**

Images can be acquired in different settings depending on the parameters that are to be measured. Examples of applications are analysis of satellite images or aerial photographies for military use, weather forecast or bedrock mapping or microscope images from an optical or electron microscope for microstructure measurements. The image scale may vary from microscopic to astronomical with principally the same operations used (Russ, 2002). As explained by Russ (2002), given the diversity of image types and sources, several general criteria can be prescribed. These are mainly: 1)The images have to be digitised. Earlier, images for computer processing were commonly acquired with a video camera mounted onto a microscope. The camera sent analogue signals to a "frame grabber" which then stored numeric values in memory. Nowadays most images are acquired digitally. 2) The need for global uniformity providing that the features look the same wherever they appear is important. This implies uniform illumination, colour, contrast and brightness. 3) Local sensitivity to variations is important so that the edges and boundaries are defined in a satisfactory way. Examples of equipment used to acquire images are: analogue video cameras or digital cameras (CCD or CMOS), scanning electron microscopes (SEM) or electron probe micro-analysers (EPMA).

Image analysis can be performed both on two-dimensional and tree-dimensional data, three dimensions demanding extremely data-capacity though. Only two dimensional data will be further discussed in this thesis.

The digital image is composed of discrete image elements or pixels with a finite area. Image acquisition hardware and software allows acquisition of images in several digital formats. The following are most common, 256x256, 512x512, 1024x1024. Also available are 64x64, 128x128, 2048x2048 and non-square formats. The software has to be calibrated so that each format has a geometric scale. It is also important to keep in mind that the amount of memory occupied is a function of image resolution. By increasing the resolution one step, the

memory occupied increases by 4 (Lastra et al., 1998). 512x512 is usually sufficient. Today most image analysis systems use 8 bits of grey-levels, but 16 bits are also available. 8 bits means 2^8=256 grey-levels where black is zero and white is 255 (Hetzner, 1998). Colour images are treated in a similar way; however the colour information is split usually in three dimensions or signals, red, green and blue (RGB) alternatively hue, saturation and intensity (HSI).

In this work image acquisition is obtained by a digital camera on the optical microscope (Paper 4) or in SEM (Papers 1-3 and 5).

5.3   IMAGE ENHANCEMENT

The images can be enhanced by applying filters or transformations. While a transformation converts each single pixel according to a certain formulae independent on the value of adjacent pixels, filters converts the centre of a matrix of pixels. Table 5-1 lists some transformation functions and some filters. The filter kernels or matrixes can consist of any defined size, 3x3, 5x5 etc. According to Russ (2002), image enhancement can be performed in either the spatial domain (the array of pixels comprising our conventional representation of image) or other domains, such as Fourier or Hough (used in EBSD, see Chapter 4.3.5). In the spatial domain, which is the one easiest available when doing classic image analysis, pixels may be modified according to rules that depend on the original pixel value. In addition, pixel values may be combined with or compared with others in their immediate neighbourhood in different ways. For image processing in the spatial domain, images are processed for enhancing the contrast and brightness, get rid of biased illumination, and to smooth the grey-levels, reduce noise and sharpen the edges (Figure 5-1). The change of grey-levels from one phase to the other generally takes place over several pixels. An edge-sharpening procedure will generally narrow the range.

Infinite possibilities concerning image enhancement filters exist, see for example Russ (2002). They are not further described here, but as Lastra et al. (1998) mentions as a rule of thumb "the general philosophy is to acquire an image with the best quality possible, and to use very few filters to improve the image".

Table 5-1. Examples of transformation functions and filters. Filtering is performed by means of matrix operations.

Transformation functions	Filters	Gaussian filter used in Figure 5-1			Laplacian filter used in Figure 5-1		
Reverse	Smoothing filters	1	2	1	-1	-1	-1
Logarithmic	Edge detection filters	2	4	2	-1	8	-1
Exponential	Sharpening filters	1	2	1	-1	-1	-1
Square							
Gamma							
Hough							
Fourier							
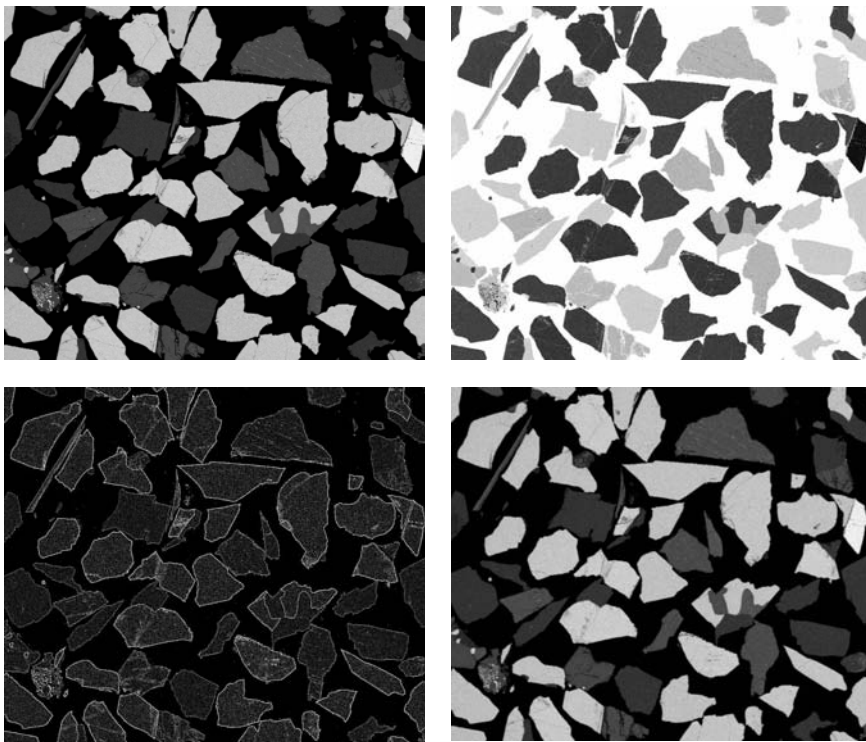
Figure 5-1. Transformation and filtering of an image. Upper left: raw image. Upper right: reversion of the grey-scale values of the image producing a photometric negative of the original image. Lower left: Edge detection by a Laplacian filter which extracts the outer contours of objects by means of the matrix in Table 5-1. Lower left: smoothing of image with a Gauss filter which attenuates the variations of light intensity in the neighbourhood of a pixel by means of the matrix in Table 5-1.

5.4   SEGMENTATION AND THRESHOLDING

As described by Russ (2002), one of the most critical steps in the process of reducing images to information is segmentation, that means distinguishing objects of interest. Lastra et al. (1998) explain that the minerals are segmented into binary images by detecting the grey-levels for each mineral. This is carried out interactively by thresholding, that means setting the lower and upper value for each maximum (see Figure 5-2). The settings are then fixed during automatic, unattended analysis (Lastra et al., 1998).
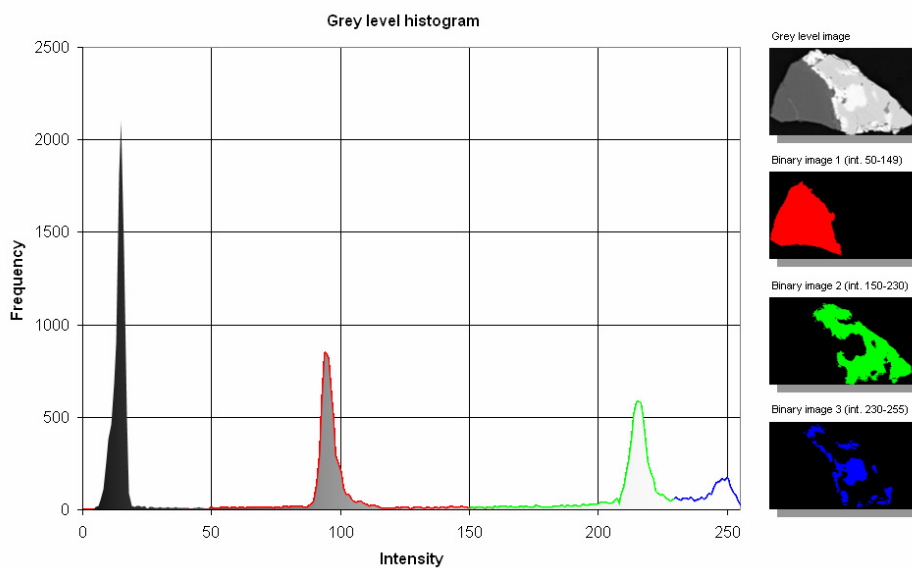
Figure 5-2. Grey level histogram and three binary images from a grey level image (upper right) consisting of 8 bits => 2^8 => 256 grey-levels. The binary images consist of 1 bit => 2^1 => 2 grey-levels. The threshold values are colour coded and also given over the binary images (Figure: Torkjell Breivik).

If there is more than one grey level or colour of interest, more windows have to be set. When segmenting images from a colour camera, three signals have to be segmented. These signals are usually red, green and blue (RGB). Important precautions are described by Lastra et. al. (1998).

For most systems the settings are fixed during automatic analysis, although there are developed systems for dynamic identification of shifted grey-levels through

a run (Schneider et al., 2004). Each of the segmented colour interval of interest is thresholded from the remaining pixels to form binary images.

Segmentation can be seen as the act of separating out information from an image while the thresholding operation is performance of this separation of features by selecting the wanted range of pixels to a foreground and rejecting all others to the background, making a binary or a two-level image where the foreground can be white and the background black or opposite (Russ, 2002). For separation of phases from backscattered electron images, segmentation by brightness is most convenient. When segmenting textures (patterns) where the average brightness is the same, frequency transforms are to be used (see e.g. Russ, 2002).

5.5 PROCESSING BINARY IMAGES

Usually, some binary operations have to be performed on binary images of the selected structures before measurements can take place. As explained by Hetzner (1998), these are mathematical morphological analyses that were mainly developed at "Ecole de Mines" in Paris. This group was responsible for developing image erosion, dilation, skeletonization and other concepts, plus the use of Boolean binary logic. There is a lot of literature in this field more thoroughly described in, for example, Russ or Hetzner (Hetzner, 1998; Russ, 2002). Most operations include modifications and combinations of the fundamental operations erosion, which removes pixels from the features in an image while dilation adds pixels to the features (Figure 5-3). The strategy for removing and adding can be somehow different but classical erosion removes any pixel touching another pixel that is part of the background (Russ, 2002). Boolean logics are used to combine images. The possibilities are AND, OR, XOR and NOT. "AND" Boolean operation with two images means that the pixels need to be white or "on" in both images to get the same colour in the resulting images. OR means that only one image needs to be white or "on" to be "on" in the resulting image and XOR demands that the pixels are white in exclusively one of the images. NOT requires only one image and simply reverses each pixel (Goldstein et al., 2003) (Figure 5-4).

The most typical reasons for applying binary operations to images of particles embedded in epoxy resin are (Lastra et al., 1998; Malvik, 1991):

- Removal of small artefacts that do not represent minerals;
- Separation of touching particles that can be misidentified as one particle;

- Removal of particles that are bigger or smaller than the fraction that has been selected;
- Removal of particles that cross the frame of the image.
- Identification of common grain boundaries for grains in a particle

Figure 5-3. Original binary image (left), three cycles of dilation of the original image (middle) and 3 cycles of erosion of the original image (right).
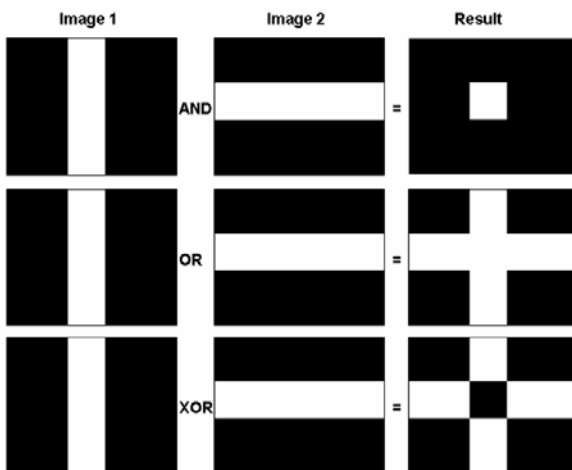
Figure 5-4. Boolean logic operations commonly used during processing of binary images. White is "on".

5.6 **MEASUREMENTS**

A range of parameters can be measured and used to characterise particles by image analysis. The way different systems select and classify objects for measurements deviates somewhat differently, but usually one finds only small variations. However, there are two types of measurements that are common to all image analysis systems. These are field-specific and object-specific measurements where field specific measurements only allow the measurement of

one given parameter for the overall field. Examples are total area or total perimeter for all structural elements Object-specific measurements consist of measurements for each identified structural element (Hetzner, 1998; Malvik, 1991) and can be grouped into four classes that are brightness, location, size and shape and for each class a variety of measurements can be made (Russ, 2002). Examples of brightness include colour-values or density, location include absolute and relative positions. Figure 5-5 shows some important object specific parameters which can be used to measure size and shape of particles and which are usually found as standard parameters in image analysis systems. These are primary feature-specific parameters. In addition some parameters derived from the basic parameters are shown. The following measurements are important during analysis of minerals with respect to mineral processing. These are described in detail by Lastra et. al. (1998),:

- Mineral quantities;
- Size distributions;
- Grain shapes and grain boundaries;
- Mineral liberation;
- Mineral associations.

Objects specific parameters

Area excluding or including the inclusion

Perimeter

Equivalent circle diameter

Maximum Feret diameter

Minimum Feret diameter

Convex hull perimeter

Derived parameters

Elongation ratio:

$$\frac{d_{max}}{d_{min}}$$

Roundness:

$$\frac{Perimeter^2}{4\pi Area}$$

Roughness:

$$\frac{Perimeter}{Conv. perimeter}$$
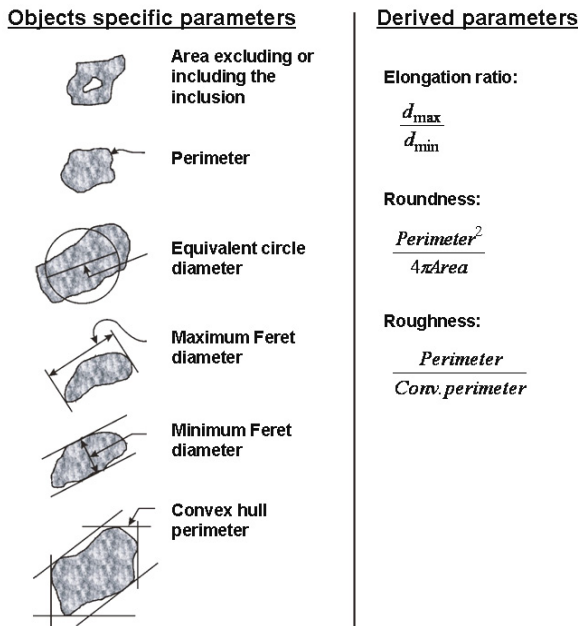
Figure 5-5. Examples of object specific measurements.

Within applied mineralogy, all features measured are involved in the characterisation of three dimensional structures viewed as a section plane in the microscope. The science of stereology further discussed in Chapter 5.10, relates measurements made in two-dimensions to the three-dimensional space. Measurement strategies and statistics are also discussed in Chapter 5.10.

5.7 ANALYSIS

In the end, the data obtained has to be analysed according to the scope of the work carried out. Typically these analyses include: tables and plots for mineral quantities, size distributions, shape factors, mineral liberation tables and mineral association tables and diagrams.

As already described, the big advantages of direct image analysis compared with indirect methods are that measurements are visual and can be checked and controlled through the process. It is also possible to quantify grain-size distributions for every mineral in the bulk material, where indirect methods only quantify the total particle size distributions. The most important advantage is nevertheless the possibility of quantifying how the minerals occur together in free and composite particles and also as mineral alterations. The best results are in any case obtained when the different methods are applied together in such a way that the advantages of every technique are utilised.

5.8 IMAGE ANALYSIS SYSTEM FOR MINERAL ANALYSIS

An image analysis system for automatic mineralogical analysis consists principally of the following components (Lastra et al., 1998):

- An imaging unit: Optical microscope with a camera or video camera preferably with colours or a Scanning electron microscope (SEM) or Microprobe (EPMA)
- A motorized stage that can be set to move precisely with software in the *x* and *y* direction. A semiautomatic system at least needs a stage that can be precisely managed manually in the *x* and *y* direction.
- An image analyser that includes calibrated image acquisition. For a *state-of-the-art* system this consists of a computer equipped with image analysis software and a graphic card connected to the imaging unit by

USB or fire wire cable. For analogue images a "frame grabber" or an analogue-to-digital converter (ADC) is necessary.

5.9   ANALYTICAL PROCEDURES

As the developments of automatic techniques proceed with unattended analyses of a high number of particles and various signals to discriminate most minerals, the statistics reach a very high level of significance for the analysed samples. The data quality however, regardless of advanced analysis techniques, will still be at the mercy of the sampling strategy. To obtain statistic valid results for the population investigated, the following analytical procedures are common practice in modal mineralogy and mineral liberation analysis:

- The sampling must be carried out so that the population investigated is representative;
- A selection appropriate for screening is split out;
- From the population of particles in which the features are to be quantified, samples are separated by screening in a series of sieves selected in such a manner that D_{max}/D_{min} is close to one. In practice, values of 1.414 or 1.2 are often retained, as recommended by Standards Organisations (Barbery, 1991);
- The samples are mounted in a plastic material, for example an epoxy resin. The particles have to be dispersed isotropically and randomly;
- Sectioning, grinding and polishing of the material-epoxy block are performed. See e.g. Reed (2005) for further descriptions of specimen preparation for SEM analysis;
- The sample is analysed by a human operator or an automatic particle analysis system;
- Each image should contain between 50 and 200 particles and the magnification should be from 30x to 400x. It means that particles >300 μm is difficult without making montages of images necessary;
- To calculate the number of images required to obtain satisfactory statistics, two approaches can be used: Either point counting statistics to calculate the number of particles or plotting of cumulative modal mineralogy for every image and see when the trend stabilises.
- The measurements are performed by means of point counting, line integration or area measurements.

- Modal mineralogy tables and total mineral liberation curves should be among the end results of liberation investigations of minerals.

5.10 STEREOLOGY

5.10.1 Basic concepts

Stereology is a mathematical methodology for obtaining three-dimensional information from measurements made in two dimensions. More generally it can be regarded as sampling theory for spatial processes. By means of stereology geometrical parameters such as number, volume, surface area, length and total curvature can be estimated. Whenever measurements are made on sections, on lines or points drawn on the section, some properties are valid in the original space while others are impossible to recover (Barbery, 1991). The most fundamental stereological relation is found in formula I. Under the conditions of the analytical procedures described in Chapter 5.9, the following statistic equalities apply:

$$\frac{\sum V_i}{\sum V_{tot}} = \frac{\sum A_i}{\sum A_{tot}} = \frac{\sum L_i}{\sum L_{tot}} = \frac{\sum P_i}{\sum P_{tot}} \qquad \textbf{I}$$

The theorems state that volume fraction equals the area fraction equals the linear fraction equals the point fraction of phase *i*. These equations were suggested already in the 19th century by Delesse (1848), Rosiwal (1898) and later Thompson (1930).

The basic equations relate 0, 1 and 2-dimentional quantities measured in the two-dimensional section plane to the more inaccessible quantities located in the three-dimensional space (Underwood, 1970). The theorems are unbiased and independent of convexity, shape, orientation or other textures. The structures measured, though, have to accord with the analytical procedures described, which mean randomness is required where uniform isotropic sections and lines are used (Barbery, 1991; Underwood, 1970). This is the reason why great care must be taken in sampling and sample preparation, as earlier described. It is also important to notice that taking the average of ratios on a particle section or intercept basis, gives a bias.

The following description is based on Barbery (1991). He says that it is also possible to obtain surface area of contact between phases in particles in a simple

and unbiased manner by using the following approach: If L_{ij} is the length of the perimeter of contact between phase i and j in a particle section of area S, then the specific surface area, Sv_{ij}, of contact in three dimensions between phase i and j is:

$$Sv_{ij} = \frac{4}{\pi} \frac{\sum (L_{ij})}{\sum (S)} \qquad\qquad \textbf{II}$$

The same kind of relation can be made with the linear intercept method. These relationships are derived without assumptions on particle shape, texture, size, etc. That is the reason why they are so powerful. But the limiting factor is still the character of the sampling and samples (Barbery, 1991). These two sets of relationships are routinely used in most image analysers. For example in flotation applications, the average composition of the surface of particles is obtained by calculating the ratio (Barbery, 1991):

$$\frac{Sv_{i,epoxy}}{Sv_{p,epoxy}} = \frac{\sum (L_{i,epoxy})}{\sum (L_{p,epoxy})} \qquad\qquad \textbf{III}$$

Coleman (1979) also provides the following expressions : The integral radius of curvature of surface estimated from the integral radius of curvature of the curve formed by the intersection of the surface with a random plane, and the length of a curve in space can be estimated by the number of intersection points of the curve with a random plane (in Barbery, 1991).

Barbery (1991) concluded that "Any other three dimensional characteristic to be assessed from plane sections can only be obtained through the use of limiting hypothesis". This is the case, for example for particle-size distribution where it among others must be assumed that particles are statistically congruent. This means particle shape is independent of particle size.

5.10.2 Sampling strategy

As already mentioned, tree approaches can be used when measuring the area fraction of a structure: point counting, line integration and area measurements. Since the measurements are made on the binary image, area measurements are heavily affected by the image enhancement and binary image processing performed on the images. The procedure in simple, but it is difficult to assess the

accuracy of the measurements. Superimposing a grid on the image instead and measuring the fraction of point that falls on the structure of interest, allows an estimation of the measurement precision (Russ, 2002). The points should be far enough apart that they provide independent measures of the structure (two points should rarely fall into the same feature). If the structure is random, the grid should be a regular square; if the structure is highly regular, the grid should be randomized to prevent bias (Russ, 2002). Point counting can be done manually in the optical microscope or by superimposing a grid by the Boolean "AND" operation on the binary image.

As mentioned in the previous chapter, it is also possible to measure surface area in an unbiased manner. Measuring the length of a boundary line in a digitised image is a error-prone task because of pixellation of the image and when the magnification is increased, more irregularities in the boundary become visible and the measured boundary is increased (Russ, 2002). The preferred method for determining surface area is consequently to place a grid of lines on the image and to count the number of intersection points which they make with the line representing the surface of interest. The relationship between the surface area per unit volume (S_V) and the number of intersections per length (P_L) is just (Russ, 2002):

$$S_V = 2 \cdot P_L \qquad\qquad \textbf{IV}$$

As further explained by Russ (2002), since this is a counting experiment, the precision can be estimated from the square root of the number of intersection points provided the lines are far enough apart that the intersections are independent events. Introducing grid lines relies on the assumption that the surfaces are isotropic. This assumption is rarely met in real structures. If the structure is not isotropic, a grid of lines that sample the structures isotropically has to be constructed. Russ (2002; Russ and Dehoff, 2001) further discuss such constructions.

In classical stereology, assumptions were made on grain-shape when size-distributions were to be measured. The most convenient shape to assume is a sphere, making it possible to calculate a matrix of α values that enable solving the distribution of sphere sizes present in the three-dimensional structure (See formula V) (Russ, 2002; Russ and Dehoff, 2001).

$$N_{V_{sphere,i}} = \sum \alpha_{i,j} \cdot N_{A_{circle,j}} \qquad\qquad \textbf{V}$$

Other shapes have also been suggested and tables of alpha coefficients for all these exist (Russ, 2002). This classical method is called unfolding. There are several drawbacks with these classical approaches, including that most particles are not spheres or another ideal shape and that shape often varies with the size. Smalls errors in assumptions produce large errors in the results. As written by Russ (2002), unfolding was a widely used method for decades, but has fallen in favour the last 20 years. Instead there has been increased emphasis on finding unbiased ways to measure structural parameters using more robust tools. Russ (2002) comments that unfolding is unfortunately still performed and that the common argument is that this gives data that can be compared from one sample to another. Even this is wrong and betrays the level of ignorance of stereological procedures (Russ, 2002).
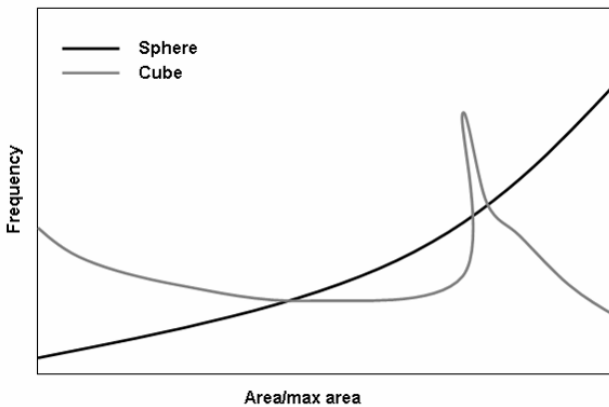
Figure 5-6. Size distribution of intercept areas produced by random sectioning assuming spheres and cubes (based on Russ, 2002).

5.10.3 Stereological conversion

When doing measurements on plane sections, it is well known that the result contains a bias due to the finite probability of observing apparently liberated sections or segments from unliberated particles (Barbery, 1991). That means that the amount of composite particles exposed is fewer than the real amount because

a composite particle, depending on the direction of cross-section, can be exposed as a liberated grain. At the same time, the amount of composite particles possessing relative equal amounts of two phases are often exposed as composite particles possessing only trace amounts of one mineral.

There are two main approaches to image analysis and stereology. The first is to make a stereological model that transforms the data to three dimensions with a certain model, or alternatively, raw data can be used, as long as possible errors from this approach are taken into account. In the case of special analysis of a homogeneous kind of texture or material, it is possible to adapt a model that describes the original space better than the raw data. For the case of general mineral liberation and association assessments on different materials, the use of raw data is preferred (Malvik, 1976). Raw data or apparent data is often used to avoid the introduction of systematic errors by applying elimination of certain grains that do not fit the grain-size or special transformations. Although the original three-dimensional space is never actually checked, results performed under the same conditions can be compared and are equally sensitive to variations as the absolute values. Trends will be correct as long as the samples are uniformly isotropic.

The correction models developed often assume ideal contact surfaces and constant grain-size. In a real material these idealised assumptions seldom hold. The intergrowths are often more complex, thus increasing the probability to be exposed as a composite particle. The size of the corrections that has to be made can therefore be discussed. The probability that a composite particle is exposed as a composite particle is therefore a function of type of intergrowths, relative amounts of minerals, grain-shape and grain-size. Some reflections regarding probabilities are found in Figure 5-7 and Figure 5-8. These curves illustrate the kind of assumptions that have to be made about grain shape in order to correct the data.

In this study, stereology is applied only to a limited extent. The principles of stereology are used, but estimates or correction factors built on assumptions for transforming two-dimensional data into three dimensions are not used. Apparent parameters observed on the section are used and regarded as a relative parameter suitable for describing a property of the minerals and for comparing with other samples. The problems are, however, approached and discussed from a stereological perspective. When dealing with a lot of different material, the main

argument against extensive use of stereological conversions, as stated by Malvik (1976), is the need for uncertain estimates that leads to an even more uncertain estimate. The danger of betraying the level of ignorance by not using or using out-of-date approaches as stated by Russ (2002) should however be avoided. More effort will therefore be put into stereological challenges in further work.
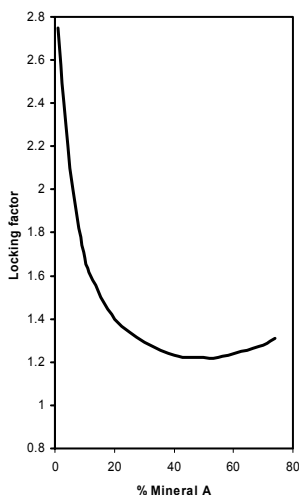
Figure 5-7. Correction factor or "locking factor" as a function of amount of phase A on the total mineral surface (based on Gaudin, 1939).
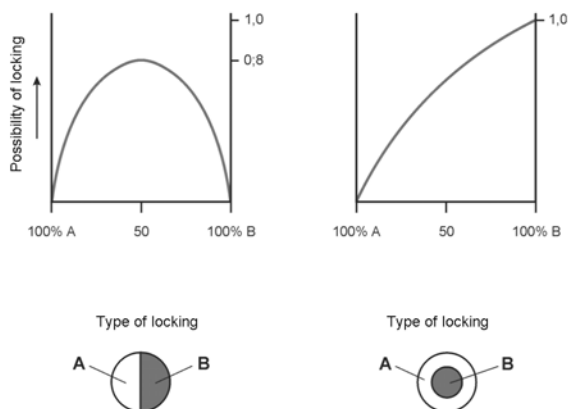
Figure 5-8. The probability that composite particles are exposed as composite particles as a function of relative amount of phases and particle morphology (based on Jones and Stewart, 1976).

5.11 **REFERENCES**

Barbery, G., 1991, Mineral liberation: measurement, simulation and practical use in mineral processing: Quebec, Canada, Les Editions GB, 351 p.

Delesse, A., 1848, Procédé méchanique pour déterminer la composition des roches: Ann, mines, v. 13, p. 379-388.

Gaudin, A. M., 1939, Principles of mineral dressing: New York, McGraw Hill.

Goldstein, J. I., Newbury, D., Joy, D., Lyman, C., Echlin, P., Lifshin, E., Sawyer, L., and Michael., J., 2003, Scanning Electron Microscopy and X-ray Microanalysis: New York, Kluwer Academic/Plenum Publishers, 689, 1 CD-ROM p.

Hetzner, D. W., 1998, Quantitative Image Analysis, Part 1 Principles: Buehler's "Tech-Notes", v. 2, p. 5.

Jones, M. P., and Stewart, P. S. P., 1976, Composite particles: London, Royal School of Mines, Imperial College.

Lastra, R., Petruk, W., and Wilson, J., 1998, Image-analysis techniques and application to mineral processing, *in* Cabri, l. J., and Vaughan, D. J., eds., Modern Approaches to Ore and Environmental Mineralogy, 27. Short Course Series: Ottawa, Ontario, Mineralogical Association of Canada, p. 327-366.

Malvik, T., 1976, En undersøkelse av malmmineralers frimalingsegenskaper, NTH, 276 p.

Malvik, T., 1991, Partikkelkarakterisering ved bruk av bildeanalyse: Konferens i Mineralteknik, Luleå, 1991.

Reed, S. J. B., 2005, Electron Microprobe Analysis and Scanning Electron Microscopy in Geology: Cambridge, Cambridge University Press, 192 p.

Rosiwal, A., 1898, Ueber geometriches Gesteinanalysen usw.: Verh. der k. k. Geolog. Reichsanstalt Wien, p. 143-175.

Russ, J. C., 2002, The Image Processing Handbook: Raleigh, CRC Press, 732 p.

Russ, J. C., and Dehoff, R. T., 2001, Practical Stereology: New York, Plenum Press.

Schneider, C. L., Neumann, R., and Alcover-Neto, A., 2004, Automated, Adaptive Thresholding Procedure for Mineral Sample Images Generated by BSE Detector: 8th International Congress on Applied Mineralogy, ICAM 2004, Sao Paulo, Brazil, 2004, p. 103-106.

Thompson, E., 1930, Quantitative Microscopic Analysis: Journal of Geology, v. 27, p. 276.

Underwood, E. E., 1970, Quantitative Stereology, Addison-Wesley Publishing Company.

Development of the Particle Texture Analysis

6.1   INTRODUCTION

The main purpose of this doctoral engineering project has been to develop and implement a technology for automatic quantification of mineral particles with respect to modal mineralogy, mineral liberation and mineral associations. There were already two commercial systems on advanced particle analyses at the initiation of this project, but as these were dedicated systems tied up to certain equipment contractors it was decided to develop a new system based on commercial EDS software suitable for a multi-purpose electron microscope laboratory. The prototype resulting from this work is called "Particle Texture Analysis" abbreviated to PTA and is compatible with the Oxford Inca Feature software for data acquisition.

6.2 BACKGROUND

6.2.1 Process mineralogy

In mineral processing, minerals are separated by means of relative differences in physical properties. To achieve efficient separation, the minerals have to be sufficiently liberated before separation. It is therefore important to quantify mineralogical characteristics that affect the behaviour of minerals during processing (Lastra et al., 1998).

Petruk (2000) describes the acquisition of quantitative data for mineral processing. He points out the strengths and weaknesses of the different bulk analysis methods and concludes that these techniques are semi-quantitative when it comes to mineralogy and give no information regarding how the minerals occur in free and composite particles. Microscope analysis, however, provides vital information in combination with bulk analysis techniques (Moen et al., 2006).

6.2.2 Existing systems

Manual methods and image analysis in the optical microscope are cheap and appropriate for many purposes (e.g. Malvik, 1998). However, generally a more advanced method is needed when studying complex or trace mineralogy, fine particles, or silicates and carbonates that cannot be uniquely defined by image analysis in the optical microscope. It is then favourable to turn to an automatic scanning electron microscope (SEM) based image analysis system (Moen et al., 2006).

This chapter will present a new automatic SEM-based system, PTA, developed at the Norwegian University of Science and Technology during the work of this thesis. Several systems have been developed for mineral liberation (Gottlieb et al., 2000; Gu, 2004; Jones and Gravilovic, 1970; King and Schneider, 1995; Petruk, 2000; Schneider et al., 2004). Recent advances, particularly in computer technology, have made fast and user-friendly mineral liberation systems possible (Gu, 2003). Backscattered electron (BSE) signals can be used to generate images from the sample from which the minerals can be quantitatively measured using modern image analysis methods. Each grain outlined from BSE images can be identified with x-ray analysis positioned at the centre of the grain or collected

from scanning the whole grain. Minerals of similar BSE intensities can be discriminated using x-ray mapping (Gu, 2003, , 2004).

6.2.3 PTA system

The Particle Texture Analysis (PTA) system developed is flexible, relatively simple to operate for a mineralogist, and based on a commercially available particle analysis system. The main principals are similar to those of the former known systems. It can be run with any instrument, depends on a standard semi-quantitative EDS system and is a useful tool for almost any kind of material. The system is therefore suitable in a multi-purpose lab. The strength and the advantages of the system will be demonstrated through practical examples from the Norwegian mineral industry where essential information for the beneficiation process is exposed.

6.3   CONCEPT

6.3.1 Sample material

The samples most frequently investigated are polished sections of mineral particles embedded in epoxy resin. Screened grain-size fractions preferably with $D_{max}/D_{min}<1.6$ (Barbery, 1991) are investigated separately. The material is generally feed, products and waste from a mineral processing plant or a laboratory.

6.3.2 General concept

The PTA data acquisition is based on Oxford Inca Feature software ran with external procedures and any scanning electron microscope. BSE images are analysed in the spatial domain by means of grey-levels, and every grain of interest is analysed by x-rays if necessary. The resulting database and the images are then post-processed offline by the PTA software that performs mineral liberation, mineral association analysis as well as mineral intergrowth analysis by combining image analysis and x-ray data.

6.3.3 Concept of data acquisition

The data acquisition is based on two different signals: the backscattered electron (BSE) signal and the characteristic x-ray signal. Polished sections of narrow grain-size fractions are mounted into the specimen chamber and a BSE image is generated. The total area of interest and running parameters regarding image acquisition and x-ray analysis are defined. Typical microscope-, image acquisition- and x-ray acquisition settings are found in Table 6-1 and Table 6-2. For each field of view a grey-scale BSE image is acquired. By image processing, the particles are segmented from the background. Features smaller than a threshold of 10-30 pixels are normally ignored because of artefacts like edge effects and shadows from micro-cracks. A particle separation procedure separating touching particles and a grey-level analysis separating monomineralic grains within the particle is performed for each particle. If an EDS spectrum has to be acquired, the coordinates of the area of every grain in the particle are returned to the microscope. These areas/grains are scanned to collect separate EDS spectra. Process time and life time must be set so that the elements of interest are detected satisfactorily to be able to discriminate between the minerals of interest.

Table 6-1. Typical SEM settings during PTA analysis.

Parameter	Setting
Working distance	15 mm
Accelerating voltage	20 kV
Gun brightness (extr. voltage)	2.1 kV
Aperture	2 (50μm) or 3 (30μm)
Beam current	0.25-0.75 nA
Magnification	40-600x

Table 6-2. Typical BSE image and x-ray acquisition settings.

Parameter	Setting
Resolution	1024*896 pixels
Image dwell time	20 microseconds/pixel
Smallest features	20 pixels
Grey image processing	Median filter, 3x3 matrix, rank 4
Binary processing	Separation
X-ray live time	0.5-2 sec
X-ray process time	4-5 (medium-high)

The whole grain area is commonly used to collect x-rays, but the centre point may also be chosen. Morphological and chemical data from all analysed grains are stored in a database. To control the time and statistics, termination criteria regarding total number of features analysed or time spent, can be set.

The mineralogy of the samples investigated should be known previous to the analysis. To be able to discriminate between the minerals that are analysed, a classification file has to be computed. The classification file is computed from single element criteria or by matching spectra. The resulting analyses have to be classified during the run or subsequently. The resulting database and images acquired by the Oxford Inca Feature software are exported to the PTA software which performs image processing and analysis for the mineral liberation and mineral association measurements offline.

6.3.4 Concept of PTA

6.3.4.1 *General*

The databases and images from every analysed grain-size fraction are imported to the PTA software. The main steps of the analysis are:

- Reading information from the INCA database;
- Processing and calibration of grey-scale and binary images;
- Identification of grains and particles to evaluate whether grains occur liberated or in composite particles and which minerals that occur together in composite particles;
- Storage of output data in the new PTA database.

When the measurements are performed, queries can be performed in the PTA database to get tables, plots and thumbnail images regarding mineral liberations, associations and intergrowth.

6.3.4.2 *Detailed structure of PTA*

The basic elements of the PTA program include:

- The analysis settings including calculated pixel-size, grey-image and binary-image processing and threshold values are read from the INCA database;
- The unique parameters for each grain including grain identification number, mineral classification, coordinates and field number are read for every grain;

- Grey-scale and binary image processing are performed;
- Pixel-size calculation is performed;
- Grain identification and indexing is performed by means of coordinate- and field information and binary images of the grains;
- Analysis of common grain boundaries for the mineral grains in a particle is performed to find the grains that belong to the particle and for being able to measure the interface between minerals. For mineral liberation and mineral association analyses, the area method is used, and the methods are based on Lastra et al. (1998). For each field:
  - A binary of every threshold interval is made;
  - Loop: for the binary image of every threshold interval, dilation of 2 pixels is performed;
  - For every dilated binary image, "AND" Boolean operation is performed together with the binary image of all other thresholds in turn (produces the boundary line between the grains in the particles in turn) see Figure 6-1;
  - Grains with a common grain boundary then belong to the same particle;
  - Every particle is then given a particle identification number;
  - And every grain is given the corresponding particle identification number in addition to the grain identification number (for grains in the same particle, the particle identification number is equal);
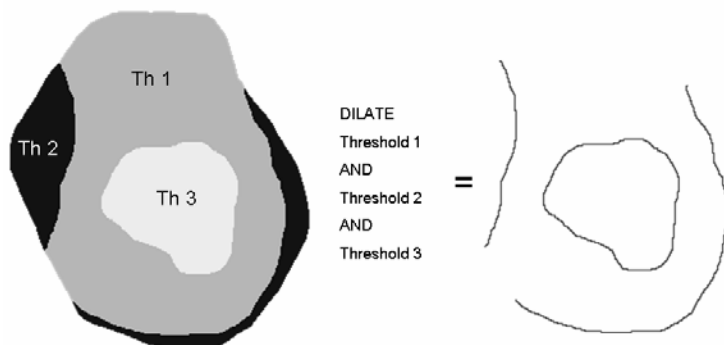
Figure 6-1. The principle of finding common grain boundaries for mineral grains in a particle (Figure: Torkjell Breivik).

- The outputs are then stored in a new PTA database including information on sample (grain-size fraction), location of raw-data database, field id, particle id, grain id, mineral id and morphology;
- From the PTA database queries may be performed to get the information of interest.

6.3.4.3 *Data that can be obtained*

Standard queries to be performed are mineral liberation of any mineral and mineral associations of any mineral. Searches on any mineral, mineral association or particle type can be done and thumbnail images can be viewed to study intergrowths etc. Minerals can easily be grouped to make a simpler picture.

6.3.4.4 *Development tools*

The PTA software is programmed in a graphic language (LabVIEW) from National Instruments (NI), using structured query language (SQL) towards databases (Access), and NI Vision library for image processing and analysis.

LabVIEW is a graphic high-level language (see Figure 6-2) that enables engineers and scientists to develop advanced applications for test, simulation, measurement and control systems. The code is drawn directly as a flow sheet (diagram) and can be test-run immediately. It is easy to monitor execution and debug code by following the data flow visually in the diagram. NI also provides a large number of functions for conditioning, mathematics, statistics, analysis and more that reduces the development time.

Human		
High-level language	Graphic language	
	Text language	
Low-level language	Assembly language	
	Machine language	
Hardware		

Figure 6-2. Levels of computer languages.

LabVIEW was chosen because of its intuitive time-saving manner, pre-build functions and its integration with other software and hardware by several standard technologies. Some programmers claim that graphic language could result in a slower compiled application than equivalent code in a text-based

language, but the main difference often depends on code optimisation rather than inherent speed.

In spite of the visual appearance graphic language has the same constructs as traditional text-based languages. It is therefore relatively straightforward to translate the software at a later stage, doing the time consuming work in another language.

6.3.5 Online with the customer

SEM-based image analysis systems are visual, and to fully utilize the results, the customer should be able to navigate within the system and try out different options. The customers from the Norwegian industry can therefore log on through a server to be able to evaluate the results alone or together with the researcher. A VNC server is used for this purpose.

6.3.6 Challenges on the way

The process of developing PTA and the interface towards Oxford Inca Feature was relatively long and complicated refining the idea how to design the software and the algorithms. The PTA was then dependent on implementing some identical data structures that were already present in Inca Feature and finding all the indexes varying from run to run. A good dialogue with Hans Otterström at Link Nordiska AB in Stockholm and the developers at Oxford Instruments, UK was therefore valuable. Oxford Instruments has been helpful providing image processing details that were essential, and Hans Otterström has assisted in making external procedures, exporting uncompressed, original images during the run and fitting some routines in INCA that did not satisfy our further use of the data. ActiveX was used to make the external procedures.

6.4 FURTHER DEVELOPMENT

6.4.1 Status

The prototype of the PTA programme is now performing well and the main structures of the programme are established and well tested. The different operations are working satisfactory, but there are obviously several areas for

improvements that will be carried out in the near future. The main areas of optimisation are discussed in the following chapters.

6.4.2 Data acquisition

A more sophisticated data acquisition procedure is needed, allowing automatic grey-scale analysis of every particle instead of interactive thresholding of the total grey-scale histogram. It will also allow a tighter interface with Inca Feature, providing integrated online measurements which make a smoother and less time-consuming system. This will be a significant improvement for the user and for the quality of the results. The implementation of this procedure is planned to be carried out by exporting the BSE image by an external procedure and treat it in separate image analysis software as follows:

- The particles are segmented from the background by grey-scale thresholding;
- An improved particle separation procedure is performed to separate touching particles;
- The grey-levels of every single particle are automatically analysed by means of distance testing of the grey-level of every pixel, detecting every grey-level region in the particles. This will make the data acquisition more flexible, avoiding unsuccessful detection of grain where the threshold values fall inside the grey-level peak;
- Grain indexing, particle indexing, morphological measurements and common grain boundary measurements are performed;
- A binary image containing separated areas for every grey-level region (or mineral grain) that is to be analysed by EDS, is returned to Inca Feature;

A more flexible routine to adjust the way of acquiring data for each grey-level choosing between morphology only, morphology and chemistry or elemental mapping to separate minerals of similar Z-contrast is also required. This routine can be implemented in the one just described.

A more integrated system also makes it possible to develop statistic stop criteria that will automatically stop the run when the criteria are met. This will be further discussed before implementation.
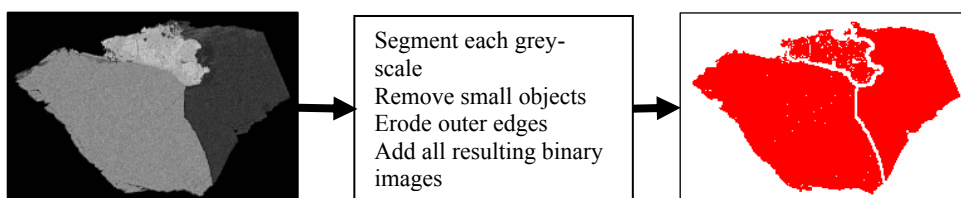
Figure 6-3. Binary image showing separated areas for every grey-level-region in a particle. By means of the separated areas in binary image, The Inca Feature software can perform individual EDS measurements for every grey-level (mineral grain) in one operation. (Figure: Torkjell Breivik).

6.4.3 Queries

At present, the data is not fully utilized in the standard queries available. Development of various queries on for example free mineral surface, contact surface between minerals, average surface composition of the particles and quantitative measurements on particle texture are a priority. In addition an improved particle search for viewing thumbnail images is desirable, making it easier to collect exactly the information requested.

Last, but not least, a better statistic evaluation of the analyses is required.

6.5 **APPLICATION EXAMPLE OF PTA ANALYSIS**

The PTA programme has already been tested on several problems for the mineral industry. Figure 6-4 - Figure 6-6, Table 6-3 and Table 6-4 show some examples of data that can be obtained. Explanations are found in the figure text.

In addition, Paper 1 titled "Particle Texture Analysis in Process Mineralogy" presented at the XXIII International Mineral Processing Congress (IMPC) in Istanbul, September 2006 also presents application of the PTA. (Moen et al., 2006).

Modal mineralogy in carbonate tailing
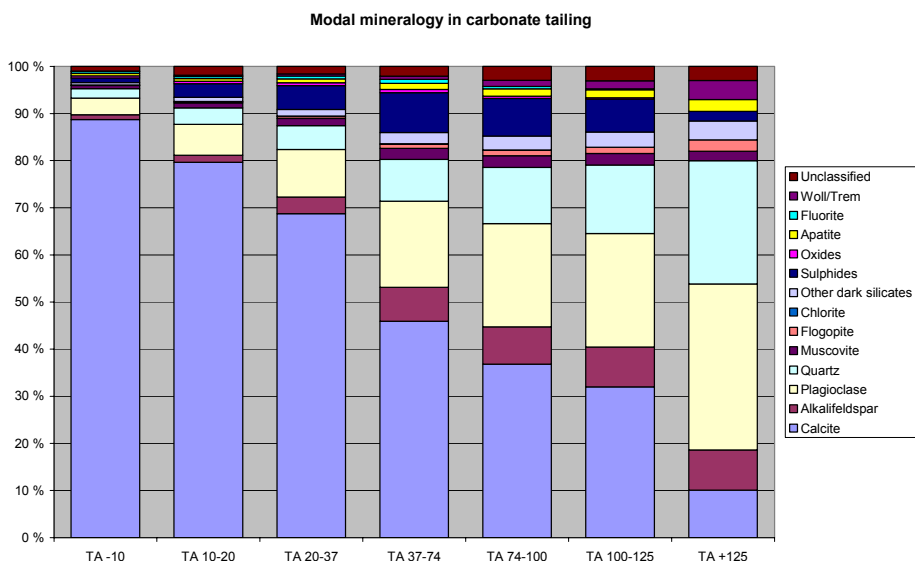
Figure 6-4. Modal mineralogy in grain-size fractions for waste from a carbonate plant displaying a major carbonate loss in the fine fractions.

Table 6-3. From the modal mineralogy of iron ore, contribution to CaO, Al$_2$O$_3$ and MnO from the gangue minerals can be calculated. The result displays which minerals that should be especially monitored in the beneficiation process.

Mineral	CaO -106μm	Al$_2$O$_3$ -106 μm	Mno -106 μm
Hematite	0.00	**0.18**	0.00
Rutil	0.00	0.00	0.00
Sulphides	0.00	0.00	0.00
Apatite	0.05	0.00	0.00
Carbonates	**1.03**	0.00	**0.31**
Plagioclase	0.00	0.03	0.00
Biotite	0.00	0.08	0.00
Quartz	0.00	0.00	0.00
Muscovite	0.00	**0.14**	0.00
Epidot	**0.34**	**0.36**	0.00
Chlorite	0.00	0.00	0.00
Amphibole	0.00	0.00	0.00
Garnet	0.04	**0.23**	**0.39**
Unclassified	0.00	0.00	0.00
Totalt	1.48	1.02	0.71

85
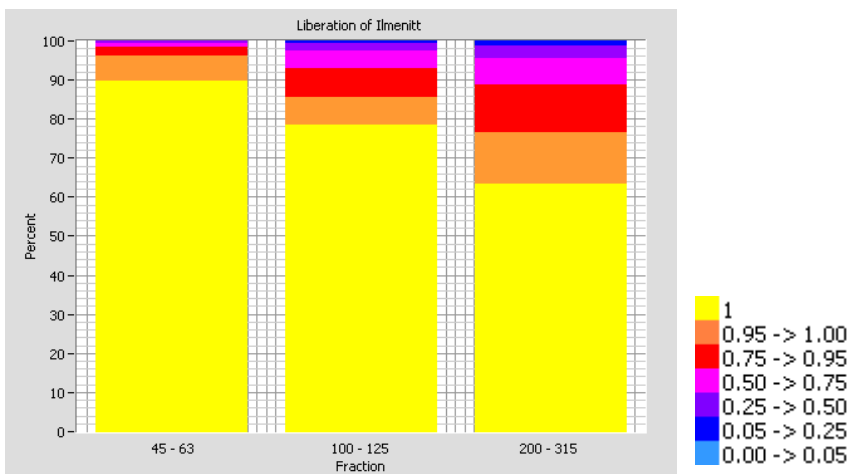
Figure 6-5. Apparent liberation of ilmenite in a raw material. The colour code reflects the grade of ilmenite in particles, where yellow is totally liberated ilmenite particles and orange reflects ilmenite particles containing less than 5 % pollution etc.

Table 6-4. Minerals associated to ilmenite in a raw material for three grain-size fractions. The minerals are grouped to make a simpler picture. The V% columns display the amount, in volume%, of this particular particle type. Intergrowths with silicates are most common while intergrowths with rutile are obviously better detected at high magnifications since the amount is increasing in the fine fractions.

Minerals associated to Ilmenite	V% 45 – 63µm	V% 100 – 125µm	V% 200 – 315µm
Ilmenite	89.7	78.6	63.2
Ilmenite/Magnetite	0.2	0.1	0
Ilmenite/Rutile	1	0.7	0.4
Ilmenite/Silicates	7	15	29.9
Ilmenite/Magnetite/Silicates	0	0.1	0.3
Ilmenite/Rutile/Silicates	0.5	0.9	0.9
Ilmenite/Magnetite/Rutile/Silicates	0	0	0
Ilmenite/Trace minerals	0.4	2.1	1.5
Ilmenite/Magnetite/Trace minerals	0.1	0.1	0.1
Ilmenite/Rutile/Trace minerals	0	0.3	0.3
Ilmenite/Silicates*/Trace minerals	1	1.4	2.8
Ilmenite/Magnetite/Silicates/Trace minerals	0.1	0.2	0.2
Ilmenite/Rutile/Silicates/Trace minerals	0	0.3	0.3
Ilmenite/Sulphides	0	0	0
Ilmenite/Silicates/Sulphides	0	0.1	0.1
Ilmenite/Magnetite/Silicates/Sulphides	0	0	0
Ilmenite/Silicates/Trace minerals/Sulphides	0	0	0
Ilmenite/Magnetite/Silicates/Trace minerals/Sulphides*	0	0	0
Ilmenite/Magnetite/Rutile/Silicates/Trace minerals/Sulphides	0	0.1	0
Sum	100	100	100
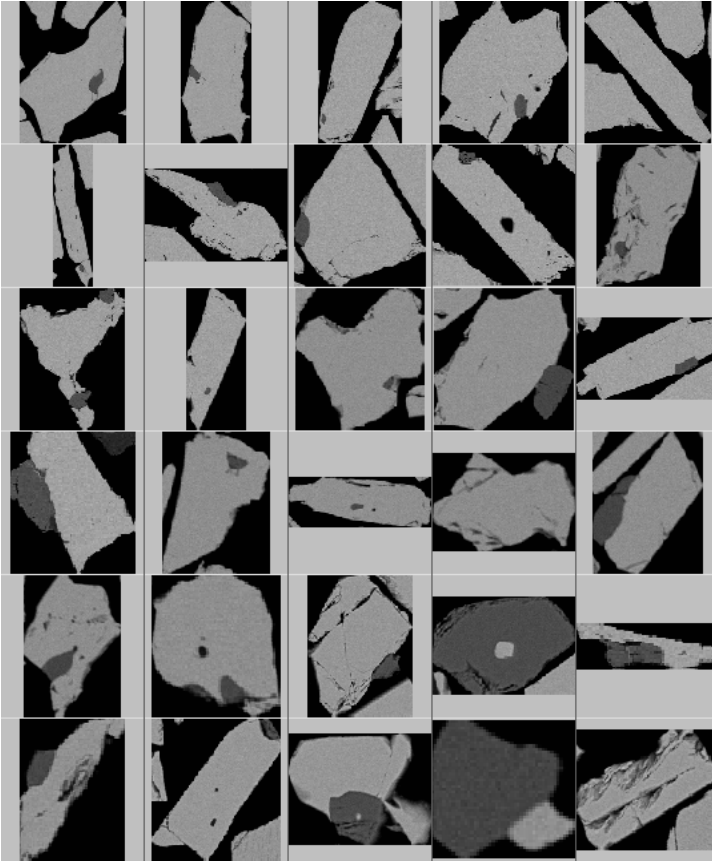
Figure 6-6. Thumbnail images of apatite (dark grey) and hematite (grey) intergrowths in a hematite concentrate. The apatite grains locked in the hematite grains are not easily separated in a beneficiation process.

6.6 **REFERENCES**

Barbery, G., 1991, Mineral liberation: measurement, simulation and practical use in mineral processing: Quebec, Canada, Les Editions GB, 351 p.

Gottlieb, P., Wilkie, G., Sutherland, D., Ho-Tun, E., Suthers, S., Perera, K., Jenkins, B., Spencer, S., Butcher, A., and Rayner, J., 2000, Using Quantitative Electron Microscopy for Process Mineral Applications: JOM Journal of Metals, v. 52, p. 24-25.

Gu, Y., 2003, Automated Scanning Electron Microscope Based Mineral Liberation Analysis: Journal of Minerals & Materials Characterization & Engineering, v. 2, p. 33-41.

Gu, Y., 2004, Rapid Mineral Liberation Analysis with X-ray and BSE Image Processing: 8th International Congress on Applied Mineralogy, ICAM 2004, Sao Paulo, Brazil, 2004, p. 119-122.

Jones, M. P., and Gravilovic, J., 1970, Automatic quantitative mineralogy in mineral technology: Rudy, v. 5, p. 189-197.

King, R. P., and Schneider, C. L., 1995, Basic image analysis for the measurement of mineral liberation, *in* Hagni, R. D., ed., Process Mineralogy XIII, 8, The Minerals, Metals & Materials Society, p. 145-157.

Lastra, R., Petruk, W., and Wilson, J., 1998, Image-analysis techniques and application to mineral processing, *in* Cabri, l. J., and Vaughan, D. J., eds., Modern Approaches to Ore and Environmental Mineralogy, 27. Short Course Series: Ottawa, Ontario, Mineralogical Association of Canada, p. 327-366.

Malvik, T., 1998, Relations between mineralogical textures and comminution characteristics for rocks and ores: XVI International Mineral Processing Congress, Amsterdam, 1998.

Moen, K., Malvik, T., Breivik, T., and Hjelen, J., 2006, Particle Texture Analysis in Process Mineralogy: XXIII IMPC 2006, Istanbul, Turkey, 2006.

Petruk, W., 2000, Applied Mineralogy in the Mining Industry: Ottawa, Ontario, Canada, Elsevier, 268 p.

Schneider, C. L., Neumann, R., and Alcover-Neto, A., 2004, Automated, Adaptive Thresholding Procedure for Mineral Sample Images Generated by BSE Detector: 8th International Congress on Applied Mineralogy, ICAM 2004, Sao Paulo, Brazil, 2004, p. 103-106.

Summary of the papers

7.1 PAPER 1: PARTICLE TEXTURE ANALYSIS IN PROCESS MINERALOGY

This paper presents a new automatic SEM based system, Particle Texture Analysis, developed at the Norwegian University of Science and Technology. The strength of the system is demonstrated through practical examples from the Norwegian mineral industry, where essential information for the beneficiation process as modal, main and trace mineralogy, mineral liberation, mineral associations and intergrowth is exposed. Through online interaction with the customer, the results can be fully utilised. The system is still a prototype that will be further developed, but the framework is established, and particle texture data can be significantly provided (Moen et al., 2006b).

7.2 PAPER 2: EBSD – A POTENTIAL SUPPLEMENTARY TECHNIQUE IN QUANTITATIVE CHARACTERISATION OF MINERALS

In this paper, the use of EBSD in applied mineralogy is discussed. Automatic identification and characterisation of mineral raw materials and beneficiated products are of major importance in mineral processing. However, minerals

show great variety in their composition and physical and chemical properties. Industrial minerals may contain the same elements in about the same amount. In these cases backscatter electron imaging or chemical analysis are not sufficient to identify the minerals. Another problem arises when microtextures are not detectable in traditional imaging or the grain-size is smaller than the x-ray spatial resolution.

As a supplementary technique in these cases, application of crystallographic information by electron backscatter diffraction (EBSD) in the scanning electron microscope (SEM) may be a suitable method. By means of EBSD, diagnostic mineral information can be achieved if indexible patterns are provided.

Until now EBSD has not been used frequently on geological samples for mineral and microstructure discrimination. In the paper the technique has been demonstrated on three Norwegian mineral raw materials and one Italian marble and the advantages and limitations of the technique are discussed (Moen et al., 2003).

7.3 PAPER 3: EBSD MICROSTRUCTURE MEASUREMENTS OF MARBLE

Bowing of crystalline marble when used as exterior thin claddings is experienced occasionally on buildings around the world. A European research project was- investigating this deterioration phenomenon and influencing intrinsic and extrinsic parameters. One of several approaches for investigation of intrinsic parameters is microstructure measurements by Electron Backscatter Diffraction (EBSD). In this paper the rock microstructures of two marbles have been investigated and the EBSD analyses show that the microstructure is intuitively different when comparing them. While the non-bowing marble shows xenoblastic microstructure with sutured grain boundaries and pronounced twinning, the bowing marble shows granoblastic and polygonal microstructure. The EBSD results indicate that the stable marble shows a stronger texture (lattice preferred orientation) than the bowing marble, which shows more random orientation. This trend confirms the statement of Barsottelli et al. (1998) and is also in accordance with proton diffraction analyses performed by the partners of the European research project (Moen et al., 2004).

90

7.4 PAPER 4:
QUANTITATIVE MEASUREMENTS OF MARBLE MICROSTRUCTURE – A MODEL FOR PREDICTING THE DETERIORATION OF MARBLE

Deterioration of marble used as exterior marble cladding panels is experienced occasionally. Many researchers have studied this effect and it is commonly concluded that the most relevant extrinsic factor is temperature variation in combination with moisture. The intrinsic factor that gives rise to the phenomenon for certain marbles lies in the microstructure. This paper presents quantitative data of different microstructure parameters in marble. By use of laboratory bowing data, the microstructure data has been linked to bowing. Development of a model to predict the bowing by means of important microstructure parameters was suggested. The results showed that by interaction of several microstructure parameters, bowing could be significantly described in a regression model. The variables that influenced the model most heavily were grain shape factors describing the roundness and roughness of the grain boundaries and of the shape of the grain size distribution curve (Moen et al., 2006a).

7.5 PAPER 5:
RECONNAISSANCE STUDY OF COMPACTION MICROSTRUCTURES IN QUARTZ GRAINS AND QUARTZ CEMENT IN DEEPLY BURIED SANDSTONES USING COMBINED PETROGRAPHY - EBSD ANALYSIS

Sandstones diagenesis involves porosity loss by mechanical and chemical compaction. In this study we have examined relations of diagenesis and microstructures in quartz grains and quartz cement in sandstones from relatively deep burial depths offshore mid Norway. Electron backscatter diffraction analysis (EBSD) has been combined with optical and cathodoluminescence petrography study of samples with different degrees of compaction and quartz cementation. Quartz cement is shown to be syntaxial to the nearest host domain (grain or subgrain), both for monogranular, polygranular, undeformed and deformed quartz. The quartz cement growth may have been initiated at different subgrain surfaces, and preserving pre-depositional deformation structures. EBSD inverse pole figure imaging shows dauphine twins to be common in all samples, both in quartz grains and quartz cement. The dauphine twins appear in grain-

grain contacts and in cement -crystal boundaries, and commonly crossing grain-cement boundaries. On basis of twin distributions we suggest that both inherited twins from the source area and twins formed by compaction-induced grain boundary deformation are present. A general problem in sedimentary rocks is to distinguish inherited from sedimentary compaction-induced deformation structures. More comprehensive following up studies are suggested to investigate the role of ductile deformation mechanisms (e.g. twinning) in sediment compaction (Mørk and Moen, 2006a, 2006b).

7.6   **REFERENCES**

Moen, K., Malvik, T., Alnæs, L., and Hjelen, J., 2006a, Quantitative measurements of Marble Microstructure - a model for predicting the deterioration of marble: Environmental Geology, v. In prep, p. 17.

Moen, K., Malvik, T., Breivik, T., and Hjelen, J., 2006b, Particle Texture Analysis in Process Mineralogy: XXIII IMPC 2006, Istanbul, Turkey, 2006b.

Moen, K., Malvik, T., Hjelen, J., and Leinum, J. R., 2003, EBSD-A Potential Supplementary Technique in Quantitative Characterisation of Minerals: XXII IMPC, Cape Town, South Africa, 2003.

Moen, K., Malvik, T., Hjelen, J., Leinum, J. R., and Alnæs, L., 2004, EBSD Microstructure Measurements of Marble: 8th International Congress on Applied Mineralogy, ICAM 2004, Sao Paulo, Brazil, 2004, p. 145-148.

Mørk, M. B. E., and Moen, K., 2006a, Reconnaissance study of compaction microstructures in quartz grains and quartz cement in deeply buried sandstones using combined petrography - EBSD analysis: In thesis Moen 2006, in prep for journal, p. 17.

Mørk, M. B. E., and Moen, K., 2006b, Textural relations of quartz grains and diagenetic quartz cement in deeply buried sandstones, offshore Norway. A petrography and SEM EBSD study: EGU06, 2006b.

General discussion

8.1 THE PROJECT

8.1.1 Purpose and scope of work

The background for this doctoral project is the need for quantification of mineralogical and microstructure parameters in the production and beneficiation of minerals. In Norway, quantitative microscopy has traditionally been measured manually or by image analysis in optical microscope. As described in the introduction chapter, the overall purpose of the project has been to develop skills and techniques on detection and quantification of mineralogy and microstructures by means of various scanning electron microscopy (SEM) techniques. A premise for success was then to develop a close cooperation with the staff at the electron microscopy laboratory at the Department of Materials Science and Engineering at the initiation of this project.

The specific objective of the project has been to develop and implement automatic SEM-based quantitative measurements on major and trace minerals in rocks, ores and milled products in order to measure modal mineralogy, microstructures and particle texture included mineral liberation and mineral association.

Through collaboration with engineers and researchers in different aspects of mineral production, the scope of work seems to have become wide. It has included development of skills in electron microscopy, development of software, implementation and testing of software, and case studies for the industry and other collaborators in fields of application from mineral processing to building materials, gold exploration, environmental issues and petroleum reservoir research. The equipment, measuring methods and the understanding of quantitative measurements of mineralogy and microstructures are however related and combine the work to a confined scope of the study.

8.1.2 Strategies

The objective of the work is described in the introduction chapter and in the chapter above. The strategy, however, to obtain the objective was to develop a particle analysis system along with competence in the field, by means of close cooperation with the industry and early publication of papers at international conferences to get feedback through the whole process.

As already mentioned, it was chosen to develop a new particle system based on commercial EDS software rather then buying one of the two commercially available systems from Australia (MLA or Quemscan). The arguments for this strategy were the fact that the laboratory is a multi-purpose laboratory, and the available commercial systems were expensive and dedicated systems dependent on predetermined microscope contractors. Another important argument for making our own system was the fact that it would also develop valuable competence along with the development of the system. Arguments against this choice are an unnecessary and slow process towards the goal of being able to do advanced particle measurements. It could have been possible to make good appointments with one of the existing contractors on building a university laboratory. A lot of skills and competence would then have been transferred from experienced people and a valuable network could have been developed.

Future choices will determine whether the best solution was chosen. Competence has been developed in the fields of quantitative analysis, electron microscopy, image analysis and programming, and a good team has evolved from the project. This team is now in position of being able to further optimise the system for a full implementation by Oxford Instruments Feature system.

However, human and economic resources must be highly prioritised to be able to put the project forward.

Because of close cooperation with the industry, extencive tasks have been carried out throughout the whole project and have driven forward the prototype of PTA. In retrospect, it has mainly been a good strategy getting the programme operative and being able to run analysis. Analyses can then be carried out at the same time as improvements and optimisation work are performed.

To gain publicity for the project and to get feedback from the researcher in the fields covered by the theses, early publications were published at international conferences. On one hand, the papers and posters published reveal that it is early work, on the other hand, this strategy led to an early contact with international research colleges in applied mineralogy.

8.2 **PAPERS**

8.2.1 **Introduction**

Five papers are included in the thesis. Paper 1 and Paper 2 present methods for quantitative measurements of minerals by means of SEM. The papers cover the principles of PTA analysis, principles of EBSD analysis and some case studies. In addition, Chapter 6 treats the development of the PTA analysis more thoroughly. These papers and chapters are discussed in Chapter 8.2.2. Papers 3, 4 and 5 present microstructure studies of marbles and deeply buried sandstones. These papers are discussed in Chapter 8.2.3 and Chapter 8.2.4.

8.2.2 **Papers1 and 2 - Quantitative characterisation of minerals in SEM**

8.2.2.1 *The PTA system*

In Paper 1 and in Chapter 5, the development, performance and use of the PTA system is described and discussed. It was chosen to develop a new system based on commercial EDS software rather then buying one.

The system is based upon image analysis of BSE images and EDS analysis. Yet the system is somewhat static, making it rather bothersome to adapt the need for EDS analysis only to certain grey-levels and only morphology measurements for the rest. For the total mineralogy analyses carried out throughout the project

period, all particles have so far been analysed by means of EDS. For rare mineral searches or studying of only the heavy minerals etc., only the relevant minerals are analysed by means of EDS, decreasing the time of analysis. On the other hand, there are some advantages using the extra analysis time needed for including EDS analysis. The chemical information leaves less of the judgement to the operator, and it is possible to check the results subsequently. This is especially important for full process evaluation. For routine investigations, a satisfactory but effective analysis should be performed using only grey-level analysis on the minerals possessing a unique grey-level.

Despite the possibilities of using both image analysis of BSE images and EDS analysis in a system like this, there are still some limitations. The main limitation is the fact that some minerals possess very similar average atomic number and thus similar grey-levels. As long as the grains are outlined by means of grey-level analysis, minerals of similar grey-levels will not be distinguished and a mixed EDS analysis will be obtained. This problem is most prominent when analysing whole rock samples where all the mineral grains are in contact with each other. All minerals of similar grey-level that are in contact will not be distinguished by using this method. In particle analysis, the problem arises only for minerals of similar grey-levels that are grown together in a particle. An example of this limitation can be seen for the sulphide minerals from Titania. When the contrast is optimised for discrimination of the silicates, ilmenite and magnetite, the sulphide mineralogy gets oversaturated (white colour) leaving no contrast between the sulphide minerals. These minerals are therefore analysed as a common sulphide-class and not as separate minerals when the total mineralogy is analysed. If the contrast is optimised for sulphide analysis, most of the minerals are discriminated, but still pentlandite and chalcopyrite will be impossible to discriminate if they are in contact. This can be solved by EDS mapping or matrix point analysis, drawing the boundaries from these.

The concept of using a commercial software contractor for data acquisition can be risky, but on the other hand, the format of the acquisition data is general and can relatively easily be adjusted to another system. The particle analysis module Oxford Inca Feature was found to be very simple in the standard form and was flexible and permitted also external procedures to adapt the acquisition for more advanced problems. Because of the possibility to perform external procedures, it is also easier to totally integrate the Inca Feature and the PTA systems. When the

systems are integrated, the flexibility will be increased significantly permitting the operator to select among the following alternatives:

- Grey-level morphologic analysis;
- Grey-level morphologic analysis and EDS spectra;
- Grey-level morphology, EDS spectra and EDS mapping to discriminate minerals of similar grey-levels.

The last alternative will then be more time consuming but allow separation of minerals like quartz/albite and pentlandite/chalcopyrite etc. These new possibilities will make it easier to adapt the way of acquiring data to the actual problem and save time and enable analysis of more samples during a night run.

Time is an important issue when it comes to particle analysis. The need for obtaining a certain level of statistic confidence by analysing a corresponding number of grains, and the time of analysis, leads to time-consuming runs especially when trace mineral analysis are to be measured. The critical points for time consumption are image acquisition and EDS live time. The image acquisition time needs to be long enough to obtain images with a satisfactory quality making the details of interest visible. The EDS live time need to be long enough to obtain sufficient counts to detect and discriminate the elements of interest. Time can therefore be decreased by decreasing the number of EDS analyses or by increasing the number of EDS detectors. The MLA system uses two EDS detectors while Quemscan uses four EDS detectors, however Quemscan uses EDS analysis instead of grey-level analysis to map and outline every mineral grain and therefore needs extraordinary good EDS capacity.

At the moment, a limited number of pre-defined queries can be performed in the resulting PTA database. From the available images and databases, an unlimited number of measurements and queries can be made. The amount of information for the process engineer is already overwhelming. The effort will therefore be prioritised on integrating the Feature and the PTA systems and making the analysis more flexible, before implementation of new queries and refining existing ones.

As described in Chapter 6.3.4.4, the PTA software is programmed in the graphic language LabVIEW from National Instruments (NI), using structured query language (SQL) towards databases (Access), and NI Vision library for image processing and analysis. Since the code is drawn directly as a flow sheet diagram and can be test-run immediately, it is easy to monitor execution and debug code

by followin the data flow visually in the diagram. NI also provides a large number of functions for conditioning, mathematics, statistics, analysis and more that reduce the development time. LabVIEW was chosen because of its intuitive time-saving manner, pre-build functions and its integration with other software and hardware by several standard technologies. Graphic language has the same constructs as traditional text-based languages. It is therefore relatively straightforward to translate the software on a later stage, doing the time-consuming work in another language.

The companies and research institutions in Norway are each not large enough to afford a dedicated particle analysis system requiring a dedicated operator. The need for a central laboratory serving the companies is therefore a good solution. The possibility to log-on to explore the results is therefore valuable to fully utilise the results. At the same time it is a future goal to introduce the PTA system on the commercial market.

8.2.2.2 *EBSD in applied mineralogy*

As described in Chapter 4.3, EBSD is a relatively new technique to the geologist and even newer to the applied mineralogist. The EBSD technique introduces a new approach to electron microscopy, making it possible to measure crystallographic properties in addition to topography, compositional contrast, chemical composition and emitted cathodoluminescence. The technique is discussed in Paper 2 and also in Chapter 4.3. In Paper 2 the application of EBSD as a tool to discriminate, among others, minerals in process mineralogy is discussed. Examples are given from ilmenite ore, forsterite/enstatite discrimination and hematite/magnetite discrimination. At the moment, EBSD is a slow and tedious technique that is not well suited to give quick particle analysis for particle texture analysis. The sample preparation is critical, the area of analysis is limited, many minerals are not easily discriminated and the sample has to be tilted during analysis. All together this does not make EBSD suitable for standard particle analysis.

These drawbacks however, do not make EBSD less interesting, but the field of application should be right and utilise what is unique about EBSD. The crystallographic approach is extremely interesting for many purposes. Future improvements and integration of various techniques will also increase the areas of use. Pattern acquisition speed (not indexed) exceeding 200 patterns/sec will

for example soon be available (Jarle Hjelen personal communication 2006). Some of the examples described in Paper 2 are not relevant for EBSD. The minerals in the ilmenite ore and enstatite/forsterite are more easily discriminated by BSE images and EDS, but for hematite/magnetite, EBSD can be relevant in cases of fine grains where optical microscopes do not have satisfactory resolution for measurements. For the discrimination of polymorphs (Al_2SiO_5, SiO_2) on the other hand, EBSD is superior since crystallography is the only characteristic that distinguish the phases. Discrimination between several minerals is not straightforward requiring thorough calibration and optimization to avoid misindexing of the patterns. The more phases introduced to the system simultaneously, and the more complex phases and crystallography, the grater the chance for misindexing.

Therefore, the area in applied mineralogy where EBSD is most useful is probably in quantitative measurements of lattice orientations and fabric parameters obtained from the measurements of orientation of crystals. When diffraction patterns are analysed in an array of steps (pixels), almost unlimited possibilities exist for making use of the data. Presentation of the orientation results in the form of maps and plots of grain boundaries (high/low angle and twin boundaries), inverse pole figure orientations, misorientation, pattern quality, grains-size, grain-shape and orientation or combinations of various information, all display information derived from the orientation data. This means that EBSD can also be used even when lattice orientation is not the main purpose of the analysis, if new information becomes visible by the use of this technique. In theoretical geology, EBSD is mostly used for studying deformation of quartz and carbonate rocks. In applied mineralogy, problems in petroleum geology for studying deformation of reservoir rocks (Mørk and Moen, 2006a, 2006b) are relevant in addition to behaviour of rock used as dimensional stones in the building industry (Moen et al., 2004).

In process mineralogy, EBSD has best potential in combination with other techniques such as image processing and analysis, and traditional particle analysis by means of BSE images and EDS measurements. The ability to segment the particles of interest and then be able to make one or a small number of measurements in the grains of interest for discrimination purposes could be useful in some situations. As concluded in Paper 2, EBSD creates together with SE images, BSE images, EDS spectras and cathodoluminescence, a complete

family of related techniques which together can discriminate most minerals and microstructures. But what is always vital, to achieve a successful result, the operator needs to possess knowledge about the techniques and the sample.

8.2.3 Papers 3 and 4 - Microstructure measurements of marble

Paper 3 describes an EBSD investigation of two marble types taken from a comprehensive study of deterioration of marbles used as exterior cladding panels ("TEAM"). The marbles were chosen because one is known to deteriorate and bow while the other remains relatively stable. Appendix 2 also show some further results from this study. From the work presented in Paper 4 on microstructures of marble, it is evident that taking out only two marbles from the sample-set is a risky project since the rocks holds a variety of microstructures and grain-sizes, and the system is multivariate and complicated. On the other hand, the two rocks compared are analogue when it comes to relative and absolute grain-size and only differ in grain-shapes, grain-boundaries and twinning formation. Some important differences can therefore be established. The results are in accordance with for example Koch and Siegesmund (2004) and show that stable marble displays a slightly more distinct lattice preferred orientation with a single c-axis maximum and a girdle distribution of the a-orientation, and the bowing marble shows more or less random lattice orientation. This is also in accordance with the appearance of the microstructure of the rocks in the microscope. The conclusions in Paper 3 and Appendix 2 diverges however slightly from former work (e.g. Koch and Siegesmund, 2004; Zeisig et al., 2002).

Bowing marble inhabits a typical polygonal, even-grained, idioblastic texture with straight grain boundaries, displaying totally recrystallised grains which show neither twinning nor undulose extinction, indicating very little deformation. The more stable marble shows an increasing grade of undulose extinction, deformation twins, some subgrain formation and widespread grain boundary migration resulting in sutured to lobate grain boundaries. As discussed by Koch and Siegesmund (2004), the lattice preferred orientation can be important for the direction-dependent bowing of certain crystalline marbles because of a big difference in expansion coefficient in the c- and a-direction. But since the strong bowing marble displays very weak or no preferred lattice

orientation, preferred orientation is secondary for the absolute bowing intensity. Direction dependent bowing is also most prominent for the bowing marble with more or less random distribution of lattice orientations. From the work in Appendix 2, it is also indicated that grain shape orientation can be equally important for direction dependent bowing giving rise to a higher number of grain boundaries normal to the foliation since the strongest bowing tendencies are also found in this direction.

From Paper 3 and 4 and the work by e.g. Alnæs et al. (2004) or Åkesson et. (2006), the grade of deformation of the marbles seems to be what is most important. The strength of the lattice preferred orientation is therefore an indication of this grade of deformation, but quantitative measurements of the lattice preferred orientation seem to be less useful than other microstructure elements described in Paper 4. Since many of the marbles used for cladding panels are relatively coarse grained, poor statistics are obtained when analysing an area of a polished section by EBSD. In the studies of e.g. Koch and Siegesmund (2004) neutron diffraction on marble cylinders of 40 mm diameter and 40 mm height were used. More representative measurements of lattice orientation of coarse samples were then obtained.

Paper 4 takes the approach of using image analysis of optical micrographs and microscopy studies and measurements for doing quantitative measurements of the microstructure. The different variables are then used in a partial least square regression to describe bowing and to be able to predict bowing in future rocks for marble cladding panels. It is evident that the deterioration problem is complex because of rocks possessing a wide variety of properties. When a prediction model is to be calculated, the size and the quality of the response dataset are extremely important parameters. As stated by e.g. Kock and Siegesmund (2004), the marbles are anisotropic and nonhomogeneous. This explains the variations between the laboratories in the bowing intensity together with slightly diverging laboratory procedures as shown in Table 3 in Paper 4. To be able to calculate a more optimised model, the distribution of bowing tendencies for each rock together with data from rocks spanning the variation-space between the extreme sample (Itq2) and the others should be available.

Paper 4, however, shows that it is possible to describe bowing by means of microscope properties. It is important to include a multivariate set of variables to cover the total variation of microstructures in the rocks that are important for

deterioration. In addition to the fact that grain-shape factors and the shape of the grain-size distribution curve showed to be most important for bowing, the model can be used as a guideline when investigating marbles for this purpose in the future.

8.2.4 Paper 5 – Microstructural relations of quartz and quartz cement

The aim of this study was to use new techniques to examine microstructural relations of quartz and quartz cement and find possible evidences of compaction-induced deformation at relatively deep burial diagenetic conditions. The motivation for the study was to get a deeper understanding of quartz cementation as a main porosity-reducing factor in deep reservoir sandstones offshore Norway (Mørk and Moen, 2006b).

The conventional methods of microscopy applied in this project are widely used in petroleum geology (optical, CL, BSE); EBSD however, is a new technique to the petroleum geologist. Cooperation between the author and Professor Mai Britt Mørk was therefore established.

Dauphiné twins are not visible by optical microscopy, but can be studied optically on a coarse level by etching polished surfaces of quartz and illuminating them at certain angles. The resolution, however, is limited as well as the information. EBSD was used to obtain information both about twinning and low angle boundaries. EBSD also confirmed the syntaxial growth of diagenetic quartz cement on quartz grains. Cathodoluminescence was therefore used to discriminate detrital grains from the quartz cement. By combining these techniques it was possible to study low angle boundaries and twins in both the detrital quartz grains and the quartz cement.

The paper clearly demonstrates the importance of combining various approaches in optical and electron microscopy to obtain the right information for interpreting mineral growth and deformation. Such combinations are valuable in various areas of geological research. It also reveals new possibilities of studying mechanisms of compaction and quartz cement growth in sandstone diaganesis. In a following-up study, compaction- and cementation-microstructures in stylolitic sandstones from the Barent Sea will be studied.

8.3 **REFERENCES**

Alnæs, L., Koch, A., Schouenborg, B., Åkesson, U., and Moen, K., 2004, Influence of Rock and Mineral properties on the durability of marble panels Dimension Stone 2004, New perspectives for a traditional building material, Prague, Czech Republik, 2004.

Koch, A., and Siegesmund, S., 2004, The combined effect of moisture and temperature on the anomalous expansion behaviour of marble: Environmental Geology, v. 46, p. 350-363.

Moen, K., Malvik, T., Hjelen, J., Leinum, J. R., and Alnæs, L., 2004, EBSD Microstructure Measurements of Marble: 8th International Congress on Applied Mineralogy, ICAM 2004, Sao Paulo, Brazil, 2004, p. 145-148.

Mørk, M. B. E., and Moen, K., 2006a, Reconnaissance study of compaction microstructures in quartz grains and quartz cement in deeply buried sandstones using combined petrography - EBSD analysis: In thesis Moen 2006, in prep for journal, p. 17.

Mørk, M. B. E., and Moen, K., 2006b, Textural relations of quartz grains and diagenetic quartz cement in deeply buried sandstones, offshore Norway. A petrography and SEM EBSD study: EGU06, 2006b.

Zeisig, A., Siegesmund, S., and Wieiss, T., 2002, Thermal expansion and its control on the durability of marbles, *in* Siegesmund, S., Wieiss, T., and Vollbrecht, A., eds., Natural Stone, Weathering Phenomena, Conservation Strategies and Case Studies, 205. Special Publications: London, Geological Society of London, p. 65-80.

Åkesson, U., Lindqvist, J. E., Schouenborg, B., and Grelk, B., 2006, Relationship between microstructure and bowing properties of calcite marble claddings: Bulletin of Engineering Geology and the Environment, v. 65, p. 73-79.

General conclusions and recommendations

9.1 CONCLUSIONS

9.1.1 Introduction

This section presents the overall conclusions from the doctoral project, and is based on the conclusions drawn in the research papers, Chapter 6, where the development of a particle analysis system (PTA) is described, and the general discussion. The conclusions presented in the following paragraphs were derived both from the development and implementation of methods as well as from investigations of geological materials.

The doctoral study has been in applied mineralogy. Advanced characterisation techniques have been developed and used as a tool for quantitatively describing geological raw materials, middlings and end products for optimal exploitation of mineralogical materials.

9.1.2 The value of quantitative microscopy

The purpose of the doctoral work was to develop and implement quantitative microscopy techniques with applications in applied mineralogy. Microscopy is a

important supplement to bulk analyses, and the interest for the project and its applications have shown that the value of what has been achieved using these techniques has been vital.

9.1.3 PTA

A method for detailed, quantitative measurements of main and trace minerals and particle texture was developed in close relation with the industry. The data acquisition is based on commercial hard- and software and the results are post-processed in the PTA software. In the future, the PTA will be further developed and integrated with Oxford Inca Feature so the full analysis can be performed simultaneously.

9.1.4 EBSD

Electron backscatter diffraction was tested and evaluated as a new approach to applied mineralogy, where the crystallographic aspect is characterised. EBSD was not found suitable for ordinary particle analysis because the analysis area is small and minerals are not easily discriminated. A combination with image processing and analysis will increase the fields of application. The technique is however superior when studying polymorphs and in quantitative measurements of lattice orientation and fabric parameters obtained from the measurements of crystal orientations.

9.1.5 Competence in the intersection geology and materials sciences

During the development and implementation of systems and techniques, competence is developed in the intersection between geology and materials technology. The research groups have become integrated with a common instrument laboratory and the knowledge to further develop the laboratory as a resource in applied mineralogical research.

9.1.6 Revitalisation of process mineralogy

The project has revitalised the area of process mineralogy in Norway and now also fully involves industrial minerals. It is aimed to develop a national

laboratory for the mineral industry where comprehensive research, development and evaluation of deposits and processes can be performed.

9.1.7 Process mineralogy case studies

Raw material, middlings and end products from the mineral industry were investigated by means of PTA analysis throughout the study. The main materials were ilmenite ore and concentrates, iron ore and concentrates, high purity quartz, ground calcium carbonate, olivine and gold ore and concentrates. Modal mineralogy, mineral liberation, mineral associations and mineral intergrowths and the contribution from various minerals to certain elements have been studied. The investigations have demonstrated the strength and the possibilities of the programme and have pushed the development of PTA forward.

9.1.8 Marble

The microstructure of marble used for exterior cladding panels was investigated with respect to deterioration. Several aspects of the microstructure were measured and analysed, and a prediction model for bowing of marble slabs calculated. For direction-dependent bowing, the grain shape orientation (foliations, lineation) is regarded as most important together with lattice preferred orientation because of extremely anisotropic thermal behaviour of calcite. The variables that influenced the intensity of bowing in the prediction model were-grain shape or roughness of the grain boundaries and the shape of the grain size distribution curve.

9.1.9 Quartz

Relations of diagenesis and microstructures in quartz grains and quartz cement in reservoir sandstones from offshore Norway were studied by means of new techniques to search for possible evidences of compaction induced deformation. A combination of optical microscopy and electron microscope techniques was used. The diagenetic quartz overgrowths were indistinguishable from the quartz host grains in EBSD maps, i.e. supporting syntaxial growth. Also in quartz overgrowths on polygranular quartz aggregates, the cement followed the orientation of the adjacent grains. Low-angle boundaries reflecting pre-depositional deformation were displayed and preserved by overgrowths of quartz

cement. This means that the cement growth was not accompanied by recrystallisation. Dauphiné twins were visualised by the EBSD method. The dauphiné twins were common both in the cemented and in the non-cemented samples and they were interpreted to have different origins. It was suggested that some of the twin distributions at quartz grain edges and quartz cement-grain contacts may be related to burial compaction. This implies a mechanism of grain-boundary deformation in burial diagenesis, which is invisible using conventional petrographic tools. The paper clearly demonstrates the importance of combining various techniques in optical and electron microscopy and reveals new possibilities of studying deformation and cement growth mechanisms.

9.2 RECOMMENDATIONS

The following recommendations are stressed in the papers and the discussion:

9.2.1 PTA

A further optimisation of the PTA system should be prioritised by means of:

- A full implementation with the Inca Feature software. This should include a more sophisticated data acquisition allowing automatic grey-scale analysis of every particle and a possibility to easily select among grey-level morphology, EDS spectra and EDS mapping to be able to discriminate between most minerals;

- More sophisticated queries for information about free mineral surface, contact surface between minerals and average surface composition and quantitative measurements on particle texture together with improved particle searches for viewing thumbnail images;

- Putting more effort into stereological challenges and better statistic evaluation of the analyses.

It is aimed to develop a national laboratory for the mineral industry where comprehensive research, development and evaluation of deposits and processes can be performed. It is also a definite goal to launch the system on the commercial market in the future.

9.2.2 EBSD

A development towards implementation of grey-scale segmentation to define the areas of analysis for EBSD-analysis should be requested. This would make EBSD more interesting in process mineralogy avoiding spending time on analysing the matrix.

9.2.3 Marble

Extensive standardised laboratory bowing data should be collected for as many calcitic marble types as possible and more microstructure measurements should be performed to generate a more optimised regression model for bowing and also for loss of strength for marbles used as exterior cladding panels. The model could be a good tool for predicting deterioration and understand more of the mechanisms involved.

9.2.4 Quartz

EBSD revealed new possibilities of studying deformation and cement growth mechanisms. Further studies of compaction and diagenesis of deeply buried reservoir sandstones focusing especially on quartz cemented stylolitic sandstones in the Barents Sea should therefore be carried out.

10. CHAPTER

References

Alnæs, L., Koch, A., Schouenborg, B., Åkesson, U., and Moen, K., 2004, Influence of Rock and Mineral properties on the durability of marble panels Dimension Stone 2004, New perspectives for a traditional building material, Prague, Czech Republik, 2004.

Alnæs, L., and Aasly, K. A., 2005, WP 5.3 Compilation of test results, *in* results, W. C. o. t., ed., Microsoft Excel: Trondheim, SINTEF Civil and Environmental Engineering, Rock and Soil Mechanics.

Amstutz, G. C., 1961, Microscopy applied to mineral dressing, Colorado School of Mines Quat., 443-482 p.

Bain, G. W., 1940, Geological, chemical and physical problems in marble industry, 1940, American Institute of Mining and Metallurgical Engineers -- Technical Publications, p. 16.

Bain, G. W., 1941, Measuring grain boundaries in crystalline rocks: J Geol, v. 49, p. 199-206.

Barbery, G., 1991, Mineral liberation: measurement, simulation and practical use in mineral processing: Quebec, Canada, Les Editions GB, 351 p.

Bunge, H. J., 1982, Texture Analysis in Materials Science: London, Butterworths.

Butcher, A., 2004, Automation, Integration and Interpretation - the Future for Process Mineralogy and Practising Mineralogists: 8th International Congress on Applied Mineralogy, ICAM 2004, Sao Paulo, Brazil, 2004.

Chayes, F., 1956, Petrographic Modal Analysis: New York, John Wiley & Sons, Inc., 113 p.

Cohen, and Monteiro, 1991, Durability and Integrity of Marble Cladding "A state of the art review": Journal of the Performance of Constructed Facilities, v. 5, p. 113-124.

Coleman, R., 1979, An ontroduction to mathematical stereology: Aarhys, Department of Mathematics, Aarhus University.

Day, A., 1993, Developments in the EBSP technique and their application to grain imaging, University of Bristol.

Delesse, A., 1848, Procédé méchanique pour déterminer la composition des roches: Ann, mines, v. 13, p. 379-388.

Dingley, D. J., 1998, Developments in on-line crystal orientation determination, Institute of Physics Conference Series, 98, p. 473-476.

Ellefmo, S. L., 2005, A probabilistic approach to the value chain of underground iron ore mining: From deposit to product, Norges teknisk-naturvitenskapelige universitet, 273 p.

Elverøy, A., Haldorsen, S., Bergh, S., Roaldset, E., Kristoffersen, Y., Haugan, P. M., Killingtveit, Å., and Eliassen, A., 1999, Geofagplanen - Plan for norsk geofaglig forskning og undervisning i U&H-sektoren, *in* NFR, ed.: Oslo, Norges forskningsråd, p. 43.

Farstad, T., Johannessen, K., and Hjelen, J., 1998, Spatial resolution of EBSP using fully automated pattern indexing: 14th Int. Congress on ELectron Microscopy ICEM 14, Cancun, Mexico, 1998, p. 753-754.

Gaudin, A. M., 1939, Principles of mineral dressing: New York, McGraw Hill.

Glagolev, A. A., 1931, Mineralogical Materials, p. 10.

Glagolev, A. A., 1934, Quantitative analysis with the microscope by the point method: Eng. Mining J, v. 135, p. 399-400.

Goldstein, I. J., 1974, Metallography - a practical tool for correlating the structures and properties of materials, ASTM Special Technical Publication 557, ASTM, p. 86.

Goldstein, J. I., Newbury, D., Echlin, P., Joy, D., Romig, A. D., Lyman, C., Fiori, C., and Lifshin, E., 1992, Scanning Electron Microscopy and X-ray Microanalysis: New York, Plenum Press, xviii, 820 p.

Goldstein, J. I., Newbury, D., Joy, D., Lyman, C., Echlin, P., Lifshin, E., Sawyer, L., and Michael., J., 2003, Scanning Electron Microscopy and X-ray Microanalysis: New York, Kluwer Academic/Plenum Publishers, 689, 1 CD-ROM p.

Gottlieb, P., Wilkie, G., Sutherland, D., Ho-Tun, E., Suthers, S., Perera, K., Jenkins, B., Spencer, S., Butcher, A., and Rayner, J., 2000, Using Quantitative Electron Microscopy for Process Mineral Applications: JOM Journal of Metals, v. 52, p. 24-25.

Grant, G., Hall, J. S., Reid, A. F., and Zuiderwyk, M. A., 1976, Multi-compositional particle characterization using the SEM-microprobe: Scanning Electron Microscopy, v. 3, p. 401-408.

Grelk, B., 2005, Review of literature and TEAM results, TEAM-project WP2, p. 40.

Grelk, B., Golterman, P., Schouenborg, B., Koch, A., and Alnæs, L., 2004, The laboratory testing of potential bowing and expansion of marble: Dimension Stone 2004, New perspectives for a traditional building material, Prague, Czech Republic, 2004.

Gu, Y., 2003, Automated Scanning Electron Microscope Based Mineral Liberation Analysis: Journal of Minerals & Materials Characterization & Engineering, v. 2, p. 33-41.

Gu, Y., 2004, Rapid Mineral Liberation Analysis with X-ray and BSE Image Processing: 8th International Congress on Applied Mineralogy, ICAM 2004, Sao Paulo, Brazil, 2004, p. 119-122.

Haddad, S. C., Worden, R. H., Prior, D. J., and Smalley, P. C., 2006, Quartz cement in the Fontainebleau Sandstone, Paris Basin, France; crystallography and implications for mechanisms of cement growth: Journal of Sedimentary Research, v. 76, p. 244-256.

Hagni, R. D., 1982, Process Mineralogy: Past, Present, and Future: Symposium on Process Mineralogy, AIME Annual Meeting, Dallas, Texas, 1982, Process Mineralogy, p. 29-36.

Hagni, R. D., 1988, The Status of Process Mineralogy in 1988: JOM Journal of Metals, v. 40, p. 25.

Hagni, R. D., 1991, A Decade of Developments in Applied Mineralogy: JOM Journal of Metals, v. 43, p. 25-26.

Hagni, R. D., 1995a, Process Mineralogy XIII: Rolla, Missouri, The Minerals, Metals & Materials Society, 377 p.

Hagni, R. D., 1995b, Recent Developments in the Application of Process Mineralogy: JOM Journal of Metals, v. 47, p. 46.

Heinrich, K. F. J., 1966, In Proceedings of the 4th International Conference on X-ray optics and Microanalysis, Paris, 1966, p. 159.

Henley, K. J., 1983, Ore dressing mineralogy - a review of techniques, applications and recent developments: 1st ICAM, Hohannesburg, South Africa, 1983, p. 175-200.

Hetzner, D. W., 1998, Quantitative Image Analysis, Part 1 Principles: Buehler's "Tech-Notes", v. 2, p. 5.

Hjelen, J., 1989, Scanning elektron-mikroskopi: Trondheim, Metallurgisk institutt, NTH, 106 p.

Hjelen, J., 1990, Teksturutvikling i Aluminium, studert ved Elektronmikrodiffraksjon (EBSP) i Scanning Elektronmikroskop, University of Trondheim.

Hjelen, J., and Nes, E., 1990, Spatial Resolution Measurements of Electron Backscatter Diffraction Patterns (EBSPs) in the Scanning Electron Microscope: XIIth International Congress for Electron Microscopy, Seattle, USA, 1990.

Hjelen, J., Ørsund, R., Hoel, E., Runde, P., Furu, T., and Nes, E., 1993, EBSP, Progress in Technique and Applications: Textures and Microstructures, v. 20, p. 29-40.

Hook, K., 1994 Look out below - The Amoco Building Cladding Failure.: Progressive Architecture, v. Feb 1975, p. 58-62.

Hough, P. V. C., 1962, Methods and means for recognizing complex patterns, 3,069,654: USA.

Humphreys, F. J., 2001, Grain and subgrain characterisation by electron backscatter diffraction: Journal of Materials Science, v. 36, p. 3833-3854.

Jacamon, F. P., and Larsen, R. B., 2005, Relationship between SEM-cathodoluminescence and trace element chemistry of quartz in granitic igneous rocks from the Oslo continental rift: Eos, v. 86(52).

Jones, M. P., 1987, Applied mineralogy: a quantitative approach: London, Graham & Trotman, 259 p.

Jones, M. P., and Gravilovic, J., 1970, Automatic quantitative mineralogy in mineral technology: Rudy, v. 5, p. 189-197.

Jones, M. P., and Horton, R., 1979, Recent developments in the stereological assessment of composite (middling) particles by linear measurements: XIth CommonwealthMining and Metallurgical Congress, London, 1979, p. 113-122.

Jones, M. P., and Stewart, P. S. P., 1976, Composite particles: London, Royal School of Mines, Imperial College.

Kessler, D. W., 1919, Physical and chemical test of the commercial marbles of the United States, Technological papers of the Bureau of Standards.

Kikuchi, S., 1928, Diffraction of cathode rays by mica: Jap. J. Phys, v. 5:83.

King, R. P., 1993, Basic image analysis for mineralogy, ICAM'93 Demonstration Workshop Manual, p. 119-139.

King, R. P., and Schneider, C. L., 1995, Basic image analysis for the measurement of mineral liberation, *in* Hagni, R. D., ed., Process Mineralogy XIII, 8, The Minerals, Metals & Materials Society, p. 145-157.

Kleber, W., 1990, Einführung in die Kristallographie: Berlin, VEB Verlag Tecknik.

Kleiv, R. A., 2001, Heavy metal adsorption on silicate tailings. A study of nepheline syenite and olivine process dust.: Unpub. Article collection thesis, Norwegian University of Science and Technology, 142 p.

Koch, A., and Siegesmund, S., 2002, Bowing of marble panels: on-site damage analysis from the Oeconomicum Building at Göttingen (Germany), *in* Siegesmund, S., Weiss, T., and Vollbrecht, A., eds., Natural Stone, Wathering Phenomena, Conservation Strategies and Case Studies, 205. Special Pubilications: London, The Geological Society of London, p. 299-314.

Koch, A., and Siegesmund, S., 2004, The combined effect of moisture and temperature on the anomalous expansion behaviour of marble: Environmental Geology, v. 46, p. 350-363.

Krieger-Lassen, N. C., 1996, The relative precision of crystal orientations measured from electron backscattering patterns: Journal of Microscopy, v. 181, p. 72-81.

Krieger-Lassen, N. C., 1998, Automatic high-precision measurements of the location and with of Kikuchi bands in electron backscatter diffraction patterns: Journal of Microscopy, v. 190, p. 375-391.

Lastra, R., Petruk, W., and Wilson, J., 1998, Image-analysis techniques and application to mineral processing, *in* Cabri, l. J., and Vaughan, D. J., eds., Modern Approaches to Ore and Environmental Mineralogy, 27. Short Course Series: Ottawa, Ontario, Mineralogical Association of Canada, p. 327-366.

Lloyd, G. E., 1985, Review of Instumentation, Techniques and Applications of SEM in mineralogy, *in* White, J. C., ed., Short Course in Applications of Electron Microscopy in the Earth Sciences, 11: Fredericton, Mineralogical Association of Canada, p. 151-188.

Lumbreras, F., and Serrat, J., 1996, Segmentation of petrographical images of marbles: Computers & Geosciences, v. 22, p. 547-558.

Malaga, K., Schouenborg, B., Alnæs, L., Bellopede, R., and Brundin, J. A., 2004, Field exposure sites and accelerated laboratory test of marble panels: Dimension Stone 2004, New perspectives for a traditional building material, Prague, Czech Republic, 14–17 June, 2004.

Malvik, T., 1976, En undersøkelse av malmmineralers frimalingsegenskaper, NTH, 276 p.

Malvik, T., 1991, Partikkelkarakterisering ved bruk av bildeanalyse: Konferens i Mineralteknik, Luleå, 1991.

Malvik, T., 1998, Relations between mineralogical textures and comminution characteristics for rocks and ores: XVI International Mineral Processing Congress, Amsterdam, 1998.

Malvik, T., 2005, Project description; Background for the programme, Strategic University Programme(SUP) "The value chain from mineral deposit to beneficiated product with emphasis on quartz": Trondheim, NTNU.

Miles, J. D., and Davy, P., 1976, Precise and general conditions for the validity of a comprehensive set of stereological fundamental formulae: Journal of Microscopy, v. 107, p. 211-216.

Moen, K., Hjelen, J., and Malvik, T., 2003a, Preparation of Quartz Samples for EBSD Analysis: Applied Mineralogy '03, Helsinki, Finland, 2003a.

Moen, K., Malvik, T., Alnæs, L., and Hjelen, J., 2006a, Quantitative measurements of Marble Microstructure - a model for predicting the deterioration of marble: Environmental Geology, v. In prep, p. 17.

Moen, K., Malvik, T., Breivik, T., and Hjelen, J., 2006b, Particle Texture Analysis in Process Mineralogy: XXIII IMPC 2006, Istanbul, Turkey, 2006b.

Moen, K., Malvik, T., Hjelen, J., and Leinum, J. R., 2003b, Automatic Material Characterization by means of SEM-techniques: 9th Euroseminar on Microscopy Applied to Building Materials, Trondheim, Norway, 2003b.

Moen, K., Malvik, T., Hjelen, J., and Leinum, J. R., 2003c, EBSD-A Potential Supplementary Technique in Quantitative Characterisation of Minerals: XXII IMPC, Cape Town, South Africa, 2003c.

Moen, K., Malvik, T., Hjelen, J., Leinum, J. R., and Alnæs, L., 2004, EBSD Microstructure Measurements of Marble: 8th International Congress on Applied Mineralogy, ICAM 2004, Sao Paulo, Brazil, 2004, p. 145-148.

Mørk, M. B. E., and Moen, K., 2006a, Reconnaissance study of compaction microstructures in quartz grains and quartz cement in deeply buried sandstones using combined petrography - EBSD analysis: In thesis Moen 2006, in prep for journal, p. 17.

Mørk, M. B. E., and Moen, K., 2006b, Textural relations of quartz grains and diagenetic quartz cement in deeply buried sandstones, offshore Norway. A petrography and SEM EBSD study: EGU06, 2006b.

NGU, 2005, Mineralressurser i Norge, Bergindustrien 2004, *in* Neeb, P.-R., ed., NGU rapport 2005.041: Trondheim, Geological Survey of Norway, NGU, p. 1-25.

Passchier, C. W., and Trouw, R. A. J., 2005, Microtectonics Berlin Springer, 366 p.

Petruk, W., 1989, The Capabilities of the Microprobe Kontron Image Analysis System: Scanning Microscopy, v. 2, p. 1247-1256.

Petruk, W., 2000, Applied Mineralogy in the Mining Industry: Ottawa, Ontario, Canada, Elsevier, 268 p.

Pettersen, T., Heiberg, G., and Hjelen, J., 1998, Measurements of spatial resolution of EBSP in the SEM as a function of atomic number and high

voltage The 14th International Congress on Electron Microscopy, Cancun, Mexico, 1998.

Pignolet-Brendom, S., and Reid, K. J., 1988, Mineralogical characterization by QUEM*SEM, *in* Carson, D. J. T., and A.H., V., eds., Process Mineralogy VIII: Warrendale, PA, TMS, p. 337-346.

Prior, D. J., Boyle, A., P., Brenker, F., Cheadle, M., C., Day, A., Lopez, G., Peruzzi, L., Potts, G., Reddy, S., Spiess, R., Timms, N., E., Trimby, P., Wheeler, J., and Zetterstrom, L., 1999, The application of electron backscatter diffraction and orientation contrast imaging in the SEM to textural problems in rocks: American Mineralogist, v. 84, p. 1741-1759.

Ramdohr, P., 1980, The ore minerals and their intergrowths, Pergamon Press, 441-1123 p.

Randle, V., 1993, Microtexture analysis. An in-depth approach to materials, 390-392 p.

Randle, V., 2003, Microtexture Determination and Its Applications, , , 146 p.

Reed, S. J. B., 2005, Electron Microprobe Analysis and Scanning Electron Microscopy in Geology: Cambridge, Cambridge University Press, 192 p.

Rosiwal, A., 1898, Ueber geometriches Gesteinanalysen usw.: Verh. der k. k. Geolog. Reichsanstalt Wien, p. 143-175.

Russ, J. C., 2002, The Image Processing Handbook: Raleigh, CRC Press, 732 p.

Russ, J. C., and Dehoff, R. T., 2001, Practical Stereology: New York, Plenum Press.

Schmidt, N.-H., and Olesen, N. O., 1989, Computer-aided determination of crystal-lattice orientation from electron channeling patterns in the SEM: The Canadian Mineralogist., v. 27, p. 15-22.

Schneider, C. L., Neumann, R., and Alcover-Neto, A., 2004, Automated, Adaptive Thresholding Procedure for Mineral Sample Images Generated by BSE Detector: 8th International Congress on Applied Mineralogy, ICAM 2004, Sao Paulo, Brazil, 2004, p. 103-106.

Schouenborg, B., Grelk, B., Alnæs, L., Brundin, J. A., Blasi, P., Yates, T., Marini, P., Tschegg, E., Unterweger, U., Tokartz, B., Kock, A., Bengtsson, T., Mladenovic, A., and Goralezyg, S., 2003, TEAM - Testing and Assessment of Marble and Limestone: International

Symposium Industrial Minerals and Building Stones, Istanbul, Turkey, Sept 15-18, 2003.

Schwartz, A. J., Kumar, M., and Adams, B. L., 2000, Electron backscatter diffraction in materials science: New York, Kluwer Academic/Plenum Publishers, XVI, 339 s. ill. p.

Shand, S. J., 1916, A recording micrometer for rock analysis: Journal of Geology, v. 24, p. 394-403.

Sørensen, B. E., Austrheim, H., and Larsen, R. B., 2005, Fluid-related recovery and deformation textures in quartz in partly retrogressed high-grade quartzites from the Bamble sector, v. 86(52).

Thompson, E., 1930, Quantitative Microscopic Analysis: Journal of Geology, v. 27, p. 276.

Underwood, E. E., 1970, Quantitative Stereology, Addison-Wesley Publishing Company.

Vaughan, J., Davidson, L., Nemchin, A., and Quinton, S., 2004, Teaching process mineralogy in Australia: Journal of Geoscience.

Weiss, T., Siegesmund, S., and Fuller, E. R., 2002, Thermal stresses and microcracking in calcite and dolomite marbles via finite element modelling, *in* Siegesmund, S., Weiss, T., and Vollbrecht, A., eds., Natural Stone , Weathering Phenomena, Conservation Strategies and Case Studies, 205: London, The Geological Society of London, p. 65-80.

Winkler, E. M., 1996, Properties of marble as building veneer: International Journal of Rock Mechanics and Mining Science & Geomechanics Abstracts, v. 33, p. 215-218.

Wittry, D. B., 1966, In Proceedings of the 4th International Conference on X-ray optics and Microanalysis, Paris, 1966, p. 168.

Wright, S., 2005, A Collection of OIM Applications, *in* Wright, S., ed., Edax TSL, p. 106.

Yates, T., Brundin, J.-A., Goltermann, P., and Grelk, B., 2004, Observations from the inspection of marble cladding in Europe: Dimension Stone 2004, New perspectives for a traditional building material, Prague, Czech Republic, 2004.

Zeisig, A., Siegesmund, S., and Wieiss, T., 2002, Thermal expansion and its control on the durability of marbles, *in* Siegesmund, S., Wieiss, T., and

Vollbrecht, A., eds., Natural Stone, Weathering Phenomena, Conservation Strategies and Case Studies, 205. Special Publications: London, Geological Society of London, p. 65-80.

Åkesson, U., 2004, Microstructures in granites and marbles in relation to their durability as a construction material, Göteborg University.

Åkesson, U., Lindqvist, J. E., Schouenborg, B., and Grelk, B., 2006, Relationship between microstructure and bowing properties of calcite marble claddings: Bulletin of Engineering Geology and the Environment, v. 65, p. 73-79.

Part Two

Paper 1

Particle Texture Analysis in Process Mineralogy

K. Moen, T. Malvik, T. Breivik, J. Hjelen
Norwegian University of Science and Technology, Trondheim, Norway
(e-mail: kari.moen@geo.ntnu.no)

ABSTRACT: This paper will present a new automatic SEM based system, Particle Texture Analysis, developed at the Norwegian University of Science and Technology. The strength of the system is demonstrated through practical examples from the Norwegian mineral industry where essential information for the beneficiation process as modal main and trace mineralogy, mineral liberation, mineral associations and intergrowth is exposed. Through online interaction with the customer, the results can be fully utilised. The system is still a prototype, but the framework is established, and particle texture data can be significantly provided.

1 INTRODUCTION

1.1 *Process mineralogy*

In mineral processing, minerals are separated by means of relative differences in physical properties. To achieve efficient separation, the minerals have to be sufficiently liberated before separation. It is therefore important to quantify mineralogical characteristics that affect the behaviour of minerals during processing (Lastra et. al. 1998).

Petruk (2000) describes the acquisition of quantitative data for mineral processing. He points out the strengths and weaknesses of the different bulk analysis methods and concludes that these techniques are semi-quantitative and give no information about how the minerals occur in free and composite particles. Microscope analysis however, provides vital information in combination with bulk analysis techniques.

1.2 *Existing systems*

Manual methods and image analysis in the optical microscope are cheap and appropriate for many purposes (e.g. Malvik 1982). However, generally a more advanced method is needed when studying complex or trace mineralogy, fine particles, or silicates and carbonates that can not be uniquely defined by image analysis in the optical microscope. It is then favourable to turn to an automatic scanning electron microscope (SEM) based image analysis system.

This paper will present a new automatic SEM based system, PTA, developed at the Norwegian University of Science and Technology. However, several systems have been developed for mineral liberation (Jones (1970), Petruk (2000), King & Schneider (1993), Gottlieb, et. al. (2000), Schneider et. al. (2004), Gu (2004). Recent advances, particularly in computer technology, have made fast and user-friendly mineral liberation systems possible (Gu 2003). Backscattered electron (BSE) signals can be used to generate images from the sample from which the minerals can be quantified using modern image analysis methods. Each grain outlined from BSE images can be identified with X-ray analysis positioned at the centre of the grain or collected from scanning the whole grain. Minerals of similar BSE intensities can be discriminated using X-ray mapping (Gu, 2003; Gu, 2004).

1.3 *PTA system*

The Particle Texture Analysis (PTA) system that is being developed at the Norwegian University of Science and Technology (NTNU) is based upon the same main principals as the former known systems. The software is however flexible, relatively simple to operate for a mineralogist, and is based on a commercially available particle analysis system. It can be run with any instrument, depends on a standard semi-quantitative EDS system and is a useful tool for almost any kind of material. The system is therefore suitable in a multi-purpose lab. The strength and the advantages of the system will be demonstrated

through practical examples from the Norwegian mineral industry where essential information for the beneficiation process is exposed.

The development was funded by the Norwegian Research Council and the mineral companies Titania, Hustadmarmor and Norwegian Crystallites.

2 MATERIALS AND METHODS

2.1 *Samples*

The samples most frequently investigated are polished sections of grinded minerals embedded in epoxy resin. Screened grain-size fractions preferably with $D_{max}/D_{min}<1.6$ (Barbery 1991) are investigated separately. The material is generally feed, concentrates or tailings from a mineral processing plant or a laboratory.

2.2 *General concept*

The Particle Texture Analysis (PTA) system is based on scanning electron microscope and Oxford Inca software. BSE images are analysed by means of grey levels, and every grain of interest is analysed by X-rays. This part is performed by means of the Oxford Inca Feature software and external procedures. The database and the images are then processed offline by the PTA software that performs mineral liberation, mineral association analysis as well as mineral intergrowth analysis and statistics by combining image analysis and X-ray data.

2.3 *Concepts of data acquisition*

Polished sections of narrow grain size fractions are put into the specimen chamber

The area of interest and running parameters regarding image acquisition and X-ray analysis are defined. For each field of view a gray scale backscattered electron image is acquired. By image analysis, the particles are thresholded from the background. A particle separation procedure to separate touching particles and a grey level analysis to separate monomineralic grains within the particle is performed for each particle. The area of every grey level of the particles is then returned to the microscope. These areas or grains are scanned to collect X-rays. Data from all analysed grains are stored in a database.

The database and images are exported to the NTNU PTA software which performs the mineral liberation and mineral association analysis offline.

2.4 *Concepts of particle texture analysis PTA*

The databases and images of every analysed grain size

fraction are imported to the software. Image analysis is performed to evaluate whether grains occur liberated or in composite particles and which minerals that occur together in composite particles. The output results in a new database where queries can be performed. Standard queries to be performed are mineral liberation of any mineral, mineral associations of any mineral and miniature images of particles of a certain texture category. Minerals can easily be grouped to make a simpler picture.

2.5 *Online with the customer*

SEM based image analysis systems are visual, and to fully utilize the results, the customer should be able to navigate within the system and try out different options. The customers from the Norwegian industry can therefore log on through a server to be able to evaluate the results alone or together with the researcher.

3 EXAMPLES FROM THE MINING INDUSTRY

3.1 *Ilmenite beneficiation*

Two different raw materials for ilmenite beneficiation were investigated because of anomalous behaviours in the lab scale process compared to normal process feed. Both materials were analysed by bulk chemical XRF analysis. The first raw material investigated was high in TiO_2 content but became surprisingly low in the lab scale concentrate.

A full mineralogy, mineral liberation and mineral association analysis was performed.

Table 1. Modal mineralogy in normal and anomalous (1) feed and concentrate

Mineral	Normal feed #	w%	Feed 1 #	w%	Normal Conc. #	w%	Conc. 1 #	w%
Ilmenite	8906	39.83	6216	42.84	13589	95.83	4610	86.46
Magnetite	27	0.20	1247	3.43	17	0.03	15	0.15
Rutile	21	0.01	29	0.08	113	0.05	31	0.07
Amfibole 1	57	1.23	209	1.98	39	0.08	26	0.26
Amfibole 2	7	0.00	41	0.02	7	0.00	16	0.02
Opyroxene	1300	14.99	2799	20.87	449	1.17	677	9.57
Cpyroxene	147	1.93	300	2.80	65	0.25	54	0.82
Biotite	814	6.72	1661	10.02	177	0.44	157	1.51
Plagioclase	3149	32.49	1646	13.67	477	1.49	60	0.62
Quartz	27	0.07	57	0.27	35	0.17	16	0.00
Zircon	9	0.04	15	0.01	5	0.00	7	0.00
Apaite	90	1.21	105	1.16	14	0.03	3	0.01
Spinel 1	1	0.00	87	0.20	4	0.00	11	0.11
Spinel 2	0	0.00	15	0.01	4	0.00	0	0.00
Calcite	31	0.17	132	1.03	29	0.00	9	0.01
Pyrite	209	0.34	111	0.43	20	0.06	12	0.09
Chalcopyrite	10	0.01	19	0.08	5	0.00	2	0.01
Ni-sulph	22	0.05	6	0.03	3	0.01	2	0.00
Mo-sulph	12	0.00	5	0.00	2	0.00	0	0.00
Titanite	0	0.00	4	0.00	2	0.00	4	0.00
Baddeleyite	3	0.00	3	0.00	2	0.00	0	0.00
Unclassified	159	0.70	460	1.06	157	0.38	79	0.29
Total	15001	100.00	15167	100.00	15215	100.00	5791	100.00

From the mineralogy it was easily recognised that the amount of orthopyroxene was significantly higher in

the anomalous raw material, and the amount of plagioclase was significantly lower. This increased amount of orthopyroxene was not removed in the concentrate. What could be the reason for this? The orthopyroxene was probably not liberated from the ilmenite. A closer look at the mineral liberation would reveal this fact.

Table 2. Mineral liberation of orthopyroxene in normal and anomalous (1) feed and concentrate

Liberation of Orthopyroxene	Normal #	Feed A	A%	Feed 1 #	A	A%
1	778	2438795.4	84.4	1564	4128601.1	79.3
0.95 -> 1.00	9	99522	3.4	27	227107.8	4.4
0.75 -> 0.95	11	59460.6	2.1	27	251642.8	4.8
0.50 -> 0.75	27	146059.5	5.1	36	255011.3	4.9
0.25 -> 0.50	20	82122.3	2.8	47	195813	3.8
0.05 -> 0.25	27	56895.7	2	87	118750.2	2.3
0.00 -> 0.05	38	7129.6	0.2	141	30147.5	0.6
Sum	910	2889994.1	100.0	1929	5207073.8	100.0

Liberation of Orthopyroxene	Normal #	Conc. A	A%	Conc. 1 #	A	A%
1	69	38285.8	15.5	219	657270.4	72.3
0.95 -> 1.00	0	0	0	1	13826.4	1.5
0.75 -> 0.95	8	31777.9	12.9	8	47358.4	5.2
0.50 -> 0.75	9	31911.9	13	13	75485.1	8.3
0.25 -> 0.50	16	43059.1	17.5	20	45054.7	5
0.05 -> 0.25	68	87120	35.4	51	56171	6.2
0.00 -> 0.05	94	14176.7	5.8	75	14169.8	1.6
Sum	264	246331.4	100.0	387	909335.8	100.0

In the feed, orthopyroxene was slightly more poorly liberated than in normal feed. In the concentrates, orthopyroxene still left in the normal concentrate, occurred mainly as composite particles. In our anomalous concentrate, however, the liberation of orthopyroxene was above 70%. The orthopyroxene should then be possible to remove. It was consequently concluded that the laboratory separation process did not work sufficiently efficiently for this sample.
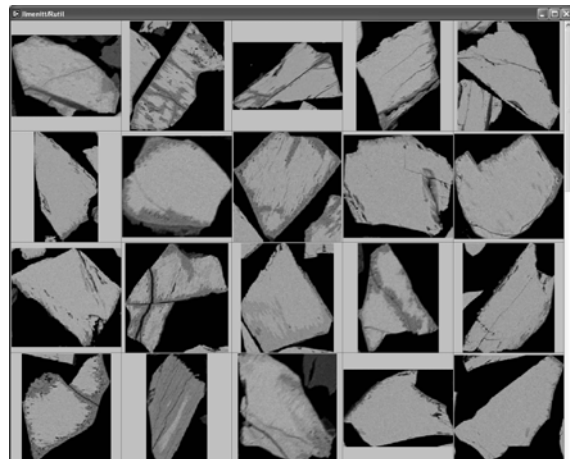
Figure 1. Thumbnail BSE images of intergrowth between ilmenite and rutile (dark)

The second anomalous raw material had a low TiO_2 content in the feed and a very high content in the concentrate. The mineralogy revealed a high content of rutile in feed and concentrate. The liberation of ilmenite was poor and thumbnail images of the rutile/ilmenite particles clearly illustrated the particle intergrowth texture (Figure 1). It was therefore concluded that the reason for high TiO_2 content in the concentrate was alteration of ilmenite into rutile which is destructive for the quality of the product.

3.2 Tailings from GCC processing

The Norwegian mineral industry has given superior attention to sustainable production and acceptance from the local environment and the society during the last decade. Looking at the tailing as a potential resource is therefore essential. In addition, knowledge of availability of elements from the special fjord fills is necessary.

Tailing from a ground calcium carbonate (GCC) plant was investigated to achieve information regarding mineralogy and how the minerals were distributed in the different grain size fractions.

More than 70 W% of the tailing consisted of calcite (Table 4). The minerals distributed differently throughout the grain size fractions (Table 3 and Figure 2). While calcite was concentrated in the fine fractions, the silicates were concentrated in the coarser fractions. The sulphides were more or less normally distributed. The majority of calcite was found in the <10 μm fraction while the majority of silicates were found in the 74-100 μm fraction (Table 4).

Table 3. Mineral distribution in fractions (W%)

Fraction	<10 μm	10-20 μm	20-37 μm	37-74 μm	74-100 μm	100-125 μm	>125 μm
Calcite	88.00	79.63	68.00	45.91	37.00	32.00	10.00
Alkalifeldspar	1.00	1.52	3.50	7.21	8.00	8.46	8.50
Plagioclase	3.50	6.54	10.00	18.28	22.00	24.08	35.00
Quartz	2.00	3.50	5.00	8.83	12.00	14.56	26.00
Muscovite	0.70	1.07	1.50	2.40	2.50	2.43	2.00
Flogopite	0.05	0.18	0.40	0.83	1.15	1.34	2.40
Chlorite	0.05	0.10	0.10	0.14	0.05	0.00	0.00
Other dark silicts.	0.50	0.89	1.40	2.35	3.00	3.20	4.00
Sulphides	1.00	2.90	5.00	8.47	8.00	6.95	2.00
Oxides	0.40	0.49	0.60	0.68	0.50	0.31	0.00
Apatite	0.50	0.62	0.83	1.30	1.55	1.70	2.50
Fluorite	0.40	0.42	0.60	0.83	0.55	0.21	0.00
Woll/Trem	0.10	0.27	0.40	0.72	1.25	1.71	4.00
Unclassified	1.00	1.40	1.60	2.06	3.00	3.06	3.00
Total in fraction	99.20	99.54	98.93	100.00	100.55	100.00	99.40

Table 4. Mineral distribution in whole sample (W%)

Fraction	<10 μm	10-20 μm	20-37 μm	37-74 μm	74-100 μm	100 125 μm	>125 μm	Total in sample
Calcite	56.40	4.99	1.86	2.31	7.51	0.34	0.05	73.42
Alkalifeldspar	0.64	0.10	0.10	0.36	1.62	0.09	0.04	2.91
Plagioclase	2.24	0.41	0.27	0.92	4.47	0.26	0.17	8.57
Quartz	1.28	0.22	0.14	0.44	2.44	0.16	0.12	4.67
Muscovite	0.45	0.07	0.04	0.12	0.51	0.03	0.01	1.21
Flogopite	0.03	0.01	0.01	0.04	0.23	0.01	0.01	0.34
Chlorite	0.03	0.01	0.00	0.01	0.01	0.00	0.00	0.06
Other dark silicts.	0.32	0.06	0.04	0.12	0.61	0.03	0.02	1.18
Sulphides	0.64	0.18	0.14	0.43	1.62	0.07	0.01	3.08
Oxides	0.26	0.03	0.02	0.03	0.10	0.00	0.00	0.44
Apatite	0.32	0.04	0.02	0.07	0.31	0.02	0.01	0.78
Fluorite	0.26	0.03	0.02	0.04	0.11	0.00	0.00	0.45
Woll/Trem	0.06	0.02	0.01	0.04	0.25	0.02	0.02	0.40
Unclassified	0.64	0.09	0.04	0.10	0.61	0.03	0.01	1.52
Total in sample	63.58	6.24	2.71	5.04	20.41	1.07	0.48	99.05
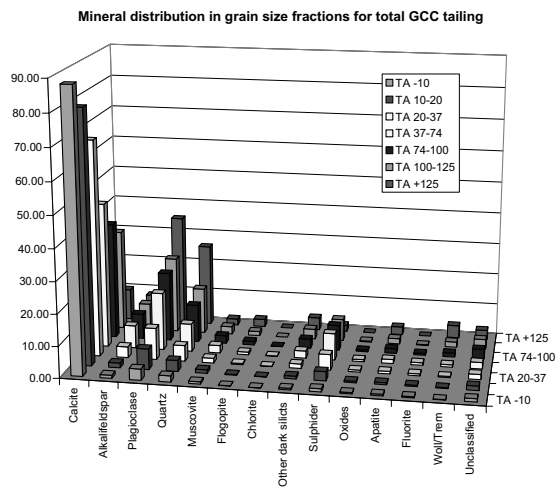
Figure 2. Mineral distribution in fractions for total GCC tailing. Data from Table 3

The importance of being able to document detailed mineralogy, how the elements are combined and verification of absence of harmful minerals is high when it comes to acceptance for special fjord fills and to be able to utilize the tailing as a resource in the future.

3.3 *High purity quartz*

The last example is from beneficiation of high purity quartz. To meet the strict product requirements, hardly all liberated trace minerals should be removed. Lattice bound elements and small traces of other minerals intergrown with quartz are the only accepted elements to occur beside SiO_2. An investigation of how the impurities occur in the feed was performed.

From the total mineral distribution it was concluded that alkalifeldspar, muscovite, biotite and calcite were the most common trace minerals (Table 5). In addition steel from the milling balls were found. Titan minerals were also important to study since titanium is an unwanted element in high purity quartz.

The minerals seemed to be highly liberated and can therefore be removed (Table 6). Only alkali feldspar and a few grains of sheet silicates, calcite and plagioclase occurred in composite particles with quartz (Figure 3). Small additional amounts of K, Na Al, Fe, Mg and Ca should therefore be expected.

Table 5. Mineral distribution in whole sample for high purity quartz feed (W%)

Fraksjon	<45 µm	45-63 µm	63-100 µm	100-125 µm	125-200 µm	200-315 µm	>315 µm	Total in sample
Quartz	16.037	7.510	11.460	7.293	20.217	22.525	14.241	99.28
Plagioclase	0.003	0.003	0.005	0.004	0.008	0.004	0.000	0.03
K-feldspar	0.023	0.012	0.019	0.012	0.029	0.019	0.006	0.12
Muscovite	0.025	0.012	0.017	0.010	0.020	0.003	0.000	0.09
Biotite	0.003	0.006	0.019	0.017	0.029	0.000	0.000	0.07
Chlorite	0.010	0.005	0.007	0.005	0.008	0.000	0.000	0.04
Calcite	0.008	0.008	0.017	0.015	0.031	0.014	0.001	0.09
Apatite	0.000	0.000	0.000	0.000	0.000	0.000	0.000	0.00
Fluorite	0.000	0.000	0.000	0.000	0.000	0.000	0.000	0.00
Sulph and oxides	0.000	0.000	0.000	0.000	0.000	0.000	0.000	0.00
Fe/steel	0.039	0.022	0.039	0.028	0.059	0.000	0.000	0.19
Titanite	0.000	0.000	0.002	0.002	0.002	0.000	0.000	0.01
Zoisite	0.001	0.001	0.001	0.000	0.000	0.000	0.000	0.00
Other	0.000	0.000	0.000	0.000	0.000	0.000	0.000	0.00
Unclassified	0.002	0.001	0.006	0.008	0.002	0.001	0.001	0.02
Total in sample	16.15	7.58	11.59	7.39	20.41	22.57	14.25	99.94

Quartz/k-feldspar

Quartz/muscovite   Quartz/chlorite
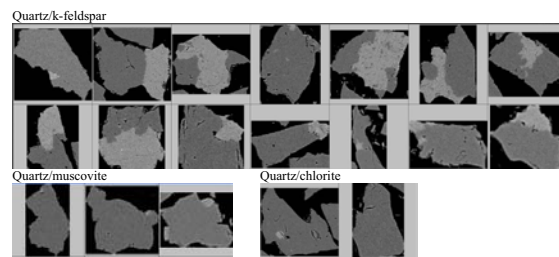
Figure 3. Thumbnail BSE images of quartz (dark) associated with alkali feldspar, muscovite and chlorite

The majority of composite particles between quartz and alkali feldspar will probably be removed during processing because the particles have got a relatively large surface of feldspar. From Table 6 it was also concluded that the very few grains of titanium minerals found in the feed, were liberated and not in composite particles with quartz. Titanium sources beside lattice bound Ti in quartz should therefore possibly be avoided in the concentrate.

Table 6. Liberation of quartz

Minerals associated to Quartz*	# 45 - 63	A 45 - 63	A% 45 - 63	# 100 - 125	A 100 - 125	A% 100 - 125	# 200 - 315	A 200 - 315	A% 200 - 315
Quartz*	14093	12048846.5	99.9	7809	39745425.8	99.7	2142	59215730.2	99.2
Quartz*/Plagioclase*	0	0	0	0	0	0	1	65932	0.1
Quartz*/Alkali feldspar*	6	6290	0.1	10	64235.9	0.2	3	124153.6	0.2
Quartz*/Muscovite	1	2290.3	0	2	20799	0.1	0	0	0
Quartz*/Plagioclase*/Alkali feldspar*/Muscovite	0	0	0	0	0	0	1	720.8	0
Quartz*/Chlorite*	0	0	0	2	24007.2	0.1	0	0	0
Quartz*/Biotite*	1	24.4	0	0	0	0	0	0	0
Quartz*/Chlorite*/Biotite*	0	0	0	1	1364.8	0	0	0	0
Quartz*/Fe/Steel*	1	29.2	0	0	0	0	0	0	0
Quartz*/Fe/Steel*/Oxides*	1	2323.1	0	0	0	0	0	0	0
Quartz*/Calcite	1	1244.8	0	0	0	0	0	0	0
Quartz*/Unclassified	0	0	0	0	0	0	5	260921.6	0.4
Quartz*/Alkali feldspar*/Muscovite/Unclassified	1	412.5	0	0	0	0	0	0	0
Quartz*/Plagioclase*/Alkali feldspar*/Muscovite/Unclassified	0	0	0	0	0	0	1	22327.9	0
Quartz*/Fe/Steel*/Unclassified	0	0	0	1	418	0	0	0	0
Sum	14105	12061460.8	100	7825	39856250.9	100	2153	59689786.2	100

4 DISCUSSION

As pointed out in the introduction, the PTA system is based upon the same principals as the former known systems, but at the time the development started, the parallel systems where dedicated to certain equipment contractors which did not fit our requirements running a multipurpose laboratory. In recent years the comparative systems have also tended against software systems rather than total soft- and hardware systems.

As was described in the introduction, the intention was to develop a flexible system, relatively simple to operate for a mineralogist, and based on commercially available components that altogether were able to quantify mineral content, mineral liberation, mineral associations and intergrowth in any kind of crystalline material.

Through the examples presented it has been demonstrated that mineralogy, both main and trace minerals, are detected and quantified, mineral liberation for all minerals are performed as well as mineral associations. Module for mineral intergrowth is not yet implemented, but collage of thumbnail images of any mineral or particle type can be viewed.

The practical application value of the system is confirmed by the interest from the mineral industry in Norway that has not had access to such systems earlier. Through online interaction with the customer, the setup can be optimised for the actual problem, and the results can be fully utilised beyond information reported by the researcher.

There are still improvements that have to be done when it comes to data acquisition, image analysis techniques, implementation of systems and automation. For instance, a statistic module to determine stop criteria based on cumulative mineral content development throughout analysis is next to be developed.

5 CONCLUSIONS

The Particle Texture Analysis (PTA) system that is being developed at the Norwegian University of Science and Technology (NTNU) is flexible, relatively simple to operate for a mineralogist, and is based on a commercially available particle analysis system.

The PTA system has an advantage when it comes to flexibility. It can be run with any instrument and depends on a standard semi-quantitative EDS system. It is a useful tool for almost any kind of material. The system is therefore suitable in a multi-purpose lab. The strength of the system is demonstrated through practical examples from the Norwegian mineral industry where essential information for the beneficiation process as modal main and trace mineralogy, mineral liberation, mineral associations and intergrowth is exposed.

Through online interaction with the customer the setup can be optimised, and the customer can evaluate the results alone or together with the researcher.

The system is still a prototype, and there are several tasks to solve and optimise, but the framework is established, and particle texture data can be significantly provided.

6 REFERENCES

Barbery G., *Mineral Liberation*, 1991, Les Edition GB, Québec, Canada, ISBN 2-9802322-0-3.

Gottlieb P., Wilkie G., Sutherland D., Ho-Tun E., Suthers S., Perera K., Jenkins B., Spencer S., Butcher A. and Rayner J., *Using quantitative electron microscopy for process mineralogy applications,* JOM Vol. 52 No. 4, April, pp 24-25 (2000).

Gu Y. *Automated Scanning Electron Microscope Based Mineral Liberation Analysis*, Journal of Minerals & Materials Characterization & Engineering, Vol2, No. 1, 33-41 (2003).

Gu Y., *Rapid Mineral Liberation Analysis with X-Ray and BSE Image Processing*, Pecchio et.al. (eds) ICAM 2004, Brazil, ISBN 85-98656-01-1, pp119-122 (2004).

Jones M.P. and Gravilovic J., *Automatic quantitative mineralogy in mineral technology*, Rudy, 5, pp 189-197 (1970).

King,R.P. & Schneider,C.L., *An Effective SEM-Based Image Analysis System for Quantitative Mineralogy*, KONA Journal, Vol.11, p 165 (1993).

Lastra R., Petruk W. and Wilson J., *Image-analysis techniques and application to mineral processing*, Modern Approaches to Ore and Environmental Mineralogy, Cabri LJ and Vaughan DJ (eds.), Mineral. Assoc. Can. Short Course, Vol 27, pp 327-366 (1998).

Malvik T., *An empirical model to establish the liberation properties of minerals*, XIV International Mineral Processing Congress proceedings, Toronto, Canada (1982).

Petruk W., *Applied Mineralogy in the Mining Industry,* 2000, Elsevier Science B.V., Amsterdam, The Netherlands, ISBN 0-444-50077-4.

Shneider C.L., Neumann R. and Alcover_Neto A., *Automated, Adaptive Thresholding Procedure for Mineral Sample Images Generated by BSE*

Detector, Applied Mineralogy, Pecchio et.al. (eds), ICAM 2004, Brazil, ISBN 85-98656-01-1, pp103-106 (2004).

Paper 2

EBSD – A POTENTIAL SUPPLEMENTARY TECHNIQUE IN QUANTITATIVE CHARACTERISATION OF MINERALS

Kari Moen and Terje Malvik

Dept. of Geology and Mineral Resources Engineering, Norwegian University of Science and Technology, Trondheim, N-7491 Norway. E-mail: *kari.moen@geo.ntnu.no* and *terje.malvik@geo.ntnu.no*

Jarle Hjelen and John Rasmus Leinum

Dept. of Materials Technology, Norwegian University of Science and Technology, Trondheim, N-7491 Norway. E-mail: *jarle.hjelen@material.ntnu.no* and j*ohn.rasmus.leinum@material.ntnu.no*

ABSTRACT

Automatic identification and characterisation of mineral raw materials and beneficiated products are of major importance in mineral processing. However, minerals show great variety in their composition and physical and chemical properties. Industrial minerals may contain the same elements in about the same amount. In these cases backscatter electron imaging or chemical analysis are not sufficient to identify the minerals. Another problem arises when micro textures are not detectable in traditional imaging or the grain size is smaller than the X-ray spatial resolution.

As a supplementary technique in these cases, application of crystallographic information by electron backscatter diffraction (EBSD) in the scanning electron microscope (SEM) may be a suitable method. By means of EBSD, diagnostic mineral information can be achieved if indexible patterns are provided.

Until now EBSD has not been used frequently on geological samples for mineral and micro structure discrimination.

The technique has been demonstrated on three Norwegian mineral raw materials and one Italian marble and shows that it has some advantages compared to traditional techniques.

Keywords: SEM, EBSD, rocks, minerals, characterisation

INTRODUCTION

Common automatic techniques describing the mineral contents and the occurrence of minerals in free and locked particles, are based on optical-, backscattered electron (BSE)- or X-ray-signals.

Especially SEM-based techniques have gained wide use, and e.g. Lastra et al.(1998) describe a system based on the combination of image analysis and electron microprobe analysis to discriminate silicates in raw material and grinding products by means of grey-level discrimination from BSE-images and X-ray spectras from energy dispersive spectrometer (EDS).

Lastra et al. (1998) state that "A further complexity arises in silicate modal analysis if the minerals to be discriminated contain the same elements". They describe a complex image analysis program which by means of grey-level ranges and different X-ray count rates, copes with very complex chemistry in modal analysis. There are also some new commercial software systems on feature analysis by backscattered and X-ray signals in combination with image analysis (e.g. Oxford Inca Feature, CSIRO QemScan).

Especially in silicates, the occurrence of similar elements in the different minerals is common. Sometimes the various minerals not only contain the same elements, but also approximately the same amount of each element. In these cases chemical analysis are not always sufficient for identification.

Another problem arises when micro textures like grain boundaries or grain size, are not detectable in traditional imaging or the grain size is smaller than the EDS resolution.

As a supplementary technique for the automatic characterisation in these cases, application of crystallographic information by EBSD is suitable (Moen et. al., 2003a).

This paper presents some experiments of this technique through three examples from Norwegian mineral raw materials and one example from Italian marble.

METHODS FOR QUANTITATIVE ANALYSIS

Through the last decades several authors have published papers concerning automatic and quantitative methods for mineral characterisation. These are among others Petruk at CANMET (Petruk, 2000), Butcher at CSIRO (Cropp et.al., 2003) and Gu at JKtech. (Gu et.al., 2003)

The methods involve image analysis of optical microscope images, BSE-images and X-ray spectras from SEM/EDS.

Optical microscopy

This is the classical tool for the investigation of minerals by means of their optical properties. Most researchers always return to this method as a reference to more advanced techniques.

The samples are prepared into thin sections for studies in transmitted light or polished sections for studies in reflected light.

If minerals are discriminated by optical signals, a light microscope may be a good tool for quantitative description using image analysis, especially for some common ore minerals. Investigation in optical microscopes give a lot of information that more advanced techniques can not give, but difficulties arise when faced with automatic analysis and high resolution. These difficulties commonly include the cases of transparent minerals. The different silicates and carbonates are in most cases impossible to discriminate automatically by optical means. It then becomes necessary to turn to methods that are based on other signals that uniquely define these minerals.

EDS – X-ray analysis

When an electron beam is focused on a sample of crystalline material, several signals are generated. Examples of signals are backscattered electrons, secondary electrons, X-rays and visible light. All of these signals can be recorded by different detectors. Characteristic X-rays give information about the chemistry of the sample, and by an EDS detector, the energy and intensity distribution of the X-rays are acquired.

For automatic modal analysis, it is possible to threshold interesting features by BSE grey levels which thereafter are scanned to count X-rays, or to scan an area and get dot-maps of the relative composition of different elements, which in turn can produce combination plots to discriminate the different minerals.

The challenge is to discriminate minerals when the chemical composition becomes quite similar or too complex or when the grain size is smaller than the EDS spatial resolution (see fig. 1). This is a topic of current interest since beneficiation of fine grained minerals demands resolution in the micron region. In these situations, a technique using alternative signals to X-rays and chemical composition may be superior.

EBSD - electron backscatter diffraction

The EBSD technique is based on the weak diffraction pattern that forms when a focused, stationary, primary electron-beam strikes a polished sample, backscatters and diffracts. The diffraction pattern is formed on a fluorescent screen and transferred by a camera to the computer (Hjelen 1990).

The technique was first developed in transmitted electron microscopy (TEM) by Alam and co-workers in 1954 (Alam et. al., 1954), who described some diffraction patterns and called them "high angle Kikuchi patterns", in recognition of related diffraction phenomena reported by Kikuchi in 1928 (Kikuchi, 1928). However, it was not until the 1970s that Venables and co-workers developed detection of backscatter diffraction to metallurgical microcrystallography in SEM, paving the way for a more widespread application of EBSD to the materials sciences in the ensuing 20 years (Venables et.al., 1973). Rapid developments in both hardware and software in the past 10 years have made EBSD easy to use and ideal for the rapid analysis
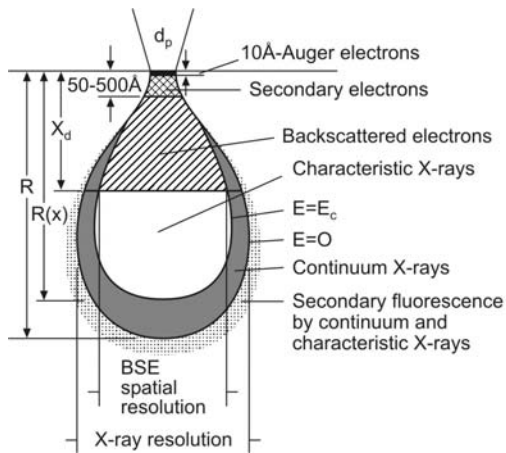
Figure 1. Interaction volume (resolution) for the signals in SEM (Goldstein 1974)
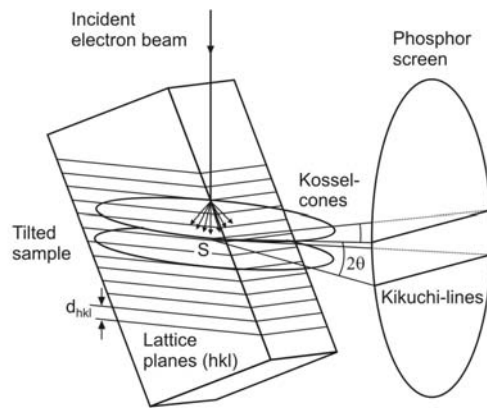

Figure 2. Origin of Kikuchi lines from EBSD (Schwartz 2000)

of microstructures of crystalline materials.

The collection of an electron backscatter diffraction pattern (EBSP) in the SEM is obtained as follows: A polished sample must be tilted to a high angle (typically 70°) inside the SEM. The electron beam is then directed at the point of interest on the sample surface. Initial elastic scattering of the incident beam causes the electrons to diverge from a point just below the sample surface and to impinge upon crystal planes in all directions. Wherever the Bragg condition for diffraction is satisfied by atomic lattice planes in the crystal, 2 cones of diffracted electrons are produced. These cones are produced for each family of lattice planes (Schwartz 2000).

These cones of electrons can be imaged using a transparent phosphor screen viewed by a sensitive camera. The camera is usually positioned horizontally, so that the phosphor screen is close to the sample in order to capture a wide angle of the diffraction patterns. Where the cones of electrons intersect with the phosphor screen, they appear as thin, bright bands (see fig. 2). These are called "Kikuchi" bands. The resulting EBSP is made up of many Kikuchi bands. Every band in the diffraction pattern represents a set of lattice planes in the crystal that is analysed, and the points of intersection between the bands represent crystallographic directions of the crystal (see fig 3). The diffraction pattern is therefore characteristic for the crystal structure and space orientation of the crystal.

EBSD software automatically locates the positions of individual Kikuchi bands and compare these to theoretical data about the relevant phase and rapidly calculates the 3-D crystallographic orientation. The whole process from start to finish can take from 0.025 sec. to more than one second dependent on the phases analysed.

For each pixel the phase and orientation are stored and can be visualised by phase or orientation maps where phase or orientation are given colour codes. Different kinds of plots can show misorientation, grain size, poles etc.. The spatial resolution of this technique is superior to X-rays, since elastic backscattered and diffracted electrons have a smaller interaction volume than X-rays. The interaction volume is dependent on acceleration voltage and atomic number of the analysed minerals, but is usually in the sub micron range.
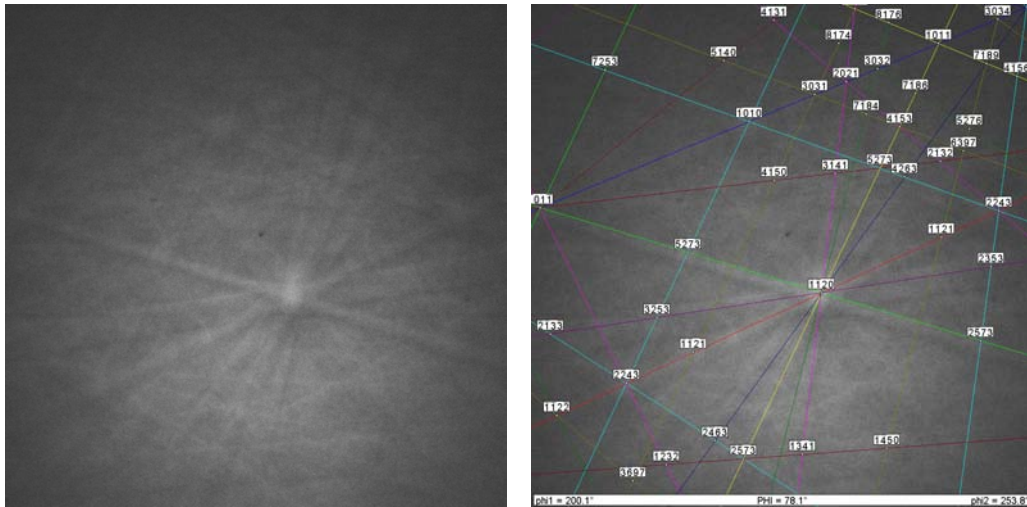
Figure 3. EBSD pattern to the left and indexed pattern to the right (Software: TSL OIM Data collection).

EXPERIMENTAL

The EBSD technique has been demonstrated on 4 different materials: **1)** ilmenite-ore from Titania A/S in Rogaland on the south-west coast of Norway, **2)** dunite (olivine stone) from A/S Olivin which is situated in Møre og Romsdal on the west coast of Norway, **3)** iron-ore from Dunderlandsdalen in Nordland in the north of Norway and **4)** marble for dimensional stone from Italy. Chemical and physical properties for the analysed minerals are given in table 1.

Table 1. Mineral properties

Mineral	Formula	Crystal structure	Space group
Ilmenite	$FeTiO_3$	Trigonal	R-3
Plagioclase	$NaAlSi_3O_8$-$CaAl_2Si_2O_8$	Tricline	C-1
Biotite	$K(Mg,Fe)_3AlSi_3O_{10}(OH,F)_2$	Monocline	C2/m
Forsterite	$Mg_{1,86}Fe_{0,14}SiO_4$	Orthorombic	Pbnm
Enstatite	$Mg_{0,94}Fe_{0,06}SiO_3$	Orthorombic	Pbca
Hematite	Fe_2O_3	Hexagonal	R-3c
Magnetite	Fe_3O_4	Cubic	Fd3m
Calcite	$CaCO_3$	Trigonal	R-3c

Preparation

The dunite specimen was prepared as polished thin sections which were ion beam etched to get a surface with as little deformation as possible and then moderately carbon coated to get rid of some charging effects because of investigations carried out on a conventional high vacuum SEM. The ilmenite and iron-ore specimens were prepared as polished sections which were then chemically-mechanically polished by colloidal silica (OP-S from Struers) in order to get a deformation-free surface (Moen et.al., 2003b). These specimens were not carbon coated (table 2).

Table 2. Sample preparation

Nb	Sample	Preparation	Ion beam etching	OP-S	Coating
1	Ilmenite-ore	Polished thin section		5 min.	
2	Dunite	Polished thin section	5kV, 5mA, 3h		carbon
3	Iron-ore	Polished section		30 sek	
4	Marble	Polished section		2.5 min.	

SEM settings

EBSD investigations of dunite were carried out on a conventional SEM equipped with EBSD hardware and software to produce grain and phase maps. Investigations of ilmenite, iron-ore and marble were carried out on a low vacuum SEM. All specimens were analysed at tilt 70° and 20 mm working distance. (table 3).

Table 3. SEM settings

Nb	Sample	SEM	EBSD hardware	EBSD software	Vacc (kV)	Vac. (Pa)	Band
1	Ilmenite-ore	Hitachi S-3500N	NORDIF CD200	Oxford Inca	20	15	Min.8
2	Dunite	JEOL 840	NORDIF CX 30	HKL Channel 5	30	10^{-3}	Min.6
3	Iron-ore	Hitachi S-3500N	NORDIF CD200	TSL OIM	25	50	5-8
4	Marble	Hitachi S-3500N	NORDIF CD200	TSL OIM	30	50	5-8

RESULTS

The results are shown as optical micrographs, electron-images and EBSD phase maps, orientation maps and orientation plots. The following vocabulary needs an explanation: "Misindexed" means that the software is indexing wrong phase or orientation for an actual pattern. "Not indexed" means that the software is not able to index the pattern at all, and "indexing fraction" means the total fraction of indexed patterns.

Figure 4 contains results from the investigation of ilmenite-ore. Image A is an absorbed electron image from the ESED-detector. Image B is a combination map of the elements Mg, Ti and Al from the EDS element dot maps which discriminate the minerals orthopyroxene, ilmenite, biotite and plagioclase. Image C is the EBSD raw map, and image D shows a noise reduced EBSD map. Legend for the EBSD image is placed above the figure text. The software had problems distinguishing between plagioclase and biotite because the acquisition parameters were not sufficiently optimised.
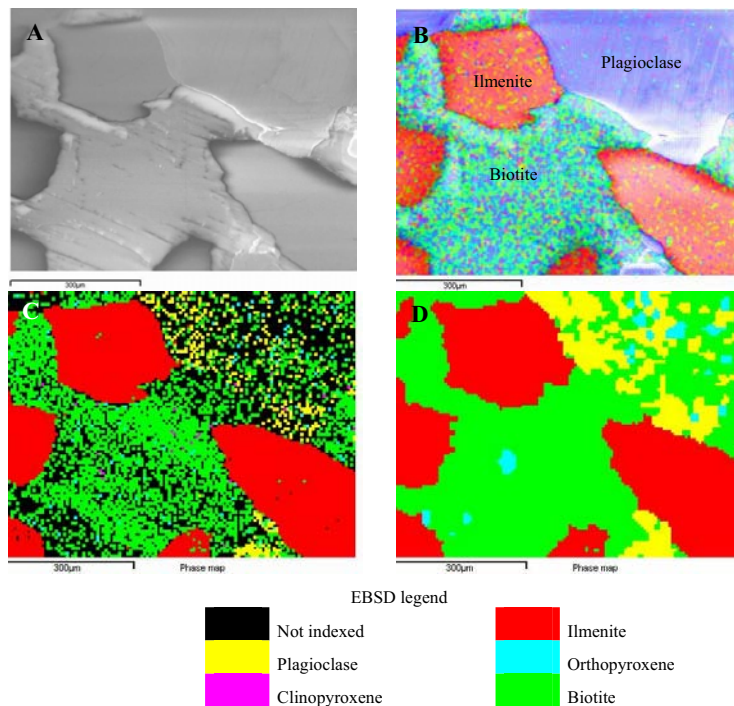

Figure 4. **A)** Electron image (ESED-detector) **B)** EDS phase map, Ti(red), Mg(green), Al(blue) **C)** EBSD raw map. **D)** EBSD enhanced map (noise reduced)

Figure 5 contains results from the investigation of dunite. Image A shows a light micrograph of enstatite in forsterite, image B shows an orientation map from the EBSD scan, image C shows a phase distribution map from the EBSD scan and image D shows a "closed" binary image from the image analyser. The "closing" procedure is applied to correct misindexing.
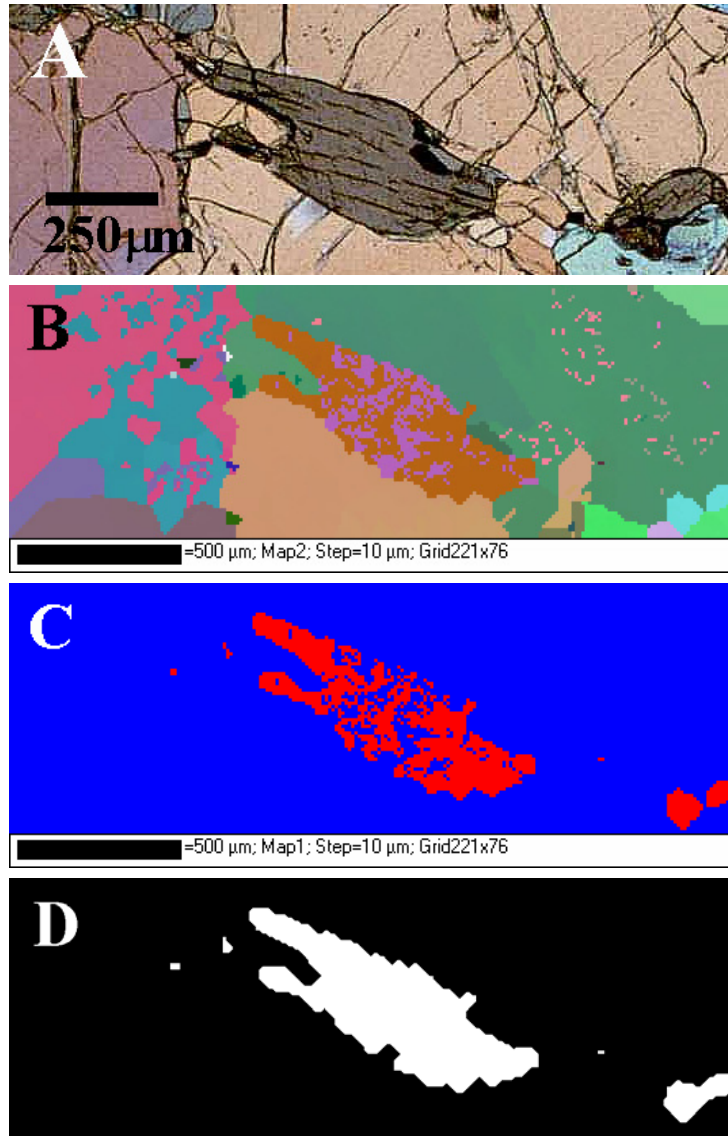

Figure 5. **A)** Optical micrograph of enstatite in forsterite. **B)** EBSD orientation map (noise reduced). **C)** EBSD phase map (noise reduced). **D)** Binary image for automatic image analysis (Enstatite 12,0 area%). "Closing" procedure applied to correct misindexing.

Figure 6 contains results from the investigation of iron-ore. Image A is an optical micrograph of a grinding product, image B is a BSE image of the same grains. Image C is the EBSD raw map which discriminates hematite and magnetite. Legend for the EBSD image is placed under the map.
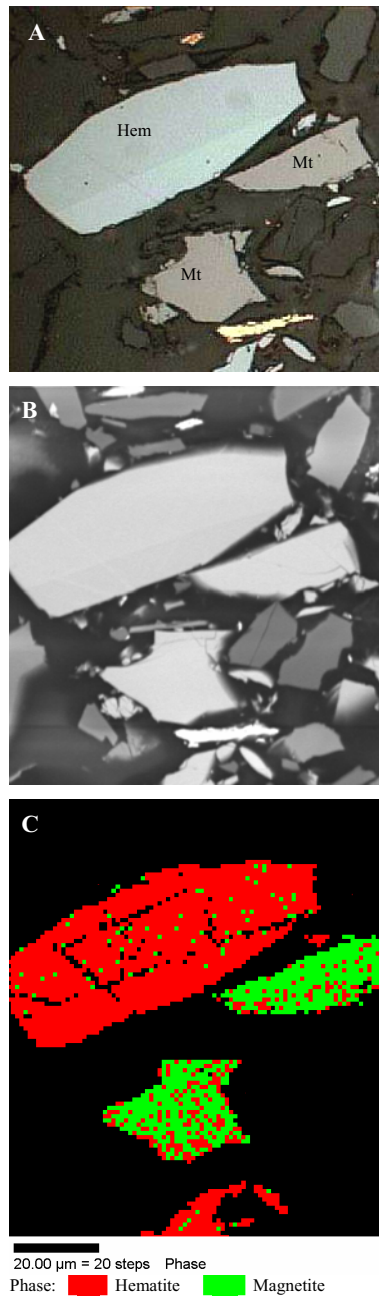
Figure 6. Iron ore **A)** Optical micrograph **B)** Electron image (BSE-detector) **C)** EBSD phase map, raw image.

Figure 7 contains results from the investigation of the microstructure of marble. The purpose is to automatically map and quantify the grain structure. Image A is an EBSD orientation map, image B shows the misorientation distribution. Image C shows the grain size distribution, image D shows the grain shape distribution and image E shows the pole figures.

Figure 7. Marble A) Orientation map B) Misorientation distribution C) Grain size distribution D) Grain shape, aspect ratios E) Pole figures.

DISCUSSION

The EBSD technique has been demonstrated on ilmenite-ore, dunite, iron-ore and marble.
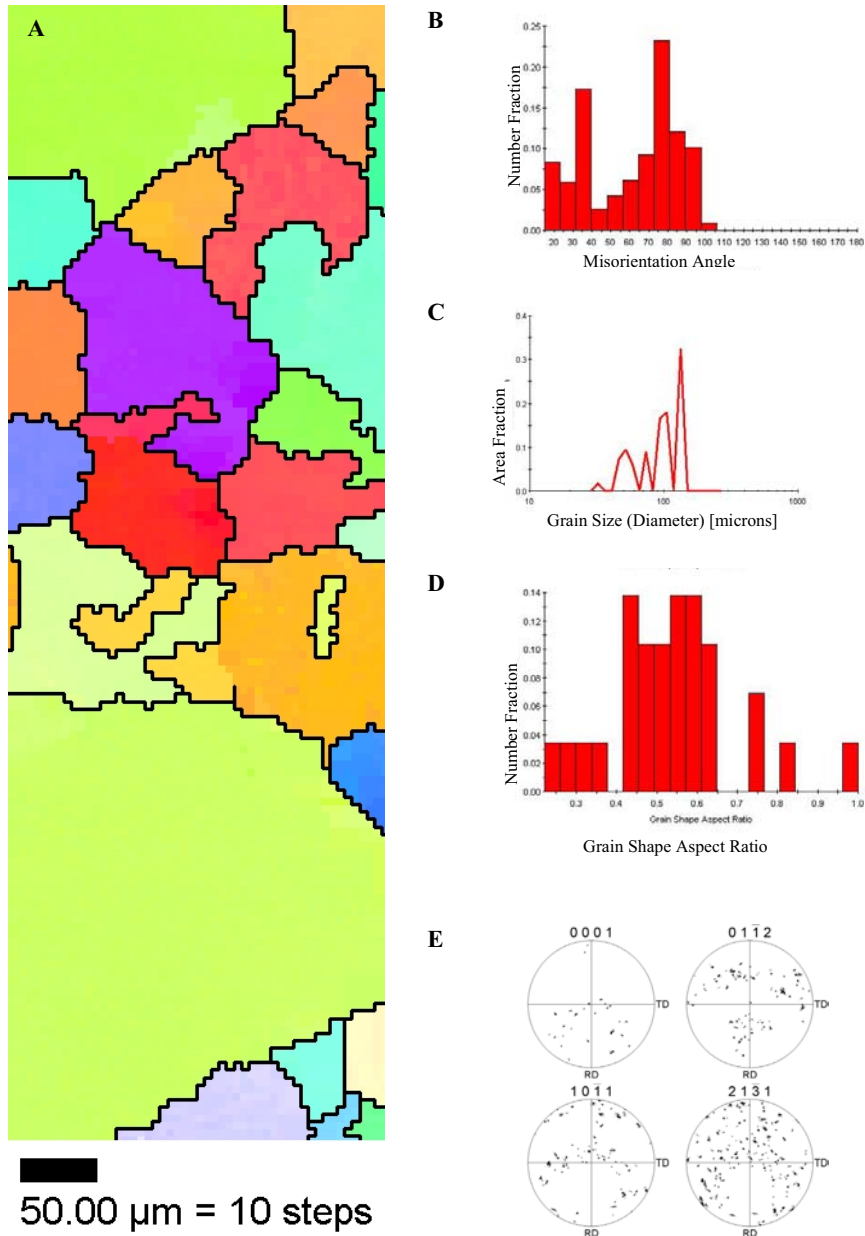
The ilmenite-ore is a noritic dyke consisting of about 20 minerals in addition to ilmenite. Some of them affect the process and product quality. The different minerals have a complex chemical composition and are removed through several steps in the process. Automatic mineral and texture quantifications of the different mineral-products are of great value for process optimisation. Most of them are discriminated by EDS. Also here, misindexing due to microfractures in the grains and not fully optimised acquisition parameters, was a bigger problem than low indexing fraction.

Dunite contains forsterite ($Mg_{1.86}Fe_{0.14}SiO_4$) and enstatite: ($Mg_{0.94}Fe_{0.06}SiO_3$) which are very similar chemically. Enstatite is unwanted in the concentrate, hence description of the occurrence of the mineral is important. During mapping, misindexing due to microfractures in the grains and bad pattern quality was a bigger problem than low indexing fraction.

The iron-ore consists of hematite (Fe_2O_3) and magnetite (Fe_3O_4). These two phases are difficult to discriminate by EDS or atomic number contrast, but is discriminated by EBSD.

Carrying out micro structure measurements in one phase, as for the marble experiment, make the indexing easier. EBSD is a unique technique for the detection of all, low and high angle grain boundaries, in any crystalline material, which is difficult by optical or electron image methods.

The charging problems that we encountered in the conventional SEM during the dunite experiment, was overcome in the low vacuum SEM without carbon coating the specimens. This led to a better diffraction pattern and better indexing.

The fact that we do not have to carbon coat the specimens, makes SEM-techniques much more useful when switching between techniques like SEM and optical microscope.

There are still some challenges to overcome before the EBSD technique is applicable as an established quantitative technique. The specimen preparation and the EBSD acquisition procedure have to be optimised to a greater degree. The experiments have indicated that misindexing is a major problem, so careful optimisation of acquisition parameters for each mineral, is important.

The image enhancement possibilities in the EBSD software is limited, so image enhancement in a conventional image analysis software might sometimes be necessary (fig. 5D).

The experiments show that EBSD is able to qualitatively discriminate minerals, which in some cases can be difficult by other automatic methods. The EBSD technique is superior as an automatic technique in discrimination of known polymorphs (Al_2O_3, SiO_2) and quantification of micro structures and fine grains. EBSD creates a complete family of related techniques together with electron imaging and X-rays analysis which together can discriminate most minerals. However, to achieve a successful result, the operator needs to possess thorough knowledge about the EBSD technique and the specimen.

CONCLUSIONS

The experiments show that EBSD is able to discriminate minerals. The technique is especially valuable when characterising materials with complex chemical composition, small grain sizes or as a method for discriminating phases of known polymorphs. Misindexing is, however, a challenge and demands some further research concerning specimen preparation and acquisition parameters.

EBSD creates a complete family of related techniques together with electron imaging and X-ray analysis, which together, can discriminate most minerals. However, to achieve a successful result, the operator needs to possess thorough knowledge about the EBSD technique and the specimen.

REFERENCES

Alam, M.N., Blackman, M., Pashley, D.W. (1954). High angel Kikuchi patterns. Proc. Royal Society of London, A221:224.

Cropp, A.F., Butcher, A.R., French, D., Gottlieb, P., O'Brien, G., Pirrie, D. (2003). Automated Measurement of Coal and Mineral Matter by QemSCAN – A New Mineralogical Tool based on Proven QEM*SEM Technology. Applied Mineralogy '03, Helsinki, Finland (in press).

Goldstein, J.I. (1973). Metallography – A practical tool for correlating the structures and properties of materials. ASTM Special Technical Publication 557, p 86.

Gu, Y., Do, M., Gay, S. (2003). Mineral identification with back-scattered electron image analysis. Applied Mineralogy '03, Helsinki, Finland (in press).

Hjelen, J. (1990): Teksturutvikling i Aluminium, studert ved Elektronmikrodiffraksjon (EBSP) i Scanning Elektronmikrosko". Ph.D.-thesis, University of Trondheim.

Kikuchi, S (1928). Diffraction of cathode rays by mica. Jap. J. Phys., 5:83.

Lastra, R., Petruk, W., Wilson, J (1998). Image-analysis techniques and applications to mineral processing. Modern Approaches to Ore and Environmental Mineralogy. COM/IMA, vol 27, pp 327-366.

Moen, K., Hjelen, J., Malvik, T., Leinum, J.R. (2003a). EBSD-a potential supplementary technique in automatic mineral characterisation. Applied Mineralogy '03, Helsinki, Finland (in press).

Moen, K., Hjelen, J., Malvik, T. (2003b). Preparation of Quartz samples for EBSD analysis. Applied Mineralogy '03, Helsinki, Finland (in press).

Petruk, W. (2000). Applied mineralogy in the mining industry. 1sted. Elsevier Science, ISBN 0-444-50077-4.

Schwartz, A. J., Kumar, M., Adams, B.L. (2000) Electron Backscatter Diffraction in Materials Science. NY, Kluwer Acadenic/ Plenum Publishers, ISBN 0-306-46487-X.

Venables, J.A., Harland, C.J. (1973). Electron Backscattering Patterns-a new crystallographic technique for use in the SEM. Scanning Electron Microscopy: Systems and Application. Institute of Physics. London and Bristol, 294.

Paper 3

EBSD Microstructure Measurements of Marble

K.Moen & T.Malvik
Department of Geology and Mineral Resources Engineering, Norwegian University of Science and Technology, Norway

J.Hjelen, J.R.Leinum
Department of Material Science, Norwegian University of Science and Technology, Norway

L.Alnæs
SINTEF Civil and Environmental Engineering, Rock and Soil Mechanics, Norway

ABSTRACT: Bowing of crystalline marble when used as exterior thin claddings is experienced occasionally on buildings around the world. A European Research Project (TEAM) is investigating this deterioration phenomenon and influencing intrinsic and extrinsic parameters. One of several approaches for investigation of intrinsic parameters is microstructure measurements by Electron Backscatter Diffraction (EBSD). The rock fabrics of two marbles have been investigated and the EBSD analyses show that the microstructure is intuitively different when comparing them. While the no bowing marble shows xenoblastic microstructure with sutured grain boundaries, subgrains and a lot of twinning, the bowing marble shows granoblastic and polygonal microstructure. The EBSD results indicate that the stable marble shows a stronger texture than the bowing marble, which shows more random orientation. This trend confirms the statement of Barsottelli et al. (1998) and is also in accordance with knowledge from materials science for metals.

1 INTRODUCTION

Several modern buildings around Europe are covered by marble claddings panels. At certain buildings the panels start to bow and loose strength after some years on the wall (see Figure 1) This phenomenon is experienced occasionally for crystalline marble when used as exterior cladding, see e.g. Cohen & Monteiro (1991), Hook (1994), and Schouenborg et al. (2001) and is assumed to be controlled by temperature variations and moisture, see Yates at al (in prep).

An extensive European research project (TEAM – Testing and Assessment of Marble and Limestone) is investigating this deterioration phenomenon and influencing intrinsic and extrinsic parameters. The project is partly funded by the European Commission under the contract no. G5RD-CT-2000-00233 (see also www.sp.se/Building/TEAM). The TEAM partners have managed to simulate bowing in the lab (Grelk et al. in prep). But why does it happen only to certain crystalline marbles? A lot of rock fabric investigations have been done (Alnæs et al. in prep), but it is difficult to quantify the important rock fabric elements by means of ordinary imaging (optical, SEM) and image analysis.

Electron Backscatter Diffraction (EBSD) detects microstructure by means of crystallography. That means preferred lattice and grain orientations, grain morphology, grain size etc. EBSD can be a potentially method for detecting and quantify such marble microstructure. The challenge is to quantify differences by EBSD and correlate the results with bowing tendencies.

This paper presents some EBSD results for two marbles, one with strong bowing and one with very weak to absent bowing experienced in both buildings and accelerated laboratory bow test.

2 ELECTRON BACKSCATTER DIFFRACTION

The EBSD technique is based on the weak diffraction pattern that forms when a focused, stationary, primary electron beam strikes a polished sample, backscatters and diffracts. The diffraction pattern is formed on a fluorescent screen and transferred by a camera to the computer (Hjelen 1990).

Rapid developments in both hardware and software in the past 10 years have made EBSD easy

Figure 1. Bowing of marble claddings (from TEAM brochure, see also www.sp.se/Building/TEAM)

Figure 2. Origin of Kikuchi lines from EBSD (Schwartz et.al. 2000)

Figure 3. EBSD patterns from 2 orientations of calcite.

to use and ideal for the rapid analysis of microstructures of crystalline materials. The collection of an electron backscatter diffraction pattern (EBSP) in the SEM is obtained as follows: A polished sample must be tilted to a high angle (typically 70°) inside the SEM. The electron beam is then directed at the point of interest on the sample surface. Initial elastic scattering of the incident beam causes the electrons to diverge from a point just below the sample surface and to impinge upon crystal planes in all directions. Wherever the Bragg condition for diffraction is satisfied by atomic lattice planes in the crystal, 2 cones of diffracted electrons are produced. These cones are produced for each family of lattice planes (Schwartz et al. 2000). These cones of electrons can be imaged using a transparent phosphor screen viewed by a sensitive camera. The camera is usually positioned horizontally, so that the phosphor screen is close to the sample in order to capture a wide angle of the diffraction patterns. Where the cones of electrons intersect with the phosphor screen, they appear as thin, bright bands (see Figure 2 and Figure 3). These are called backscatter "Kikuchi" bands (Kikuchi 1928). The resulting EBSP is made up of many Kikuchi bands. Every band in the diffraction pattern represents a set of lattice planes in the crystal that is analysed, and the points of intersection between the bands represent crystallographic directions of the crystal (see Figure 3). The diffraction pattern is therefore characteristic for the crystal structure and space orientation of the crystal.
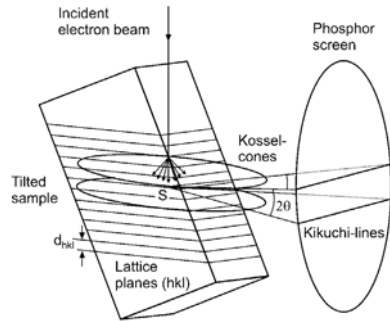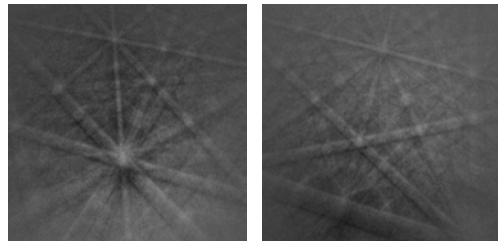
The EBSD software automatically locates the positions of individual Kikuchi bands, compares these to theoretical data about the relevant phase and rapidly calculates the 3-D crystallographic orientation. The whole process from start to finish can take from 0.025 sec. to more than one second dependent on the phases analysed.

For each pixel the phase and orientation are stored and can be visualised by phase or orientation maps where phase or orientation are given colour codes. Different kinds of plots can show misorientation, grain size, poles etc. The spatial resolution of this technique is superior to x-rays, since elastic backscattered and diffracted electrons have a smaller interaction volume than x-rays. The interaction volume is dependent on acceleration voltage and atomic number of the analysed minerals, but is usually in the sub micron range. (Moen et al. 2003)

3 EXPERIMENTAL

3.1 Sampling and preparation

The marble specimens are sampled from two neighbouring quarries. Both are calcitic marbles (calcite content > 99 %weight), but one has a problem with bowing while the other has not. For the EBSD analyses the specimens were prepared by cutting, grinding and polishing, to give a polished rock section of diameter 25 mm. A chemical-

mechanical polishing was performed in the end, to make a deformation free surface that makes lattice diffraction possible.

3.2 Microscopy

Before put into the Scanning Electron Microscope (SEM), the sample is covered by aluminium foil along the flanks and carbon paint along the edges to make it as conductive as possible without carbon coating it. To get an optimal EBSD pattern, the analysis is performed in a low vacuum SEM without a conductive carbon layer.

The equipment applied for the experiments is listed in Table 1 and the running and processing conditions in Table 2.

Table 1. Equipment applied for EBSD mapping

Equipment	Type
Low-vacuum SEM	Hitachi S-3500N
EBSD camera	Nordif EBSD dig. camera
EBSD software	TSL, OIM version 3,08/3,5

Table 2 Running and processing conditions for EBSD mapping

Parameter	Setting
WD	20 mm
V_{acc}	20 kV
Pressure	40 Pa
Tilt	70°
Magnification	90x
Binning	2x2
Step size	5 μm
Processing	Gaussian convolution Half with 15° Expansion L=22 Harmonic calculus

4 RESULTS

The results are presented in Figure 4 as orientations maps colour coded by the inverse pole figure (top) and grain boundary map including grains with preferred lattice orientation (bottom), in Figure 5 as pole figures and in Figure 6 as grain size distributions (top) and misorientation angle plots (bottom).

No bowing marble: Bowing marble:
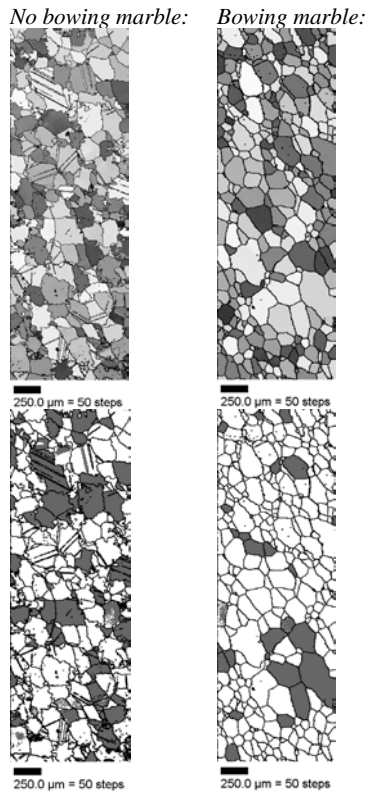

Figure 4. Inverse pole maps (top), grain boundary maps including grains with a preferred orientation (plotting in the dark maxima of the <0001> pole figures (bottom).
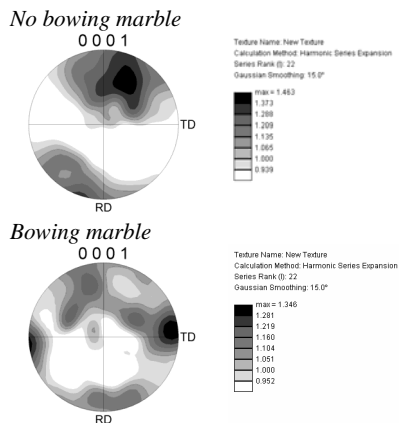

Figure 5. Pole figures of orientation densities in logarithmic scale, upper hemisphere, equal area projection: no bowing marble (top), bowing marble (bottom) based on stage scan of more than 6000 grains.
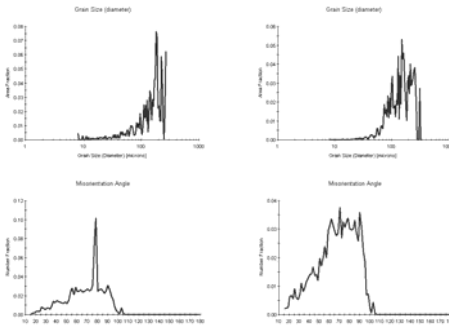
147

No bowing marble: *Bowing marble:*

Figure 6. Grain size distribution (top) and misorientation angles (bottom). The peak around 77° characterising the no bowing marble represents the twin boundaries.

5 CONCLUSIONS

EBSD seems to be well suited to describe microstructure elements in marble (e.g. grain size distribution, grain boundary geometry, grain shape preferred orientation, and lattice preferred orientation (texture)).The first experiments are regarded as successful and are presented here.

The feature characteristics of the two marbles are intuitively different. While the no bowing marble shows a lot of subgrains, twinning and sutured grain boundaries (xenoblastic microstructure), the bowing marble shows clean grain boundaries, equally distributed grain size and almost no twinning. This means granoblastic and polygonal microstructure with triple point grain boundary intersections of approximately 120°, which is typical for a statically recrystallised microstructure (Pieri et al. 2001).

From Figure 5, one can see that the stable marble has got one distinct pole (dark maximum) in the (0001) pole figure, while the bowing marble has the orientations more smeared out. Figure 4 (bottom) shows grains with a preferred lattice orientation, which means grains plotting in the maximum of the pole figures. In the bowing marble it is seen fewer grains with a preferred lattice orientation. The figures 4-5 indicate that the stable marble shows more preferred orientation (stronger texture) than the bowing marble, which on the other side shows a more random orientation. This trend is in accordance with the findings of Koch and Siegesmund (in press) and also confirms the statement of Barsottelli et al. (Barsotelli, Fratini & Giorgetti 1998) who cite Rosenholts and Smith,1950: "Decohesion of marble due to thermal expansion anisotropy of the calcite crystal only occurs in marble with weak or absent crystallographic orientation".

The findings are also in accordance with knowledge from material science for metals where it is known that recrystallised metal, free of tension and weak crystallographic orientation, is ductile and easy to form. Contrary, deformed metal contains preferred crystal orientation and a great number of dislocations, which reinforce the structure and makes it more resistant against external forces.

The EBSD technique is at present in use for investigation of additional marble types and also to study the potential relationship between bowing, in *situ* rock stresses and rock fabric.

6 REFERENCES

Alnæs, L., Koch, A., Schouenborg, B., Åkesson, U. & Moen, K. 2004. Influence of Rock and Mineral properties on the durability of marble panels. *In prep. Proc. Dimension Stone 2004.*

Barsottelli, M., Fratini, F. & Giorgetti. 1998. Microfabric and alteration in Carrara marble: a preliminary study. *Science and technology for Cultural Heritage 7* (2), 115-126.

Cohen & Monteiro 1991: Durability and Integrity of Marble Cladding " A state of the art review". *Journal of the Performance of Constructed Facilities.* 5(2), pp 113-124.

Grelk, B., Golterman, P, Schouenborg, Koch, A. & Alnæs, L. 2004. The laboratory testing of potential bowing and expansion of marble. *In. prep. Proc. Dimension Stone 2004.*

Hjelen J, 1990. Teksturutvikling i Aluminium, studert ved Elektronmikrodiffraksjon (EBSP) i Scanning Elektronmikrosko. Ph.D. Thesis. Trondheim, Norway: University of Trondheim.

Hook, K. 1994: Look out below – The Amoco Building Cladding Failure. *Progressive Architecture,* Feb., 75, pp 58-62.

Kikuchi S, 1928. Diffraction of cathode rays by mica. Jap. J. Phys, 1928. 5:83.

Koch, A. & Siegesmund, S. 2004. The combined effect of moisture and temperature on the anomalous expansion behavior of marble. *In*: S. Siegesmund, H. Viles & T. Weiss (eds), *Stone Decay hazards; Environmental Geology*, in press.

Moen K, Malvik T, Hjelen J, Leinum JR, 2003 Automatic Material Characterization by means of SEM-techniques, Proceeding, 9th Euroseminar on Microscopy Applied to Building Materials, Ed: M.A:T:M: Broekmans et.al

Nordtest 2000, Field method for measurement of bowing of cladding panels, http://www.sp.se/building/team/results.htm

Pieri M, Burlini L, Kunze K, Stretton I, Olgaard DL, 2001. Rheological and microstructural evolution of Carrara marble with high shear strain: results from high temperature torsion experiments. Journal of Structural Geology. 23;9, p 1393-1413.

Schouenborg, B., Grelk, B., Alnæs, L., Brundin, J.A., Blasi, P., Yates, T., Marini, P., Tschegg, E., Unterweger, U., Tokartz, B., Kock, A., Bengtsson, T., Mladenovic, A & Goralezyg, S. 2003: TEAM – Testing adn Assessment of Marble and Limestone.

Schwartz AJ, Kumar M, Adams BL, 2000. Electron Backscatter Diffraction in Materials Science. NY, Kluwer Acadenic/ Plenum Publishers, ISBN 0-306-46487-X.

Yates, T.; Brundin, J-A; Goltermann, P. & Grelk, B., 2004. Observations from the inspection of marble cladding in Europe. *In prep. Proc. Dimension Stone 2004.*

Paper 4

Quantitative measurements of marble microstructure -a model for predicting the deterioration of marble

K.Moen & T.Malvik

Department of Geology and Mineral Resources Engineering, Norwegian University of Science and Technology, Norway

L.Alnæs

SINTEF Building and Infrastructure, Rock and Soil Mechanics, Norway

J.Hjelen

Department of Materials Science and Engineering, Norwegian University of Science and Technology, Norway

ABSTRACT:

Deterioration of marble used as exterior marble cladding panels is experienced occasionally. Many researchers have studied this effect and it is commonly concluded that the most relevant extrinsic factors are temperature variation in combination with moisture. The intrinsic factors that give rice to the phenomenon for certain marbles can be found in the microstructure. This paper presents quantitative data of different microstructure parameters in marble. By use of laboratory bowing data, two models for prediction of bowing by means of important microstructure parameters were suggested. The results showed that by interaction of several microstructure parameters, bowing could be significantly described in a regression model. The variables that influenced the models most heavily were grain-shape factors describing the roundness and roughness of the grain boundaries together with the shape of the grain-size distribution curve.

Keywords: Marble, deterioration, microstructure, characterisation, microscopy, quantification

1 INTRODUCTION

As the building frameworks were introduced to the construction sector, the natural stone was not used for carrying the constructions any longer. Nowadays thin cladding panels of 20-40 mm are rather used. Several modern buildings are covered by marble claddings panels and at certain buildings the panels start to bow and loose strength after some years, Figure 1. The complete replacement of façade panels of some prestigious buildings like the Amoco building in Chicago and the Finlandia Hall in Helsinki are often referred examples of this phenomenon that is assumed to be controlled by marble type, temperature variations, moisture and time. It is experienced occasionally for crystalline marble only when used as exterior cladding, and has been studied by several authors investigating intrinsic and extrinsic parameters, see e.g. Kessler (1919), Cohen & Monteiro (1991), Hook (1994), Winkler (1996), Zeisig et al. (2002), Schouenborg et al. (2003), Yates et al. (2004),

Figure 1. Warping marble cladding panels at the Finlandia Hall, Helsinki. Photo: TEAM project.

Grelk et al. (2004), Koch & Siegesmund (2004), Alnæs et al. (2004) and Åkesson et al. (2006).

Some authors have studied the extrinsic factors and corresponding response from the rocks (Kessler, 1919; Koch and Siegesmund, 2002; Winkler, 1996; Yates et al., 2004). It was found that the process of bowing can not be explained by chemical weathering and acid rain. Kessler (1919) found that repeated heating lead to permanent dilatations due to microfracturing while Winkler (1996) favoured the role of oriented water molecules that enter and expand the stone capillaries enough to permit entry of ordinary water.

An extensive European research project "Testing and Assessment of Marble and Limestone" (TEAM) 2000-2005, was investigating this deterioration phenomenon and influencing intrinsic and extrinsic parameters (Grelk, 2005). The "TEAM" partners managed to simulate bowing and loss of strength in the laboratory (Grelk et al., 2004) and a major question asked was: Why does it happen only to certain crystalline marbles?

Numerous rock response and rock microstructure investigations were performed and reported in papers and reports by the "TEAM" partners on more than 50 rock types throughout the project (e.g. Alnæs et al., 2004; Grelk et al., 2004; Koch and Siegesmund, 2004; Yates et al., 2004; Åkesson et al., 2006). Permanent dilatations due to microfracturing and the strong anisotropic thermal dilatation for calcite ($26 \times 10^{-6} K^{-1}$ parallel to crystallographic c-axis and $-6 \times 10^{-6} K^{-1}$ parallel to the a-axis) are among important mechanisms mentioned (Weiss et al., 2002), together with lattice preferred orientation, grains-shape preferred orientation and the nature of the grain boundaries and grain-size distribution (Koch and Siegesmund, 2004; Zeisig et al., 2002; Åkesson et al., 2006), but no straightforward conclusions were established.

Most samples investigated show deterioration due to thermal and moisture treatment. As stated by Zeisig et al. (2002), this cannot be explained without taking into account the rock mineralogy and the microstructure. However, the microstructure cannot be reduced to one or a small number of parameters (grain-size, grain-shape etc.), because degradation is controlled by an interaction of several microstructure parameters. In his review article, Grelk (2005) mentions that in order to correlate the properties of the marble to its microstructure; there is a need to quantify the degree of granoblasticity/xenoblasticity of the marbles.

This paper presents quantitative data of different microstructure parameters in marble. The term microstructure is used in accordance with Passchier and Trouw (2005) and includes complete spatial and geometrical configuration of all components of a rock including grain-size distribution, grain-shapes, grain-shape preferred orientation, grain boundary morphology, size and orientation of micro cracks and lattice preferred orientation (texture in material sciences) etc. By use of laboratory bowing data acquired by the partners of the "TEAM" project, the microstructure data is linked to bowing. Development of a model to predict the bowing by means of measured microstructure parameters is suggested further on. The results show that the microstructure is correlated with deterioration tendencies, and based on interaction of several parameters the bowing response can be described.

2 EXPERIMENTAL

2.1 Rock samples

Commercial types of marble were investigated. They were sampled by the "TEAM" project partners from quarries around Europe situated in Greece, Italy, Norway, Portugal and Sweden. They were all calcitic or dolomitic marbles with quartz, biotite, muscovite, phlogopite, sulphides and oxides as accessory minerals. Figure 3 shows microphotographs of the marble microstructures, and the most important characteristics of the microstructure elements are summarised in Table 3. Marble codes were used instead of locations or names due to confidentiality reasons.

2.2 Characterisation of marble microstructure

The specimens were prepared to polished thin sections of thickness 30 μm by cutting, vacuum impregnation, grinding and polishing. Manual quantification was carried out to describe distinct microstructure parameters including shape of grains, shape of grains aggregates, grain boundaries, cleavage, twinning and number of adjacent grains. Image analysis was also carried out to quantify some of the important microstructure elements such as 2D grain-size distribution and grain-shape factors. Since most specimens were sampled randomly according to foliation planes and lineation directions, no reference coordinate system was introduced.

2.3 Microscopy

By optical microscopy of polished thin sections the marbles were characterised by relevant parameters organised in simple quantification categories, following Passchier and Trouw (2005). By means of a coding system described in Table 1, the best correlated and relevant variables were included in the regression model.

Table 1. Some examples from the coding system used for characterising the microstructures in the microscope.

Shape of grains			Shape of grain aggregates			Grain Boundaries	
Idioblastic/euhedral	1		Polygonal	1		Straight (mosaic)	1
Hypidioblastisc/subhedral	2		Interlobate	2		Lobate / caries	2
Xenoblastic/anhedral	3		Amoeboid	3		Sutured	3

Subgrain growth		Twinning of carbonate		Signs of cleavage	
None	0	No	0	No	0
Weak	1	Weak	1	Weak	1
Medium	2	Medium	2	Medium	2
Strong	3	Strong	3	Strong	3

2.4 Image analysis

2.4.1 General

To quantify grain-size distribution and shape factors, micrographs taken in the optical microscope were analysed by means of two-dimensional image analysis. To be able to threshold the grain boundaries without getting disturbed by the distinct cleavage planes and carbonate twin boundaries, manually contouring was performed. An advanced automatic segmentation routine developed by Lumbreras and Serrat (1996) could alternatively be tested

in the future. Measured microstructure parameters by means of image analysis and derived parameters are displayed in Table 2.

Table 2. Measured microstructure parameters applied for characterising the marbles

Parameter	Abbreviation	Definition
Area	A	Area of grain
Equivalent circle diameter	ECD	$ECD = 2 \times \sqrt{\dfrac{A}{\pi}}$
Grain size percentiles	D50 (also D5, D10, D20, D90)	The ECD where 50 area% of the grains are smaller
Perimeter	P	The length of the outer boundary of the grain
Convex perimeter	P_c	Perimeter of the convex hull of the grain
Circumference	C	$ECD \times \pi$
Adjacent grain analysis	AGA	Number of adjacent grains for the median sized grains (Åkesson, 2004)
Roughness 1	Rg1	P/P_c
Roughness 2	Rg2	$\dfrac{P}{\sqrt{A}}$
Roughness 3	Rg3	P/C
Roundness	Ro	$\dfrac{4\pi A}{P^2}$

2.4.2 Grain-size distribution

The two-dimensional (2D) grain-size distributions were obtained by area analysis of 500-3000 grains for each sample. The grain-size distribution is presented as apparent cumulative area % as a function of apparent equivalent grain diameter (ECD) in *μm*. Ratios reflecting the shape of the distributions were also tested in the multivariate analysis. The ratios were defined as D5/D10, D5/D20, D10/D50 and D10/D90.

2.4.3 Shape factors

Grain-shape factors reflecting the irregularity of grain boundaries (roughness and roundness), Table 2, were chosen to describe the microstructure in addition to the grain-size distribution. Since most specimens were sampled randomly according to foliation planes and lineation directions, variables depending on sample orientation, like aspect-ratio and grain-shape orientation, were not taken into account in this paper. These aspects are excellent treated by Koch and Siegesmund (2004) and is further discussed in the discussion chapter.

Shape factors describing roundness and roughness include measurements of grain perimeter. As King and Schneider (1995) explain, the measurement of perimeter by image analysis is subject to uncertainty because it is dependent of the digital pixel size and the resolution at which the original image is generated. If the images originate from different magnifications, error is introduced. This is referred to as the fractal problem. The images of this study originated from two different magnifications (2.5x and 5x). The image analysis software subsamples the boundary points to approximate a smoother, more accurate perimeter. These values were used in this analysis.

2.5 Adjacent grain analysis

Åkesson et al. (2004) have described microstructures quantitatively by using adjacent grain analysis, AGA, and achieved good correlation between AGA and bowing observed on buildings. Since calcite belongs to the hexagonal crystal system, a polygonal, equigranular, idioblastic texture with straight grain boundaries will give rise to crystals sharing grain boundaries with six grains, which are referred to as *adjacent grains* AG (Figure 2) (Åkesson, 2004). Increasing grade of deformation with grain boundary migration, bulging and subgrain formation leading to lobate or sutured grain boundaries and more inequigranular grain-sizes will result in an increasing number of adjacent grains. In an inequigranular rock, the largest crystals can have the highest number of adjacent grains whereas the smallest crystals can have less than six adjacent grains. A larger number of adjacent grains also occur in rocks with complex grain boundaries (Figure 2). Both of these microstructures can increase the number of adjacent grains in comparison with a polygonal, equigranular texture. This relation was observed by Bain (1941) in an investigation of grain-border measurements on several types of marbles (Åkesson, 2004).

The number of adjacent grains was counted for at least 100 median sized grains from each sample following Åkesson (2004).
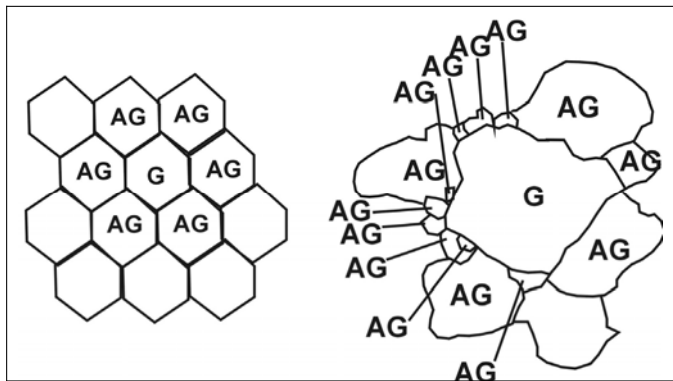

Figure 2. Schematic image of an ideal polygonal texture (left) and a seriate interlobate texture (right). The figure also illustrates how the adjacent grains AG are counted (with permission from Åkesson et al., 2006)

2.6 Mineralogy

Modal mineralogy is regarded as important for the deterioration potential. Most marbles however, possesses only traces of other minerals. Mineralogical analyses existed for most samples in the dataset. Some simple scatterplots were performed on the data, but since the calcitic marbles were pure and the statistical material regarding laboratory bowing of dolomitic marbles was poor in this dataset, no further efforts were done to establish relations between carbonate and silicate mineralogy and deterioration potential. The dolomitic samples were therefore removed from the dataset.

2.7 Response data

Response data is the dependent variable in a regression model and is in this case a general term for the measurements on physical response from the marble when exposed to different

stresses like heat, moisture, seismic, point load etc. The response dataset from the "TEAM" project contained a huge amount of outputs. Since most partners had performed measurements on a limited set of samples, only very few of these could be used to compute a prediction model. The input data or the independent variables were in this case the microstructure data.

From Grelk (2005) it is explained that deterioration of marble panels involves several parameters and properties where "bowing" is the most obvious phenomenon, but it is often followed by volume changes. The most serious phenomenon is nevertheless loss of strength which may progress so far as to total loss of cohesion between the grains. The result may be cracking of panels, spalling around anchor points or ultimately failure of the panels (Grelk, 2005).

When possible correlation between deterioration and microstructure should be found, a response dataset of good data quality had to be available. The "TEAM" project partners had experienced that getting representative response data at the same magnitude from the different laboratories was not straightforward since the marbles were both nonhomogeneous and anisotropic (Koch and Siegesmund, 2004). Since the most serious phenomenon is loss of strength, this parameter should then be used as the main response parameter. However, available data on this property was not numerous. On the other hand, bowing data from laboratory bowing after 25 wetting and heating cycles was available for most samples and collected by several laboratories. These data was therefore applied in the calculations for constructing a prediction model. Bowing data from the Sintef (1), Unigoe (2) and Rambøll (3) laboratories was used since these laboratories had performed most tests. In addition to absolute bowing, expansion and loss of strength measurements, the development of these responses during cyclic heating and moisture treatment give characteristic hysteresis graphs (see e.g. Koch and Siegesmund, 2004). Experimental setup and references to procedures and standards for laboratory bowing tests are also found in this paper.

2.8   Data analysis

2.8.1   Correlation

Correlation was calculated to measure the degree of linear relationship between bowing data from three laboratories. To obtain a reliable prediction model, the response data needs good quality and the correlation should therefore be high between the laboratories.

The correlation coefficient assumes a value between -1 and $+1$. If one variable tends to increase as the other decreases, the correlation coefficient is negative. Conversely, if the two variables tend to increase together the correlation coefficient is positive. For a two-tailed test of the correlation: H_0: $\rho = 0$ versus H_1: $\rho \neq 0$ where ρ is the correlation between a pair of variables. The p-values displayed in Table 4, are for the hypothesis test of the correlation coefficient being zero.

2.8.2   PLS Regression

The available dataset had more variables than rock types and variables that were multicollinear. Multicollinearity means that some variables are correlated. Ordinary regression analysis cannot be performed under these circumstances with collinear data in addition to the fact that there are more variables than samples. The problem was solved by performing regression on latent variables which are independent, instead of the original variables.

The principle of the method can be described as follows: In a dataset, correlated variables contain approximately the same information. If several variables are correlated with each other, this suggests that there is an underlying phenomenon that is more fundamental than the actual variables. By principal component analysis (PCA) (eigenvector analysis) the data is

6

projected onto a lower dimensional space. The projection provides an alternative set of variables to those given in the original data table. These new variables are independent, linear combinations of the original variables and referred to as latent variables. The loadings are the weights needed to define the latent variable. The loadings define the magnitude of influence this variable has on the construction of the latent variable. The score of the samples is the projection of the sample down onto the latent variable axis.

PCA is performed by calculating the covariance/variance (or correlation) matrix for the variables. From this the eigenvectors can be calculated with corresponding eigenvalues. This new eigenvector matrix makes the basis for the analysis. The eigenvectors are rotated in relation to the original coordinate space and have some new and useful properties of linear independence in addition to the fact that the loadings describe the degree of variance that are described by the different PCs. The rotation of the PCs has to be optimized. To take into account the best directions in both the variable space and the "bowing" space (X and Y) Partial Least Squares regression (PLS) can be used. Here the latent vectors in X have maximum relevance for Y.


3 RESULTS

3.1   General

The results found in this chapter benefit from results obtained in the "TEAM" project. The microstructure measurements are a part of this study whereas the rock response data was obtained by the "TEAM" partners (collected by Alnæs and Aasly, 2005). All data used can be found in this dataset.

3.2   Microscopy

Figure 3 displays photomicrographs of the investigated rocks. The marbles possessed a variety of microstructures and grain-sizes from equigranular, idioblastic texture with straight grain boundaries and totally recrystallised grains showing neither twinning nor undulose extinction (Itq2), to microstructures of undulose extinction, deformation twins, subgrain formation and widespread grain boundary migration resulting in sutured to lobate grain boundaries and seriate shape of grain aggregates (Itq1 and 3).

Table 3 gives an overview of the results from the characterisation of the rocks. Characteristic values from the image analysis are also found here including 2D grain-size distribution percentiles, grain-shape factors and adjacent grain analysis (AGA). Average bowing data from the three laboratories used in the analysis is also included.
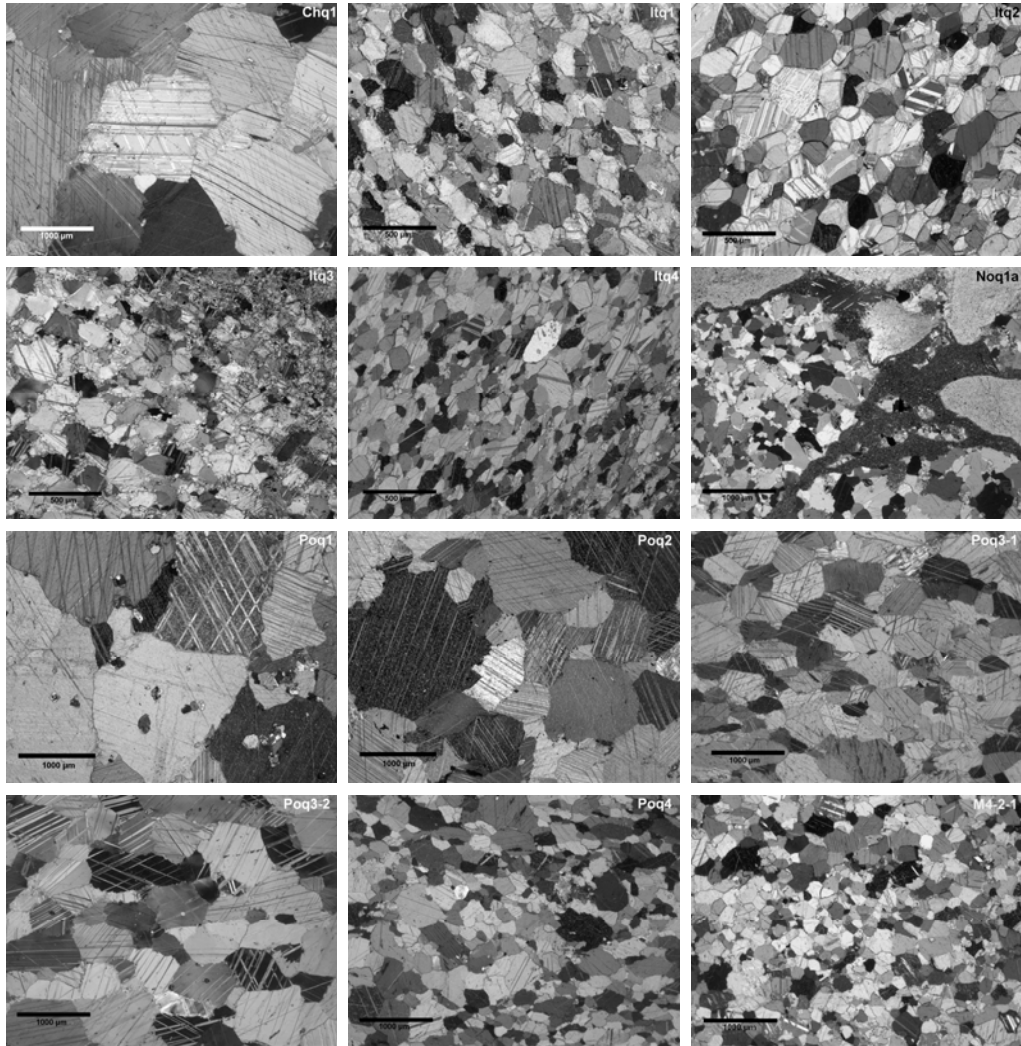
Figure 3. Microstructure of the investigated marbles. Scalebar is displayed in the lower left corner and sample code in the upper right corner.

Table 3. Overview of important microstructure elements of the marbles investigated.

| Marble	Comp	Crystal	Grain boundaries	Shape of grain	Subgrain	2D grain-size					Shape factors (50 percentiles)				AGA	Spherical bowing 25 cycl. (mm/m)		
		growth		aggregates	growth	D5	D10	D20	D50	D90	Rg1	Rg2	Ro3	Ro		Lab. 1	Lab. 2	Lab. 3
Chq1	cc	Hypidiobl	Lobate(straight)	Interlobate(polyg)	None(weak)	163	228	319	508	648	1.84	4.57	1.28	0.40	9		0.485	0.639
Grq-1	dol	Xenobl	Sutured	Interlobate	Strong	49	83	154	369	591		4.48	1.27	0.42	10	0.037	0.140	0.171
Itq1	cc	Hypidiobl	Lobate / caries	Interlobate	Weak	42	55	75	119	200	1.55	4.18	1.18	0.49	8	1.123	0.180	0.903
Itq2	cc	Idiobl	Straight	Polygonal	None	68	86	113	173	371	1.54	4.65	1.31	0.40	7	7.735	2.891	4.709
Itq3	cc	Xenobl	Sutured	Interlobate	Strong	31	45	69	127	231	1.70	4.31	1.29	0.41	8	0.054	0.217	0.300
Itq4-1	cc	Idiobl	Straight(lobate)	Interlobate	None	35	47	61	97	174	1.46	4.57	1.29	0.41	8	2.246		0.434
Itq4-2	cc	Idiobl	Straight(lobate)	Interlobate	Weak	28	35	46	71	123	1.36	4.57	1.29	0.41	8			
Noq-1a	cc	Xenobl	Lobate / caries	Interlobate	Weak	39	57	85	159	547	1.65	4.77	1.37	0.36	9	0.651		
Noq-1b	cc	Xenobl	Lobate / caries	Interloateb	Weak													
Poq1x	other	Hypidiobl	Lobate(straight)	Polyg(interlob)	None	80	109	183	387	652	1.80	4.85	1.37	0.35	13		0.906	0.637
Poq1y	other	Hypidiobl	Lobate(straight)	Polyg(interlob)	None	79	105	160	416	652	1.60	4.85	1.38	0.36				0.340
Poq1z	other	Hypidiobl	Lobate/caries	Polyg(interlob)	None	94	155	290	462	647	1.87	4.74	1.33	0.38			1.066	0.157
Poq2x	cc	Hypidiobl	Lobate/caries	Polygonal	Weak	190	236	303	439	629	1.72	4.55	1.28	0.42	8		0.977	0.877
Poq2y	cc	Hypidiobl	Lobate(straight)	Polygonal	None	227	275	362	489	639	1.56	4.44	1.26	0.43				0.846
Poq2z	cc	Hypidiobl	Lobate/caries	Polyg(interlob)	None	207	265	345	502	641	1.55	4.47	1.27	0.42			1.194	0.829
Poq3-1	cc	Hypidiobl	Straight	Polygonal	Weak	141	176	238	375	555	1.87	4.48	1.28	0.42	7		0.536	0.379
Poq3-2	cc	Hypidiobl	Sutured	Polygonal	Medium	144	171	212	401	647	1.76	4.47	1.27	0.42	8			
Poq4	cc	Hypidiobl	Lobate (straight)	Interlob(polyg)	None	79	104	139	219	377	1.47	4.60	1.30	0.44	8		0.526	0.309
Siq2	dol	Idiobl	Straight	Polygonal	None	57	68	87	126	181					8	0.140		0.137
Seq1	dol	Xenobl	Lobate/caries	Interlobate	None	101	133	181	289	451					8	0.486		0.009
M-1-2	cc	Xenobl	Sutured	Amoeboid	Weak											0.614		
M-2-2	cc	Hypidiobl	Straight	Polygonal	None													
M-3-2	dol	Idiobl	Straight	Polygonal	Noen											0.040		
M4-1-1	cc	Hypidiobl	Straight(lobate)	Polygonal	None	75	97	127	189	283	1.60	4.35	1.23	0.44	8	1.369		0.923
M4-1-2	cc	Hypidiobl	Lobate(straight)	Polygonal	Medium	65	82	103	155	227	1.55	4.21	1.19	0.46	8			
M4-2-1	cc	Hypidiobl(idiobl)	Lobate(straight)	Polygonal	Weak	81	101	127	184	293	1.54	4.32	1.22	0.46	7	1.326		0.857
M4-2-2	cc	Idiobl(hypidiobl)	Straight	Polygonal	None(weak)	67	87	104	152	230	1.56	4.18	1.19	0.49	7			
M4-3-1	cc	Hypidiobl	Straight(lobate)	Interlobate	Weak	75	89	113	163	249	1.55	4.32	1.22	0.46	8	1.560		0.886
M4-3-2	cc	Hypidiobl	Straight	Polygonal	None	67	81	102	142	219	1.58	4.25	1.20	0.47	7			

3.3 Image analysis

3.3.1 Grain size distribution

The grain-size distribution was plotted as apparent cumulative area % as a function of apparent equivalent grain diameter (ECD) in *μm*. D50 ranged from 80 to 540 *μm*. Five different grain-size percentiles are presented in Table 3. In addition to absolute grain-sizes, ratios reflecting the shape of the cumulative curves were tested in the multivariate analysis to investigate correlation with deterioration. The ratios were defined as D5/D10, D5/D20, D10/D50 and D10/D90. The coarsest rocks came out finer than in reality because of too many grains crossing the image boundary when using the 2.5x objective.

3.3.2 Shape factors

Four different grain-shape factors were calculated, though describing very similar phenomena of the grains, namely roughness and roundness, see Table 2. The shape-factor distributions were plotted as apparent cumulative area % as a function of shape-factors, and the cumulative 50%-percentile values were used in the analysis.

3.4 Adjacent grain analysis

The number of adjacent grains was analysed following the procedure of Åkesson (2004). Median values and the standard deviation of the population are shown in Figure 4
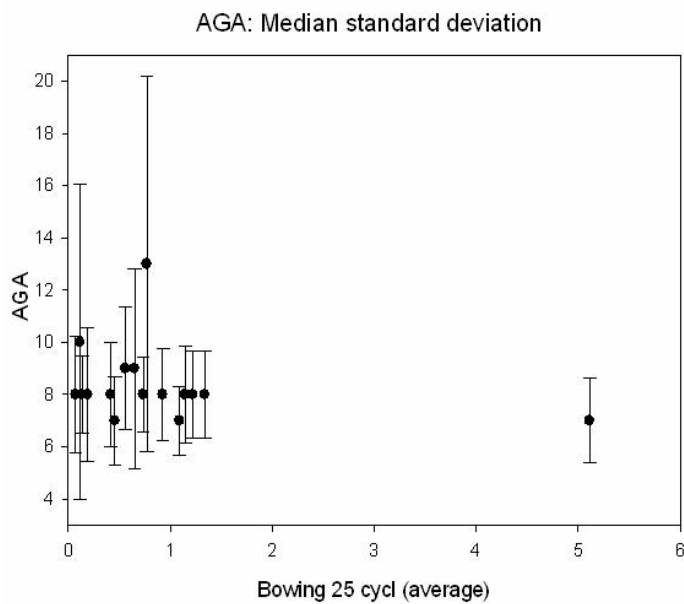
Figure 4. Bowing plotted versus AGA (median ± standard deviation). Poq1x (AGA=13) is anomalous because of a polygonal shape of grain aggregates with additional small grains (not subgrains) adding up the number of adjacent grains, see Figure 3

3.5 Mineralogy

Laboratory bowing experiments on dolomitic marbles showed very little bowing potential. It is evident that dolomite and calcite possess different properties when it comes to thermal dilatation, surface tension and deformation. Because of poor statistics on laboratory bowing of dolomitic samples, they were removed from the dataset used in the analyses.

3.6 Response data

Table 4 shows the correlation matrix for bowing between three laboratories. The statistics are poor and the sample Itq2 has an extreme bowing potential compared to the other samples. The high value is real, but must be carefully treated in the analysis since it will influence the models heavily. As seen from the table, the correlation is good when the sample Itq2 is included and poor when it is excluded. The number of samples was few due to little overlap especially between the data from Laboratory 1 and 2.

Table 4. Correlation matrix for bowing between the laboratories. Cell contents: Pearson correlation, p-value and number of samples in calculation. Correlation is calculated both with sample Itq2 included in and excluded from the dataset.

	Itq2 included		Itq2 excluded	
	(1) SINTEF	(2) UNIGOE	(1) SINTEF	(2) UNIGOE
(2)UNIGOE	0.990 0.090 3		-1.000 * 2	
(3) Ramböll	0.965 0.000 7	0.923 0.001 8	0.286 0.583 6	0.079 0.866 7

3.7 Multivariate statistics

3.7.1 Regression model

Partial Least Square Regression (PLS) was performed on the calcitic marbles and the regression coefficients for each variable are found in Table 5. For the rocks where multiple samples were investigated, average values were used. Because of few samples the final model was calculated without cross-validation since leaving one value out would influence the model heavily. The "mean contribution from variable" column indicates the impact from each variable on the bowing.

Table 5. Regression coefficients and "mean contribution from variable" for two models of average bowing after 25 cycles (mm/m). Average bowing is calculated from the data of laboratories 1-3. Model 1 is calculated with sample Itq2 included and Model 2 with Itq2 excluded.

	Model 1: Regression Coefficient for average bowing Itq2 included Based on 4 components	Mean contribution from variable (%)	Model 2: Regression Coefficient for average bowing Itq2 excluded Based on 5 components	Mean contribution from variable (%)
Constant	24.8314		7.93521	
D5	-0.0005	0	0.00086	0
D10	-0.0002	0	0.00017	0
D20	0.0001	0	-0.00026	0
D50	0.0002	0	-0.00039	1
D90	0.0013	2	0.00049	1
D5/D10	-0.0214	5	0.02909	12
D5/D20	-0.0267	4	0.02883	9
D10/D90	-0.0583	4	0.0014	0
D50/D90	-0.0398	7	-0.01886	6
Roughness 1A50	0.5097	2	-0.14941	1
Roughness 2 A50	-1.7181	22	-1.32225	34
Roughness 3 A50	-9.1454	33	-1.24007	9
Roundness A50	8.9408	11	-6.65376	16
AGA	0.0079	0	0.08212	4
Shape of grains	-0.6744	4	-0.24427	3
Subgrain growth	-0.1996	0	-0.10381	0
Grain Boundaries	-0.1231	1	0.17072	1
Shape of grain aggregates	-0.8233	3	-0.03447	0
Signs of cleavage	0.0827	0	0.00307	0
Twinning of carbonate	0.4342	1	0.23245	1
Sum		100		100

3.7.2 Actual versus calculated bowing

Figure 5 shows calculated bowing plotted versus average laboratory bowing after 25 cycles calculated from data of Laboratories 1-3 for the two calculated models from Table 5. Because the points are in a linear pattern, from the bottom left-hand corner to the top right-hand corner, the response plot indicates that the model fits the data adequately. In the analysis of variance for Model 1 and 2, both p-values were less than 0.05 indicating that the models were significant.

By studying the residuals and the leverage of the variable in the models, no outlyers were indicated. Some samples had high leverage values. This is because of few samples in the calculation leading to heavy influence from some individuals in the model.
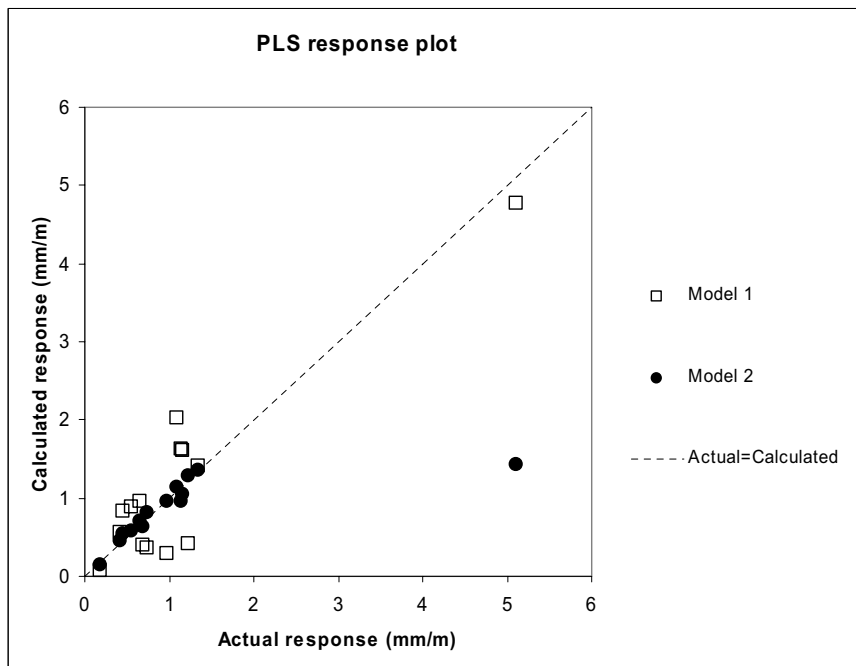
Figure 5. Calculated bowing from Model 1 and 2 in Table 5 plotted versus average laboratory bowing after 25 cycles. Dotted line indicates perfect correlation. Model 1 is calculated with the extreme sample Itq2 included while in Model 2 Itq2 is excluded from the calculation.

4 DISCUSSION

4.1 Aim

As formulated in the introduction, the aim of this paper was to quantify important microstructure parameters in marble used as cladding panels and use the parameters in a model that can describe and predict the deterioration of marble.

Repeated heating and wetting cycles are found by several authors to generate these deterioration problems, but the fundamental explanation lies in the microstructure. The variables used in the model should be relatively easy to obtain from the rock. The purpose, however, was not only to be able to predict future deterioration by simple microstructure measurements, but also to be able to define the most important properties for deterioration. If the variance of the deterioration data distribution could be explained by the measured microstructure properties, one step forward was made. As already pointed out by many authors, there is no simple relation between deterioration and microstructure, rather a complex multivariate one.

The results found in this paper benefit from results obtained in the "TEAM" project. The response data possessed a major variance between the laboratories because of both nonhomogeneous and anisotropic samples analysed, and slightly diverging laboratory procedures. Standardised laboratory test routines were developed and drafts of laboratory test methods have been presented to the European Standardisation of Natural Stone.

4.2   Response data

Bowing data from three laboratories was used in the analysis. There was very little overlap between the data from Laboratory 1 and 2, but from Table 4 the correlation of bowing data between the laboratories shows that the correlation was good as long as sample Itq2 was included in the dataset. When this sample was removed, the correlation became poor. The reason was that the data was now not spanning the sample space, and only samples showing relatively small magnitude of bowing were found in the remaining dataset. This means that the magnitude of bowing for the remaining samples possessed a high degree of uncertainty and the input data could be regarded as not ideal. Itq2 is known for its true and extreme deterioration potential and could not be regarded as an outlyer. The problem was rather vacancy of samples spanning the sample space between Itq2 and the other samples. It was a problem, however, that Itq2 influenced the model significantly. Keeping this in mind, the data was still used in Model 1.

4.3   Microstructure parameters and correlation with bowing

The marbles investigated possessed a variety of microstructures ranging from idioblastic, polygonal and equigranular grain texture with straight grain boundaries to xenoblastic marbles of undulose extinction, deformation twins, subgrain formation and widespread grain boundary migration resulting in sutured to lobate grain boundaries.

They were characterised under the microscope by certain properties. Some of these properties displayed weak trends in relation to bowing as already pointed out by several authors summarized by Grelk (2005). By means of the coding system from Table 1, the properties could be used in the statistic model. Also for some of the variables from automatic image analysis, weak trends could be seen. As already pointed out by several authors (Alnæs et al., 2004; Grelk, 2005), marbles prone to deterioration are found both among the relatively finer and relatively coarser marbles. The shape of the grain-size distribution curves and the shape of the grains, on the other hand, are more interesting regarding deterioration. The variables were poorly correlated with bowing one by one, but some of the variables showed weak trends with bowing. The variables that seemed to have strongest trends towards bowing were: "Roughness 1", "Roughness 2", "Roughness 3", "Roundness", D5/D10, D5/D20, D50/D90 and AGA, from image analysis and: "Shape of grains", "Subgrain growth", "Grain boundaries", "Shape of grain aggregates" and "Twinning", from microscopy.

To be able to evaluate the variables properly, methods that take the interaction of variables into account had to be used.

4.4   Mineralogy

It is reported by various authors that dolomitic marbles behave differently from calcitic. This is confirmed by the data from "TEAM", but the number of samples in this study was too few to make a conclusion. Since the statistic material regarding dolomitic marbles was poor in this dataset, no further efforts were made to establish relations between mineralogy and deterioration potential, and the dolomitic samples were therefore removed from the dataset.

Grelk (2005) reports that documented cases of bowing marble principally involve calcitic marble. Bowing of dolomitic marble also occur, however, not in the same magnitude (Malaga et al., 2004). Alnæs et al. (2004) found that both calcitic and dolomitic marble types as well as polymineralic varieties may behave similarly on building facades. No clear relationship between mineralogy and deformation potential was established by the "TEAM" project, but there is a strong indication that dolomitic samples behave differently from calcitic marble. If dolomitic marbles resist deterioration in the term of bowing, more than calcitic marbles, it can

be due to different physical properties including less anisotropic thermal expansion and poorer capillarity properties.

4.5   Analysis

The analysed dataset contained collinear data and had more variables than samples. Partial least square regression was therefore used. Figure 5 shows calculated bowing versus average laboratory bowing for two models calculated from the dataset. The quality of the input bowing data and the statistics were poor, but the models still describe bowing adequately. It is important to note, however, that because of very few data, each sample influenced the model heavily. This is most prominent for the sample Itq2. Two models were therefore calculated where Model 1 was constructed from all data while Model 2 was constructed with Itq2 excluded form the dataset. It is indicated from Figure 5 that since Model 1 displays a relatively poor fit in the lower region but a very good fit for Itq2, while Model 2 shows a very good fit in the lower region but a poor fit for Itq2, that the full explanation for the bowing potential of Itq2 is not found in the measured microstructure data. However, the bowing potential of the other samples is quite well described in Model 2. It would therefore be very useful to analyse more samples with bowing potential between Itq2 and the others to be sure to span the whole sample space. Then a final model could be calculated. Because of few samples, the final model was calculated without cross-validation since leaving one value out would influence the model heavily. For the same reason, prediction intervals were not included. They would anyhow be very wide.

On the other hand, the models show strong trends, and from Table 5, the contribution from the different variables can be studied. The Roughness factors 2 and 3 and Roundness influenced the bowing most heavily. These were all derived from the same measurement of perimeter and area for each grain and describe similar phenomenon. This is not according to Zeisig et al. (2002) that conclude that grain boundary morphology does not play such an important role as was previously assessed. On the other hand, they refer to the shape of grain aggregates that did not have an important contribution in Model 1 and 2 either. It is evident that the grain-shape factors describe irregularities that are important for bowing better than classification of shape of grain aggregates (polygonal, interlobate, amoeboid) or shape of grains (idioblastic, hypidioblastic, xenoblastic).

In addition, the shape of the grain-size distribution curves (D5/D10, D5/D20 and D50/D90) was secondary important. These ratios describe the degree of inequigranularity of the samples. The irregularity of grain boundaries caused by small grains, subgrains and grain boundary migration is stated as important for reinforcing the rock (Alnæs et al., 2004; Zeisig et al., 2002; Åkesson et al., 2006).

Some of the microscope characteristics (shape of grains, grain boundaries, shape of grain aggregates) also contributed, while the absolute grain-size had hardly any influence.

In Model 1, AGA had no influence while in Model 2 it had some. As can be seen from Figure 4, AGA does not very well catch up the vital properties for bowing. This is contrary to Åkesson et al. (2006) who found very good correlation. This fact can be due to investigation of different populations of microstructrues (Åkesson et al. (2006) tested 5 rocks) or due to slightly different performance of the measurements.

It is important to keep in mind that only one or a few sections were investigated for each rock. As already mentioned, the rocks are nonhomogeneous and anisotropic and each section covers only some square centimetres, which does not necessarily represent the rock satisfactory.

5 CONCLUSIONS

To be able to predict deterioration of marble cladding panels, and to study important microstructure parameters influencing deterioration, two models for prediction of bowing of cladding panels were calculated. They were based on quantitative microstructure measurements of 11 different rocks.

The results obtained in this study indicated that deterioration is independent of absolute grain-size. On the other hand, shape of the grain-size distribution curve contributed to bowing in the regression model. The inequigranularity of the rock was therefore assumed important.

The grain-shape influenced the bowing most heavily and showed that these factors describe irregularities that are important for bowing better than classification of shape of grain aggregates (polygonal, interlobate, amoeboid) or shape of grains (idioblastic, hypidioblastic, xenoblastic).

AGA had no influence in Model 1 and some influence in Model 2. The weak contribution can be due to investigation of different populations of microstructrues than Åkesson et al.(2006).

The parameters used in the model are relatively easy to quantify when investigating a new sample, and the regression model shows that it is possible to predict bowing by means of microstructure measurements. When standardised laboratory bowing measurements are collected from all samples, an improved model based on the variation within each rock and between rocks should be developed.

The conclusions of this paper are still under discussion with the "TEAM" project partners awaiting the final evaluation.

6 ACKNOWLEDGEMENTS

7 REFERENCES

Alnæs, L., Koch, A., Schouenborg, B., Åkesson, U., and Moen, K., 2004, Influence of Rock and Mineral properties on the durability of marble panels Dimension Stone 2004, New perspectives for a traditional building material, Prague, Czech Republi, 2004.

Alnæs, L., and Aasly, K. A., 2005, WP 5.3 Compilation of test results, *in* results, W. C. o. t., ed., Microsoft Excel: Trondheim, SINTEF Civil and Environmental Engineering, Rock and Soil Mechanics.

Bain, G. W., 1941, Measuring grain boundaries in crystalline rocks: J Geol, v. 49, p. 199-206.

Cohen, and Monteiro, 1991, Durability and Integrity of Marble Cladding "A state of the art review": Journal of the Performance of Constructed Facilities, v. 5, p. 113-124.

Grelk, B., 2005, Review of literature and TEAM results, TEAM-project WP2, p. 40.

Grelk, B., Golterman, P., Schouenborg, B., Koch, A., and Alnæs, L., 2004, The laboratory testing of potential bowing and expansion of marble: Dimension Stone 2004, New perspectives for a traditional building material, Prague, Czech Republic, 2004.

Hook, K., 1994 Look out below - The Amoco Building Cladding Failure.: Progressive Architecture, v. Feb 1975, p. 58-62.

Kessler, D. W., 1919, Physical and chemical test of the commercial marbles of the United States, Technological papers of the Bureau of Standards.

King, R. P., and Schneider, C. L., 1995, Basic image analysis for the measurement of mineral liberation, *in* Hagni, R. D., ed., Process Mineralogy XIII, 8, The Minerals, Metals & Materials Society, p. 145-157.

Koch, A., and Siegesmund, S., 2002, Bowing of marble panels: on-site damage analysis from the Oeconomicum Building at Göttingen (Germany), *in* Siegesmund, S., Weiss, T., and Vollbrecht, A., eds., Natural Stone, Wathering Phenomena, Conservation Strategies and Case Studies, 205. Special Pubilications: London, The Geological Society of London, p. 299-314.

Koch, A., and Siegesmund, S., 2004, The combined effect of moisture and temperature on the anomalous expansion behaviour of marble: Environmental Geology, v. 46, p. 350-363.

Lumbreras, F., and Serrat, J., 1996, Segmentation of petrographical images of marbles: Computers & Geosciences, v. 22, p. 547-558.

Malaga, K., Schouenborg, B., Alnæs, L., Bellopede, R., and Brundin, J. A., 2004, Field exposure sites and accelerated laboratory test of marble panels: Dimension Stone 2004, New perspectives for a traditional building material, Prague, Czech Republic, 14–17 June, 2004.

Passchier, C. W., and Trouw, R. A. J., 2005, Microtectonics Berlin Springer, 366 p.

Schouenborg, B., Grelk, B., Alnæs, L., Brundin, J. A., Blasi, P., Yates, T., Marini, P., Tschegg, E., Unterweger, U., Tokartz, B., Kock, A., Bengtsson, T., Mladenovic, A., and Goralezyg, S., 2003, TEAM - Testing and Assessment of Marble and Limestone: International Symposium Industrial Minerals and Building Stones, Istanbul, Turkey, Sept 15-18, 2003.

Weiss, T., Siegesmund, S., and Fuller, E. R., 2002, Thermal stresses and microcracking in calcite and dolomite marbles via finite element modelling, *in* Siegesmund, S., Weiss, T., and Vollbrecht, A., eds., Natural Stone , Weathering Phenomena, Conservation Strategies and Case Studies, 205: London, The Geological Society of London, p. 65-80.

Winkler, E. M., 1996, Properties of marble as building veneer: International Journal of Rock Mechanics and Mining Science & Geomechanics Abstracts, v. 33, p. 215-218.

Yates, T., Brundin, J.-A., Goltermann, P., and Grelk, B., 2004, Observations from the inspection of marble cladding in Europe: Dimension Stone 2004, New perspectives for a traditional building material, Prague, Czech Republic, 2004.

Zeisig, A., Siegesmund, S., and Wieiss, T., 2002, Thermal expansion and its control on the durability of marbles, *in* Siegesmund, S., Wieiss, T., and Vollbrecht, A., eds., Natural Stone, Weathering Phenomena, Conservation Strategies and Case Studies, 205. Special Publications: London, Geological Society of London, p. 65-80.

Åkesson, U., 2004, Microstructures in granites and marbles in relation to their durability as a construction material, Göteborg University.

Åkesson, U., Lindqvist, J. E., Schouenborg, B., and Grelk, B., 2006, Relationship between microstructure and bowing properties of calcite marble claddings: Bulletin of Engineering Geology and the Environment, v. 65, p. 73-79.

Paper 5

Reconnaissance study of compaction microstructures in quartz grains and quartz cement in deeply buried sandstones using combined petrography - EBSD analysis

Mai Britt E. Mørk*, Kari Moen

Department of Geology and Mineral resources Engineering, NTNU, N-7491 Trondheim, Norway.
* corresponding author: mai.britt.mork@ntnu.no, Tel. +4773594812, Fax. +4773594814

Abstract

Sandstones diagenesis involves porosity loss by mechanical and chemical compaction. In this study we have examined relations of diagenesis and microstructures in quartz grains and quartz cement in sandstones from relatively deep burial depths offshore mid Norway. Electron backscatter diffraction analysis (EBSD) has been combined with optical and cathodoluminescence petrography study of samples with different degrees of compaction and quartz cementation. Quartz cement is shown to be syntaxial to the nearest host domain (grain or subgrain), both for monogranular, polygranular, undeformed and deformed quartz. The quartz cement growth may have been initiated at different subgrain surfaces, and preserving pre-depositional deformation structures. EBSD inverse pole figure imaging shows dauphinè twins to be common in all samples, both in quartz grains and quartz cement. The dauphinè twins appear in grain-grain contacts and in cement -crystal boundaries, and commonly crossing grain-cement boundaries. On basis of twin distributions we suggest that both inherited twins from the source area and twins formed by compaction-induced grain boundary deformation are present. A general problem in sedimentary rocks is to distinguish inherited from sedimentary compaction-induced deformation structures. More comprehensive following up studies are suggested to investigate the role of ductile deformation mechanisms (e.g. twinning) in sediment compaction.

Keywords: sandstone, compaction, diagenesis, quartz cement, EBSD analysis

1. Introduction

Sediments undergo compaction and porosity reduction during burial and diagenesis. The processes of sediment compaction are commonly divided broadly into mechanical compaction at relatively shallow depth (e.g. < 2.5 km depth) and chemical compaction at deeper burial. Mechanical compaction involves grain rotation grain breaking, and squeezing of ductile grains and pore collapse (e.g. Boggs, 1992; Chester et al., 2004). Chemical compaction involves dissolution, element transport and cementation. However, the spatial two-division is broad and over-simplified, as the actual processes are dependent on combinations of several geological parameters. The rate and degree of sandstone compaction is influenced both by burial rate, sediment composition, mechanical strength and petrophysical properties, as well as temperature, pressure and stress conditions, and in reality, compaction may be composed of both mechanical and chemical processes in both regimes.

In deeply buried siliciclastic sediments quartz cementation is one of the most important porosity reducing factors (e.g. Bjørlykke et al., 1986; McBride, 1989; Worden and Burley, 2003). Various sources of silica, including pressure solution (e.g. at stylolites) have been discussed in the literature, and mechanisms involved in pressure solution have been reviewed and discussed elsewhere (e.g. Renard et al., 2000). Chemical compaction involving quartz
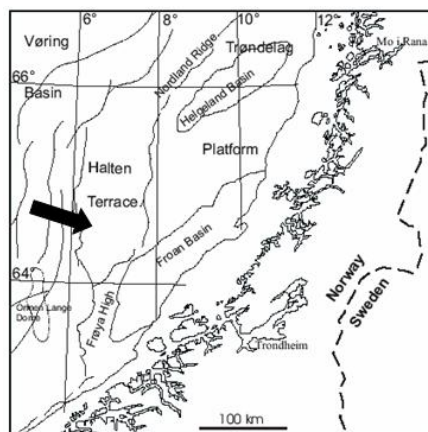
Fig. 1 Location of the Halten Terrace ("Haltenbanken petroleum province") in the Norwegian Sea offshore mid Norway. Names offshore refer to main structural elements (see Blystad et al., 1995).

cementation has been correlated to a given temperature interval, and the dissolution process to generate silica cement is enhanced by interaction of quartz grains with adjacent mica or clay minerals rather than by grain boundary stress (Thompson, 1959; Bjørkum, 1996; Oelkers et al., 1996; Renard and Ortoleva, 1997; Walderhaug and Bjørkum, 2003). In recent models of quartz cementation stress is considered insignificant in promoting dissolution at grain contacts (Bjørkum, 1996; Renard et al., 2000). However, the role of stress induced deformation in deep burial diagenesis may be difficult to document as mechanical deformation structures may in some cases be obliterated by later chemical diagenesis. Cathodoluminescence imaging has a potential to identify deformation structures in quartz grains such as cemented microfractures. By using this method, Makowitz and Milliken (2003) showed that mechanical deformation had taken place in several stages in relation to quartz cementation in Frio Formation sandstones in the Gulf of Mexico. Micro-fracturing had taken place both before, during and after quartz cementation. Fisher et al. (1999) attributed mechanical compaction structures of sandstone at deep (>4.5 km) burial to situations where the rate of stress increase had been higher than the rate of "chemical compaction processes".

In this study we examine if new petrographic methods can provide novel information of micro-structures in quartz grains and quartz overgrowths that can be connected to diagenetic compaction. We combine conventional optical petrography and cathodoluminescence analysis with electron backscatter diffraction (EBSD) analysis. We postulate that this type of approach may have a potential to increase our knowledge of deformation and compaction processes in burial diagenesis. The EBSD technique is relatively new in material sciences (Schmidt and Olesen, 1989; Prior et al., 1999; Schwartz et al., 2000), and has proven successful in fabric analysis in structural geology (e.g. van Daalen et al., 1999; Lloyd, 2000) and study of mineral growth mechanisms in igneous and metamorphic petrology (Piazolo et al., 2004; Terry and Heidelbach, 2006). Haddad et al. (2006) recently identified different growth zones in quartz cement by using EBSD technique from diagenetic systems from very shallow burial depths. In contrast, we present data from relatively deep burial to examine possible microstructures in relation to burial compaction and cementation. The selected sandstones are from exploration wells in central areas of the Halten Terrace (Fig. 1), in the main petroleum exploration area offshore mid Norway in the Norwegian Sea. The aim is to search for indicators that may help interpreting compaction and deformation mechanisms in quartz-rich sandstones.

2. Analytical procedure

Polished thin sections were examined by optical microscopy for petrographic sandstone characterisation, diagenetic interpretation and selection of samples for study. Areas of EBSD analysis were selected and identified by SEM backscatter electron images and cathodoluminescence.

The EBSD technique is based on the weak diffraction pattern that forms when a focused, stationary, primary electron beam strikes a polished sample, backscatters and diffracts. The diffraction pattern is formed on a fluorescent screen and transferred by a camera to the computer (Hjelen, 1990). The sample was tilted to a high angle (70°) inside the SEM. Scattering of the incident electron beam causes electrons to diverge from a point just below the sample surface and impinge upon crystal planes in all directions. Wherever the Bragg condition for diffraction is satisfied by atomic lattice planes in the crystal, two cones of diffracted electrons are produced for each family of lattice planes (Schwartz et al., 2000). Backscatter "Kikuchi" bands (Kikuchi, 1928) appear where the cones of electrons intersect with the phosphor screen. The points of intersection between the bands represent crystallographic directions, and the diffraction patterns (e.g. Appendix 1) are characteristic for the crystal structure and space orientation of the crystal. The EBSD software automatically locates the positions of individual Kikuchi bands, compares these to theoretical data of the relevant phase and rapidly calculates 3-D crystallographic orientations. For each pixel the orientation is stored and can be visualised by orientation maps and plots. The interaction volume is dependent on acceleration voltage and atomic number of the analysed minerals, but is usually in the sub- micron range (Moen et al., 2003). To be able to get EBSD patterns that can be indexed, the crystal lattice at the sample surface has to be undeformed. To obtain this, a post-mechanical preparation is required (Lloyd, 1985). After mechanical polishing of the quartz samples, the surface damage in the uppermost layers was therefore removed by chemical-mechanical polishing (illustration in Moen et al., 2003).

To get optimal EBSD patterns, the analyses were performed in a low vacuum SEM (Hitachi S-3500N) without a conductive carbon layer. The equipment applied for the experiments includes a Nordif EBSD digital camera, and using the TSL, OIM software. The following running and processing conditions for EBSD mapping were applied: WD 20 mm, 20kV accelerating voltage, <30 Pa pressure, 70° tilt, binning 2x2.

3. Geological framework

The early Mesozoic sedimentation history in the Norwegian Sea - Haltenbanken area was related to tectonic rifting, followed by Cretaceous and Tertiary post-rift subsidence and pronounced Neogene subsidence (Spencer et al., 1993), and the present burial depths are close to the maximum burial depths of the studied formations. The regional geothermal gradient has been fairly high through time, possibly as high as 35ºC/km (Oelkers et al., 1996). Sandstone diagenesis and quartz cementation of Jurassic reservoir sandstones have been discussed from adjacent areas (Bjørlykke et al., 1986; Ehrenberg, 1990; Storvoll et al., 2002), and extensive quartz cementation and dissolution at stylolites are documented to occur from 3.5-4.5 km burial (Bjørlykke et al., 1989). The main quartz cementation is interpreted to have taken place at temperatures of 80-120ºC (Walderhaug, 1994), relatively late in the burial history. Findings of unusual high porosity values in the deepest buried sandstones are ascribed to inhibition of quartz cementation by presence of grain-coating chlorite or illite/chlorite (Ehrenberg, 1993;

Storvoll et al., 2002). However, for the Middle Jurassic Garn Formation Ehrenberg (1990) concluded that most porosity loss occurred by relatively early compaction at less than 2 km burial, and that compaction had a greater impact on porosity loss than had quartz cementation. Ehrenberg (1990) also described onset of extensive grain dissolution and illitisation at burial depths greater than 3.5km.

Samples for the present study were selected from cores in different exploration wells to cover sandstones with different diagenetic compaction/cementation relations. The sandstones are from formations of Jurassic and Cretaceous age. Using an average geotherm of 30ºC/km the studied samples from depths 3.2 – 5 km imply maximum burial temperatures of ~100-150ºC, or ~115-175ºC using the above mentioned value of 35ºC/km (Oelkers et al., 1996). Thus all samples are from depths within the "window" of extensive thermally induced quartz cementation, assuming the given geothermal gradients.

4. Sandstone petrography and diagenesis

Three categories of sandstones are described below, respectively sandstones of extensive degree of quartz cementation (category A, Fig. 2a), deeply buried sandstone with very little quartz cementation (category B, Fig. 2c) and a stylolite-bearing sandstone with minor clay matrix and clay laminae (category C, Fig. 5a). Mineralogical compositions are quantified by petrographic modal analyses using 600 counts (Table 1). The compositions are relatively quartz-rich, classifying as subarkosic arenite (Pettijohn et al., 1972). The detrital mineralogy suggests a provenance of relatively high grade metamorphic rocks similar to time analogous sandstone formations in more proximal settings to the south of the study area (Mørk and Johnsen, 2005). Both eastern and western areas of the Caledonides may have contributed to the Jurassic sands in the Haltenbanken area (Gjelberg et al., 1987; Brekke et al., 2001), whereas western and northern marginal areas, including Greenland, may have been sources for the Cretaceous sandstone formations (Morton and Grant, 1998; Brekke et al., 2001).

Diagenetic minerals and interpreted paragenetic sequences are described below. Diagenetic quartz overgrowths on quartz grains have been identified in the optical microscope by location of dust/inclusion rinds and by grain shapes and textural relations, and have been confirmed also by cathodoluminescence images (Figs. 2a,b and 3).

4.1. Category A. Quartz-cemented samples
Sample 3185 (Cretaceous) Medium to coarse-grained, moderate-well sorted sandstone with 24% quartz cement (Fig. 3a) and 14% porosity. Presence of glauconite suggests eogenesis in marine environments prior to the burial diagenesis. The main phase of mesogenetic quartz cementation is predated also by pore-filling kaolinite. The latest mesogenetic event after quartz cementation involved formation of coarse carbonate cement (sporadic distributed) and dissolution of feldspar.

Sample 4205 (Lower Jurassic) Medium to very coarse-grained, poor to moderate sorted with 19% quartz cement (Fig. 2a) and 7% porosity. Clay-mineral coatings around quartz are interpreted as early diagenetic and appear to predate dissolution of detrital feldspar grains.
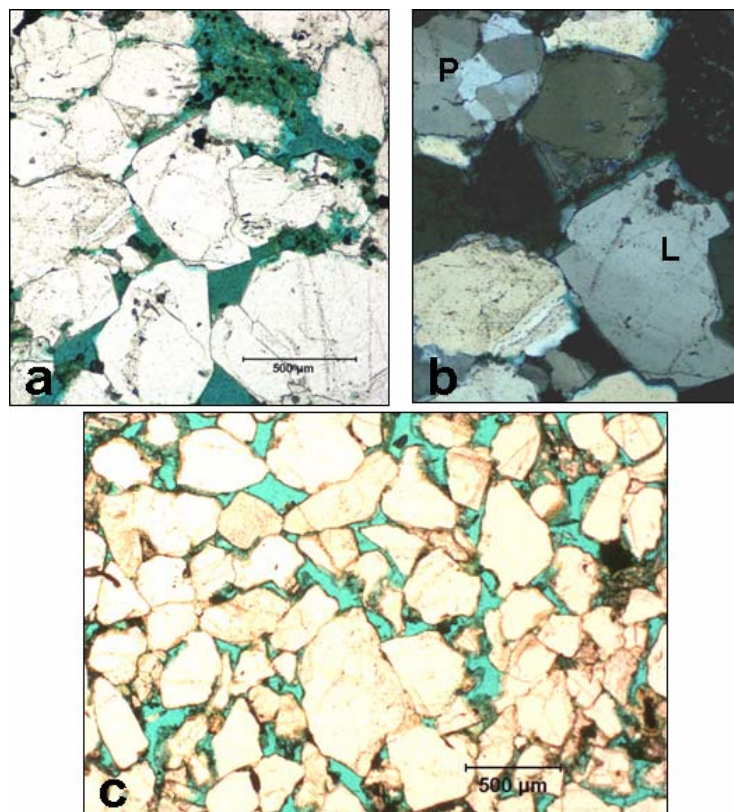
Fig. 2 Optical micrographs. a) Sandstone category A (4205) shows porosity loss due to quartz cementation. b) Close up of a in crossed polars show examples of quartz overgrowths on grains with low angle boundaries (L) and on polygranular grains (P). c) Sandstone category B (5040) showing porosity-loss due to dense grain packing. Porosity is shown by blue colour in (a) and (c).

Table 1a Modal analysis (%) of sandstones selected for EBSD study. IGV refers to inter-granular volume, excluding replacive cement (Table 1b).

Kate -gory	Sample	Qtz	Qtz pgr	Fsp	Mic	Rfr	Cly- lam	Aut. cly	Carb cem	Opq cem	Qtz cem	Por	Total IGV
A	3185	47	0	5	<1	4	0	5	<1	0	24	16	41
A	4205	48	12	6	1	0	0	4	1	2	19	7	28
B	5040	59	7	7	2	1	0	6	7	2	2	9	18
C	5243	51	8	10	<1	0	4	5	14	<1	2	5	16

Table 1b Supplementary data from modal analysis.

Analysis	Replacive cement	Porefill. cement	Porosity secondary	Porosity primary	IGV
3185	3	25	<1	16	41
4205	4	22	2	6	28
5040	7	10	1	8	18
5243	7	14	3	2	16

Mineral abbreviations: Qtz = quartz, Pgr = polygranular, Fsp = feldspar, Mic = mica, Rfr = rock fragment, Cly lam = clay laminae, Aut cly = authigenic clay minerals, Carb cem = carbonate cement, Opq = opaque cement, pyrite, Por = porosity.

Kaolinite, pyrite and siderite predate the main phase of mesogenetic quartz cementation. The siderite is preferentially located within biotite. The quartz cement growth was postdated by dissolution of detrital feldspar and by growth of carbonate cement (minor).

4.2. Category B. Samples with limited quartz cement
Sample 5040 (Lower Jurassic) Medium to coarse-grained, well sorted sandstone with 9% porosity and only 2% quartz cement. This sample has relatively dense grain packing (Fig. 2c). The detrital quartz and feldspar grains have thin clay-mineral coatings which may have prevented quartz cementation (cf. Ehrenberg, 1993; Storvoll et al., 2002). The clay mineral coatings also preserve the outline of partly dissolved feldspar grains. Carbonate cement in partly dissolved feldspar grains postdate the clay-mineral coatings and the dissolution of feldspar. Presence of compacted and folded mica flakes enclosed in the carbonate support the interpretation of a late carbonate cement phase. The paragenetic sequence is: 1) formation of clay-mineral coatings, 2) compaction and bending of mica, 3) growth of siderite and pyrite in local domains, 4) dissolution of feldspar, and 5) growth of coarse carbonate cements.

4.3. Category C. Sample with stylolite lamina
Sample 5243 (Lower Jurassic) Medium to very coarse-grained, poorly sorted, sandstone with clay laminae with 5% porosity and only minor (2%) quartz cement. Stylolites are developed at the thin clay lamina (Fig. 6a). The stylolite formation and mica compaction is postdated by feldspar dissolution and late carbonate cement. The low porosity reflects a combination of clay matrix, mechanical compaction and late carbonate cement.

4.4. Porosity reduction and compaction
Compaction is volume reduction due to overburden stress, largely related to porosity reduction. As both compaction and cementation have taken place, porosity does not give a correct value for the amount of compaction. In such cases, changes in intergranular volume (IGV) as defined by the sum of porosity and pore-filling cements may give better indications of compaction. Uncertainties in calculating IGV may be related to interpretation of dissolution porosity and replacive cements which are subtracted from the IGV values (Table 1b). The quartz cemented samples 3185 and 4205 show both higher porosity and higher intergranular volume (IGV) than in the less-cemented and deeper buried samples 5040 and 5243 (Table 1a,b).

The IGV of sample 3185 of 41% is close to primary porosity values in arenitic sandstones in spite of burial depths of 3 km. This means that much of the quartz cement may be of relatively early mesogenetic origin. Compared to porosity data and IGV compaction curves for sandstones from other areas (Beard & Weyl 1973, Paxton et al. 2002) sample 3185 is nearly uncompacted. Sample 4205 with IGV of 28% is also somewhat less compacted than the average for 4 km burial on IGV-depth curves (Paxton et al., 2002; Worden and Burley, 2003). As it was less well sorted than sample 3185, original porosity values may have been less. Quartz cementation may have occurred relatively early during mesogenesis as it was also interpreted to predate late carbonate cement.

The arenitic sandstone 5040 (category B) has IGV values of 18% which implies considerable compaction, and this compaction may have been facilitated also by chemical dissolution, e.g. by feldspar dissolution. The limit of mechanical compaction-reduced IGV is inferred to be 26% at >2.5km burial (Paxton et al., 2002). The matrix and stylolite bearing sample (categoryC) has an IGV of 16%, but as the amount of original matrix is uncertain it does not
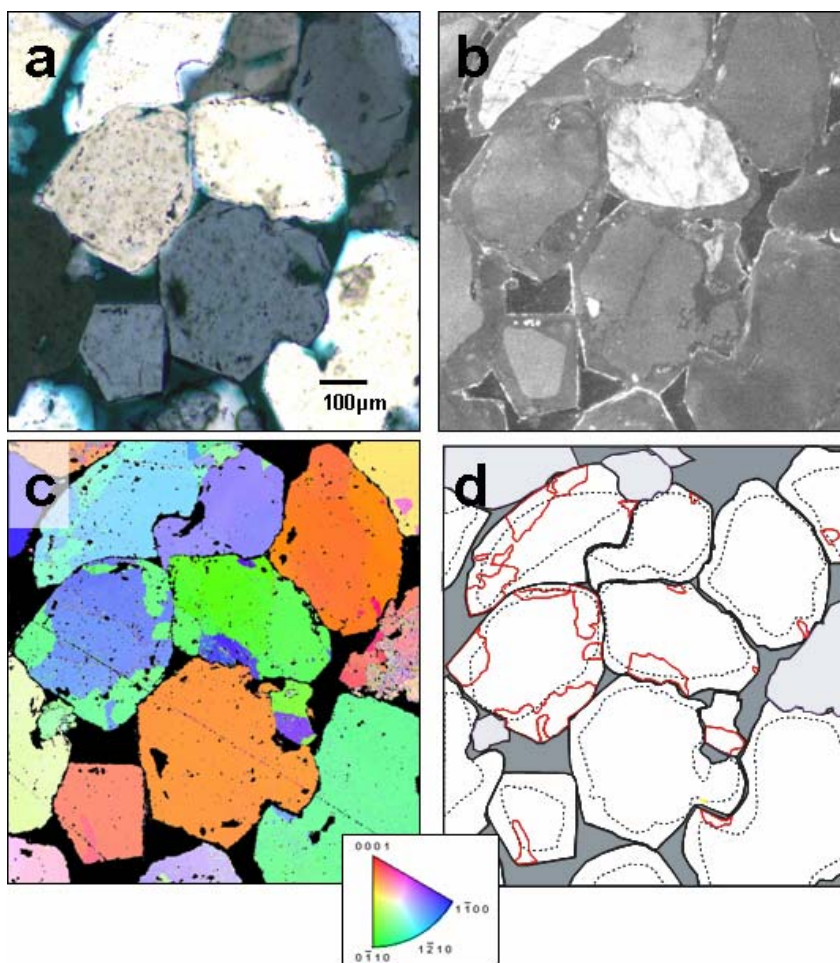
Fig. 3. Microstructural relations of quartz cement overgrowths and dauphiné twins, sample 3185. a) Optical micrograph (crossed polars). b) Cathodoluminescence image showing the overgrowths as dark rims on the quartz grains. c) EBSD orientation image of quartz, step size 1μm. Crystal orientation normal to the image plane is shown by colour code in the small inset figure. d) Composite sketch showing quartz with overgrowths (white, original detrital grain boundaries are shown by dotted line) and dauphiné twins (red boundary lines).

indicate degree of compaction. However, assuming dissolution at stylolites, compaction could have been considerable. Some of the pore-filling cement postdated compaction as supported by observation of relatively late carbonate cements.

In summary, based on the IGV's sandstones from category B and C show evidence of significant compaction which may be a combination of mechanical and chemical compaction. Large IGV's in category A sandstones show that quartz cementation may have occurred relatively early in mesogenesis and was more important than compaction in reducing porosity. Assuming the hypothesis that compaction caused deformation at detrital grain boundaries we would expect to see more compaction induced deformation features in the category B sandstone than in the others.

5. Microstructures of quartz grains and quartz cement

The detrital quartz grains in all the sandstone categories can be divided into monogranular (90-75%) and polygranular (10-25%) grains. Quartz cement occurs as syntaxial overgrowths on both mono- and polycrystalline quartz grains. Where quartz overgrowths are present on polygranular grains the overgrowths show similar crystallographic orientation as the different crystals they overgrow, giving slight variation in crystal orientation within an overgrowth. This is seen in optical microscope (e.g. Fig. 2b, 5f), and confirmed by EBSD analyses (e.g. Fig. 5e, see below).

EBSD data are represented as crystal orientation maps prepared from inverse pole figures (Figures 3b, 4b, 5a,d and 6b). The colour code refers to crystallographic orientation vertical to the sample (image) plane. The EBSD images are compared with optical microscope images and SEM backscattered electron images of the same areas as well as cathodoluminescence images. The data are also represented in special grain boundary maps that verify distributions of high angle boundaries, low angle boundaries and 60° twin boundaries (e.g. Fig. 5b,e).

5.1. Low angle boundaries and cement
A high proportion of the monogranular quartz grains show distinct low-angle boundaries in all the studied samples, identified both optically and by EBSD analysis. Subgrains are defined by maximum misorientations of 10° (Vernon, 2004, White 1977). These boundaries can be interpreted as "walls" of organised dislocations formed by strain redistribution (recovery) by dislocation creep in the crystals (Vernon, 2004). Subgrain microstructures in quartz are very common in regional metamorphic rocks. In sedimentary deposits such features are noted in detrital quartz grains and rock fragments even at very shallow burial, suggesting that they are inherited from the source rocks.

Where quartz overgrowths are present on grains with subgrains defined by low-angle boundaries the overgrowth show similar crystallographic orientation as the different subgrains (Fig. 2b,5f). This is confirmed by EBSD analyses (Fig. 5e). The observation of low angle boundaries both in detrital quartz grains and in the quartz cement is unexpected as low angle boundaries are associated with deformation at metamorphic conditions (e.g. Vernon, 2004). These features may be related to growth controlled by the detrital host lattice, or alternatively, to deformation during the burial. The first alternative means that different subgrains in the detrital quartz controlled the optical orientation of the overgrowth, and that the cement growth was initiated at different sub-surfaces. The second alternative, that subgrain boundaries formed in response to deformation after cement growth may be less likely, as the mechanisms of subgrain formation operate at higher temperature conditions (e.g. Vernon, 2004; Passchier and Trouw, 2005).

5.2. Dauphinè twinning
Dauphinè twins are related by a 180° (or apparent 60°) rotation about the quartz c(0001) axis. Such twins are not visible by optical microscopy, but they can be identified by the electron backscatter diffraction techniques (Schmidt and Olesen, 1989). Dauphinè twinning may emanate from a region of contact with a neighbouring grain. Several processes can cause dauphinè twinning: structural inversion from β- to α-quartz during cooling (Putnis, 1992; Nord, 1994), grain boundary migration due to contact metamorphic heating (Piazolo et al., 2005) and stress (e.g. Frondel, 1962; Lloyd, 2000; Wenk et al., 2005). Lloyd (2000) interpreted dauphinè twinning in quartz to stress induced grain-contact features due to faulting. Experimental results by Laughner et al. (1979) showing that dauphinè twins could be
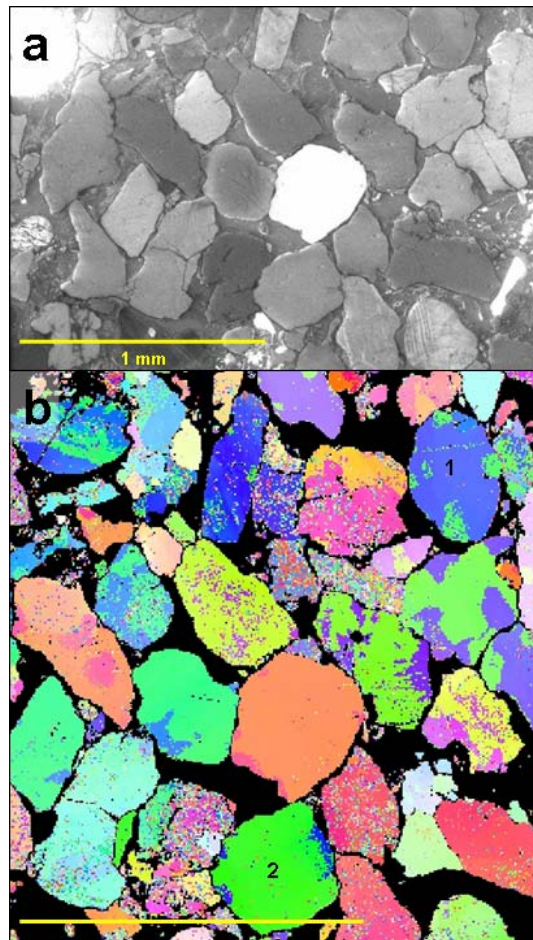
Fig. 4. Cathodoluminescence image (a) and EBSD inverse pole figure map (b) of relatively densely packed sandstone (sample 5040). Note patchy dauphiné twin distributions. Pixel sized spots are considered to be noise due to mis-indexing. Step size: 5μm.

formed in quartz at stresses down to 0.9 kb may in particular have relevance to burial diagenetic regimes comparable to the present study.

5.2.1. Category A. Quartz cemented sandstones
Sample 3185: Dauphinè-twins occur as small patches at long contacts and at quartz cement edges, in some cases crosscutting cement-grain boundaries. Twins are also developed in overgrowths in contact with pyrite which predates the quartz cement. Fig. 3c,d shows dauphinè twins restricted to cement rims as well as dauphinè twins that include both cement and outer parts of host grains. *Sample 4205* shows similar features as described above for 3185. The dauphiné twins are located at long grain boundaries, in quartz-cemented zones and in contact with other grains or cement zones. The twin boundaries appear to crosscut fluid-inclusion trails marking the "pre-cement" grain boundary and zones at grain edges.

5.2.2. Category B. Sandstone with limited quartz cement
Sample 5040: This sandstone shows examples of patchy dauphinè-twin localisation at detrital grain edges near the contact with other quartz grains (Fig. 4b, see in particular grains marked

1 and 2). Twins are also developed adjacent to patchy carbonate cement or clay mineral and carbonate rims. Some twin patches are developed at long contacts. Such twin distributions at grain boundaries may suggest a relation to post depositional compaction deformation. However, dauphinè-twins in quartz also occur near to pores (Fig. 4b), but it is possible that other grains may be in contact when considering 3d space. It is also possible that adjacent grains may have been dissolved during a later event. Fig. 5 shows that dauphiné twins tend to be elongated parallel to subgrain boundaries.

5.2.3. Category C. Sandstone with stylolite lamina
Sample 5243: Quartz grains are elongated and share long contacts subparallel to the stylolite seam and at a steep, oblique angle. The EBSD image (Fig. 6b) indicates a random orientation of quartz grains along the stylolite. Patchy dauphinè-twin bodies occur on one or both sides of high angle, long grain contacts (e.g. grain 1, Fig. 6b), and occasionally at grain edges (grain 2). Other grains show dauphiné twins that may be inherited.

5.3. Relation to subgrains
In total, on basis of the studied samples, dauphinè-twins are seen to occur in quartz grains with or without subgrains, sub-parallel to low angle boundaries or located only in parts of subgrains or across subgrain boundaries.
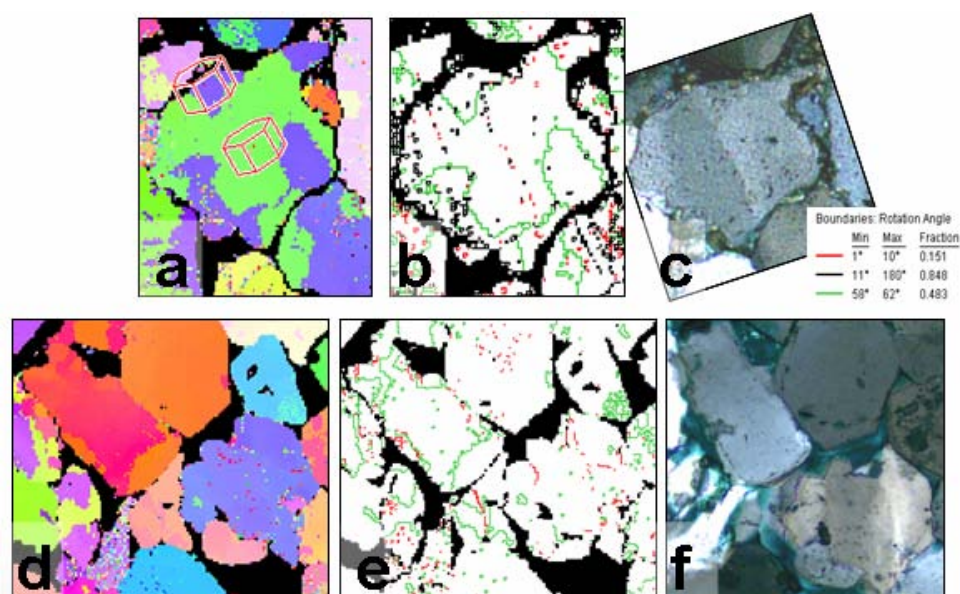
Fig. 5. Twins and low angle boundaries. a) EBSD image (sample 5040, detail of Fig. 3) showing Dauphiné twins. b) Low angle <10º boundaries shown in red and 60º twin boundaries in green. Step size: 5 microns. Smallest, one-pixel sized spots are considered to be noise due to mis-indexing. c) Low angle boundaries shown in optical micrograph (crossed polars). d) EBSD image (sample 3185) showing dauphiné twins. e) Low angle boundaries and twin boundaries. f) Optical micrograph showing continuation of low angle boundaries into quartz overgrowths.
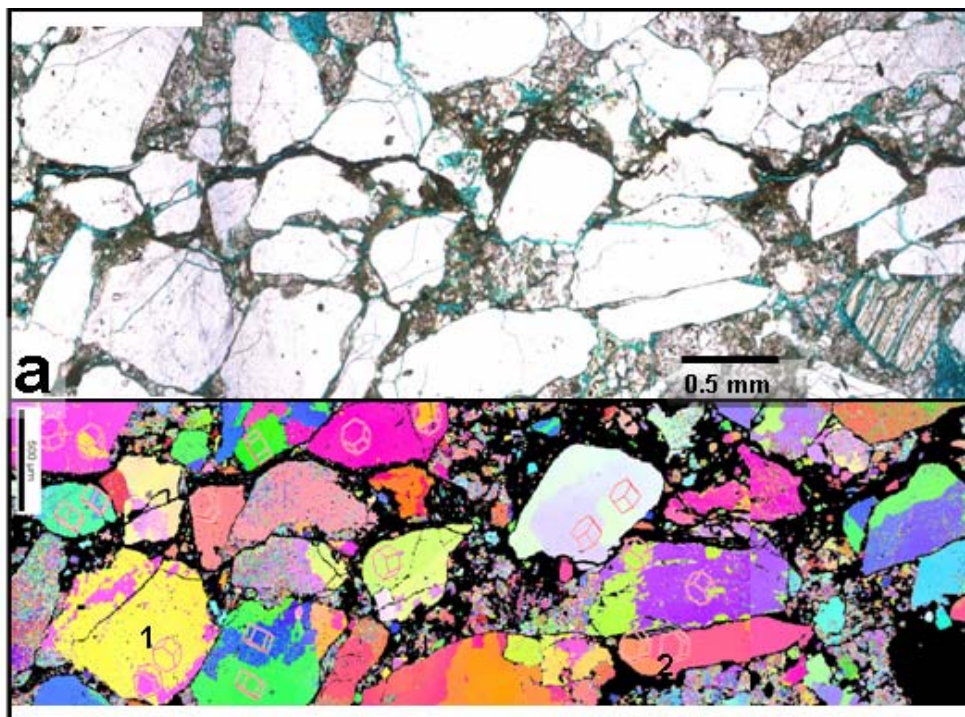
Fig. 6. a) Optical images (plane polars) of stylolite bearing sandstone 5243. Quartz grains (white), clay matrix and carbonate cement (brown), porosity (blue). Note partly dissolved feldspar (lower right side). b) EBSD image and crystal orientation symbols showing examples of 60 º rotation around the c-axis. Step size 5 microns.

6. Discussion

The studied sandstones have been buried to 3-5 km depths at similar geothermal conditions, but experienced different main compaction mechanisms. Quartz cementation was the main porosity reducing factor in category A sandstones and mechanical compaction and chemical dissolution in category B and C sandstones. This was concluded on basis of interpreted intergranular volumes and paragenetic sequences. Late carbonate cementation appears to have postdated main compaction and quartz cementation in all cases. The interpretation of relatively early mesogenetic quartz cementation in the younger of the category A sandstones is different from developments elsewhere at Haltenbanken (e.g. Bjørlykke et al., 1986; Ehrenberg 1990). Probably it reflects that extensive quartz cementation may be related to distinct thermal or tectonic events (e.g. Gluyas et al., 1993). Early formed clay coatings observed in one of the category A sandstones had not prevented quartz cementation.

Poor degree of quartz cementation may have been prevented by clay mineral coatings in the compacted category B sandstone. In cases with dominance of mechanical compaction we note that feldspar dissolution may have played a role in increasing amount of compaction. The matrix bearing stylolite sandstone (category C) experienced compaction by a combination of mechanical grain rotation and stylolite formation before a late event of feldspar dissolution and carbonate growth.

EBSD analysis shows frequent distribution of dauphinè twins in all three categories of sandstones. Assuming that they are related to compaction, the category B sandstones would probably be more influenced by grain contact stresses than the quartz cemented and matrix richer sandstones. The longer cement contacts and presence of matrix would both tend to reduce grain boundary stress, and it is a question if twins would develop at the contact between the different quartz cement overgrowths.

The dauphinè twins could in principle have formed 1) in the metamorphic source area prior to erosion and deposition (inherited), 2) by compaction deformation at grain boundaries prior to quartz cementation, 3) by deformation following quartz cementation or 4) the twins may be growth features controlled by pre-existing twins in the host grains (case 1 or 2 in combination with diagenetic quartz cement growth).

The twin patches show different distributions and size, and some of the larger ones located within or across grains are most certainly inherited from the metamorphic or igneous sources. However, there are also distinct relations of twin distributions to syn- and post-deformational textural features. In the sandstone without quartz cement dauphiné twins are located near grain contacts, near pores and some within grains. The apparent spatial relationship to the present sedimentary grain contacts suggest that they formed in response to compaction induced stresses. Such an interpretation may be supported by the documentation of stress induced dauphiné twins in the literature, some of which may be comparable to the pressures of diagenetic burial conditions (Laughner et al., 1979).

The relation of dauphiné twins to quartz overgrowths have been identified by combining EBSD images with optical microscopy and cathodoluminescence images (Figs 3 and 5). The patchy dauphiné twins are seen to crosscut the original quartz grain-quartz overgrowth boundaries. Occasionally they appear only in the quartz overgrowth, but more frequently they are located at the cement contacts between different grains, in cement in contact with early formed pyrite, and also in cement near to pores (e.g. 3185, 4205). These relations give evidence of twin formation during and/or after the quartz cement growth. However, they do not prove if they formed as growth twins controlled by older twins in the detrital grain or if they formed due to later compaction induced deformation. A possible interpretation is that the smaller twin patches aligned in the cement and around grain-cement boundaries are due to diagentic compaction, whereas larger patches, dominantly within the detrital grains are inherited twins.

Time and temperature aspects of diagenetic compaction differ from the stress situations related to faulting and impact processes which may have caused more instantaneous dauphiné twin formation (e.g. Lloyd, 2000; Wenk et al., 2005). Diagenetic processes related to burial are likely to be much slower. However, stress conditions may change more rapid on local scales due to changes in pore fluid pressure, cementation and dissolution. Deep burial or post quartz cementation deformation microstructures described in the literature seem to be limited to microfracturing (e.g. Fisher et al., 1999; Makowitz and Milliken, 2003). Bjørkum (1996) found no evidence of grain boundary deformation at grain-grain boundaries in quartz cemented, stylolitic samples.

In general it is difficult to distinguish between compaction induced and inherited deformation structures in sedimentary formations. However, on the basis of the present study we suggest that the EBSD method may be used to map deformation microstructures and in combination with other methods to examine relations between diagenetic cement growth and deformation.

Late cementation would lead to annealing of older fractures and deformation zones, and make it more difficult to assign correct relations between deformation and present configuration of load bearing grains. More detailed studies could be designed to compare microstructures and dauphiné twin distribution of load-bearing and non-load bearing quartz grains and twin formation at grain-grain, grain-cement and cement-cement boundaries. Selective dissolution of other minerals like feldspar may complicate interpretation of stress distributions, and deformation structures may also have been influenced by earlier cements.

7. Conclusions

- Diagenetic quartz overgrowths in deeply buried sandstones are indistinguishable from the quartz host grains by the EBSD technique, i.e. supporting syntaxial growth.

- Quartz overgrowths on polygranular quartz aggregates follow the orientation of the adjacent grains.

- Low-angle boundaries reflecting pre-depositional deformation are displayed and preserved by overgrowths of quartz cement. This means that the cement growth was not accompanied by recrystallisation.

- Dauphiné twins are visualised by the EBSD method and they show the following relations:
  o Occurrence at grain edges, at long contacts and in general near to adjacent grains.
  o Occurrence in quartz cemented zones and adjacent to other cement such as carbonate and pyrite.
  o Different spatial relations to subgrain boundaries in quartz, in some cases showing sub-parallel relations.

The dauphiné twins are common in the cemented and in the non-cemented samples and they may have different origins. However, we suggest that some of the twin distributions at quartz grain edges and quartz cement-grain contacts may be related to burial compaction. This implies a mechanism of grain-boundary deformation in burial diagenesis, which is invisible by conventional petrographic tools. However, the different techniques must be combined to study the detailed relations of compaction and cementation.

8. Acknowledgements

9. References

Beard, D.C., Weyl, P.K., 1973. Influence of texture on porosity and permeability of unconsolidated sand. AAPG Bulletin 57, 349-369.

Bjørkum, P.A., 1996. How important is pressure in causing dissolution of quartz in sandstones? Journal of Sedimentary Research 66, 147-154.

Bjørlykke, K., Aagaard, P., Dypvik, H., Hastings, D.S., Harper, A.S., 1986. Diagenesis and reservoir properties of Jurassic sandstones from the Haltenbanken area, offshore mid Norway. In: Spencer, A.M. (Ed.), Habitat of Hydrocarbons on the Norwegian Continental Shelf. Norwegian Petroleum Society, Graham & Trotman, 275-286.

Bjørlykke, K., Ramm, M., Saigal, G.C., 1989. Sandstone diagenesis and porosity modification during basin evolution. Geologische Rundshau 68, 1151-1171.

Blystad, P., Brekke, H., Færseth, R.B., Larsen, B.T., Skogseid, J., Tørudbakken, B., 1995. Structural elements of the Norwegian continental shelf. Part II: The Norwegian Sea Region. Norwegian Petroleum Directorate-Bulletin No 8.

Boggs, S. Jr., 1992. Petrology of sedimentary rocks. Macmillan Publishing Company.

Brekke, H., Sjulstad, H.I., Magnus, C.,Williams, R. 2001. Sedimentary environments offshore Norway - an overview. In: Martinsen, O.J., Dreyer, T. (Eds.). Sedimentary Environments Offshore Norway - Palaeozoic to Recent. Norwegian Petroleum Society Special Publication 10, 7-37.

Chester, J.S., Lenz, S.C., Chester, F.M., Lang, R.A., 2004. Mechanism of compaction of quartz sand at diagenetic conditions. Earth and Planetary Science Letters 220, 435-451.

Ehrenberg, S.N., 1990. Relationship between diagenesis and reservoir quality in sandstones of the Garn formation, Haltenbanken, Mid-Norwegian continental shelf. AAPG Bulletin 74, 1538-1558.

Ehrenberg, S.N., 1993. Preservation of anomalously high porosity in deeply buried sandstones by grain-coating chlorite: examples from the Norwegian continental shelf. AAPG Bulletin 77, 1260-1286.

Fisher, Q.J., Casey, M., Clennel, M.B., Knipe, R.J., 1999. Mechanical compaction of deeply buried sandstones of the North Sea. Marine and Petroleum Geology 16, 605-618.

Frondel, C., 1962. Dana's System of Mineralogy: III Silica Minerals. John Wiley and Sons, New York.

Gjelberg, J., Dreyer, T., Høie, A., Tjelland, T., Lilleng, T., 1987. Late Jurassic to Mid-Jurassic sandbody development on the Barents and Mid-Norwegian shelf. In: Brooks, J., Glennie, K. (Eds.), Petroleum Geology of Northwest Europe. Graham and Trotman, London, 1105-1129.

Gluyas, J.G., Robinson, A.G., Grant, S.M., 1993. Geochemical evidence for a temporal control on sandstone cementation. In: Horbury, A.D., Robinson, A.G. (Eds.), Diagenesis and Basin Development. AAPG Studies in Geology 36, 23-34.

Goldstein, R.H., Rossi, C., 2002. Recrystallisation in quartz overgrowths. Journal of Sedimentary Research 72, 432-440.

Haddad, S.C., Worden, R.H., Prior, D.J., Smalley, P.C., 2006. Quartz cement in the Fountainbleau sandstone, Paris Basin, France: crystallography and implications for mechanisms of cement growth. Journal of Sedimentary Research 76, 244-256.

Hjelen J., 1990. Teksturutvikling i Aluminium, studert ved Elektronmikrodiffraksjon (EBSP) i Scanning Elektronmikrosko. Ph.D. Thesis, University of Trondheim, Norway.

Kikuchi S., 1928. Diffraction of cathode rays by mica. Japanese Journal of Physics 5, 83.

Laughner, J.W, Cline, T.W., Newnham, R.E., Cross, L.E., 1979. Acoustic emissions from stress-induced Dauphiné twinning in quartz. Physics and Chemistry of Minerals 4, 129-137.

Lloyd, G. E., 1985. Review of Instumentation, Techniques and Applications of SEM in mineralogy. In: White, J. C. (Ed.), Short Course in Applications of Electron Microscopy in the Earth Sciences, 11: Fredericton, Mineralogical Association of Canada, 151-188.

Lloyd, G.E., 2000. Grain boundary contact effects during faulting of quartzite: an SEM/EBSD analysis. Journal of Structural Geology 22, 1675-1693.

Makowitz, A., Milliken, K.L., 2003. Quantification of brittle deformation in burial compaction, Frio and Mount Simon Formation sandstones. Journal of Sedimentary Research 73, 1007-1021.

McBride, E.F., 1989. Quartz cement in sandstones: a review. Earch Science Reviews 26, 69-112.

Moen, K., Hjelen, J., Malvik, T., 2003. Preparation of Quartz samples for EBSD analysis [Poster]. Applied Mineralogy '03, Helsinki 2003. Applied Mineralogy '03, CD.

Moen K., Malvik T, Hjelen J., Leinum J.R., 2003. Automatic Material Characterization by means of SEM-techniques. In: Broekmans, M.A.T.M., Jensen, V., Brattli, B. (Eds.), Proceeding, 9th Euroseminar on Microscopy Applied to Building Materials.

Morton, A.C., Grant, S., 1998. Cretaceous depositional systems in the Norwegian Sea: heavy mineral constraints. AAPG Bulletin 82, 274-290.

Mørk, M.B.E., Johnsen, S.O., 2005. Jurassic sandstone provenance and basement erosion in the Møre margin – Froan Basin area. Norges geologiske undersøkelse, Bulletin 443, 5-18.

Nord, G.L., 1994. Transformation-induced twin-boundaries in minerals. Phase Transitions 48, 107-134.

Oelkers, E.H., Bjørkum, P.A., Murphy, W.M., 1996. A petrographic and computational investigation of quartz cementation and porosity reduction in North Sea sandstones. American Journal of Science 296, 420-452.

Passchier, C.W., Trouw, R.A.J., 2005. Microtectonics. Springer Berlin Heidelberg New York.

Paxton, S.T., Szabo, J.O., Ajdukiewicz, J.M, Klimentidis, R.E., 2002. Construction of an intergranular volume compaction curve for evaluating and predicting compaction and porosity loss in rigid-grain sandstone reservoirs. AAPG Bulletin 86, 2047-2067.

Pettijohn, F.J., Potter, P.E., Siever, R., 1972. Sand and Sandstone. New York - Heidelberg - Berlin, Springer-Verlag.

Piazolo, S., Prior, D.J., Holness, M.D., 2005. The use of combined cathodoluminescence and EBSD analysis: a case study investigating grain boundary migration mechanisms in quartz. Journal of Microscopy 217, 152-161.

Prior, D.J., Boyle, A.P., Brenker, F. Cheadle, M.C., Day, A., Lopez, G., Peruzzi, L., Potts, G.J., Reddy, S., Spiess, R., Timms, N.E., Trimby, P., Wheeler, J., Zetterström, L., 1999. The application of electron backscatter diffraction and orientation contrast imaging in the SEM to textural problems in rocks. American Mineralogist 84, 1741-1759.

Putnis, A., 1992. Introduction to Mineral Sciences. Cambridge University Press, Cambridge.

Renard, F., Ortoleva, P., 1997. Water film at grain-grain contacts: Debye-Huckel osmoic model of stress, salinity and mineralogy dependence. Geochimica et Cosmochimica Acta 61, 1963-1970.

Renard, F., Brosse, É., Gratier, J.P., 2000. The different processes involved in the mechanism of pressure solution in quartz-rich rocks and their interactions. Special Publications International Association of Sedimentologists 29, 67-78.

Schmidt, N.H., Olesen, N.O., 1989. Computer-aided determination of crystal lattice orientation from electron channeling patterns in the SEM. Canadian Mineralogist 27, 15–22.

Schwartz A.J., Kumar M., Adams B.L., 2000. Electron Backscatter Diffraction in Materials Science. NY, Kluwer Acadenic/ Plenum Publishers, ISBN 0-306-46487-X.

Spencer, A.M., Birkeland, Ø., Koch, J.-O., 1993. Petroleum geology of the proven hydrocarbon basins, offshore Norway. First Break 11, 161-176.

Storvoll, V., Bjørlykke, K., Karlsen, D., Saigal, G., 2002. Porosity preservation in reservoir sandstones due to grain-coating illite: a study of the Jurassic Garn Formation from the Kristin and Lavrans fields, offshore Mid-Norway. Marine and Petroleum Geology 19, 767-782.

Terry, M.P., Heidelbach, F., 2006. Deformation enhanced metamorphic reactions and the rheology of high-pressure shear zones, Western Gneiss region, Norway. Journal of metamorphic Geology 24, 3-18.

Thomson, A., 1959. Pressure solution and porosity. In: H.A. Ireland (Ed.), Silica in sediments. SEPM Special publication 7, 92-111.

van Daalen, M., Heilbronner, R., Kunze, K., 1999. Orientation analysis of localized shear deformation in quartz fibres at the brittle-ductile transition. Tectonophysics, 303, 83-107.

Vernon, R.H., 2004. A practical guide to rock microstructure. Cambridge University Press.

Walderhaug, O., 1994. Temperatures of quartz cementation in Jurassic sandstones from the Norwegian continental shelf – Evidence from fluid inclusions: Journal of Sedimentary Research 64, 311-323.

Walderhaug, O., Bjørkum, P.A., 2003. The effect of stylolite spacing on quartz cementation in the Lower Jurassic Stø Formation, southern Barents Sea. Journal of Sedimentary Research 73, 146-156.

White, S.H., 1977. Geological significance of recovery and recrystallisation processes in quartz. Tectonophysics 39, 143-170.

Wenk, H.-R., Lonardelli, I., Vogel, S.C., Tullis, J., 2005. Dauphiné twinning as evidence for an impact origin of preferred orientaiton in quartzite: an example from Vredefort, South Africa. Geological Society of America 33, 273-276.

Worden, R.H., Burley, S.D., 2003. Sandstone diagenesis: The evolution of sand to stone. In: Burley, S.D., Worden, R.H. (Eds.), Sandstone Diagenesis. Recent and Ancient. Reprint Series 4 of the International Association of Sedimentologists, Blackwell Publishing, 3-44.

Appendix

Example of electron backscatter diffraction patterns from mother grain and dauphiné twin (Fig. A1). a) Mother grain with the following orientation in Euler space: phi 1: 200.1º, PHI:78.1º and phi 2: 253.8º. b) Twin grain with the following orientation: phi 1: 200.9º, PHI: 77.3º and phi 2: 194.9º. The mis-orientation is 59 degrees around the crystallographic c-axis (59@<0001>).
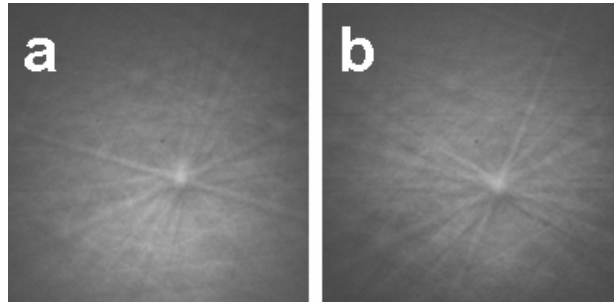
Appendix

INTRODUCTION

The following sections give some additional examples of case studies that have been carried out by means of EBSD analysis. These are not presented in any of the papers but further demonstrate the importance and strength of advanced characterisation methods. The first case was presented as a poster at Applied Mineralogy'03 in Helsinki in 2003, the second case shows some further results from the work presented in Paper 3 presented at ICAM 2004 in Sao Paulo, Brazil. The last case presents a limited investigation carried out as a part of the doctoral project of Steinar Ellefmo in 2005. The EBSD results were not published in his thesis.

1 PREPARATION OF QUARTZ SAMPLES FOR EBSD ANALYSIS

Introduction

Electron backscatter diffraction (EBSD) in scanning electron microscopy (SEM) is a powerful, supplementary technique in mineral discrimination analysis in addition to traditional optical, X-ray and electron microscopy analysis. The technique has up till now mostly been applied in orientation analysis of mono phase materials and more rarely on geological samples for mineral discrimination analysis, but will probably find a wider application together with the low vacuum SEM. The EBSD technique provides diagnostic mineral information, if an electron backscatter pattern with distinct bands is achieved. The quality of diffraction patterns is strongly dependent on the sample preparation. The sample needs to have a polished undisturbed crystal surface.

A preparation study has therefore been performed on quartz as a foundation for obtaining optimal electron backscatter diffraction patterns (EBSP) during EBSD analysis of geological samples.

EBSP - Electron Backscatter diffraction Pattern

The EBSD technique is based on a weak diffraction pattern that forms when primary electrons are backscattered and diffracted from a crystal in a polished sample. The diffraction pattern is formed on a fluorescent screen and transferred by a camera to the computer (Hjelen, 1990).

Surface deformation removal

To get an indexible pattern, the crystal lattice at the sample surface has to be undeformed. To obtain this, a post-mechanical preparation is required (Lloyd, 1985). After mechanical polishing, the surface damage in the uppermost layers has to be removed by either electro-polishing, etching, ion sputtering or chemical-mechanical polishing (colloid silica). Insulating samples should be gently carbon coated or low vacuum must be employed in the SEM. This study involves chemical-mechanical polishing of quartz samples by colloidal silica suspension which is the most common method for geological samples.

General EBSD sample preparation

1) Mechanical polishing
2) Removal of surface damage by
   -electro polishing
   -etching
   -ion sputtering
   -chemical-mechanical polishing (colloid silica)
3) Insulating samples should be gently carbon coated or low vacuum must be employed in the SEM.

Experiments

A quartz sample from a pegmatite was mechanically polished to 0,25 microns. Backscatter patterns from the same grain were generated after different times of chemical-mechanical polishing by colloidal silica suspension (50 vol% OP-S from Struers). Figure 1 shows the effect from increasing polishing times on the pattern quality.

The backscatter pattern is also dependent on the SEM running parameters. The experiment was carried out on a Hitachi S-3500N low vacuum SEM equipped with a Nordif EBSD-detector and both TSL and Oxford Crystal EBSD software. The sample was tilted to 70°, the accelerating voltage was 25 kV, the working distance set to 20 mm and the pressure in the chamber was 30 Pa. Subsequently, quartz powders encapsulated in epoxy were chemically-mechanically polished with high and low degree of pressure and colloidal silica concentration to see the effects (Figure 2).
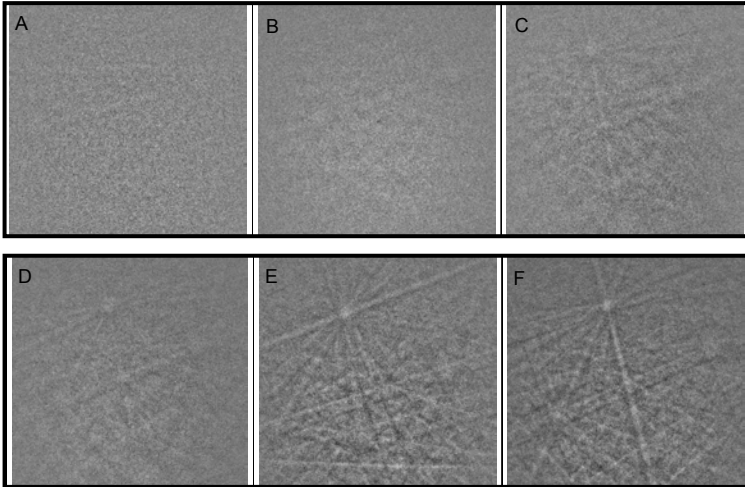
Figure 1. Diffraction patterns from quartz after increasing time of colloid silica polishing. A) 0 sec, B) 10 sec, C) 20 sec, D) 30 sec, E) 60 sec, F) 240 sec.
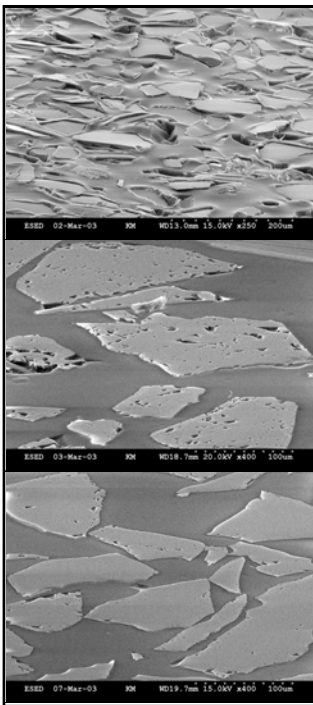
Topography due to aggressive polishing. 5 min of concentrated OP-S polishing, high pressure.

Less topography between quartz and epoxy, but distinct in the quartz. 90 sec. of concentrated OP-S polishing, high pressure.

Minimal topography. The sample is polished for 30 minutes by low pressure and in diluted silica suspension.

Figure 2. Illustration of topography due to differences in polishing properties. All images from samples of quartz powder encapsulated in epoxy (environmental secondary electron detector (ESED)).

Conclusions

After ordinary mechanical polishing, the uppermost atom layers are deformed and no or only diffuse diffraction patterns are generated. After only seconds of colloidal silica polishing, a reasonable pattern may be achieved. The pattern quality converges very quickly against an optimum pattern which is generated after about 30-60 seconds.

One problem regarding too intense polishing, is the generation of topography due to differences in polishing properties between minerals, epoxy and within cracks. To avoid topography, the pressure on the sample on the cloth and the concentration of the colloidal silica suspension should be decreased. This chapter was presented as a poster at the 2nd International Applied Mineralogy Symposium, "Applied Mineralogy '03" in Helsinki, Finland 17-18 March 2003 (Moen et al., 2003).

2 EBSD MICROSTRUCTURE MEASUREMENTS OF MARBLE

Introduction

On modern buildings, stone is used as thin cladding panels rather than for carrying the constructions. Several modern buildings are covered by marble claddings panels and at certain buildings the panels start to bow and loose strength after some years. The phenomenon is assumed to be controlled by marble type, temperature variations, moisture and time. Several studies have been performed to study this behaviour investigating intrinsic and extrinsic parameters (Alnæs et al., 2004; Grelk, 2005; Koch and Siegesmund, 2004; Schouenborg et al., 2003; Winkler, 1996; Yates et al., 2004; Zeisig et al., 2002; Åkesson et al., 2006). Specialised laboratory test procedures have also been developed to be able to predict the behaviour of the marbles.

A small experiment using EBSD to study preferred lattice orientation and preferred grain shape orientation and connect these parameters to direction-dependent bowing and intensity of bowing was carried out.

Experimental

Sampling and preparation

The marble specimens were sampled from two neighbouring quarries. Both were calcitic marbles (calcite content > 99 %weight), but one had a significant highe bowing potential than the other. For the EBSD analyses the specimens were prepared by cutting, grinding and polishing, to give a polished rock section of diameter 25 mm. A chemical-mechanical polishing was performed in the end, to make a deformation free surface that makes lattice diffraction possible. Both samples were from the sample set of the European research project "TEAM" (Testing and Assessment of Marble and Limestone 2000-2005, contract no. G5RD-CT-2000-00233).

Microscopy

To get an optimal EBSD pattern, the analyses were performed in a low-vacuum SEM without a conductive carbon layer. The equipment applied for the experiments is listed in Table 1 and the running and processing conditions in Table 2.

Table 1 Equipment applied for EBSD mapping

Equipment	Type
Low-vacuum SEM	Hitachi S-3500N
EBSD camera	Nordif EBSD dig. camera
EBSD software	TSL, OIM version 3,08/3,5

Table 2 Running and processing conditions for EBSD mapping

| Parameter	Setting
WD	20 mm
V_{acc}	20 kV
Pressure	40 Pa
Tilt	70°
Magnification	90x
Binning	2x2
Step size	5 μm
Processing	Gaussian convolution Half with 15° Expansion L=22 Harmonic calculus

Results
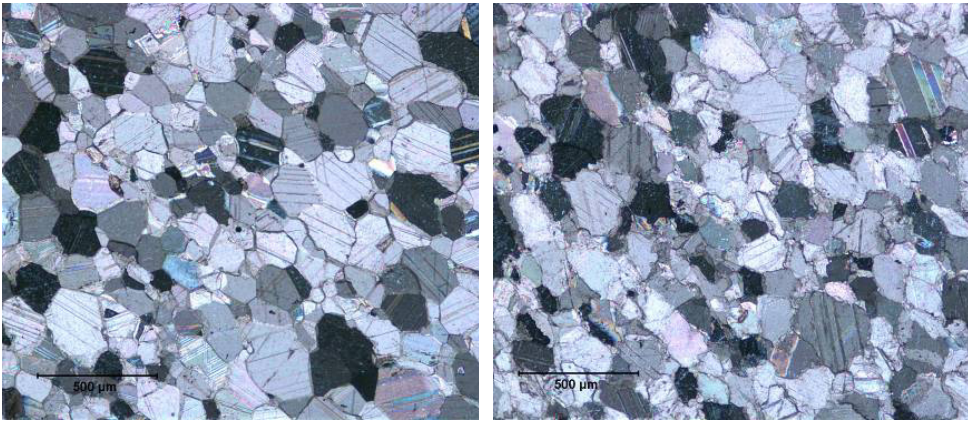
Figure 3. Optical micrographs, crossed polars, of bowing marble to the left and no bowing marble to the right. Both are calcitic marbles from neighbouring quarries. The bowing marble possesses euhedral grains and polygonal shape of grain aggregates and straight grain boundaries while the no bowing marble possesses sub- to anhedral shape of grains and interlobate to amoeboid shape of grain aggregates and lobate to sutured grain boundaries.
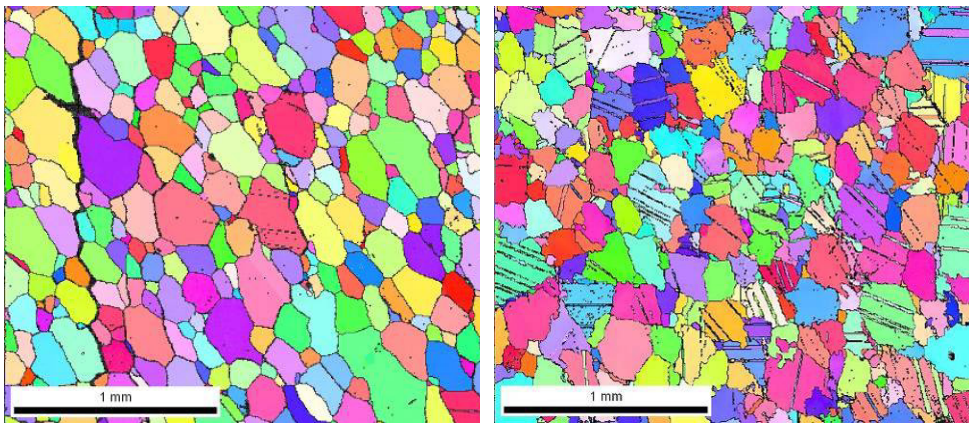

Figure 4. Inverse pole figure maps of bowing marble to the left and no bowing marble to the right. The left marble possess major twinning and grain boundary migration.
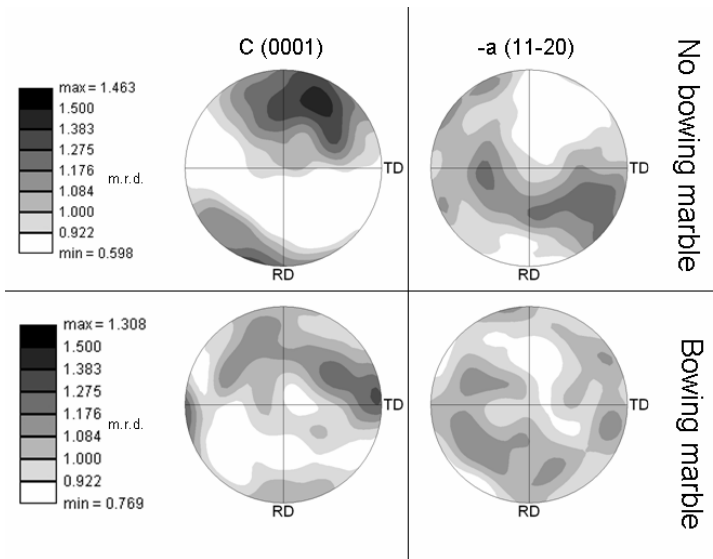
Figure 5. Pole figures of lattice preferred orientation. Lattice orientation is plotted in upper hemisphere, equal area projection, logarithmic scale (multiples of random distribution), harmonic series expansion, rank 22, Gaussian half width 15deg and around 6000 grains were analysed. RD is parallel to y direction. The no bowing marble displays a single c-axis maximum and a girdle a-axis distribution while the bowing marble shows a less pronounced distribution. Both marbles however display nearly random distribution (1.30 and 1.46 mrd).
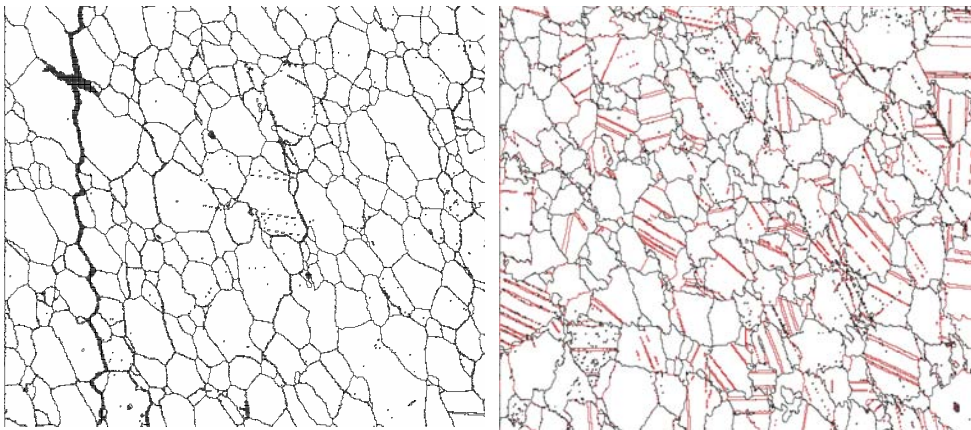
Figure 6. Whenever the lattice orientation is changed, a grain boundary is defined. The grain boundary maps were used to measure grain shape orientation, see Figure 7. The twin-boundaries (in red) were removed before measuring the grain shape orientations.
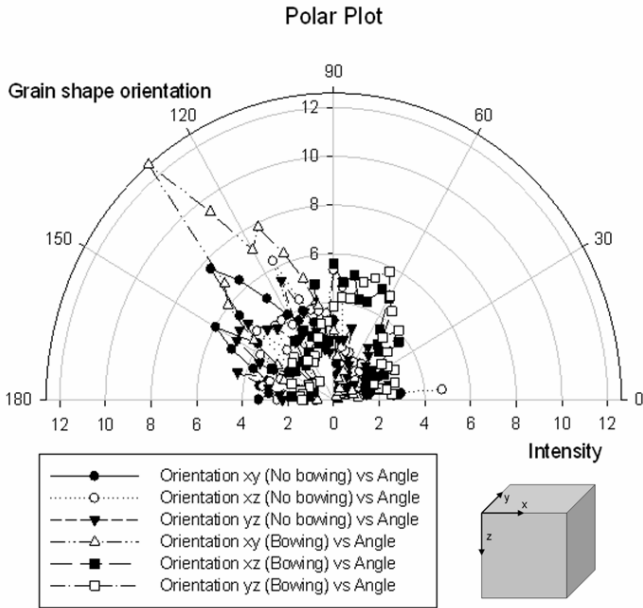
Figure 7. Polar plot of grain shape orientations for three orthogonal sections, xy, xz and yz for bowing and non-bowing marble. The only distinct orientation maximum is for the xy plane of bowing marble at 130°.
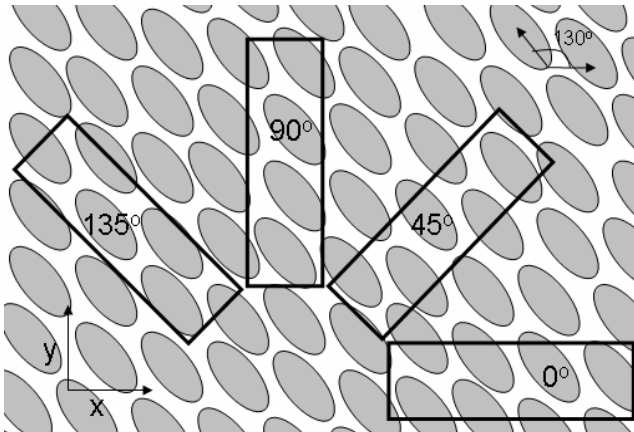
Figure 8. The orientation distribution displays a weak preferred 130° orientation for the xy-plane of bowing marble. Elongation and orientation of the grains will therefore give rice to different numbers of grain boundaries along the longer dimension of the laboratory marble slabs when the slabs are cut in different directions. The 45° slab will contain the highest number of grain boundaries along the longer dimension whereas the 135° slab will contain the lowest number of grain boundaries.

Table 3. Spherical bowing (mm/m) after 50 heating and wetting cycles for marble slabs cut in four directions. Marble Itq1 shows weak bowing tendencies while marble Itq2 shows distinct bowing. For the bowing marble (Itq2), the 45° slab displays the highest magnitude of bowing whereas the 135° slab show the lowest magnitude of bowing. This is correlated to the relative number of grain boundaries indicated in Figure 8. The no bowing marble also shows inhomogeneous bowing tendencies with highest magnitude in the 90° direction. (Alnæs and Aasly, 2005)

Marble	0° (par - x)	45° (45° -x)	90°(nor - x)	135° (135°- x)
Itq1 (No bowing)	1.53	1.89	2.20	0.90
Itq2 (Bowing)	10.07	13.62	10.17	8.25

Discussion and conclusions

From the measurements of two marbles some hypothesis can be drawn. These can be discussed according to findings of previous published work. The research documented in Paper 4 in this thesis covering microstructure measurements on several marble types, discover that the behaviours of the marbles are complex and a study of only two marbles will miss the spanning of the different variables. However, hypothesis from the study are:

- Totally recrystallised rocks with few signs of deformation, that means straight grain boundaries and polygonal grains are more disposed for deterioration than deformed rocks that have undergone grain boundary migration, bulging and subgrain growth leading to inequigranular grain sizes, xenoblastic grain shapes, interlobate to amoeboid shape of grain aggregates, lobate to sutured grain boundaries, twinning and sub grains that all together are annealing the structure. This is in accordance with earlier work e.g. (Alnæs et al., 2004; Kessler, 1919; Koch and Siegesmund, 2004; Schouenborg et al., 2003; Winkler, 1996; Yates et al., 2004; Zeisig et al., 2002; Åkesson et al., 2006). Which parameters that are most important, on the other hand, is not clear. Various conclusions are drawn here. While Winkler states that cogwheel-like interlocks of the grains are important for stabilising the rock, Zeisig et al. (Zeisig et al., 2002) conclude that boundary morphology, i.e. the irregularity of grain boundaries, does not play such an important role as was previously assessed.

- The non-bowing marble has slightly stronger lattice preferred orientation. This implies that lattice preferred orientation cannot explain

9

the magnitude of bowing, but can explain some of the direction-dependence of bowing. The lattice preferred orientation of numerous marbles is studied by Siegesmund and his co-workers by means of neutron diffraction (e.g. Koch and Siegesmund, 2004; Zeisig et al., 2002). The results from this study are in accordance with the work of Siegesmund. Koch and Siegesmund (Koch and Siegesmund, 2004) conclude that lattice preferred orientation clearly controls the degree of bowing and that the direction of maximum bowing is linked to the c-axis maximum. According to Koch and Siegesmund's own results and from Figure 5, the strongest bowing marbles display the weakest lattice preferred orientation. This should imply that lattice preferred orientation is not that important for the bowing intensity. For the direction-dependent bowing however, it seems more important. Calcite is known to have extremely anisotropic thermal behaviour with thermal dilatation of $26 \times 10^{-6} K^{-1}$ parallel to the crystallographic c-axis and $-6 \times 10^{-6} K^{-1}$ perpendicular to it, i.e. parallel to the a-axis (Kleber, 1990). A preferred lattice orientation can therefore give rice to anisotropic bowing behaviour. However, the bowing marble displays the largest direction-dependent bowing, but shows the weakest lattice preferred orientation.

- The marble with most pronounced grain shape preferred orientation (foliation) show the strongest direction dependent bowing. This is in accordance with (Koch and Siegesmund, 2004), but they conclude that lattice preferred orientation is most important. From the results of Kock and Siegesmund (2004) and the results above, it is more appropriate to make the conclusion that foliation is most important. From the work above from Paper 4, it is evident that deterioration is caused by a complex interaction of several properties.

The main conclusions from the work are however that lattice and grain preferred orientation is most important for the direction dependent bowing while irregularities of the grain boundaries and the shape of the grain size distribution curve are most important for the intensity of bowing.

3 EBSD MEASUREMENTS OF LAMELLAS IN HEMATITE

Small exsolution lamellas were detected in some hematite grains by Steinar L. Ellefmo and Suzanne McEnroe (Ellefmo, 2005) while studying sections of iron ore from Rana in Norway, in optical microscope. The lamellas were only resolved in oil immersion objective. Metamorphism has induced deformation twins in the hematite and the exsolution lamellas may be parallel, sub parallel or perpendicular to the deformation twins (Ellefmo, 2005), see Figure 9. The ore has undergone three to four phases of folding, thus it is assumed that different generations of deformation twins are formed.

Ramdohr (1980) has observed the same texture, however the origin and characteristics remain unexplained, and McEnroe (personal communication with Ellefmo 2004) has observed similar textures in Australian iron ores.

Due to similar reflectance, however in anti-phase, the lamellas were assumed to be of the same mineral as the hematite mother grain. This was confirmed in the SEM where the lamellas were not detected by means of backscattered electrons, which indicate that they are of the same average atomic number as the mother grain and must be regarded as micro-twin lamellas. By use of EBSD, a hematite grain containing lamellas were investigated and the twins could be further studied, see Figure 10. The misorientation was found to be 90 degrees about the <2 -2 0 1> axis of rotation.
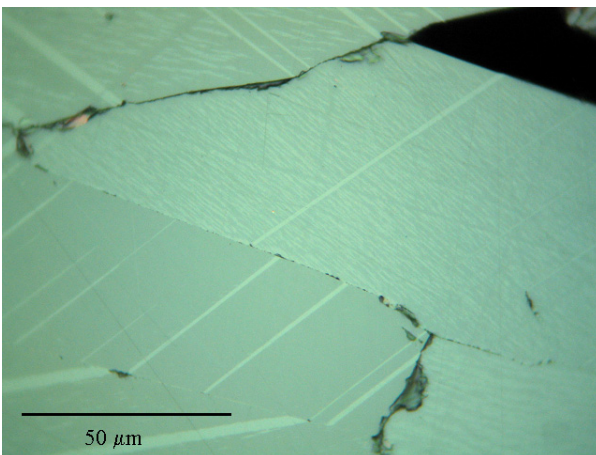
Figure 9. Small lamellas of micro twin deformation in the hematite, oil immersion, reflected light. (Photo: Steinar L. Ellefmo).
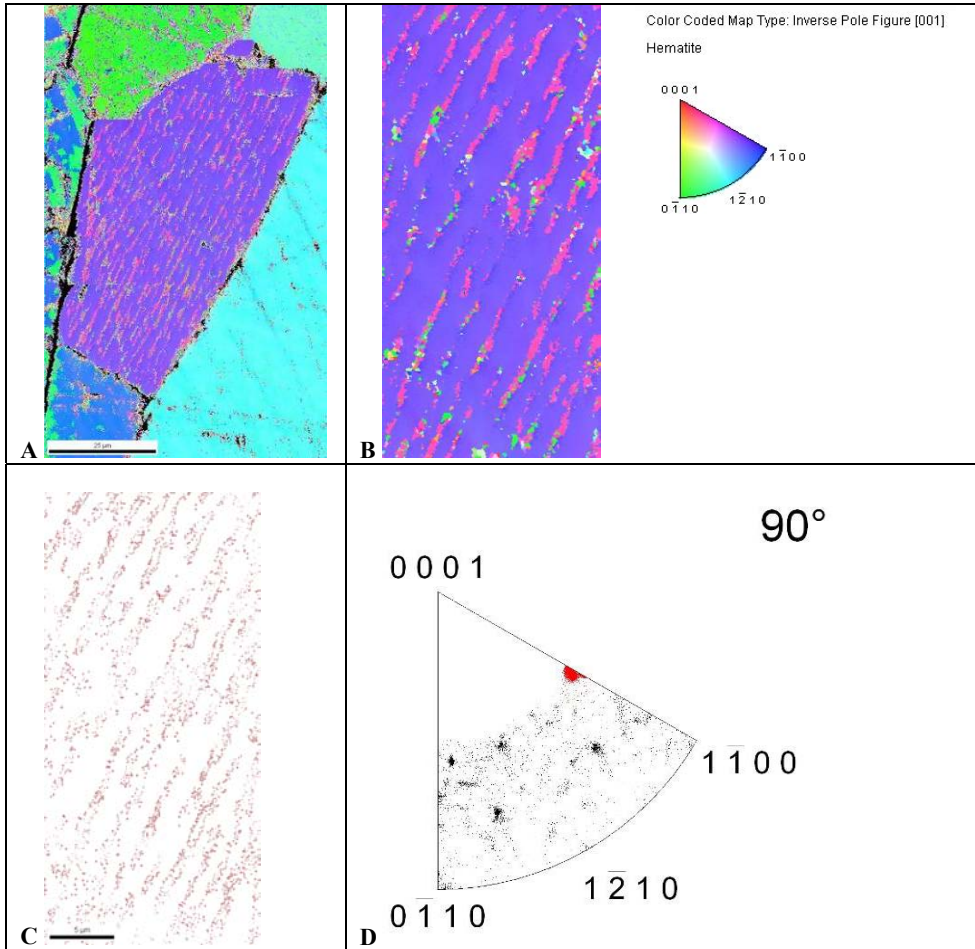
Figure 10. A) EBSD inverse pole figure map of hematite grain containing lamellas. B) Close up of grain from A. C) Twin boundaries. D) Inverse pole figure of axis of rotation at 90° misorientation. The red population shows the boundaries from C. Misorientation between parent and daughter is 90@<2 -2 0 1>.

REFERENCES

Alnæs, L., Koch, A., Schouenborg, B., Åkesson, U., and Moen, K., 2004, Influence of Rock and Mineral properties on the durability of marble panels Dimension Stone 2004, New perspectives for a traditional building material, Prague, Czech Republik, 2004.

Alnæs, L., and Aasly, K. A., 2005, WP 5.3 Compilation of test results, *in* results, W. C. o. t., ed., Microsoft Excel: Trondheim, SINTEF Civil and Environmental Engineering, Rock and Soil Mechanics.

Ellefmo, S. L., 2005, A probabilistic approach to the value chain of underground iron ore mining: From deposit to product, Norges teknisk-naturvitenskapelige universitet, 273 p.

Grelk, B., 2005, Review of literature and TEAM results, TEAM-project WP2, p. 40.

Hjelen, J., 1990, Teksturutvikling i Aluminium, studert ved Elektronmikrodiffraksjon (EBSP) i Scanning Elektronmikroskop, University of Trondheim.

Kessler, D. W., 1919, Physical and chemical test of the commercial marbles of the United States, Technological papers of the Bureau of Standards.

Kleber, W., 1990, Einführung in die Kristallographie: Berlin, VEB Verlag Tecknik.

Koch, A., and Siegesmund, S., 2004, The combined effect of moisture and temperature on the anomalous expansion behaviour of marble: Environmental Geology, v. 46, p. 350-363.

Lloyd, G. E., 1985, Review of Instumentation, Techniques and Applications of SEM in mineralogy, *in* White, J. C., ed., Short Course in Applications of Electron Microscopy in the Earth Sciences, 11: Fredericton, Mineralogical Association of Canada, p. 151-188.

Moen, K., Hjelen, J., and Malvik, T., 2003, Preparation of Quartz Samples for EBSD Analysis: Applied Mineralogy '03, Helsinki, Finland, 2003.

Ramdohr, P., 1980, The ore minerals and their intergrowths, Pergamon Press, 441-1123 p.

Schouenborg, B., Grelk, B., Alnæs, L., Brundin, J. A., Blasi, P., Yates, T., Marini, P., Tschegg, E., Unterweger, U., Tokartz, B., Kock, A., Bengtsson, T., Mladenovic, A., and Goralezyg, S., 2003, TEAM - Testing and Assessment of Marble and Limestone: International Symposium Industrial Minerals and Building Stones, Istanbul, Turkey, Sept 15-18, 2003.

Winkler, E. M., 1996, Properties of marble as building veneer: International Journal of Rock Mechanics and Mining Science & Geomechanics Abstracts, v. 33, p. 215-218.

Yates, T., Brundin, J.-A., Goltermann, P., and Grelk, B., 2004, Observations from the inspection of marble cladding in Europe: Dimension Stone 2004, New perspectives for a traditional building material, Prague, Czech Republic, 2004.

Zeisig, A., Siegesmund, S., and Wieiss, T., 2002, Thermal expansion and its control on the durability of marbles, *in* Siegesmund, S., Wieiss, T., and Vollbrecht, A., eds., Natural Stone, Weathering Phenomena, Conservation Strategies and Case Studies, 205. Special Publications: London, Geological Society of London, p. 65-80.

Åkesson, U., Lindqvist, J. E., Schouenborg, B., and Grelk, B., 2006, Relationship between microstructure and bowing properties of calcite marble claddings: Bulletin of Engineering Geology and the Environment, v. 65, p. 73-79.